Targeting Waddlia chondrophila development cycle using genetic tools and metabolomics

Walter, Chantal

UNIVERSITÉ DE GENÈVE **FACULTÉ DES SCIENCES**

Section des Sciences Pharmaceutiques
Laboratoire de Pharmacognosie
Département de Botanique et Biologie Végétale

Professeur Muriel Cuendet
Docteur Philippe Christen
Docteur Karl Perron

Targeting *Waddlia chondrophila* development cycle using genetic tools and metabolomics

THÈSE

Présentée à la Faculté des sciences de l'Université de Genève
pour obtenir le grade de Docteur ès sciences, mention sciences pharmaceutiques

Par

Chantal Walter

de
Mümliswil-Ramiswil (SO)

Thèse N° 5337

GENÈVE
Atelier d'impression ReproMail
2019

UNIVERSITÉ
DE GENÈVE
FACULTÉ DES SCIENCES

DOCTORAT ÈS SCIENCES, MENTION SCIENCES PHARMACEUTIQUES

Thèse de Madame Chantal WALTER

intitulée :

«Targeting *Waddlia Chondrophila* Development Cycle Using Genetic Tools and Metabolomics»

La Faculté des sciences, sur le préavis de Madame M. CUENDET LICEA, professeure associée et directrice de thèse (Section des sciences pharmaceutiques), Monsieur P. CHRISTEN, docteur et codirecteur de thèse (Section des sciences pharmaceutiques), Monsieur K. PERRON, docteur et codirecteur de thèse (Département de botanique et biologie végétale - Section des sciences pharmaceutiques), Monsieur S. RUDAZ, professeur associé (Section des sciences pharmaceutiques), Monsieur I. XENARIOS, professeur titulaire (Département de biochimie, Faculté des sciences, Université de Genève et Département formation recherche, Ludwig Institute for Cancer Research, Centre hospitalier universitaire vaudois, Université de Lausanne, Suisse), Monsieur S. SUTOUR, docteur (Neuchâtel Platform of Analytical Chemistry, Université de Neuchâtel, Suisse), autorise l'impression de la présente thèse, sans exprimer d'opinion sur les propositions qui y sont énoncées.

Genève, le 29 avril 2019

Thèse - 5337 -

Le Doyen

N.B. - La thèse doit porter la déclaration précédente et remplir les conditions énumérées dans les "Informations relatives aux thèses de doctorat à l'Université de Genève".

I. Abstract

Chlamydia sp. are the major cause of bacterial eye infection in the world. They are also responsible for several urogenital infections. The consequences of such untreated infections can be blindness and infertility. According to the World Health Organization, more than 131 million people were newly infected in 2016 and *Chlamydia* infections in the world's population is still on the rise. At the moment, their treatment is based on antibiotics such as macrolides and tetracyclines. However, since general antibiotic resistance and frequency of persistent infections in the world are rapidly increasing, it is necessary to develop new strategies to treat these bacterial infections. These human pathogens are all Gram-negative intracellular bacteria and members of the-phylum *Chlamydiae.* The *Chlamydiae* member *Waddlia chondrophila* is especially interesting as a model organism since it shares the same intracellular development cycle as the other members of the phylum, but is less pathogenic. The biphasic development cycle comprises the infectious form, called the elementary body (EB) and the non-infectious metabolically active form, the reticulate body (RB). This developmental cycle is the focus of the work presented here. It is unique to the *Chlamydiae* and thus is of interest in the search for novel anti-chlamydial targets and drugs.

Patterns of gene expression, which are up- or down-regulated during this development cycle were identified and in some cases this temporal gene expression has been linked to the activity of specific transcription factors (TF). There are relatively few TFs within the *Chlamydiae*, and only eight are common throughout the phylum. These latter appear to be important for progress through the developmental cycle. The *W. chondrophila* TF Euo is a major regulator of the late phase gene expression when the differentiation from RBs to EBs occurs. It is found only in the *Chlamydiae* and thus was chosen as a target in the search for specific inhibitors. Since no experimental genetic system is currently available for studying *Chlamydiae,* and manipulating the *Chlamydiae* genome to create specific mutations has not been possible thus far, a high throughput screening procedure was developed in a heterologous system, *Escherichia coli.* For these experiments, the *W. chondrophila* Euo was co-expressed with a reporter plasmid containing a known Euo promoter fused to *β*-galactosidase (LacZ). This made it possible to measure Euo activity in an experimentally tractable host, without the need to culture the *Chlamydia* cells.

Natural products encompass a wide range of chemically diverse molecules and in the past have also proved to be a rich source of potential antibiotics. In this study, a total of around 175 plant extracts and 2700 natural products were screened against of Euo. The method proved suitable for use in high-throughput screening mode although unfortunately no active compound emerged.

A different strategy was therefore adopted focusing on another chlamydial TF, DksA. Unlike Euo, DksA is present in a wide range of bacteria including *E. coli* and *Pseudomonas aeruginosa*. This suggested the possibility of investigating *W. chondrophila* DksA function by genetic complementation of DksA mutants of *E. coli* and *P. aeruginosa*, with the subsequent aim of developing a screening protocol to identify *W. chondrophila* DksA inhibitors. DksA is a DNA-independent TF which binds to RNA polymerase through the so-called secondary channel. In *E. coli*, DksA is known to be a key regulator of the stringent response to unfavourable growth conditions, such as amino acid starvation, iron limitation or changes in pH of the environment. Its major effects on gene expression are down-regulation of rRNA transcription and up-regulation of genes required for synthesis of several amino acids. In *P. aeruginosa*, DksA is known to be involved in production of pyocyanin, an important virulence factor. For the complementation experiments, *W. chondrophila dksA* was transformed into *dksA* mutant strains of *E. coli* and *P. aeruginosa* and tested for its ability to complement the host cell mutation. However, no restoration of DksA function in either *E. coli* or *P. aeruginosa* DksA was observed in any of these tests.

Given the difficulties encountered in studying the function of recombinant chlamydial TFs in a heterologous host, a very different approach was adopted in which changes in the metabolites associated with progress through the chlamydial developmental cycle were investigated in a mammalian cell host. For these experiments, the Vero monkey kidney epithelial cells were infected with *W. chondrophila* and the cellular metabolites were monitored at early and late stage of the development cycle, corresponding to the transition from the RB stage to the final EB stage of infection. The results obtained using ultra-high performance liquid chromatography time-of-flight mass spectrometry revealed three metabolites which were increased during the late stage of the developmental cycle, and which were not present in non-infected cells. Molecular networks generated from the tandem mass spectra (MS^2) showed a cluster of the three increased masses, although they could not be identified by dereplication, probably due to the lack of an extensive database of *Chlamydiae* metabolites. According to MS^2 and high resolution mass spectra data, these molecules are probably lipids. Indeed, the MS^2 spectra of all three compounds showed a fragmentation ion which could tentatively be assigned to cholesterol with a loss of the alcohol group as water. The network clustering, the MS^2 spectra and the high resolution mass spectra of these three metabolites produced in *W. chondrophila*-infected Vero cells suggest that they are as yet unknown metabolites, with a cholesteryl ester structure and a diamide side chain.

In conclusion, different approaches were used in this work with the aim of understanding the biology of the chlamydial infectious cycle, and ultimately of identifying new targets and anti-chlamydial drugs. Although, the screening of natural products yielded no significant positive

results, this research provides a generic screening tool, which could be used to search for inhibitors of other chlamydial TFs. The complementation approach using the chlamydial TF DksA, expressed in the corresponding mutants of two other Gram-negative bacteria, *E. coli* and *P. aeruginosa,* showed no complementation, thus suggesting differences in the regulation and/or function of DksA between these diverse bacterial species. Finally, the metabolomics research revealed the presence of putative new metabolites characteristic of different stages during the development cycle. These metabolites are probably unique, and thus could be characteristic for *W. chondrophila* infections.

Overall, this work presents several strategies using high throughput screening, genetic complementation, and metabolomics to investigate the *W. chondrophila* development cycle. While targeting specific TFs did not yield useful results, the findings of the metabolomic study has provided novel insight into the *W. chondrophila* development cycle, which in the future could offer a promising starting point for identifying specific and druggable targets to perturb the chlamydial infectious cycle.

II. Résumé

Les bactéries du genre *Chlamydia* sont la principale cause d'infection oculaire bactérienne dans le monde. Elles sont également responsables de plusieurs infections urogénitales. Les conséquences de ces infections peuvent être respectivement la cécité et l'infertilité. Selon l'Organisation mondiale de la santé, plus de 131 millions de personnes ont été atteintes en 2016, et les infections à *Chlamydia* dans la population mondiale ne cessent d'augmenter. Actuellement, le traitement est basé sur des antibiotiques tels que les macrolides et les tétracyclines. Cependant, comme la résistance générale aux antibiotiques et la fréquence des infections persistantes dans le monde augmentent rapidement, il s'est avéré nécessaire de développer de nouvelles stratégies pour traiter ces infections bactériennes. Ces pathogènes humains sont tous des bactéries intracellulaires Gram-négatives et membres de l'embranchement *Chlamydiae*. Parmi ceux-ci, *Waddlia chondrophila* est particulièrement intéressant comme organisme modèle car il partage le même cycle de développement intracellulaire que les autres membres de l'embranchement, tout en étant moins pathogène. Le cycle de développement biphasique comprend la forme infectieuse, appelée corps élémentaire (CE) et la forme métaboliquement active non infectieuse, le corps réticulé (CR). Ce cycle de développement est le principal centre d'intérêt du travail présenté ici. Il est unique aux *Chlamydiae* et présente donc un intérêt dans la recherche de nouvelles cibles et de nouveaux médicaments.

Les gènes dont l'expression est modulée au cours de ce cycle de développement, ont été identifiés, montrant également l'importance de certains facteurs de transcription (FT). Il y a relativement peu de FT identifiés chez les *Chlamydiae*, et seulement huit sont communs à tout l'embranchement. Ces derniers semblent importants pour la progression du pathogène tout au long de son cycle de développement. Le FT Euo de *W. chondrophila* est l'un des principaux régulateurs de l'expression génique en phase tardive lorsque la différenciation des CRs en CEs se produit. Il n'est présent que dans les *Chlamydiae* et a donc été choisi comme cible dans la recherche d'inhibiteurs spécifiques. Aucun système génétique expérimental n'étant actuellement disponible pour l'étude des *Chlamydiae*, et la manipulation du génome des *Chlamydiae* pour créer des mutations spécifiques n'ayant pas encore été possible, un procédé de criblage à haut débit a été développé dans un système hétérologue, avec *Escherichia coli*. Pour ces expériences, le FT Euo de *W. chondrophila* a été co-exprimé avec un plasmide rapporteur contenant un promoteur reconnu par Euo fusionné au gène codant pour la *β*-galactosidase (LacZ). Ceci a permis de mesurer l'activité d'Euo dans *E. coli*, sans avoir besoin de cultiver la bactérie *W. chondrophila.*

Les produits naturels englobent un large éventail de molécules et qui se sont également avérés dans le passé être une riche source d'antibiotiques potentiels. Dans cette étude, environ 175 extraits de plantes et 2700 produits naturels ont été testés contre l'activité d'Euo. La méthode s'est avérée appropriée pour une utilisation en criblage à haut débit, bien qu'aucun composé actif n'a malheureusement pu être identifié.

Une stratégie différente a donc été adoptée, axée sur un autre FT de *W. chondrophila*, la protéine DksA. Contrairement à Euo DksA est présent dans une large gamme de bactéries dont *E. coli* et *Pseudomonas aeruginosa*. Cela donne la possibilité d'étudier la fonction de DksA de *W. chondrophila* par complémentation génétique des mutants DksA d' *E. coli* et de *P. aeruginosa*, dans le but de développer un protocole de criblage pour identifier les inhibiteurs de ce DksA. Ce dernier est un FT indépendant de l'ADN qui se lie à l'ARN polymérase par le canal secondaire. Dans le cas d'*E. coli*, il est reconnu comme l'un des principaux régulateurs de la réponse stringente, permettant de répondre aux conditions de croissance défavorables, telles que la privation d'acides aminés, la limitation du fer ou les changements du pH de l'environnement. Ses principaux effets sur l'expression des gènes sont la répression de la transcription des ARN ribosomiques et l'induction de l'expression des gènes nécessaires à la synthèse de plusieurs acides aminés. Chez *P. aeruginosa*, il est impliqué dans la production de pyocyanine, un facteur de virulence important. De manière à investiguer la fonction de cette protéine, *dksA* de *W. chondrophila* a été transformé dans des mutants *dksA* d'*E. coli* et de *P. aeruginosa*. La possibilité de complémenter les mutations a alors été testée. Aucune restauration de la fonction de DksA chez *E. coli* ou *P. aeruginosa* n'a été observée dans ces tests.

Considérant les difficultés rencontrées dans l'étude de la fonction des FTs de *W. chondrophila* recombinants chez un hôte hétérologue, une approche différente a été adoptée. Dans cette approche les changements dans la composition en métabolites durant le cycle de développement de *W. chondrophila* ont été étudiés. Pour ces expériences, des cellules épithéliales rénales de singe Vero ont été infectées par *W. chondrophila* et la composition en métabolites cellulaires a été mesurée au début et à la fin du cycle de développement, ce qui correspond à la transition du stade CR au stade CE final de l'infection. Les résultats obtenus par chromatographie liquide à ultra-haute performance avec détection par spectrométrie de masse à temps de vol ont révélé la présence de trois métabolites dont les concentrations étaient augmentées à la fin du cycle de développement et qui n'étaient pas présents dans les cellules non infectées. Les réseaux moléculaires générés à partir des spectres de masse en tandem (MS^2) ont montré une augmentation pour trois masses. Elles n'ont pas été identifiées par déréplication, en raison de l'absence d'une grande base de données des métabolites de *Chlamydiae*. Selon les données MS^2 et les spectres de masse à haute résolution, ces

molécules appartiennent probablement à la classe des lipides. En effet, les spectres MS^2 des trois composés ont montré un ion de fragmentation qui pourrait être attribué au cholestérol avec une perte du groupe alcool sous forme d'eau. Après regroupement en réseau, les spectres MS^2 et les spectres de masse à haute résolution de ces trois métabolites produits dans les cellules de Vero infectées par *W. chondrophila* suggèrent qu'il s'agit de métabolites encore inconnus, avec un squelette cholestérol estérifié et une chaîne latérale diamidique.

En conclusion, différentes approches ont été utilisées dans ce travail dans le but de bloquer l'activité de FTs, de comprendre la biologie du cycle infectieux de *Chlamydia*, et finalement d'identifier de nouvelles cibles et des molécules contre ces bactéries. Bien que le criblage de produits naturels n'a donné aucun résultat positif significatif, cette recherche fournit un outil de dépistage génétique qui pourrait être utilisé pour rechercher les inhibiteurs d'autres FT dans le groupe des *Chlamydiae*. L'approche par complémentation utilisant le FT DksA de *W. chondrophila*, exprimé dans les mutants correspondants de deux autres bactéries Gram-négatives, *E. coli* et *P. aeruginosa*, n'a montré aucune complémentation, ce qui suggère des différences dans la régulation et/ou la fonction de DksA entre ces diverses espèces bactériennes. Enfin, la recherche en métabolomique a révélé la présence de nouveaux métabolites présumés caractéristiques des différents stades du cycle de développement. Ces métabolites sont probablement uniques et pourraient donc être caractéristiques des infections à *W. chondrophila.*

Dans l'ensemble, ce travail présente plusieurs stratégies utilisant le criblage à haut débit, la complémentation génétique et la métabolomique pour étudier le cycle de développement de *W. chondrophila*. Bien que les expériences visant à bloquer l'activité de FT spécifiques n'ont pas donné de résultats positifs, l'étude métabolomique a fourni de nouvelles informations sur le cycle de développement de *W. chondrophila*, qui pourraient dans l'avenir offrir un point de départ prometteur pour identifier des cibles spécifiques et médicamenteuses pour perturber le cycle infectieux de *W. chondrophila*.

III. Remerciements

C'était un rêve et le rêve est devenu une réalité, une réalisation.

L'obtention de mon doctorat n'aurait pas été possible sans une grande équipe qui m'a soutenue et m'a guidée tout au long de mon parcours et de mes années à Genève. Permettez-moi donc de vous nommer tous et de vous exprimer ma profonde gratitude, mes remerciements et mon respect:

Prof. Muriel Cuendet pour m'avoir donné l'opportunité de faire ce projet de doctorat; les membres du jury, Prof. Ioannis Xenarios (Département de biochimie, Faculté des sciences, Université de Genève et Département formation recherche, Ludwig Institute for Cancer Research, Centre hospitalier universitaire vaudois, Université de Lausanne, Suisse), Prof. Serge Rudaz (Faculté des sciences pharmaceutiques, Université de Genève, Genève, Suisse) et Dr Sylvain Sutour (Neuchâtel Platform of Analytical chemistry, Université de Neuchâtel, Suisse) pour l'évaluation de mon travail; Dr Karl Perron, co-superviseur pour son mentorat et ses conseils; Dr Philippe Christen co-superviseur pour les précieuses discussions et conseils; Prof. Gilbert Greub, Dr Marie de Barsy et Prof. Patrick Viollier pour les collaborations constructives et pour leur confiance; Dr Gerardo Turcatti et Dr Marc Chambon du BSF à Lausanne pour avoir partagé avec moi leur collection de produits naturels.

Prof. Jean-Luc Wolfender, pour les nombreuses discussions lors des réunions de groupe et son équipe qui a réalisé l'analyse en spectrométrie de masse. Je présente mes remerciements particulièrement à Dr Pierre-Marie Allard dont les connaissances approfondies en métabolomique ont été inestimables; Dr Samuel Bertrand, Dr Guillaume Marti et Dr Julien Boccard qui ont partagé leurs connaissances dans le domaine de la spectrométrie de masse et de l'analyse des données; Dr Mélanie Marguerettaz et Verena Ducret, qui m'ont gentiment montré les techniques de microbiologie et de biologie moléculaire; les membres des groupes de pharmacognosie, phytochimie et produits naturels bioactifs, et microbiologie pour leur contribution professionnelle à ma thèse, mais aussi pour leur soutien personnel et leur agréable coopération: Betty, Manuel, Sara et Sandrine de l'unité de microbiologie; Amina, Vincent, Mark, Antonio, Vera, Joëlle, Quentin, Soura, Olivier, Adlin, Nicolas, Caroline, Noémie, Aymeric de la Section des sciences pharmaceutiques; Frédéric Borlat et Natalie Schregle, pour l'appui technique et administratif. Dr Laurence Marcourt pour le soutien à l'interprétation des spectres RMN; Davide pour avoir partagé l'activité d'enseignement et les belles discussions durant ces années; Dr Andreas Nievergelt-Meier, qui m'a enseigné les techniques générales de la culture de cellules eucaryotes.

Tous mes amis, surtout: Sylvie Haas, Andrea Schou, Nur Tanrisever, Adam Zimke, Stefan Erni, Jeanine Gerber, Dr Sandra Balzer et Dr Mariam Martin Mnatsakanyan qui m'ont soutenue

au-delà du "Röstigraben", d'Allemagne et d'Australie, à leur manière. Je tiens également à remercier le Fonds national suisse de la recherche scientifique pour le financement de ce projet, ainsi que la Fondation Ernest et Lucie Schmidheiny pour m'avoir soutenue avec une subvention pour l'achat de la collection de produits naturels.

A la fin, je voudrais mentionner les personnes qui représentent tout pour moi: ma famille, y compris Dr Zaki Sleiman et sa famille. Merci pour votre présence et pour votre patience durant ces années. J'apprécie tous vos soutiens et votre présence à côté de moi. Je ne pouvais pas souhaiter mieux.

IV. Table of contents

V. List of figures

VI. List of tables

VII. Abbreviations

Amp	Ampicillin
ATP	Adenosine triphosphate
Bp	Base pairs
BLAST	Basic local alignment search tool
***β*-ME**	*β*-mercaptoethanol
Cb	Carbenicillin
ChEBI	Chemical entities of biological interest
C. pneumoniae	*Chlamydia pneumoniae*
C. psittaci	*Chlamydia psittaci*
C. trachomatis	*Chlamydia trachomatis*
CM	Chloramphenicol
CPAF	Protease-like activity factor
CTP	Cytidine triphosphate
DDAOG	9H-(1,3-dichloro-9,9-dimethylacridin-2-one-7-yl) *β*-D-galactopyranoside
dH_2O	Deionized water
DMSO	Dimethyl sulfoxide
DNA	Deoxyribonucleic acid
DNP	Dictionary of natural products
2D-PAGE	Two-dimensional polyacrylamide gel electrophoresis
EB	Elementary body
E. coli	*Escherichia coli*
ECMDB	*E. coli* metabolome database
EDTA	Ethylenediaminetetraacetic acid
EMSA	Electrophoretic mobility shift assay
ESI	Electrospray ionization
Euo	Early upstream open reading frame
FA	Formic acid
GC	Gas chromatography
Gm	Gentamicin
H	Hour(s)
HILIC	Hydrophilic interaction liquid chromatography
HIV	Human immunodeficiency virus
HMDB	Human metabolome database
HRMS	High resolution mass spectrometry
IPTG	Isopropyl *β*-D-1-thiogalactopyranoside
KM	Kanamycin
LB	Luria-Bertani broth
LBA	Luria-Bertani broth containing agar
LC	Liquid chromatography
MALDI	Matrix-assisted laser-desorption-ionization
Mbp	Mega-base pairs
MeOH	Methanol
MIC	Minimal inhibitory concentration
Min	Minute(s)
MS	Mass spectrometry
MS^2	Tandem mass spectrometry

MUG	4-methylumbelliferyl-*β*-D-glucuronide
m/z	Mass-to-charge ratio
NMR	Nuclear magnetic resonance
NCE	New chemical entity
npt-II	*Neomycin phosphotransferase II*
OD	Optical density
ONPG	*o*-nitrophenyl *β*-D-galactopyranoside
PCA	Principal component analysis
PCR	Polymerase chain reaction
P. aeruginosa	*Pseudomonas aeruginosa*
PBS	Phosphate buffer saline
PG	Peptidoglycan
p.i.	Post-infection
ppGpp	Guanosine tetraphosphate
OPLS-DA	Orthogonal partial least squares discriminant analysis
QC	Quality control
RB	Reticulate body
RNA	Ribonucleic acid
RP	Reverse phase
rrn	Genes encoding the rRNA
RT	Room temperature
S	Second(s)
SCBF	Secondary channel-binding factors
SDS	Sodium dodecyl sulfate
SPE	Solid phase extraction
S. aureus	*Staphylococcus aureus*
SST	System suitability test
TCA	Trichloroacetic acid
Tet	Tetracycline
TF	Transcription factor
TOF	Time-of-flight
UHPLC	Ultra-high performance liquid chromatography
UHPLC-MS	Ultra-high performance liquid chromatography coupled to mass spectrometry
USA	United States of America
UTP	Uridine triphosphate
UV	Ultraviolet
VIP	Variable importance in projection
W. chondrophila	*Waddlia chondrophila*
WHO	World Health Organization
X-Gal	5-bromo-4-chloro-3-indolyl *β*-D-galactopyranoside

Chapter 1: General introduction

1.1 Current antibacterial drug discovery

Following the discovery of penicillin by Alexander Fleming in the early 20th century, and the 'golden age' in the 1950s when the majority of antibacterial molecules were discovered, the number of new antibiotics on the market over the past 25 years has been extremely low [1].

There are a number of reasons for this. Firstly, finding novel chemical classes with antibacterial activity has proved difficult. Secondly, to be successful any new chemical entity (NCE) must have a low tendency to select for resistant strains [2], otherwise, by the time the molecule arrives on the market, resistant bacteria may have already evolved. Thirdly, developing new antibiotics is relatively expensive and novel drugs tend to be used in small quantities as last-line treatments, and thus may not be commercially viable. For these reasons, several big pharmaceutical companies have stopped research on antibiotics in favour of other therapeutic areas such as cancer and neurodegeneration.

As a consequence, development of new antibacterial drugs is in the so-called “post-antibiotic” era. In other words, the large majority of newly approved drugs are based on minor modifications to existing scaffolds or simply on improved formulation, and third or even fourth generation forms of antimicrobial agents have been developed with the aim of maintaining effectiveness by avoiding development of resistance [3]. In the current development pipeline, there are 51 potential new antibiotics of which only eight are considered innovative, and suitable for the treatment of antibiotic resistant bacteria [4]. Furthermore, the World Health Organization (WHO) recently announced that the number of NCEs currently in development, will not be capable of fighting the growing risk of antibiotic resistance [4]. At the same time, it is estimated that drug-resistant infections could cause 10 million deaths per year worldwide by 2050 [5]. Therefore, novel innovative strategies are urgently needed in order to fill the antibiotic pipeline.

1.2 Global epidemiology of *Chlamydiae* infections

The leading cause of bacterial eye disease (trachoma) and the most frequent cause of sexually transmitted bacterial diseases in the world are both due to infection with the human pathogen *Chlamydia trachomatis* of the phylum *Chlamydiae* [6, 7]. In 2016, WHO reported that *C. trachomatis* was responsible for 131 million new cases of sexually transmitted infections and for 85 million reported cases of blindness worldwide, and most of these cases were treatable [8, 9]. Tragically however, the incidence of trachoma and sexually transmitted bacterial diseases are on the increase. In 2016 for example, 11,013 new *C. trachomatis* infections were described in Switzerland, 8% more than in the previous year. The same increasing trend can be observed in other European countries, as well as in the United States of America (USA) [10]. The largest number of new infections (around 75%) is found in young women (15-24 years old). Most of the time, the bacterial infection is asymptomatic and remains untreated, which can lead subsequently to urogenital infections such as cervicitis, urethritis and pelvic inflammatory disease [11]. Severe reproductive complications such as infertility and ectopic pregnancy may also result from such untreated infections [12-14]. The estimated direct medical cost of *C. trachomatis* treatment and complications resulting from infection, for the period between 2002-2011 was over 500 million dollars in the USA alone [15]. Studies have shown that chlamydial infections can also facilitate transmission and persistence of pathogenic viruses such as HIV (human immunodeficiency virus) and human papillomavirus [16, 17]. In addition, transmission of *C. trachomatis* from the mother with cervical chlamydial infection to the newborn during parturition was also reported [18]. Besides the urogenital tract infections, several studies have shown that *C. trachomatis* can be involved in the pathogenesis of several chronic diseases, including asthma, arthritis, and atherosclerosis [19-22]. Other reported human pathogens of the phylum *Chlamydiae* are *C. pneumoniae* and the zoonotically acquired *C. psittaci*. These pathogens can cause rare forms of respiratory infections and atypical pneumonia [23]. Transmission of *C. psittaci* to humans is acquired from an avian reservoir [24].

1.3 Biology of *Chlamydiae*

1.3.1 Phylogeny and related organisms

The phylum *Chlamydiae* comprises obligate intracellular Gram-negative bacteria and is part of the *Planctomycetes-Verrucomicrobia-Chlamydiae* bacterial superphylum containing a wide range of members, including some human pathogens, abundant soil microbes and bacterial strains important for the marine nitrogen cycle (Figure 1.1) [25].

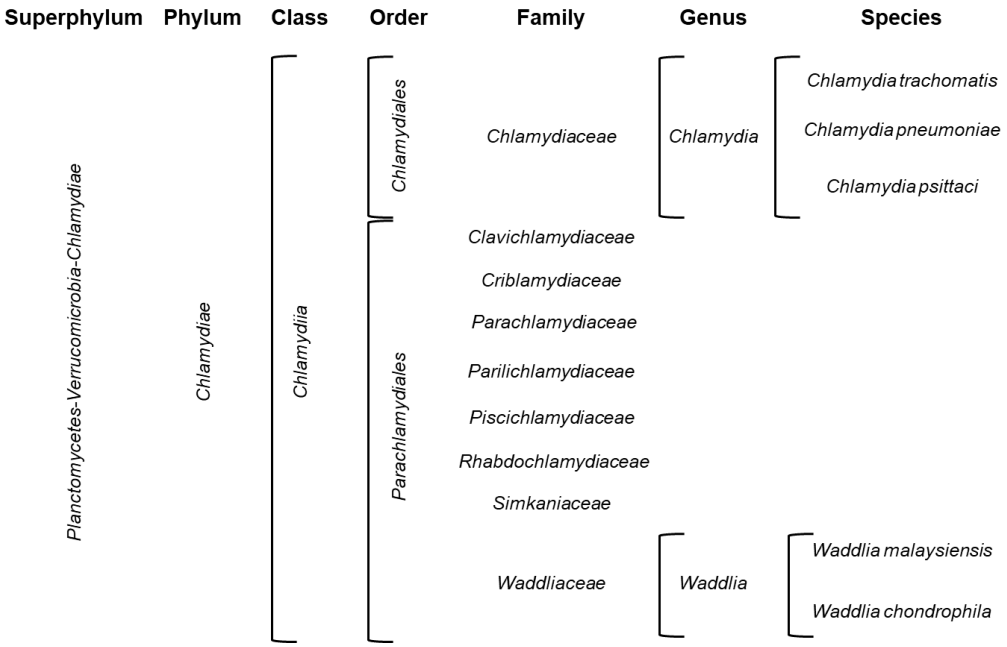

Figure 1.1. Classification of the phylum *Chlamydiae*.
Genera and species only mentioned in this thesis are shown. Adapted from Gupta *et al*. [26] and Chua *et al*. [27].

This phylum now contains the single class *Chlamydiia* with two orders *Chlamydiales* and *Parachlamydiales*. This was proposed recently taking into account the degree of conservation of signature sequences in the DNA and proteins within the phylum [26].

Chlamydiaceae was the first family to be described in this phylum in 1945 and was thought to be the only family until the 1990s when a total of nine ecologically and genetically diverse families (*Chlamydiaceae, Clavichlamydiaceae*, *Criblamydiaceae*, *Parachlamydiaceae, Parilichlamydiaceae, Piscichlamydiaceae*, *Rhabdochlamydiaceae*, *Simkaniaceae,* and *Waddliaceae) w*ere recognized, based on 16S rRNA analyzes and phenotypic characteristics [28-32]. Indeed, the more recently included *Chlamydiae* families are sometimes referred to in the literature as *Chlamydia*-related organisms or environmental *Chlamydiae,* since initially they were isolated mainly from environmental sources [33]. The original family *Chlamydiaceae* comprises the single genus *Chlamydia*. This genus includes the three human pathogens *C.*

trachomatis, C. pneumoniae and C. psittaci, with *C. trachomatis* strains being the most widely studied. These strains can be further classified by the serovar-specific antigens into two human biovars and further subtyped by serotypes (15-19) [34, 35]. The *C. trachomatis* trachoma biovar includes the ocular serotypes A, B, Ba, C, the leading cause of non-congenital blindness in developing nations, and the urogenital serotypes D-K, which are the sexually transmitted bacteria. The second *C. trachomatis* biovar is the lymphogranuloma venereum biovar, serovars L1-L3, responsible for lymphogranuloma venereum [36].

1.3.2 Genome

The complete sequence of the *C. trachomatis* genome was published in 1998. It contains 1.04 Mega-base pairs (Mbp) with around 900-1200 genes and an estimated 895 protein coding sequences. By comparison, the *Escherichia coli* genome consists of 4.6 Mbp and about 5000 genes [37, 38]. The reduced genome complexity is typical for obligate intracellular pathogens dependant on host-encoded functions. A comparative genomic study of different members of the family *Chlamydiaceae* showed a high degree of genome conservation in terms of size, number of coding sequences, nucleotide sequence homology and genomic synteny (conserved gene proximity along the chromosome) [39]. A core set of 560 genes are shared by all *Chlamydiae*, of which 27 are specific to *Chlamydiae* and are not present in any other cellular organisms sequenced to date [40]. Among these conserved genes are transcription factors (TFs), housekeeping genes related to the intracellular lifecycle, and a further 122 genes, which encode proteins with currently unknown function [40].

1.3.3 TFs

TFs are involved in the regulation of the chlamydial intracellular development cycle. They regulate gene expression by binding regulatory regions within bacterial promoters. They can function either as activators, repressors or dual regulators of gene expression. In 2015, Domman and Horn identified 73 putative regulatory regions in *Chlamydiae* containing either an experimentally determined DNA-binding domain and/or sequence homology to known regulatory motifs. These regulators were found to be present at varying frequency throughout the phylum [41]. Thus, members of the *Chlamydiaceae* harbour relatively few (12-15) TFs, which most likely function in core chlamydial biology, such as the developmental cycle. By comparison, the free-living Gram-negative bacteria *E. coli* contains about 300 genes, which express known or predicted TFs [42].

1.4 *Chlamydiae* pathogenesis mechanisms

1.4.1 Intracellular development cycle

All *Chlamydiae* members have a characteristic two-phase intracellular development cycle (Figure 1.2) [43], which starts with the entry into the host cell of the small infectious and metabolically inert form, called the elementary body (0.2 to 0.3 µm, EB). EBs are incorporated into a membrane-bound, parasitophorous inclusion, where they differentiate into larger non-infectious reticulate bodies (1 µm, RB). In the inclusion, the metabolically active RBs use the host cell metabolites to grow and divide through binary fission [44]. The inclusion also provides a protective niche to escape from the host cell endocytic pathways, evading lysosomal fusion [45]. Following RB growth, they differentiate back into EBs and exit by cell lysis and extrusion to infect other host cells [46]. Only EBs can survive in the extracellular environment [47].

Based on temporal gene expression patterns, the chlamydial development cycle can be divided into early, middle and late phases of the cycle [48, 49]. In the early phase, genes involved in macromolecular synthesis are expressed to establish the intracellular niche. The mid-cycle genes are essential for actively dividing bacteria and the late cycle gene products are required when RBs differentiate back to EBs [48]. This temporal pattern of gene expression is regulated by highly conserved TFs that interact with specific DNA-binding domains to either activate or repress gene transcription. The duration of the cycle varies between *Chlamydiae* members. In *C. trachomatis*, early transcription initiation occurs within 1-2 h post-infection (p.i.), the mid-cycle genes are expressed by 3-18 h, and the late cycle genes appear after 20-48 h [48].

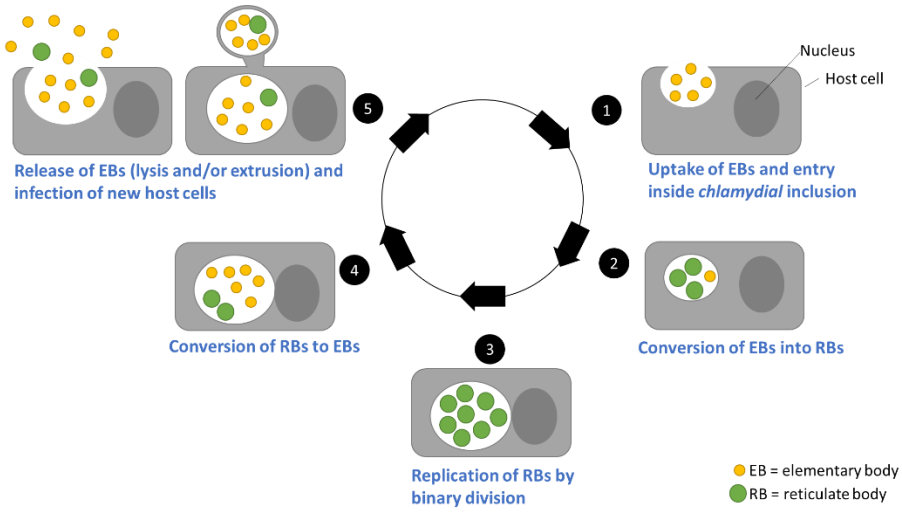

Figure 1.2. The *Chlamydia* developmental cycle.
The *Chlamydia* developmental cycle in which EBs infect the host cell (1), convert into RBs (2) and then replicate by binary division (3). The RBs convert back to EBs (4) that are then released (5) to infect new host cells. Adapted from Abdelrahman and Belland [50].

1.4.2 Persistent form

Under certain stressful conditions, such as the interferon-gamma-induced immunological response, the presence of antibiotics (penicillin G or other *β*-lactam antibiotic exposures), or nutrient-starvation (amino acids, iron or glucose deprivation), the *Chlamydiae* RB can develop into a characteristic reversible state, referred as the persistent form [51-53]. In this state, known as the aberrant RB phenotype (AB), the bacteria are still viable and non-infectious [54]. The ABs do not differentiate into EBs, rather the persistent form represents a bacterial strategy to escape the host immune response for months or even years. When the environmental stressor is removed or the appropriate nutrients are replenished, *Chlamydia*e resume their normal development and produce EBs [55, 56]. The persistent form has been implicated in the etiology of several chronic diseases.

1.4.3 Interaction with the host cell

Like other Gram-negative bacteria, *Chlamydiae* produce a functional needle-like apparatus, the type III secretion system (T3SS), to deliver proteins, also known as effectors through the inclusion membrane and into the host cell cytosol during the development cycle [57]. A characteristic of the *Chlamydiae* is the location of the T3SS within the EB, which unlike in other bacteria is restricted to one hemisphere of the EB surface [58, 59]. This concentrates the T3SS-secreted proteins, and increases the speed and efficacy of subverting the host signalling pathways vital for bacterial intracellular lifestyle [60].

A *Yersinia* T3SS-specific inhibitor, a benzohydrazide compound, also repressed progression of the *C. trachomatis* development cycle in HeLa and Vero cells [61]. This finding led to the conclusion that T3SS activity is important for the survival and pathogenesis of the bacteria in the intracellular environment of the host [62, 63]. However, the function of all chlamydial effectors is not yet known, and little homology between the effector proteins of different members of the phylum *Chlamydiae* has been found, probably because of the differing survival mechanisms employed in a diverse range of host cells [33].

Chlamydiae are dependent on the eukaryotic host cell metabolism, and the effector proteins are able to subvert many cellular processes including the host cell cytoskeletal functions, to promote the survival and thus the pathogenesis of the bacteria [64]. The host cell cytoskeleton is important for many cellular processes such as cell division and motility, vesicle and organelle movement, and the maintenance of cell shape [65]. The effector proteins of *Chlamydiae* manipulate the host cell cytoskeleton to promote interaction with various organelles such as mitochondria, lipid droplets, multivesicular bodies, the Golgi and the

endoplasmatic reticulum (ER) thus delivering key macromolecules to the inclusion, including lipids, amino acids and nucleotides [66].

Lipids, such as sphingomyelin and cholesterol act as signalling molecules in many cellular functions and are present in the inclusion membrane of *Chlamydiae*. Cholesterol-rich microdomains in the plasma membrane of the host cells (also called lipid rafts), play a key role during pathogen attachment and entry into the host cell. Lipid rafts are known to be important components of cell signalling and endocytosis, and often represent the bacterial target during pathogenesis [67]. However, the main source of host lipids is the Golgi apparatus [68], located in the cytoplasm of the host cell, close to the ER and the cell nucleus. The Golgi is responsible for the transport, modification and packaging of proteins and lipids into vesicles. Chlamydial infection induces fragmentation of the Golgi apparatus providing access to the lipid components [69]. The multivesicular bodies provide a further source of sphingomyelin and cholesterol. They can also be co-opted by *Chlamydiae* and have been shown to be important for *Chlamydiae* replication [70]. The transfer of the lipids to the inclusion involves the formation of specific ER-inclusion contact sites [71].

The *Chlamydiae* are auxotrophic for many amino acids, *C. trachomatis* being able to produce only aspartate, glycine and tryptophan. *Chlamydiae* can acquire essential amino acids through host-cell protein degradation by the lysosomes [72]. *Chlamydiae* are also auxotrophic for three of the four ribonucleoside triphosphates (adenosine triphosphate (ATP), guanosine triphosphate and uridine triphosphate (UTP)). Surprisingly, cytidine triphosphate (CTP) can be obtained from the host cell or can be produced from UTP by the bacterially-encoded CTP synthetase. The presence of this specific gene suggests that the bacterial anabolic metabolism is limited to the synthesis of molecules that the bacteria cannot get from the host in sufficient quantities [73]. In contrast, *Chlamydiae* do not import deoxyribonucleotide triphosphates from their host cells and instead use the bacterial genome-encoded ribonucleotide reductase to modify the imported ribonucleotides for DNA synthesis. The ribonucleotide reductase encoding genes are negatively controlled by the TF NrdR [74]. Overall, these bacteria-host interactions permit the acquisition of nutrients and metabolites for inclusion, for membrane stability and expansion and for bacterial proliferation.

1.5 Current *Chlamydiae* therapies

1.5.1 Conventional therapy: Antibiotics

Chlamydial infections in humans are classically treated with macrolide (usually azithromycin) and tetracycline (typically doxycycline) antibiotics [75]. Some *Chlamydiae* strains are also sensitive to penicillin-type antibiotics, which inhibit the transpeptidase that catalyses the cross-linking of peptidoglycan (PG), the final step in cell wall biosynthesis [43]. However, the existence of PG in the chlamydial cell wall has been highly debated [76-78]. The cell wall-structure of the two development forms shows notable differences. The cell wall of EBs is rigid and osmotically stable, probably due to the presence of disulfide cross-linked protein complexes in the outer membrane [79], whereas upon differentiation into RBs, the cysteine-rich proteins are depleted and the cell wall structure changes, becoming less compact and more sensitive to disruption by detergents [79]. Furthermore, treatment with penicillin G was found to prevent the differentiation of RBs into EBs, leading to the bacterial persistent form discussed above [80], and this has largely precluded its use in the clinic. Thus currently, chlamydial infections are mainly treated with azithromycin or doxycycline even though resistance of *Chlamydiae* to these two classes of antibiotics has been frequently described in the literature, and indeed *in vitro* experiments have shown that the use of sub-inhibitory concentrations of azithromycin can lead to the appearance of resistance mutations in the 23S rRNA gene [81].

Non-genetic mechanisms may also contribute to the failure of antibiotics *in vivo*. Certain environments appear to slow down the chlamydial growth thus leading to appearance of the persistent form of the bacteria, which is more resistant to antibiotic treatment [82, 83]. For example, rectal infections [84] and infection of circulating human monocytes [85], frequently give rise to appearance of the persistent form of the bacteria thus resulting in resistance to treatment and prolonged infections [86].

1.5.2 Prevention

Since antibiotic resistance is on the rise globally, prevention of bacterial infections plays an increasingly important role. *C. trachomatis* is spread through personal contact (via hands, clothes or bedding) and by disease-spreading flies that have been in contact with discharge from the eyes of an infected person. Therefore, improvements in living standards, disease awareness and in a primary health care are required. In 1998, the WHO implemented a "Global Elimination of Trachoma by 2020" program (GET 2020), based on the SAFE strategy (Surgery for entropion/trichiasis, Antibiotics for infectious trachoma, Facial cleanliness to reduce transmission, and Environmental improvements) [87]. Since the start of SAFE, chlamydial eye infections have decreased significantly in previously endemic areas [88].

In parallel, screenings of sexually active young adults for *Chlamydia* infections are performed in order to prevent sexual transmission of the bacteria. Such screenings aim at detecting infection in healthy people at risk, prior to clinical manifestation of disease. Nowadays, the annual *Chlamydia* screening for sexually active female patients at risk is highly recommended by numerous professional medical associations [89]. In the USA and Australia, *Chlamydia* screening is recommended for women up to the age of 25, and in the UK the recommendation applies to both women and men up to the same age [90]. Nevertheless, the number of cases per year in these countries is still increasing, possibly due to improved detection through wider screening programmes and the use of more sensitive tests.

1.5.3 *Chlamydia* vaccine development

A vaccine designed to protect against *C. trachomatis* genital and ocular infections is urgently needed, but despite dedicated efforts spanning many decades, no effective vaccines have yet been approved for the use in humans. Preclinical studies in animal models showed that short-lived natural immunity develops following primary infection [91], and these promising results were the starting point for a new era in vaccine development.

To ensure the safety of patients and to reduce the risk of adverse reactions, only essential, bacterial-specific antigens have been used for vaccine development [92] and much attention has focused on the *C. trachomatis* major outer membrane protein (MOMP), which is part of the chlamydial outer membrane complex (COMC) [93]. MOMP is present in all *Chlamydiae* [94, 95]. It functions as a large porin, which forms a channel through the cell membrane and could be a promising target for the development of recombinant vaccines [96]. The difficulty in using MOMP has been its complex structure [97, 98] and numerous animal studies have

failed when the denatured form of recombinant MOMP was used as antigen [99]. Nevertheless, a MOMP-based vaccine currently in phase I clinical trial makes use of a potent human-compatible cationic liposomal adjuvant (CAF01) to achieve a strong immune response [96, 100, 101]. Apart from its use in vaccine development, the MOMP can be also used for antibody-based diagnostics.

Another potential vaccine candidate in preclinical development is the complex of polymorphic membrane proteins (PMPs), also present in the COMC. A vaccine formulation containing both MOMP and PMP were shown to be antigenic in early studies on *C. trachomatis* infected mice [102]. Finally, a recent approach using live-attenuated influenza A virus as a delivery vehicle for *Chlamydia* vaccines has shown encouraging results [103]. Thus overall, despite past failures, the new programmes for vaccine development now offer promising possibilities in the fight against the growing incidence of *Chlamydia* infections worldwide.

1.6 Antibacterial drug discovery strategies

Antibiotics against *Chlamydia* and other bacteria have traditionally been discovered through cell-based screening assays, which measure inhibition of bacterial growth. Since *Chlamydia* are obligate intracellular pathogens, the cell-based screening assays against this organism rely on infection of a host cell, which complicates assay development.

Natural products constitute a vast untapped source of molecules from diverse terrestrial and marine environments [104] and have provided many new antibacterial compounds [105]. For example, a screening for novel anti-chlamydial metabolites derived from marine-microorganisms led to the isolation of pyocyanin, a known virulence factor secreted by *Pseudomonas aeruginosa* [106]. This molecule inhibits the infectivity of EBs thus reducing the number and size of chlamydial inclusions, and in addition induces production of antimicrobial intracellular reactive oxygen species [106]. Unfortunately, exposure to higher concentrations of pyocyanin showed cytotoxicity in humans with negative consequences for various tissues such as the nervous system, the vascular system and the liver [107]. Nevertheless, pyocyanin could provide a starting point for chemical optimization aimed at reducing toxicity while at the same time maintaining anti-chlamydial activity. Other recently performed screenings have revealed natural products with anti-chlamydial activity, such as an antibacterial peptide from spiders, sterols from marine sponges, and dimeric indole derivatives from marine sponge actinomycetes [108-110]. Unfortunately, natural product screening has so far failed to identify novel classes of antimicrobials [3, 111].

In addition to screening assays based on host-cell survival, more sophisticated methods exist using cell-based phenotypic screens. In such screens, the goal is to identify compounds that selectively affect a particular pathway such as the methylerythritol phosphate pathway for bacterial isoprenoid biosynthesis [112]. The precise biological target of the active compounds can then be determined in a second step.

The lack of an experimentally tractable genetic system in *Chlamydiae*, and the difficulty in introducing exogenous DNA and obtaining stable transformants [113] have further complicated working with this organism. The rigid cell wall of EBs makes them refractory to DNA uptake, and while the RBs may be less impermeable to DNA, their intracellular and intra-inclusion location makes accessibility more difficult [114]. Furthermore, the observed incompatibility when two plasmids are present in the same cell (the recombinant plasmid together with an endogenous plasmid frequently present in the *Chlamydiae*), can lead to plasmid instability over time, and can also decrease the transformation efficiency. Furthermore, the use of antibiotics to improve stability of plasmid-encoded resistance markers

is restricted by U.S. Centers for Disease Control and Prevention guidelines [114, 115], and only a limited range of commonly antibiotics such as tetracycline and erythromycin are permitted for clinical treatment regimens.

A third approach to antibacterial screening, which does not rely on a cell-based assay, is an *in-vitro* target-based screen. Such screens have been made possible through a combination of whole genome-based bioinformatics, which has identified hitherto unknown targets [116] together with high-throughput procedures for chemical synthesis. While this targeted approach has great potential for drug discovery, it has failed thus far to discover new antibacterial drugs. This is partly through the inability of many active molecules to enter the bacterial cell [117], or having done so, to escape the efflux pathways; and partly through the propensity of such molecules to select for resistant mutations in the target gene [118].

1.7 *Waddlia chondrophila* as a model organism of *Chlamydiae*

Described as a bacterium causing abortion in ruminants, and with some documented cases of miscarriage in women, *W. chondrophila* is especially interesting as a model of chlamydial pathogenesis. In addition, it has been linked to rare cases of respiratory infections [119, 120]. *W. chondrophila* was first isolated from tissues of an aborted bovine fetus in 1986 at the Washington Animal Disease Diagnostic Laboratory, and the acronym WADDL gave rise to the name of this organism [29, 121].

W. chondrophila has a *Chlamydia*-specific biphasic development cycle with a fast replication time, consisting of early-cycle (0-8 h), mid-cycle (8-24 h) and late-cycle (24+ h) [122]. In contrast to other members of the phylum *Chlamydiae*, *W. chondrophila* has a broad host range, replicating within various species of amoeba and human macrophages, as well as in diverse human cell lines (e.g. human A549 pneumocytes, human Ishikawa endometrial cells) and primate Vero kidney cells (epithelial kidney cells from *Cercopithecus aethiops)* [123, 124]. Its natural hosts and main reservoir are most likely the amoebae [40], and experiments with amoebae have allowed its pathogenic potential to be assessed without the need to work with infected mammalian cells [125]. Growth *in vitro* can be inhibited with azithromycin and doxycycline [121, 126] and these two compounds represent the most common treatments for chlamydial infections in human. Interestingly, EBs of *W. chondrophila* (600 nm) are around twice the size of those in *C. trachomatis*, which has proved useful in studying the precise subcellular localization of proteins in this model organism [126, 127].

Apart from morphological differences, the mode of interaction with the host cell also differs between *W. chondrophila* and other members of the phylum. In *W. chondrophila,* host cell

mitochondria, lipid droplets and ER are recruited to the inclusions, possibly providing ATP and lipids for bacterial intracellular replication and their rapid growth cycle [45, 128, 129]. Curiously, the 2.1 Mb genome of *W. chondrophila* is around twice that of other members of the *Chlamydiaceae* [33] and encodes around twice as many proteins. This reflects the higher capacity of this strain for biosynthesis of nucleotides and amino-acids, Indeed, *W. chondrophila* possesses genes to produce at least seven more amino acids (alanine, asparagine, aspartate, cysteine, glutamate, glutamine, glycine, proline, serine, threonine, methionine) than *C. trachomatis* [57], and this greater autonomy may provide the basis for its higher growth rate and broader host range [57]. Despite these differences, similarities in the regulation of gene expression are observed. Comparison of the TFs between *W. chondrophila* and *C. trachomatis* reveals 20 and 13 annotated TFs, respectively, with 10 TFs common to both strains (Figure 1.3). The latter were also found in most other members of the phylum *Chlamydiae* and have been described as playing an important role in the regulation of genes required for the chlamydial developmental cycle [122].

		C. trachomatis D/UW-3/Cx	*W. chondrophila* WSU	Description
Transcription factors	*atoC*			Sigma-54 interaction
	chxR			OmpR/PhoB-type
	dcrA			Divalent cation-dependent regulator A
	dksA			DksA C4-type
	euo			Early upstream open reading frame
	fmdB			Putative regulatory protein, FmdB, Zinc ribbon domain
	fur			Ferric uptake regulator protein
	grgA			Putative transcriptional regulator
	hrcA			Heat-inducible transcription repressor HrcA
	lexA			LexA repressor
	nrdR			Transcriptional repressor NrdR
	pc1472			Putative transcriptional regulator
	phoU			Putitive phosphate transport regulator
	pUV_18090			Putative transcriptional regulator
	sNE_A03110			Putative transcriptional regulator
	trpR			Trp operon repressor
	wcw_0478			Putative HTH-type transcriptional repressor
	wcw_0617			Translational regulator CsrA
	wcw_p0015			Putative transcriptional regulator
	wHTH			WHTH_DNA-bd_dom
	ybjN			Putative sensory transduction regulator
	yebC			Probable transcriptional regulatory protein
	ytgR			Probable metal transport system membrane protein CT_069
	Total TFs present	13	20	

Figure 1.3. TF genes present or absent in *C. trachomatis* and *W. chondrophila*.
The presence (green) or absence (red) of genes encoding TFs in the genomes of *C. trachomatis* and *W. chondrophila* is shown (adapted from Domman and Horn [41]). Descriptions of the encoded proteins are derived from the annotated UniProt database [130].

1.8 Antibacterial target identification strategies

A major bottleneck in antibacterial drug discovery remains the target identification. In general, antibacterial drugs target are cell wall synthesis, membrane function, bacterial ribosomes or specific metabolic pathways such as folic acid synthesis or DNA/RNA synthesis. Approximately 130 antibiotics are currently marketed, while the number of antibacterial targets is estimated to be only about 40 [131]. This relatively small number of targets is due to the fact that the antibiotic discoveries were based on the classical cell-based screening assays, in which the inherent difficulty is understanding the mechanism of action of the 'hit' compound. The specific targets in such screens are mostly unknown and need to be determined using biochemical and molecular biology methods in a second step.

Based on genomic sequence data, it has been estimated that less than 0.1% of possible therapeutic targets are currently exploited [132], suggesting that there is still a vast unexplored potential for novel antibiotics. Therefore improved, more effective strategies for target identification based on genomic, proteomic or metabolomic approaches, are needed (Figure 1.4). These 'OMIC' approaches can provide a more comprehensive understanding of the biological processes under investigation, and thus may lead to more effective screens for discovery of new targets and drugs.

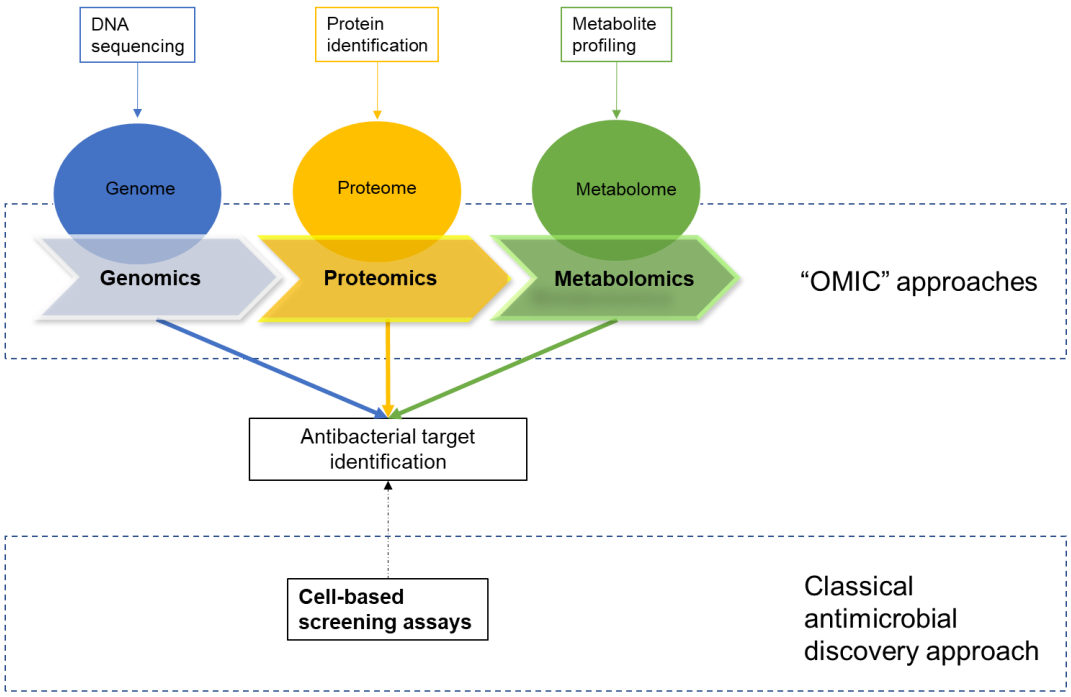

Figure 1.4. Approaches for novel antibacterial target identification.
Strategies for the determination of antibacterial targets based on the three OMIC approaches, genomic, proteomic and metabolomic, and on the classical antimicrobial discovery approach, the cell-based screening assays, whereby a compound is selected for its antibacterial activity, and the target is determined in a second step by biochemical and molecular biology methods.

1.8.1 Genomic approach

The modern era of molecular genetic analysis of bacterial genomes started with the sequencing of the entire *Haemophilus influenzae* genome in 1995 [133]. Since then, the sequences of many other bacterial genomes have been determined. By 1997, 11 complete genome sequences were published; by 1998, the complete genome of *C. trachomatis* had been determined [37] and today, fully annotated genomes of over 100 microorganisms are available in public databases [134, 135]. This has facilitated the search for bacteria-specific functions and targets, and has opened the way to rich new possibilities for antibacterial drug discovery [3]. The development of homology-based bioinformatic tools such as basic local alignment search tool (BLAST) [136] and FASTA [137] allow identification of sequences that are specific to medically important pathogens, while at the same time, enabling exclusion of those genes which show strong homology to their human orthologues, and which consequently may lead to off-target effects in the clinic. Therefore, by combining recent methodologies, proteins specific to pathogens can be selected as targets, with priority given to those which are essential for bacterial viability [138].

Recently, a bioinformatics analysis of the *C. trachomatis* genome identified a number of hypothetical proteins with potential as novel drug targets [139]. Hypothetical proteins are those, which can be predicted based on nucleic acid sequence data but whose existence has not been demonstrated experimentally and whose function is unknown [140]. Using this approach, Turab *et al*. identified 269 hypothetical proteins in *C. trachomatis* and were able to assign functions to 89 of them, including enzymes, transporters and proteins involved in biosynthesis and regulatory processes. While the genomic approach may identify new potential drug targets involved in bacterial virulence or their mechanism of pathogenesis [139], there are nevertheless limitations to this approach: insensitivity to an inhibitor could result from functional redundancy of non homologous gene products [141]; some important target structures such outer membranes and proteoglycans are not defined by discrete gene products. Therefore, these structures and the pathways involved in their generation are more amenable to whole-cell phenotypic screening strategies [142]. Although the genome contains all the protein coding information, sequence analysis alone cannot directly predict the total proteome that an organism is capable of generating in specific physiological states. Therefore proteomics, or global protein analysis, provides an additional valuable approach to identify novel drug targets.

1.8.2 Proteomic approach

The proteome is defined by the complete set of proteins that an organism produces in different environments and under various growth conditions [143]. In contrast to the analysis of the genome, it provides a more dynamic assessment of gene expression. Early attempts to study the effects of different environments and external stress factors on the bacterial proteome employed high resolution two-dimensional polyacrylamide gel electrophoresis (2D-PAGE) [144-146]. Typically, protein separation was based on differences in isoelectric point in the first dimension and molecular weight of the fully denatured protein in the second dimension. Furthermore in such gels, certain post-translational modifications can also be identified using radioactive labelling of antibody based procedures [147]. A catalogue of proteins describing protein expression levels under a given set of circumstances, such as during different phases of a disease, can be established with 2D-PAGE. Today, many 2D-PAGE-based protein maps are available, including those of *C. pneumoniae* and *C. trachomatis* [148, 149].

In addition, 2D-PAGE can be combined with mass spectrometry (MS) procedures such as matrix-assisted laser-desorption-ionization (MALD)–time-of-flight MS capable of identifying individual silver-stained proteins extracted from the 2D-gel [150]. Ideally, an individual protein sequence can then be linked to the corresponding open reading frame in the bacterial genome, and the protein can be characterized by classical molecular biology and biochemical methods.

The main disadvantages of 2D-PAGE for proteomics is that not all proteins are well separated in 2D-gels, and low abundance proteins may not be detectable even with sensitive staining methods [151]. On the other hand, proteomics based on 2D gels can lead to the discovery of subsets of expressed proteins, known as “proteomic signatures”, which can be characteristic for a particular physiological state [152], and can be crucial for bacterial survival, making them interesting as potential antibacterial targets [151]. Using the latter approach, the different expression levels of *C. pneumoniae* proteins at several stages of the infection cycle, between acute and persistent infection, and in the extracellular EB have been characterized [149, 153, 154]. This has led to the identification of new antigens for anti-chlamydial vaccines. It also led to the identification of chlamydial effector proteins, including the protease-like activity factor (CPAF) conserved in all *Chlamydiae* [155, 156]. CPAF is a major chlamydial virulence factor, which is secreted into the cytoplasm during the acute infection of the host cell and acts as an atypical serine protease by cleaving and degrading specific host proteins [157-159]. To date, at least 16 host substrates have been reported, making CPAF an interesting potential therapeutic target [160].

1.8.3 Metabolomic approach

Metabolites are generally though to include all low molecular weight components, typically less than 1500 Da, present in a biological system. Metabolomics aims at the identification and quantification of all possible metabolites present in a given set of experimental conditions [161]. Such changes can occur in response to physiological or pathological stimuli or as a result of genetic modifications [162]. It can be considered as the metabolic complement of functional genomics, since it allows the detection of biochemical reaction intermediates, which are characteristic of different cellular pathways [163, 164]. Nowadays, metabolomics is widely used in drug discovery for the identification of disease or toxicity biomarkers, and in understanding drug mode-of-action through changes in cellular metabolism [165, 166].

Metabolomics can be further subdivided according to the class of metabolites analyzed, such as glycomics (the study of sugars) and lipidomics (the study of lipids), for example, and two alternative approaches exist, known as targeted and untargeted metabolomics. The former focuses on the identification and quantification of specific metabolites (or metabolic classes) with known chemical properties and the advantage of this approach is that the sample preparation can be tailored to select only those classes of compounds, which are relevant to the investigation [167]. The second approach aims to measure all the metabolites present in a given biological system using nuclear magnetic resonance (NMR) and MS-based techniques [161]. The untargeted profiling strategy is especially applicable in the search for new biomarkers. Full coverage of the entire metabolome is not possible using only one single technique [168] due to the wide difference in concentrations of the intracellular metabolites, and the huge diversity of chemical structures and properties. Therefore, complete qualification and quantification of a metabolome requires a combination of various protocols based on both MS and NMR analyses. MS is used either as stand-alone procedure or coupled to separation techniques, such as gas chromatography (GC–MS), liquid chromatography (LC–MS), or capillary electrophoresis (CE–MS) [169]. The choice of analytical platform is determined by the physico-chemical properties of the metabolite(s) and the complexity of the sample to be investigated. The CE–MS technique is mostly seen as complementary to LC–MS and GC–MS, and it is especially suitable for the detection of charged metabolites [170]. The second leading analytical approach used in metabolomics is NMR spectroscopy. NMR has the advantage of being non-destructive and highly reproducible, and where possible, it is the method of choice in elucidating structures of unknown metabolites. The major drawback of NMR is its lower sensitivity compared to MS. The two approaches used in combination can each contribute valuable complementary information.

In medical microbiology, various MS-based metabolomic applications exist, including diagnosis of infections [171] or in investigating the mechanism of action of a given antibacterial compound [172]. In microbiology research, MS-based metabolomics has been applied in the metabolite flux analysis, and elucidation of gene and enzyme function. In industrial fermentation it has been used to monitor the production of specific metabolites [173] such as antibiotics. Since metabolic intermediates reflect the activity of enzymatic pathways and networks, it can also provide information about the physiological state of the cell and the effects of microbial interactions [174]. Such a metabolomic approach was applied in a recent study on the development cycle of *C. pneumoniae* in HEp-2 cells to investigate time dependent activation of different pathways during the replicative phase of the development cycle, resulting in the detection of some unique metabolites in infected cell extracts [175]. Such key metabolites for a specific bacterial state, also known as biomarkers can then be further used for drug target or diagnostic research. Thus, metabolomics offers a valuable approach for elucidating the chemical response of bacteria during the developmental cycle or following changes in the environmental conditions.

1.9 Aims of the thesis

(i) To develop a screening method for measuring the activity of selected, chlamydial TFs in a heterologous host (*E. coli*), and to use this method to screen a collection of plant extracts and natural products for molecules capable of interfering with TF DNA-binding activity.

(ii) To evaluate the function of the chlamydial TF, DksA by genetic complementation of the DksA mutant strains of *E. coli* and *P. aeruginosa*, with the subsequent aim of developing a screening for DksA inhibitors.

(iii) To highlight changes in the intracellular development cycle of *W. chondrophila* using a metabolomic approach in order to identify potential biomarker candidates for drug target research.

Chapter 2: Development of a method to screen plant extracts and natural products for inhibitors of developmentally important TFs from *W. chondrophila*

2.1 Introduction

Chlamydiae is a group of bacteria responsible for multiple human diseases worldwide [176, 177]. While chlamydial infections can be treated with antibiotics, which interfere with protein or nucleic acid synthesis in the metabolically active chlamydial RBs, such treatments fail to affect the metabolically inactive forms including the EBs and the viable persistent form [178-180]. This often results in prolonged therapy, which is costly and frequently leads to the development of drug resistance [181]. Thus, there is a current need to investigate new approaches and to develop novel anti-chlamydial agents [182, 183].

Natural products are more diverse, and generally more complex than experimentally-derived synthetic and combinatorial molecules. They have a higher hit rate in high throughput screening (HTS) campaigns [184] and they have contributed greatly to the history of the antibiotic drug discovery [185-187]. From 1981−2014, 140 NCEs have been approved by the FDA for the medical indication of bacterial infection. Of these, 59% were either natural products, or their derivatives, isolated from microorganisms [188]. In addition, a recent review by Chandra *et al.* [189] has highlighted the potential of plant-based molecules to combat the increasingly widespread resistance to current antimicrobials.

Plant-derived polyphenolic compounds, initially identified as antioxidants for use in the treatment of cardiovascular diseases, were also found to exhibit anti-chlamydial activity [105], and catechins, another group of polyphenolic compounds, showed *in vitro* inhibitory effects on the proliferation of *C. trachomatis* and *C. pneumoniae* [190]. In addition, the secondary plant metabolite resveratrol (3,5,4′-trihydroxystilbene), which belongs to the class of polyphenolic compounds called stilbenes, was recently shown to exhibit dose-dependent inhibition of chlamydial growth in a mouse fibroblast cell line [191]. Resveratrol is found in grape skin [192], and was first isolated by Takaoka in 1940 from the roots of white hellebore (*Veratrum grandiflorum* O. Loes.) [193]. Indeed, this polyphenolic compound is now known to be present in over 100 medicinal and edible plants. Apart from its antioxidant and cardioprotective properties, it has been reported to exhibit antibacterial activity against several Gram-positive and Gram-negative bacteria [194]. In another class of plant-derived compounds, the flavonoids, luteolin was shown to reduce inflammation and bacterial load *in vivo* following acute infection of mice with *C. pneumoniae* [195], although another flavonoid quercetin, which was shown to be effective in eradicating *C. pneumoniae* in HL cell cultures [196], had no effect in the mouse model described above.

The chlamydial developmental cycle requires the temporal expression of stage-specific genes, which are tightly regulated by TFs [197, 198]. Of these, four TFs NrdR, HrcA, PhoB, and Euo

are conserved among most members of the phylum *Chlamydiae* and belong to the so called "core set" of TFs [122]. NrdR controls the expression of genes involved in DNA synthesis and repair [74]; the heat-sensitive HrcA regulates expression of heat shock genes during stressful conditions [199, 200]; PhoB, a member of the PhoB-superfamily, regulates the bacterial phosphate response and is involved in bacterial survival [122, 201]; and the early upstream open reading frame (Euo) acts as a master TF, targeting the promoters of more than 100 late genes during the development cycle [202]. Euo was found to be expressed early in chlamydial replication cycle, when the EB to RB transition takes place, and it was also found to be present in the persistent form [122, 203, 204]. Euo was first described as a protease specific for the chlamydial H1-like histone Hc1 [205], although no evidence for the degradation of Hc1 protein was found using His-tagged Euo preparations with extracts of *C. psittaci* [203]. Since all of the TFs mentioned above are highly conserved among the *Chlamydiae* and are important in the regulation of bacterial growth, they could provide excellent targets for novel anti-chlamydial drugs [206].

Currently, tests of growth inhibition during chlamydial infection are performed in eukaryotic cells at 24 to 72 h p.i., which is costly and time-consuming [207, 208]. Since *Chlamydiae* are obligate intracellular pathogens and genetic manipulation is complicated, an approach using a heterologous *E. coli*-based system was initiated to screen for molecules able to inhibit TFs.

E. coli are genetically tractable organisms and gene expression studies based on gene fusions are frequently performed in these bacteria [209]. To facilitate these studies, a wide choice of reporter systems is available. The early gene regulation studies were based on expression of *β*-galactosidase, an enzyme encoded by the bacterial *lacZ* gene, and for which, in 1972, Miller developed a colorimetric assay using the substrate *o*-nitrophenyl *β*-D-galactopyranoside (ONPG) [210]. Subsequently, numerous other *β*-galactosidase substrates have been developed mostly for use in liquid media, such as the fluorescent substrates 4-methylumbelliferyl-*β*-D-glucuronide (MUG) and the 9H-(1,3-dichloro-9,9-dimethylacridin-2-one-7-yl) *β*-D-galactopyranoside (DDAOG) [211-213]. For experiments on solid media, the chromogenic substrate, 5-bromo-4-chloro-3-indolyl *β*-D-galactopyranoside (X-Gal) [214, 215], which develops a blue coloration upon cleavage by *β*-galactosidase is most frequently used.

In addition to *lacZ*, other reporter systems have been developed, such as the *neomycin phosphotransferase II* (*npt-II*) gene, which confers resistance to the aminoglycosides neomycin and kanamycin (Kan) [216, 217], and the *luxAB* gene, which catalyses light emission in the presence of long-chain aliphatic aldehydes [218]. The light-producing enzyme luciferase, which is found naturally in fireflies and in luminous marine and terrestrial microorganisms is also commonly used as a reporter gene to detect gene activity and is often

used in eukaryotic cells [219]. These reporter systems and numerous others provide a wide choice of readouts for development of transcription-based screening methods [220].

Here, the objective was to develop a screening assay in *E. coli* for inhibitors of *Chlamydiae* TFs, by co-expressing a plasmid encoding the TF with a second reporter plasmid containing the TF DNA binding motif fused to a reporter gene. The TFs chosen for this study are all repressors of gene transcription required during the *W. chondrophila* development cycle. The goal was to optimise the method to screen for TF inhibitors in a collection of plant extracts and natural products. The prediction was that successful candidates would interfere with the chlamydial development cycle and thus would reduce the infectious yield in the clinical setting.

2.2 Materials and Methods

2.2.1 Chemicals

Standard chemicals were obtained from Fluka Chemie AG, Buchs, Switzerland or Merck KGaA, Darmstadt, Germany.

2.2.2 Bacterial strains, plasmids and growth conditions

E. coli Top10 cells were routinely grown at 37°C in liquid Luria-Bertani (LB) medium or on LBA plates (LB containing 1.5% (w/v) agar) (both from US Biological, Salem, MA, USA). For stable plasmid maintenance, antibiotics (all purchased from AppliChem GmbH, Darmstadt, Germany) were added to media at the following final concentrations: gentamicin 10 µg/mL (Gm10), tetracycline 10 µg/mL (Tet10), chloramphenicol 20 µg/mL (CM20) and ampicillin 100 µg/mL (Amp100). The bacterial strain and the plasmids used are listed in Table 2.1. Plasmids were introduced into competent *E. coli* strains by heat-shock at 42°C for 2 min, allowed to recover for 1h at 37°C in LB without antibiotic then transferred to LBA plates with the appropriate antibiotics at 37°C overnight [221].

Table 2.1. Bacterial strains and plasmids.

Strains and plasmids	Relevant characteristics	Source
E. coli		
Top10	F-*mcrA* Δ(*mrr-hsd*RMS-*mcr*BC) Φ80*lacZ* ΔM15 Δ*lac*X74 *rec*A1 *ara*D139 Δ(*araleu*)7697 *gal*U *gal*K *rps*L (Str^R) *end*A1*nup*G	*
Plasmids		
pJGZ290	p290lacZ, Tet^r	[222]
pKT25	Kan^r	[223]
pUG3.1-lacI	*lacI*, CM^r	gift from P. Viollier
pMA-RQ	T5-lacO, Amp^r	gift from P. Viollier
pJAMA8	*luxAB* based promoter-probe vector, Ap^r	[224]
pBAD-Euo	*W. chondrophila euo* on pBAD, Amp^r	[122]
pJGZ290prhs9_lacZ	DBM *rhs9* on p290lacZ, Tet^r	[122]
pwcw1705_lacZ	DBM *wcw1705* on p290lacZ, Tet^r	[122]
pHrcA_lacZ	DBM *hrcA* on p290lacZ, Tet^r	[122]
pPhoB_lacZ	DBM *phoB* on p290lacZ, Tet^r	[122]
pNrdR_triple_consensus_lacZ	DBM *nrdR* on p290lacZ, Tet^r	gift from P. Viollier
pJGZ290_Kan^r	*kan^r* on pJGZ290, Tet^r and Kan^r	this study
pJGZ290lacO_lacZ	*placO* on pJGZ290, Tet^r	this study
pJGZ290lacO_Kan^r	*placO* on pJGZ290_Kan^r, Tet^r	this study
pJGZ290_luxAB	*luxAB* on pJGZ290, Tet^r	this study

pJGZ290lacO_LuxAB	*placO* on pJGZ290_luxAB, Tet^r	this study
pMT335-NrdR	*W. chondrophila nrdR* on pMT335, Gm^r	gift from P. Viollier
pMT335-HrcA	*W. chondrophila hrcA* on pMT335, Gm^r	gift from P. Viollier
pMT335-PhoB	*W. chondrophila phoB* on pMT335, Gm^r	gift from P. Viollier
pSRK	IPTG-inducible lac promoter, Gm^r	[225]
pSRK-NrdR	IPTG-inducible *nrdR*, Gm^r	this study
pSRK-HrcA	IPTG-inducible *hrcA*, Gm^r	this study
pSRK-PhoB	IPTG-inducible *phoB*, Gm^r	this study
pSRK-Euo	IPTG-inducible *euo*, Gm^r	[122]

*Thermo Fisher Scientific, Waltham, MA, USA.
Abbreviations of antibiotics: Kan: kanamycin; Gm: gentamicin; Amp: ampicillin; Tet: tetracycline; CM: chloramphenicol.
IPTG: isopropyl *β*-D-1-thiogalactopyranoside; DBM: DNA binding motif.

Table 2.2. Primers used for Sanger DNA sequence analysis and *Kan^r* cloning.

Primers	Gene	Sequences (5'-3')	Purpose
Lac290 up		TGACGGCTATCACCATCAT	Sequencing
M13-20 down		GTAAAACGACGGCCAGT	
HindIII-Kan^r up	*Kan^r*	gccAAGCTTTGATGGCAGGTTGGGCGTCG	Cloning
Pst1-Kan^r down	*Kan^r*	gccCTGCAGGACAGGATGAGGATCGTTTC	

The restriction sites are underlined.

Table 2.3. Promoters sequences.

Promoter name	Sequences (5'-3')
placO	AATTGTGAGCGGATAACAATTACGAGCTTCATGCACAGTGAAATCATGAA AAATTTATTTGCTTTGTGAGCGGATAACAATTATAATATGTGGAATTGTGA GCGCTCACAATTCCACA
NrdR_triple_consensus_lacZ	GGATCCAATTGTGAGCGGATAACAATTACGAGCTTCATGCACAGTGAAA TCATGAAAAATTTATTTGCTTTGTGAGCGGATAACAATTATAATATGTGG ACTTCTCATCCGAAGCTGGCAAAAGGGATTTCGGATAAACAAGTTGGGA AGCAGCGAAAAGTAGGTGATTTTACTCACCCTTCGAAGACTCCAAAAGG AGTGCGATTA
Promoter name	**DNA binding motif sequences (5'-3')**
prhs9	GTAAAGTTTGCATTT
pwcw1705	TTTAGGCTAACCATG
pHrcA	TAGCAAATAGCTTTGTTGAGTGCTAA
pPhoB	CACGCGGGAAATGTTAAGTTT

The T5 promoter sequence is underlined.

2.2.3 DNA manipulation and cloning procedures

Restriction enzymes, T4 DNA ligase, calf intestinal alkaline phosphatase and *Pfu* DNA polymerase (Promega Corporation, Madison, WI, USA) or (New England Biolabs, Ipswich, MA, USA). Standard protocols for DNA modification and cloning were followed [221]. For plasmid purification, the GenElute™ plasmid miniprep kit (Sigma-Aldrich, Buchs, Switzerland), was used according to the supplier's instructions. All plasmid inserts were verified by Sanger DNA sequencing (Fasteris SA, Geneva, Switzerland) using the standard primers Lac290-up and M13-20-down (Table 2.2).

Promoter sequences:

Promoter sequences for the *lacO* operator, NrdR_triple_consensus_lacZ, pHrcA, pPhoB, prhs9 and pwcw1705 were designed by Prof. Viollier from the Department of Microbiology and Molecular Medicine of the University of Geneva and synthesized by Life Technologies™, Carlsbad, CA, USA (Table 2.3).

Plasmid constructs:

pJGZ290lacO_lacZ: The *lacO* region of plasmid pMA-RQ was excised by digestion with *EcoRI* and *BamHI* and inserted into the corresponding sites of pJGZ290 (Table 2.1).

pJGZ290lacO_Kan^r: The *Kan^r* gene (794 bp) was amplified from pKT25 using the primers HindIII-Kan^r-up and Pst1-Kan^r-down (Table 2.2), restriction digested and inserted into the HindIII and PstI sites of pJGZ290 (pJGZ290_Kan^r) (Table 2.1). The lacO region was then excised from plasmids pMA-RQ by digestion with *EcoRI* and *BamHI* and inserted into the corresponding sites of pJGZ290_Kan^r (Table 2.1).

pJGZ290lacO_LuxAB: To obtain the LuxAB coding sequence (2061 bp), plasmid pJAMA8 was digested with *BamHI,* flush ended using the Klenow enzyme and digested with *XbaI.* LuxAB was inserted into the *XbaI* and *HpaI* sites of the vector pJGZ290lacO (Table 2.1).

TFs *NrdR, HrcA* and *PhoB:* The pSRK vector containing an isopropyl *β*-D-1-thiogalactopyranoside (IPTG)-inducible *lac* promoter (Table 2.1) was used to express TFs NrdR, HrcA and PhoB. The sequences were excised from pMT335-NrdR, pMT335-HrcA and pMT335-PhoB (Table 2.1) using *NdeI* and *SacI*, and cloned into pSRK cleaved using the same enzymes. The resulting plasmids pSRK-NrdR, pSRK-HrcA and pSRK-PhoB (Table 2.1) were verified by digestion with *NdeI* and *SacI* followed by gel electrophoresis on a 1.5% (w/v) agarose gel (MP Biomedicals, Santa Ana, CA, USA) containing 1x UltraPure™ TBE buffer (Thermo Fisher Scientific).

Co-transformation of E. coli:

Reporter plasmids, pJGZ290lacO_lacZ, pJGZ290lacO_Kan^r or pJGZ290lacO_LuxAB were co-transformed with plasmid pUG3.1 containing *lacI* as described above. Clones were selected on solid medium containing the appropriate selection antibiotics. Similarly, plasmids pSRK-NrdR, pSRK-HrcA or pSRK-PhoB were co-transformed with reporter plasmids pNrdR_triple_consensus_lacZ, pHrcA_lacZ or pPhoB_lacZ (Table 2.1).

2.2.4 Reporter assays

2.2.4.1 Kan reporter assay by minimum inhibitory concentration (MIC)

Kan activity tests were performed in 96 well culture plates (Corning Incorporated, Corning, NY, USA) following previously described protocols [226, 227]. Briefly, *E. coli* transformed with the plasmids pJGZ290lacO_Kan^R and pUG3.1-lacI were inoculated into 0.9% (w/v) NaCl with or without 1 mM IPTG at a density matching the 0.5 McFarland turbidity standard from bioMérieux® SA, Marcy l'Etoile, France, (~150×10^6 CFU·mL^{-1}). Kan was tested at increasing concentrations as specified. To follow bacterial growth, the redox sensitive colorimetric dye, iodonitrotetrazolium chloride (INT) (Sigma-Aldrich) in dH_2O was filter sterilised and added to each well at a final concentration of 0.2 mg/mL. Plates were incubated at 37°C for 24 h. The first clear well of the dilution series was noted as the MIC for Kan.

2.2.4.2 Kan reporter assay by antibiogram

Agar disk-diffusion testing was performed using the protocol described elsewhere [228]. Briefly, freshly growing *E. coli* containing plasmids pJGZ290lacO_Kan^R and pUG3.1-lacI were inoculated into 1 mL 0.9% (w/v) NaCl to a density corresponding to 0.5 McFarland turbidity standard (~150 × 10^6 CFU·mL^{-1}) and the inoculum was spread uniformly over the entire surface of LBA plates either with or without 1 mM IPTG. Sterile discs (bioMérieux® SA) were placed on the agar and different concentrations of Kan were added to each disc. Plates were incubated for 24 h at 37°C, and the diameters of growth inhibition zones were measured.

2.2.4.3 LuxAB reporter-based assay

For *luxAB* activity measurements, a previously described protocol [218] was adapted as follows. *E. coli* cells transformed with pJGZ290lacO_LuxAB and pUG3.1-lacI were grown overnight in LB containing the appropriate antibiotics, then diluted in the same medium to an optical density (OD) of 0.05 at a wavelength of 600 nm. Tubes containing 973 µL of selection medium were prepared, equilibrated to 37°C, and 17 µL of the diluted culture was added. The tubes were incubated at 37°C for 30 min on a shaker at 260 rpm. Expression of *luxAB* was induced by addition of 1 mM IPTG and incubation was continued for 3 h at 37°C, 260 rpm. To measure *luxAB* activity, 200 µL of bacterial suspension was transferred to the wells of a white polystyrene 96-well plate (Nunc™) (Thermo Fisher Scientific) and the reaction was started by addition of 2 mM *n*-decanal in EtOH:dH_2O (1:1). After 3 min of incubation, *luxAB* activity was measured over 10 s in a BioTek® Synergy 2 plate reader (Gain: 150) using Gen5 Software 2.04.11 (BioTek® Instruments Inc., Winooski, VT, USA). Z-factors were calculated using the following formula [229]:

$$\text{Z-factor} = 1 - \frac{3 * \text{SD}(\text{IPTG}^+) + 3 * \text{SD}(\text{IPTG}^-)}{\text{Mean}(\text{IPTG}^+) - \text{Mean}(\text{IPTG}^-)}$$

IPTG$^-$, reporter activity in absence of IPTG.
IPTG$^+$, reporter activity in presence of IPTG.
SD, standard deviation.

2.2.4.4 Measurement of LacZ reporter gene activity using X-Gal

E. coli transformed with pJGZ290lacO_lacZ and pUG3.1-lacI were spread on LBA plate containing 40 µg/mL (X-Gal, AppliChem) with or without 1 mM IPTG and incubated for 24 h at 37°C.

2.2.4.5 Measurement of LacZ reporter gene activity using ONPG

LacZ activity was measured according to the protocol described by Miller [210].

LacZ activity measurement of LacI: Overnight cultures of *E. coli* transformed with pJGZ290lacO_lacZ and pUG3.1-lacI were diluted to an OD_{600} of 0.05 in LB containing appropriate antibiotics. To induce *lacZ* expression, IPTG was added to a final concentration of 1 mM and incubation was continued for 3 h at 37°C, 260 rpm. The OD_{600} measurement of each culture was recorded.100 µL aliquots of cells were lysed in 700 µL Z-Buffer containing 50 mM *β*-ME (Sigma-Aldrich). Z-buffer was prepared as follows: 60 mM Na_2HPO_4, 40 mM NaH_2PO_4, 10 mM KCl and 1 mM $MgSO_4$, pH 7.0 and sterilized by autoclaving at 121°C for 15 min. A tube containing Z-buffer only was used as a blank. Ten µL of 0.1% (v/v) SDS (AppliChem), and 20 µL of chloroform were added to each tube and the mixtures were vortexed for 10 s at maximum speed. Tubes were incubated at 28°C for 5 min. To start the reaction, 200 µL of ONPG (Fluka Chemie) solution in Z-buffer containing *β*-ME was added to each tube and vortexed. The time taken for each tube to reach a pale-yellow colour was recorded. Reactions were stopped by addition of 500 µL of 1 M Na_2CO_3 and transferred to ice. Tubes were centrifuged at maximum speed (14000 rpm) for 5 min and OD_{420} was recorded. LacZ activity (Miller units) was calculated according to the equation:

$$\text{LacZ activity (Miller Units)} = \frac{1000 * OD_{420}}{(OD_{600} * t * V)}$$

Time (t) calculated in min and volume (V) in mL.
OD_{420}: Optical density measured at 420 nm.
OD_{600}: Optical density measured at 600 nm.

LacZ activity measurement of TFs: Overnight cultures of *E. coli* co-transformed with each of the pSRK-TF plasmids together with the corresponding pJGZ290_lacZ plasmid in which lacZ expression is under control of the TF DNA binding motif, were diluted 1:50 in LB supplemented with the appropriate antibiotics, and incubated at 37°C, 260 rpm until an OD_{600} of 0.5-0.8. Cultures were induced with 1 mM IPTG for 3 h at 37°C, 260 rpm and LacZ activity was measured as described above using the ONPG substrate.

2.2.4.6 Measurement of LacZ reporter gene activity using ONPG in 96-well plate format

Overnight cultures of *E. coli* co-transformed with pJGZ290prhs9_lacZ and pSRK-Euo, and with pJGZ290prhs9_lacZ and pSRK as a control, were diluted 1:50 with LB and incubated at 37°C, 260 rpm to an OD_{600} of 0.5-0.8. Cultures were induced with 1 mM IPTG and 190 µL aliquots were dispensed immediately into the wells of a 96-well plate. Plant extracts were added to cultures at a final concentration of 40 µg/mL and incubated for 3 h at 37°C, 260 rpm. Final values for OD_{600}, OD_{420} and OD_{550} were recorded in a plate reader. (Since plates were not centrifuged, light scattering was estimated as $OD_{550} \times 1.75$ and was subtracted from the reading at 420 nm). LacZ activity measurement was performed according to Griffith and Richard [230], and Miller units were calculated as described by Miller [210]. Briefly, 100 µL aliquots of the cell suspension were permeabilized in DeepWell™ 96-well plates (Nunc™) (Thermo Fisher Scientific) containing 1 mL Z-Buffer, 20 µL of 0.1% (v/v) SDS and 40 µL chloroform. Lysates were mixed by pipetting up and down 20 times. To measure LacZ activity, 20 µL of 4 mg/mL ONPG (in Z-buffer containing 0.27% (v/v) β-ME) was added and incubated for 10 min. Reactions were terminated by addition of 50 µL of 1 M Na_2CO_3.

For subsequent high throughput screening applications, alternative methods for cell lysis were investigated due to the incompatibility of using chloroform in standard 96-well plates. The following reagents were tested according to the suppliers' instructions: PopCulture® reagent (Sigma-Aldrich) 1% (v/v) rLysozyme 40 U/µL (Sigma-Aldrich), B-PER® reagent (Thermo Fisher Scientific), CelLytic™ express (Sigma-Aldrich), FastBreak™ reagent solution 10x (Promega) and Cell Culture Lysis reagent 5x (Promega). For high throughput assays the FastBreak™ reagent was selected.

2.2.5 Western blot

Buffers, solutions and reagents for Western blotting were prepared as previously described [221].

For NrdR, HrcA and PhoB analysis, overnight cultures of *E. coli,* transformed with pSRK-NrdR, pSRK-HrcA, pSRK-PhoB or the empty vector pSRK, were diluted to an OD_{600} of 0.05 with LB containing gentamicin, and incubated with 0, 0.1 or 1 mM IPTG at 37°C, 260 rpm for 3 h. The OD_{600} was recorded and 1 mL of each culture was centrifuged at maximal speed to pellet the cells. Cell pellets were resuspended in 2x sample buffer to obtain a final protein concentration of 2 mg/mL, assuming that 1 OD_{600} unit corresponds to 5×10^8 cells and 0.175 mg/mL of total proteins. Samples were sonicated to fragment the DNA and proteins were denaturated at 90°C for 5 min. Thirty µg aliquots of each sample were loaded on a 4-15% Mini-PROTEAN® TGXTM

precast protein gels (Pierce™, Bio-Rad, Hercules, CA, USA) and run at 30 mA for 30 min in Tris-glycine SDS buffer (AppliChem). The PageRuler™ pre-stained protein ladder (Thermo Fisher Scientific) provided molecular weight standards. Proteins were transferred electrophoretically to a 0.45 µm nitrocellulose membrane (Whatman®, Dassel, Germany) in Transfer buffer at 250 mA, for 2.5 h in the cold room. Homogeneous transfer of proteins to the membrane was checked by staining with 2% Ponceau S solution. Non-specific binding to membranes was blocked using 4% (w/v) milk powder in TBST for 1 h with constant agitation. Primary antibodies against TFs NrdR, HrcA and PhoB were obtained from Prof. Viollier. Antibodies were diluted 1:5000 in 4% (w/v) milk-TBST and added to membranes for 2 h at RT with gentle agitation. After 3 washes with TBST and once with 4% (w/v) milk-TBST for 10 min, membranes were incubated with peroxidase-coupled anti-rabbit IgG (whole molecule) (Sigma-Aldrich) diluted 1:5000 in 4% (w/v) milk-TBST for 45 min with gentle agitation. Proteins were detected by chemiluminescence as previously described [59]. Membranes were exposed immediately to autoradiographic film and images were developed using the SRX-101A film processor (Konica Corporation, Tokyo, Japan).

For Euo analysis, an overnight culture of *E. coli* transformed with pJGZ290prhs9_lacZ and pSRK-Euo was diluted into fresh medium containing antibiotics, and Euo expression was induced as described above in the presence of 0, 0.05, 0.1, 0.5 and 1 mM IPTG. After 3 h, 30 µg aliquots of each sample were prepared for electrophoresis as described above, loaded onto 4-20% Mini-PROTEAN® TGX™ precast protein gels and run at 100 V for 80 min in Native Page™ running buffer (AppliChem) supplemented with 0.1% (v/v) SDS. Proteins were transferred to a 0.2 µM nitrocellulose membrane using the iBlot™ 2 system (Thermo Fisher Scientific). Uniform transfer of protein was confirmed by staining with 2% Ponceau S solution and membranes were processed as described above using the rabbit anti-Euo primary antibody from Prof. Viollier at a dilution of 1:5000.

2.2.6 Plant extracts and natural products

Collections of 175 plant extracts from the Swiss Alps and 74 natural products (all at 4 mg/mL in DMSO) were available in the lab. A library of 2640 natural products (at 10 mM in DMSO) was purchased from the NCCR Chemical Biology collection provided by the BSF-ACCESS screening platform, EPFL, Lausanne, Switzerland. Additional compounds were obtained from commercial sources as indicated: apigenin 7-O-glucoside (Fluka Chemie), (+)-gallocatechin (AnalytiCon Discovery GmbH, Potsdam, Germany), (-)-gallocatechin (Sigma-Aldrich), kaempferol (Sigma-Aldrich), luteolin (Sigma-Aldrich), naringenin (Carl Roth, Karlsruhe, Germany) and resveratrol (AppliChem).

2.2.7 Euo minimal inhibitory concentration assay

Minimal inhibitory concentrations (MIC) of plant extracts were determined as previously described [226, 227]. Briefly, plant extracts were tested at 200 µg/mL for growth inhibition of *E. coli* co-expressing the plasmids pJGZ290prhs9_lacZ and pSRK-Euo.

2.2.8 High throughput screening for Euo inhibitory compounds

Overnight cultures of *E. coli* transformed with pJGZ290prhs9lacZ and pSRK (control), or pJGZ290prhs9_lacZ and pSRK-Euo, were diluted 1:50 in fresh selection medium, and incubated at 37°C, 260 rpm until OD_{600} of 0.5-0.8. Expression of Euo was induced by addition of 1 mM IPTG and 100 µL aliquots of cells were transferred to black 96-well clear bottom plates (Corning Incorporated) containing 40 µg/mL plant extracts or 100 µM natural products, all in 1% (v/v) DMSO. Control wells contained 1% DMSO alone. Plates were incubated for 3 h at 37°C, 260 rpm. The OD_{600} of each well was then recorded and cells were lysed by addition of FastBreak™ reagent to a final concentration of 10% (v/v) followed by incubation for 15 min at room temperature (RT) on an orbital shaker at 250 rpm. To measure LacZ activity, the galactosidase substrate, DDAOG (Thermo Fisher Scientific), was added to a final concentration of 5.5 µM and the fluorescence signal at $F_{590/680}$ was recorded for 10 min at 28°C using Synergy HT microplate reader (gain: 90, optics position: top, read height: 1.00 mm). LacZ activity in DDAOG units was calculated using the Gen5 version 2.04.11 software (BioTek® Instruments) as follows:

$$\text{LacZ activity (DDAOG Units)} = \frac{F_{590/680}}{(OD_{600} * t)}$$

Time (t) calculated in min.
$F_{590/680}$: Excitation/emission at 590/680 nm.
OD_{600}: Optical density measured at 600 nm.

2.2.9 Experimental design

Experimental replicates were performed using starting cultures derived from independent bacterial colonies as described in the legends to Figures.

2.3 Results and Discussion

2.3.1 Validation of reporter systems

Three gene-based reporter systems, *npt-II*, (neomycin phosphotransferase-II, which confers resistance to Kan) *luxAB* (bioluminescent readout in the presence of decanal) and *lacZ* (a colorimetric, *β*-galactosidase-based readout), were tested for their activity in *E. coli* and for their suitability as a readout in a high throughput screening format. For these preliminary experiments, the *E. coli* lac operator (*lac*O)/lac repressor (LacI) system was used. In this system, LacI acts as a transcriptional repressor by binding to *lacO* inserted upstream of the reporter gene (Figure 2.1A). IPTG binding to the LacI repressor releases it from *lacO* allowing transcription of the reporter gene to occur (Figure 2.1B). The reporter dependent signal can then be measured [231, 232]. In preliminary experiments the suitability of each of the three reporter systems was tested.

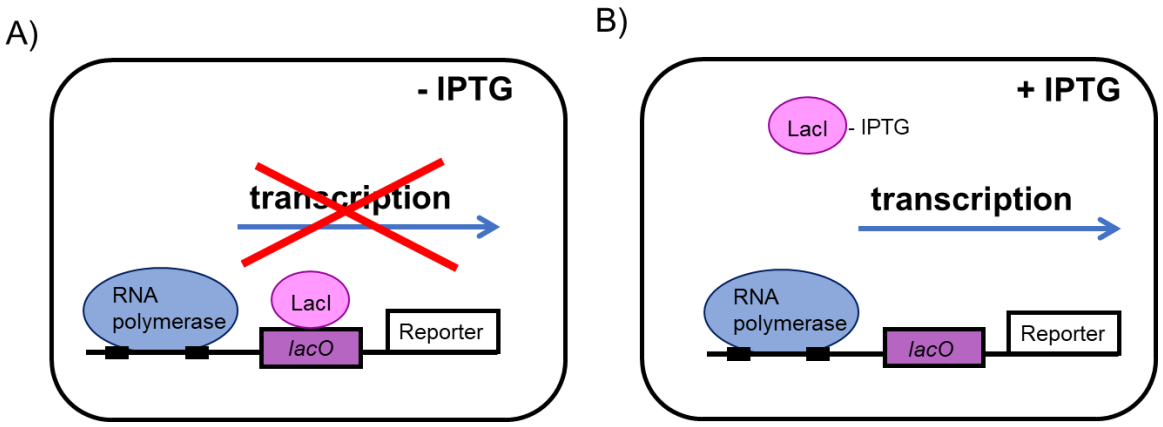

Figure 2.1. Schematic representation of the lac operator (*lac*O)/lac repressor (LacI) system in *E. coli*. (A) In absence of IPTG, LacI binds to *lacO* located upstream of the reporter gene and inhibits transcription. (B) In the presence of IPTG, LacI binds to IPTG, the reporter gene is transcribed and the corresponding signal can be measured.

npt-II (Kan^r)

E. coli cells co-transformed with plasmids pJGZ290lacO_Kan^r and pUG3.1-lacI were tested using different concentrations of Kan in the presence or absence of IPTG. The minimal inhibition concentration (MIC) was determined as described in section 2.2.5.1, and shown to be 205 µg/mL and 51 µg/mL in presence or absence of IPTG, respectively (Figure 2.2A). This provides a sufficient window for detecting differences between the induced and repressed conditions in the *E. coli* lac operator (*lac*O)/lac repressor (LacI) system. This finding may be different in the final screening method with the chlamydial TFs and their corresponding DNA binding motifs co-transformed into *E. coli*.

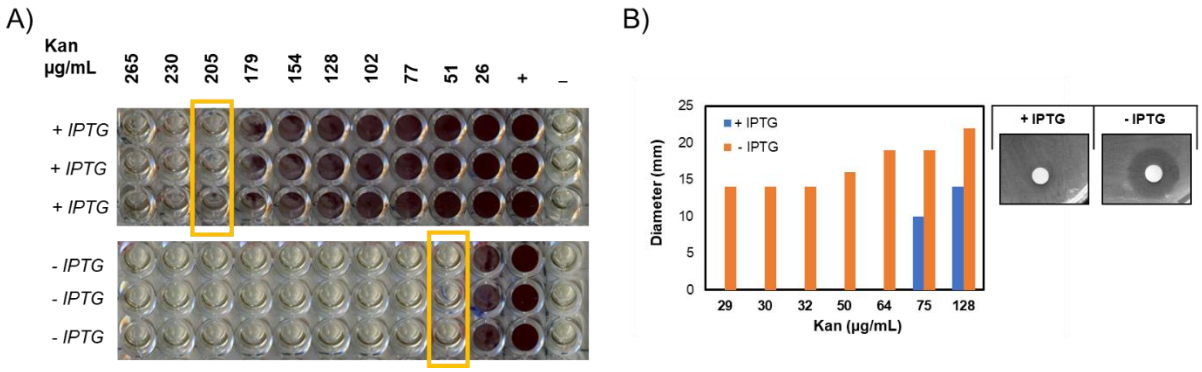

Figure 2.2. Activity test of Kan reporter.
(A) MIC of Kan in the presence (top) or absence (bottom) of IPTG. *E. coli* expressed both pJGZ290lacO_Kan^r and pUG3.1-lacI, and Kan was tested at the concentrations indicated. In positive control (+) no Kan was added and in negative control (-) no cells were present. Growth was detected using the redox sensitive dye INT (section 2.2.5.1). Experiments were done in triplicate and the wells indicating the MIC are framed in yellow. (B) Antibiogram assay. Zones of inhibition were measured on LBA plates containing discs with different concentrations of kanamycin (left). The discs impregnated with 64 µg/mL Kan in the presence and absence of IPTG are shown (right).

An antibiogram test with these bacterial strains using different concentrations of Kan in the presence and absence of IPTG, showed that 64 µg/mL Kan resulted in the largest difference (19 mm) in the diameters of the growth inhibition zones (Figure 2.2B). However, the strain was sensitive to higher concentrations of Kan even in the presence of IPTG. This result revealed the limitation of the antibiogram using the Kan reporter at higher Kan concentrations in the operator (lacO)/lac repressor (LacI) system and showed that the Kan reporter system could be useful for screening, although the antibiogram procedure, while having the advantage of being simple, inexpensive, and easy to interpret did not provide a reliable readout. Furthermore, quantification of bacteria-free zones on agar plates is not suitable for use in high-throughput format. The MIC assay shares the same advantages as the antibiogram assay, but also has the same disadvantage of requiring a relatively long incubation time (24 h). Performing MIC assays without the bacterial cell metabolism indicator INT may be possible but could lead to difficulties in the readout due to the presence of pigments such as anthocyanins, betalains, carotenoids and xanthophylls in plant extracts, which could lead to erroneous results [233]. Overall, the MIC assay could be used to screen plant extracts and natural products, but because of the long incubation times, it was decided not to be proceed further with this reporter system.

luxAB

The bioluminescent *luxAB* reporter system contains the *luxA* and *luxB* genes, which together, in the presence of the chemical decanal, generate a light signal. In this test, *E. coli* expressing plasmids pJGZ290lacO_luxAB and pUG3.1-lacI, were grown with and without IPTG induction of *luxAB* (Figure 2.3). A repression activity of 90% was measured and a Z-factor of 0.5 was calculated. The Z-factor is a coefficient used to calculate the robustness of the screening and the optimal screening window [229]. A Z-factor in the range of 0.5-1 indicates a good screening procedure, whereas a Z-factor below 0.5 would be unsatisfactory [234].

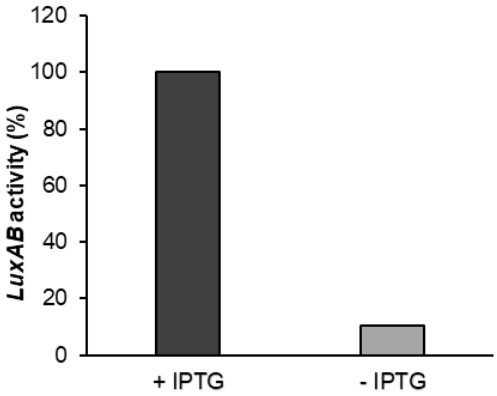

Figure 2.3. Effect of IPTG on *luxAB* gene-based reporter activity.
LuxAB activity in *E. coli* expressing both pJGZ290lacO_LuxAB and pUG3.1-lacI was measured in presence and absence of IPTG. Experiments were performed in technical triplicates on two different occasions and mean values are represented.

In conclusion, the *luxAB* gene-based reporter is functional and can be used as a quantitative screening method. The use of this reporter for testing plant extracts and natural products in gene expression studies in *E. coli* has been previously described [235].

lacZ

Expression of the *β*-galactosidase gene (*lacZ)* was tested as a third possible reporter system. LacZ activity can be followed either on plates or in liquid medium, and various substrates are available for detection of the enzymatic reaction. In Figure 2.4, the LacZ activity of *E. coli* expressing pJGZ290lacO_lacZ and pUG3.1-lacI was followed in liquid medium by adding the colorimetric substrate ONPG, in presence or absence of IPTG.

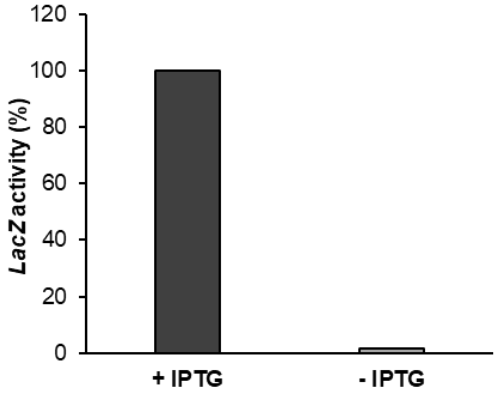

Figure 2.4. Functional test of *lacZ* gene-based reporter.
E. coli containing both pJGZ290lacO_lacZ and pUG3.1-lacI were tested following the protocol described in section 2.2.5.4. Experiment were performed in technical triplicates on two different days and mean values are represented.

In liquid medium, a repression activity of 98% is seen and a Z-factor of 0.7 was calculated (Figure 2.4). In contrast, on solid medium, no obvious difference between the two conditions was observed using X-gal as a substrate (data not shown), possibly due to its high sensitivity to background levels of *β*-galactosidase in non-induced cells.

In conclusion, both the *luxAB* and *lacZ* gene-based reporter systems showed a Z-factor higher than 0.5, making both assays suitable for quantitative screening in 96-well plates. To evaluate, which of the two assays would be better suited for screening plant extracts and natural products, the effect on the readout of the presence of DMSO, the solvent used for sample solubilisation and storage, was tested (Figure 2.5).

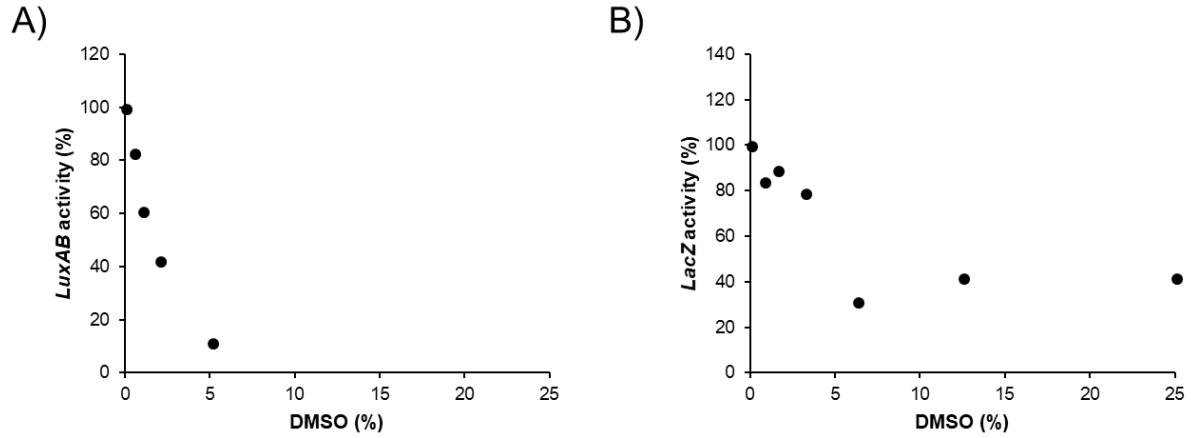

Figure 2.5. Influence of DMSO on the *luxAB* and *lacZ* readouts.
(A) *LuxAB* reporter gene assay was performed with *E. coli* pJGZ290lacO_luxAB using different DMSO concentrations, following the protocol described in section 2.2.5.3. (B) *LacZ* reporter gene assay was performed with *E. coli* pJGZ290_lacZ using different DMSO concentrations following the protocol described in section 2.2.5.4. Experiments were done in technical triplicates and mean values are represented.

In conclusion, this experiment showed that the *LuxAB*-based assay was more sensitive to the presence of DMSO (Figure 2.5A) than the *lacZ*-based assay. In the latter case, up to 3% DMSO in the reaction mix had minimal effect on the readout (Figure 2.5B). Additionally, no effect on bacterial growth was observed using 1.5% DMSO.

Overall, the validation of the three reporter systems showed that the *lacZ* readout in liquid medium is the most robust, and the most suitable for use in high throughput screening for TF inhibitors present in plant extracts and natural products. Therefore, LacZ reporter was chosen to set up the screening for transcription repressors as detailed below.

2.3.2 Selection of target TFs

Four *W. chondrophila* TFs, NrdR, HrcA, PhoB and Euo, were tested as potential targets for the inhibitor screening (Figure 2.6). All TFs are conserved among most members of the phylum *Chlamydiae*, and all are likely to be involved in regulating the intracellular developmental cycle.

HrcA and PhoB

For the set-up of the screening assays containing the TFs HrcA and PhoB, their endogenous promoters containing the corresponding DNA binding motifs were inserted upstream of the *lacZ* reporter gene. HrcA and PhoB have been shown to bind their own promoter sequences *in vitro* [236-239].

Euo

For the TF Euo, two different promoters were tested. First the rhs9 promoter, which is the endogenous promoter of the *rhs* genes and present in a broad range of Gram-negative bacteria [240]. The definitive function of the target genes has yet to be assigned. The *rhsT* gene of *P. aeruginosa*, which belongs to the rhs family, encodes a virulence determinant important for the pathogenesis of this strain [241]. A second sequence containing the Euo DNA binding motif was the promoter of the gene pwcw1705 which has a predicted ATPase and/or kinase function [122].

NrdR

In contrast to the natural promoters discussed above, the NrdR promoter was designed by Prof. Viollier. This synthetic sequence contains three NrdR DNA-binding motifs and is referred to as pJGZ290NrdR_triple_consensus_lacZ.

For simplicity, *E. coli* co-transformed with the NrdR, HrcA, PhoB or Euo reporter plasmids (pJGZ290NrdR_triple_consensus_lacZ, pJGZ290pHrcA_lacZ, pJGZ290pPhoB_lacZ, and pJGZ290pwcw1705_lacZ or pJGZ290prhs9_lacZ) together with the corresponding IPTG-inducible TF plasmid (pSRK-NrdR, pSRK-HrcA, pSRK-PhoB, or pSRK-Euo) are referred as NrdR+, HrcA+, PhoB+, Euo1705+ and Euo9+. As negative controls each of the reporter

plasmids co-transformed with the pSRK empty vector are referred to as NrdR-, HrcA-, PhoB- and Euo1705-/Euo9-, respectively.

A)

TF	DBM
Euo	Pwcw1705
Euo	Prhs9
HrcA	PhrcA
NrdR	PnrdR
PhoB	PphoB

B)

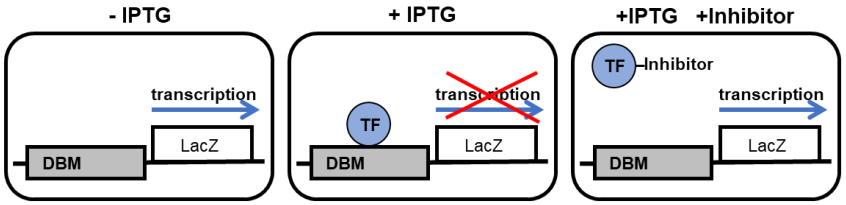

Figure 2.6. Set-up of the screening assay in which the TFs NrdR, HrcA, PhoB and Euo, and their corresponding DNA binding motifs are co-expressed in *E. coli*.
(A) The TFs analyzed and their cognate DNA binding motifs (DBM) are shown. For Euo, two binding motifs were tested as described in the text. In (B), an *E. coli* cell co-expressing the IPTG-inducible TF and its corresponding reporter plasmid is shown. In the absence of IPGT, lacZ is transcribed and signal can be measured (left panel). Following IPTG induction of the TF, *lacZ* transcription is repressed (middle panel). In presence of IPGT and a TF inhibitor, expression of *lacZ* can be detected (right panel).

The expression of the TFs NrdR, HrcA, PhoB and Euo was tested by western blotting. *E. coli* cultures transformed with each of the pSRK-TF plasmids were grown in different concentrations of IPTG as shown in Figure 2.7. Antibodies against NrdR (wcw_1751), HrcA (wcw_1636), PhoB (wcw_0128) and Euo (wcw_1683) detected proteins with the expected molecular weights of 15 kDa, 35 kDa, 25 kDa and 17kDa respectively (arrows in Figure 2.7A-D).

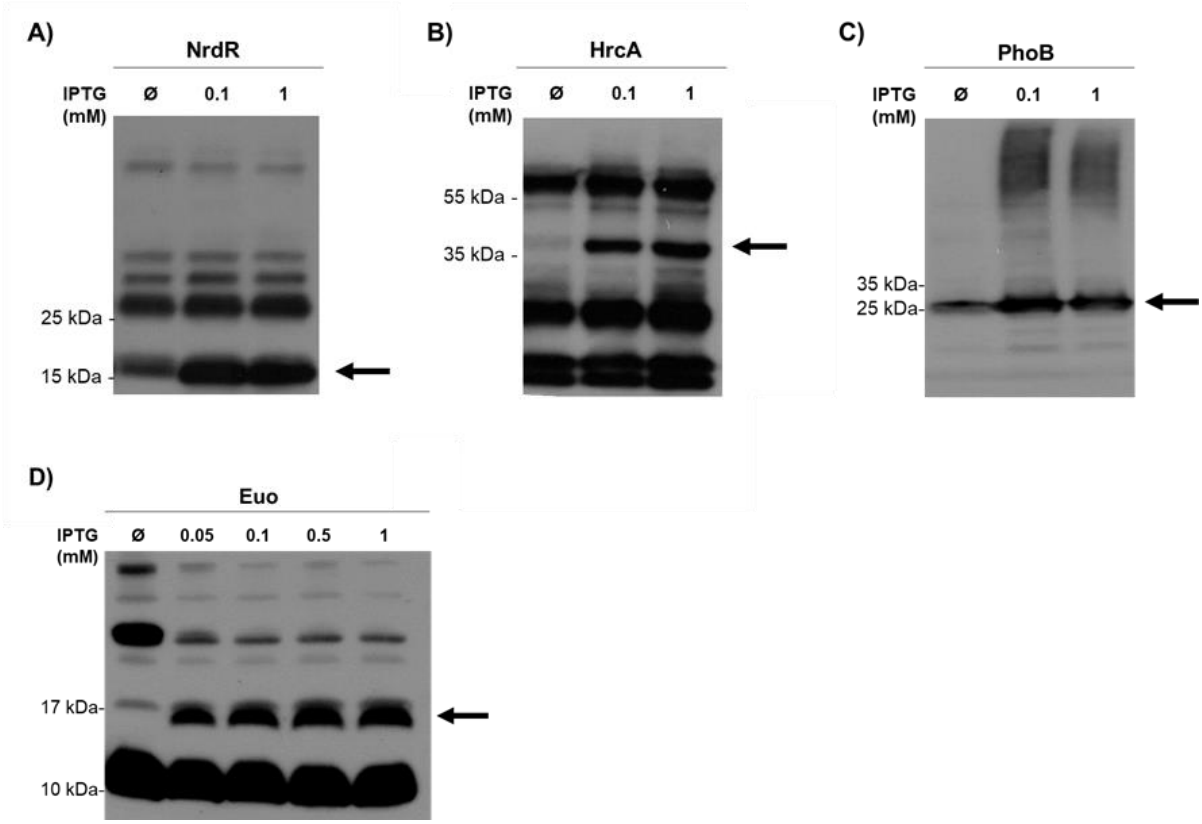

Figure 2.7. Expression of NrdR (A), HrcA (B), PhoB (C) and Euo (D) in vector pSRK using various IPTG concentrations.
Bands corresponding to the TFs are indicated by an arrow.

However, in cells grown without IPTG, bands corresponding to the TFs NrdR, HrcA and PhoB are also present, suggesting either that these promoters have a basal, uninduced level of expression, or that these antibodies also recognise their *E. coli* homologues. On the other hand, endogenous expression was not observed in the case of Euo, which is absent in *E. coli*. Moreover, this TF is the only conserved TF unique to the *Chlamydiae*, showing more than 70% sequence homology between *W. chondrophila* and most other members of the phylum [122].

LacZ activity was tested in *E. coli* transformed with the IPTG-inducible expression plasmids encoding NrdR, HrcA, PhoB and Euo and the corresponding reporter plasmids. Cultures were induced with or without 1 mM IPTG as described in section 2.2.5.4 and the results are shown in Figure 2.8.

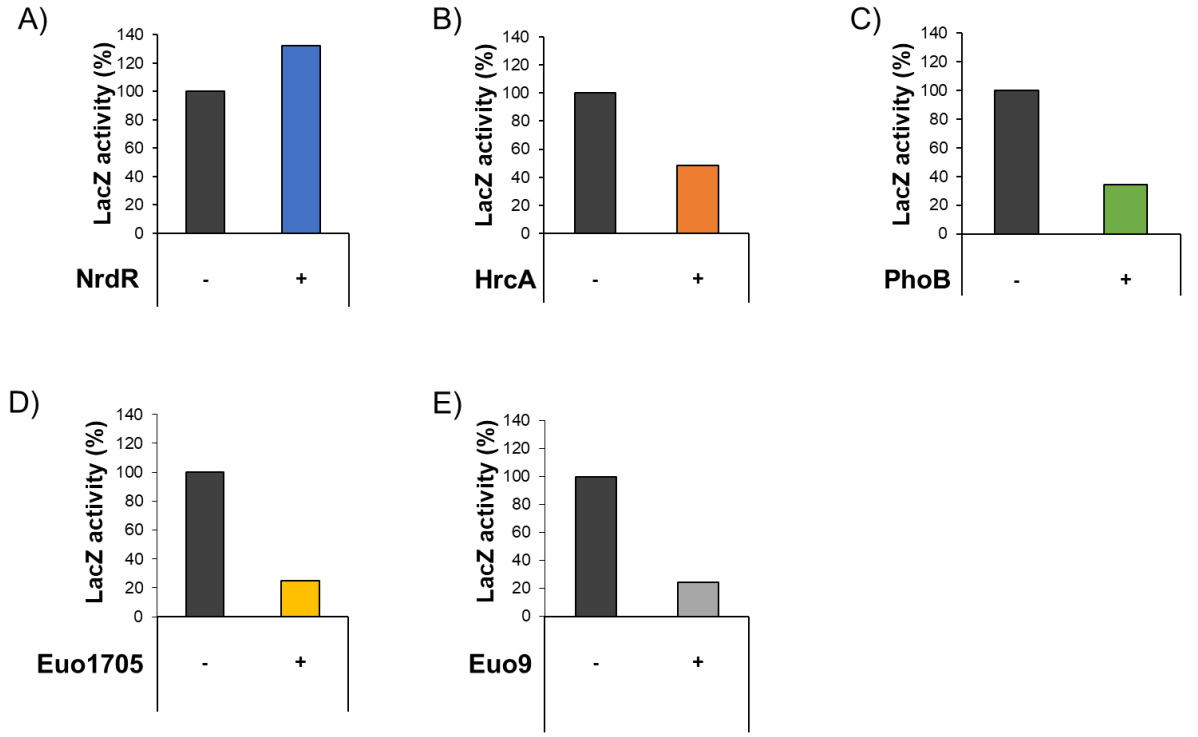

Figure 2.8. LacZ activity results of chlamydial TF NrdR, HrcA, PhoB and Euo.
Overnight cultures of *E. coli* containing both NrdR- or NrdR+ (A), HrcA- or HrcA+ (B), PhoB- or PhoB+ (C), Euo1705- and Euo1705+ (D), and Euo9- or Euo9+) (E) were measured following the protocol described in part 2.2.5.4 at 1 mM IPTG. Experiments were done in technical triplicates and mean values are represented.

In this system NrdR showed no inhibitory activity at 1 mM IPTG (Figure 2.8A). For HrcA (Figure 2.8B) and PhoB (Figure 2.8C), a maximum LacZ repression activity of 51 and 66% respectively could be measured. This is in agreement with previously published results in which HrcA and PhoB showed similar LacZ repression activity when expressed from the arabinose inducible plasmid, pBAD to chart the landscape of TF specificities resulted in similar LacZ repression activity [122]. Calculated Z-factors for HrcA and PhoB gave a value which was too low (0.4) in the case of HrcA, but good (0.9) in the case of PhoB. The highest transcriptional repression activity of the four TFs was seen for Euo, at around 80%, with similar activities being measured using both DNA binding motifs Pwcw1705 and Prhs9 (Figure 2.8D and 2.8E). Similar repression activity of Euo was also described previously in the literature [122]. The two promoters containing DNA binding motifs for Euo (Pwcw1705 and Prhs9) showed similar repression activity, although the calculated Z-factor was higher for Prhs9 (0.7) compared to Pwcw1705 (0.4). The large difference between these Z-values can be explained by the higher variability in Pwcw1705 data (data not shown). From these results, due to its highest transcriptional repression activity and the best Z-factor for a screening method, the IPTG inducible plasmid pSRK expressing *Euo* and the promoter containing DNA binding motif

for Euo Prhs9 were selected for the screen. In the future work, Euo9- and Euo9+ are referred as Euo- and Euo+.

In addition, in view of the results using PhoB, in particular the high Z-factor value obtained, this system was also retained as a potential secondary assay to confirm possible positive results.

2.3.3 Set up of the screening method – parameter optimisation

2.3.3.1 Bacterial concentration prior to induction

Starting concentrations as measured by OD_{600} were tested as shown in Figure 2.9. A fresh overnight culture of Euo+ diluted to a starting concentration of OD_{600} 0.05 showed no IPTG-dependent difference in transcriptional repression, whereas a repression activity of 52% was calculated when induction was started with a bacterial culture diluted to an OD_{600} of 0.5.

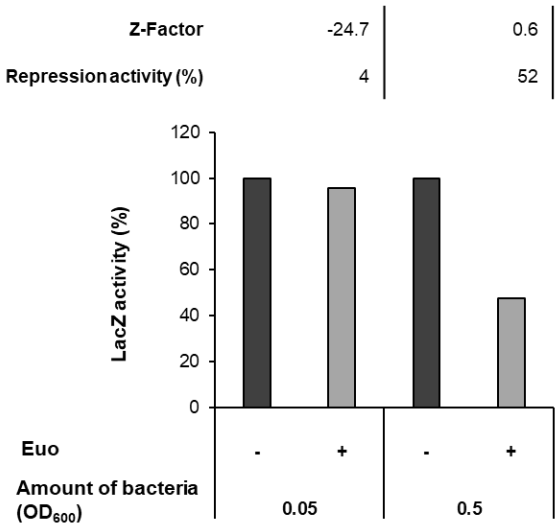

Figure 2.9. *LacZ* reporter gene expression as a function of bacterial starting concentration.
O/N cultures of Euo- and Euo+ in LB were diluted to OD_{600} 0.05 or 0.5 and expression was induced by addition of 1 mM IPTG. LacZ activity was measured following protocol in part 2.2.5.4. Experiments were done in technical triplicates and mean values are represented.

In this case, transcriptional repression was lower than the previously described (76% in Figure 2.8) probably due to a difference in the longer time of adaptation of the culture to the new environmental conditions in the experiments shown in Figure 2.9. In the final screening protocol, overnight cultures were first diluted 1:50 and grown to an OD_{600} of 0.5-0.8, thus allowing the bacteria to enter the exponential growth phase prior to addition of IPTG.

2.3.3.2 IPTG concentration

The relationship between IPTG concentration and repression of *lacZ* transcription was determined (Figure 2.10). IPTG concentrations of 0, 0.05, 0.1 and 1 mM, were compared. All concentrations of IPTG reduced LacZ activity. Z-factors and repression activities were calculated for each condition and the highest values (0.8 and 78%) were obtained using a final concentration of 1 mM IPTG.

In absence of IPTG, a similar LacZ activity could be measured between Euo- and Euo+ (Figure 2.10). This relationship between IPTG concentration and LacZ activity is in agreement with the Euo western blotting results (Figure 2.7), which showed that expression of Euo is under control of IPTG, and in the absence of induction, no Euo is expressed. Therefore, in the screening protocol, IPTG is used at a final concentration of 1 mM.

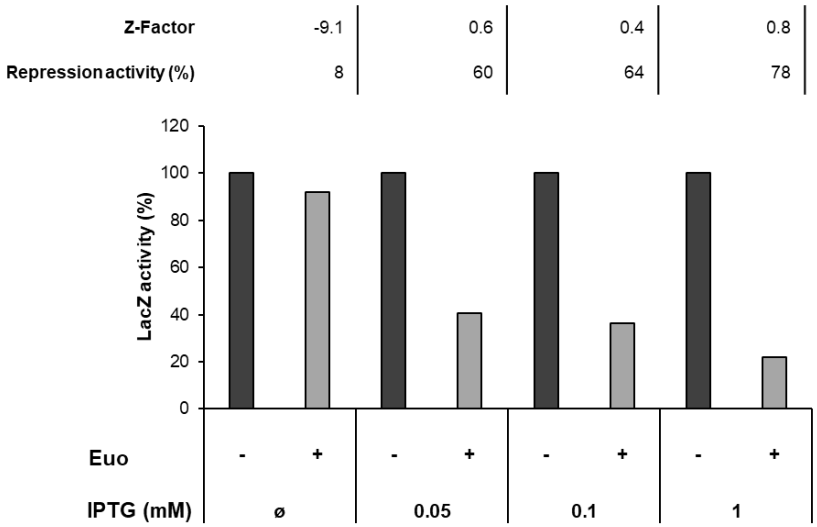

Figure 2.10. Effect of different IPTG concentrations on LacZ activity.
Expression of LacZ was measured in Euo- and Euo+ using different IPTG concentrations, and control measured in absence of IPTG following protocol described in part 2.2.5.4. Experiments were done in technical triplicates and mean values are represented.

As IPTG can be toxic for bacteria at higher concentrations [242], the influence of 1 mM IPTG *per se* on growth was tested at different bacterial starting concentrations (OD_{600} of 0.13 and 0.6). IPTG had no effect on bacterial growth (data not shown), indicating that 1 mM IPTG can be used in the final screening method.

2.3.3.3 Induction time

To determine the optimal time of induction, Euo+ and Euo- cultures were induced with 1mM IPTG and grown for 1, 2, 3 and 4 h after addition of 1 mM IPTG. The induced level of LacZ activity in each culture was measured using ONPG as substrate (section 2.2.5.6) and the results are shown in Figure 2.11.

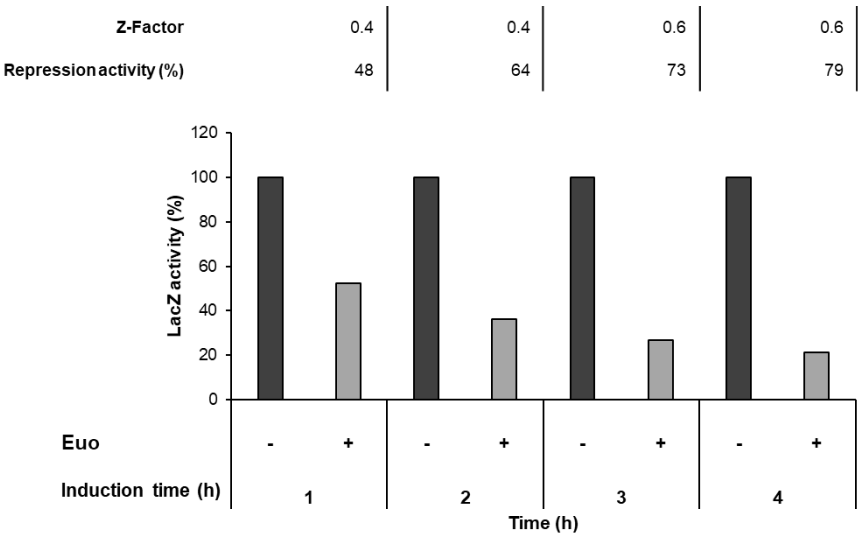

Figure 2.11. Expression of LacZ as a function of post-induction time.
Expression of LacZ in Euo- and Euo+ transformed cells, was measured at different times post-induction following the protocol described in part 2.2.5.5. Experiments were done in technical triplicates and mean value are represented.

Using the ONPG assay, the highest repression activity of LacZ (79%) and the strongest Z-factor (0.6) were measured at 4 h post-induction, while at 3 h post-induction, 73% repression activity and a Z-factor of 0.6 were measured. Thus, in the interest of increasing the screening throughput, LacZ activity was measured at 3 h post-induction in the final screen. Measurement of LacZ activity was also tested at different times after addition of the substrate ONPG (data not shown), and a reaction time of 10 min was selected for the screening protocol.

To test many samples at high throughput, it was important to compare different procedures for the final readout phase. For this, the LacZ activity was measured in the traditional Miller assay in culture tubes (protocol 2.2.5.4) and compared to the 96 well plate format measured using a plate reader (protocol 2.2.5.5). No significant difference in values was obtained using the different measurement procedures (data not shown).

From these initial analyses, the screening method 1 was established. This method combined the advantages of using the *Chlamydia*-specific TF, Euo with an efficient screening method based on the 96-well plate format. To complete the preliminary set up phase it was also necessary to investigate possible interference of the plant extracts on signal measurement. This led to further optimisation of the screening as follows.

Library samples were dissolved in DMSO and tests on the influence of DMSO on LacZ activity have already been described in section 2.3.1 using the operator (*lac*O)/lac repressor (lacI) system in *E. coli*. Furthermore, MIC determination of different DMSO concentrations using the *E. coli* strain containing Euo+ showed normal growth at 5% DMSO and a MIC of 12.5% DMSO (data not shown). In the final screening method, a maximal concentration of 1% DMSO was chosen, which had no impact either on the measured LacZ activity or on the cell growth.

2.3.4 Further method optimisation

In order to consume as little as possible of the precious test compounds during the project, the total sample volume of method 1, 200 µL, was reduced to 100 µL, resulting in similar values for Z-factor and repression activity (0.9 and 84%, compared to 0.8, and 80%, respectively) (data not shown). Furthermore, the cell culture dilution step in method 1 did not affect repression activity of Euo and Z-factor between OD_{600} of a non-diluted culture and a 1:4 diluted culture (data not shown). These findings led to the conclusion that the total sample size can be reduced, and the dilution step in method 1 can be eliminated without consequences for the validity of the screening method.

2.3.4.1 Lysis buffer optimisation

The screening was optimised to perform the assay in 96 well plates. The traditional method for measuring LacZ activity in tubes (as performed by Miller) uses a mixture of chloroform/SDS in Z-Buffer containing β-ME to lyse the cells [210]. Chloroform is not suitable for use in standard 96 well plates, since it dissolves polystyrene [243]. Therefore, alternative lysis procedures without chloroform were tested, which would be compatible with standard 96 well plates, and also with the ONPG-based *lacZ* reporter assay. Numerous lysis reagents were tested. The PopCulture® Reagent containing 1% rLysozyme 40 U/µL [243] and Cell Culture Lysis Reagent (CCLR) were not suitable for the screening due to the production of foam, which interfered with the absorbance measurement of ONPG. Using CelLytic™ Express, a Z-factor of 0.9 and a repression activity of 60% were calculated, however, this reagent is supplied as

a powder to be added directly to the samples and thus is difficult to use in a 96-well plate format. Cooled FastBreak™ Reagent and B-PER® Reagent both resulted in a good Z-factor (0.6) and similar repression activity (78% for FastBreak™ Reagent and 72% for PER® Reagent) (Figure 2.12).

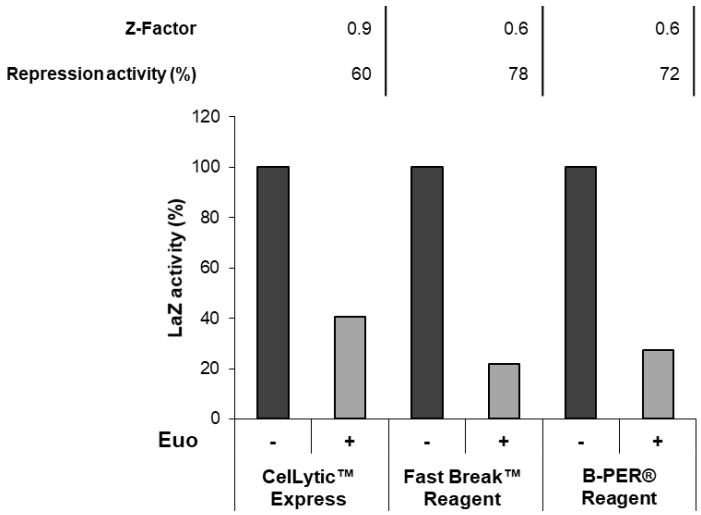

Figure 2.12. In-culture bacterial cell lysis with CelLytic™ Express, FastBreak™ Reagent and B-PER® Reagent.
LacZ activity of Euo- and Euo+ was measured after cell lysis in the presence of various reagents at RT for 15 min and 350 rpm. Experiments were performed in technical triplicates and mean values are represented.

FastBreak™ Reagent was selected for use in the screening method. Tests of different solvents for ONPG (DMF, MeOH, DMSO and dH_2O) showed that DMF resulted in protein or cell debri precipitation) and MeOH and DMSO resulted in foam production. dH_2O showed no interference with cell culture and lysis buffer and was used for these experiments.

2.3.4.2 Substrate DDAOG

The final stage in optimising the screening procedure was to replace the colorimetric substrate ONPG with the fluorescent substrate DDAOG in order to limit the impact of the pigmented plant extracts and natural products. In addition, DDAOG has a wide separation between the excitation and emission wavelengths (590 and 680 nm [212]) thus further reducing the chance of false positive results. For use in combination with FastBreak™ Reagent, DDAOG was dissolved in dH_2O. Without cell lysis, no LacZ activity is detected in the presence of DDAOG. Lysis by FastBreak™ Reagent and measurement of LacZ activity in the presence of various

concentrations of DDAOG resulted in a good Z-factor of 0.5 and a repression activity of Euo of 78% at 5.5 µM DDAOG (Figure 2.13). 5.5 µM DDAOG was therefore chosen as the substrate for the final screen.

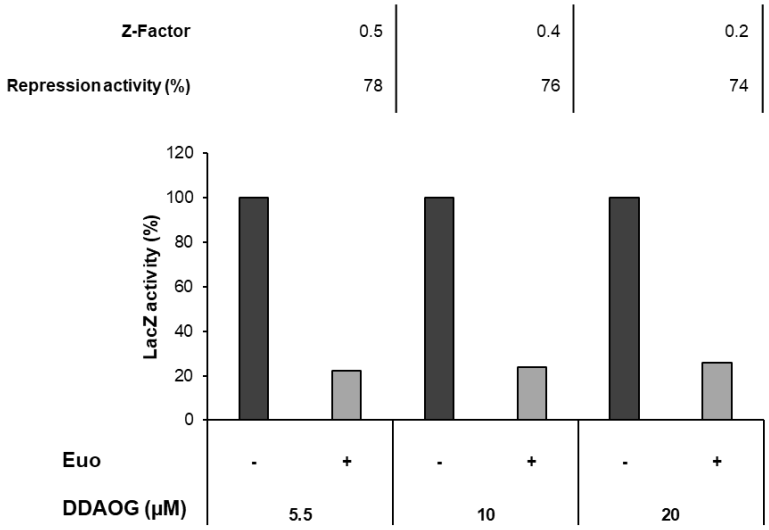

Figure 2.13. *β*-Galactosidase assay optimisation with DDAOG as substrate. LacZ activity of Euo- and Euo+ was measured using indicated DDAOG concentrations. Cells were lysed by FastBreak™ Reagent. For all experiments, protocol described in part 2.2.9 was followed. Experiments were performed in technical triplicates and mean value are represented.

The modifications to screening method 1 led to the final screening method 2 optimised for natural products and plant extracts, as illustrated in Figure 2.14. This second method combines the advantages of the 96-well plate format, an efficient and compatible lysis procedure, and a fluorescent substrate to minimise the impact of pigmented plant extracts and natural products.

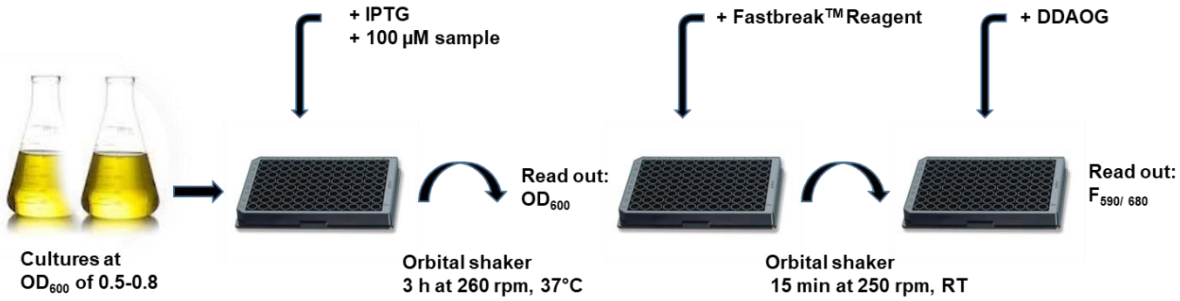

Figure 2.14. Illustration of screening method 2 to identify molecules that alter the ability of the TF Euo to interact with its cognate DNA binding site (Method 2).

2.3.5 Screening of plant extracts and natural products for their ability to repress the activity of Euo

The effect of 175 plant extracts from the Swiss Alps was tested on *E. coli* growth and their effect on Euo repression activity was measured. Alpine plants have been shown to harbor a huge unexplored potential for novel chemical structures [244].

Plant extracts were first tested for growth inhibition of *E. coli* containing Euo+ at 200 µg/mL in 96-well plates. None of the plant extracts showed bacterial toxicity (data not shown). The plant extracts were then tested for Euo repression activity at 40 µg/mL using screening method 1.

Comparison of the cultures treated with plant extracts and the untreated control cultures revealed no significant Euo inhibitory activity associated with any of the compounds (Figure 2.15 and 2.16), even though several plant extracts were found to enhance the repression activity of Euo, which could also affect bacterial cell cycle progression.

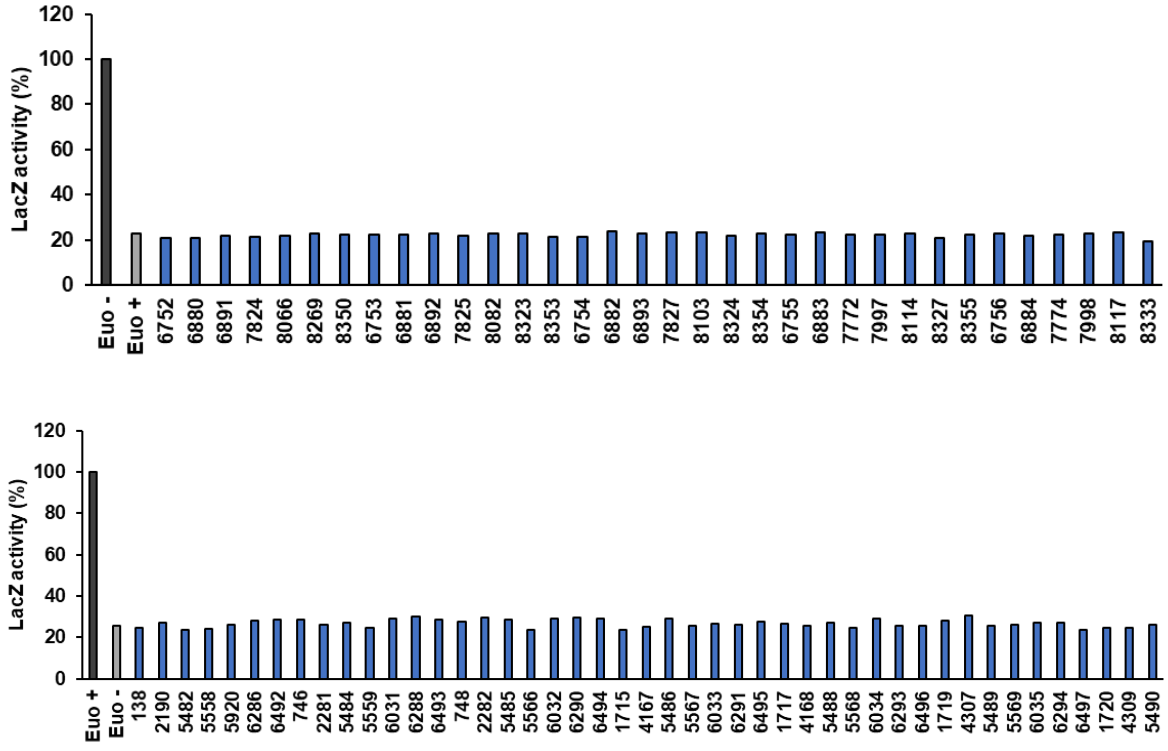

Figure 2.15. Screening results of 175 plant extracts at 40 µg/mL for Euo repression activity.
Experiments were performed in technical duplicates and mean values are represented (plate 1-2 of 5).

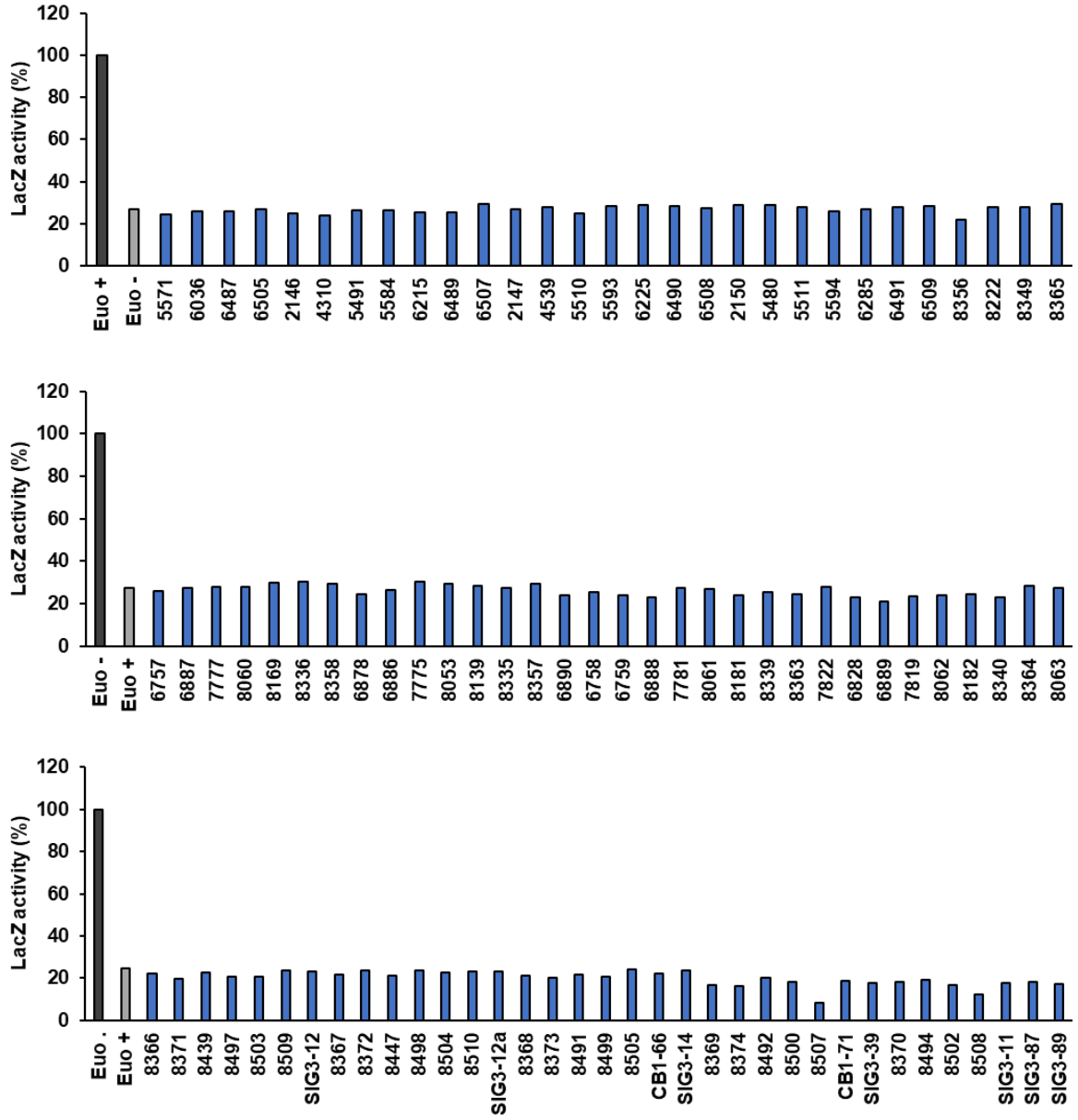

Figure 2.16. Screening results of 175 plant extracts at 40 µg/mL for Euo repression activity.
Experiments were performed in technical duplicates and mean values are represented (plate 3-5 of 5).

The analysis was then extended to include the 74 natural products. All were tested at 40 µg/mL for Euo repression activity using method 1 (Figure 2.17). Resveratrol (at 43.75, 87.5, 175 and 350 µM) and apigenin 7-O-glucoside (at 100, 200 and 400 µM) were also tested. Four compounds (harmine (6-H9) at 188 µM, quercetin 7-O-glucoside (6-B1) at 86 µM, resveratrol at 350 µM and apigenin 7-O-glucoside at 200 and 400 µM) showed weak repression, between 7-17%, of Euo activity.

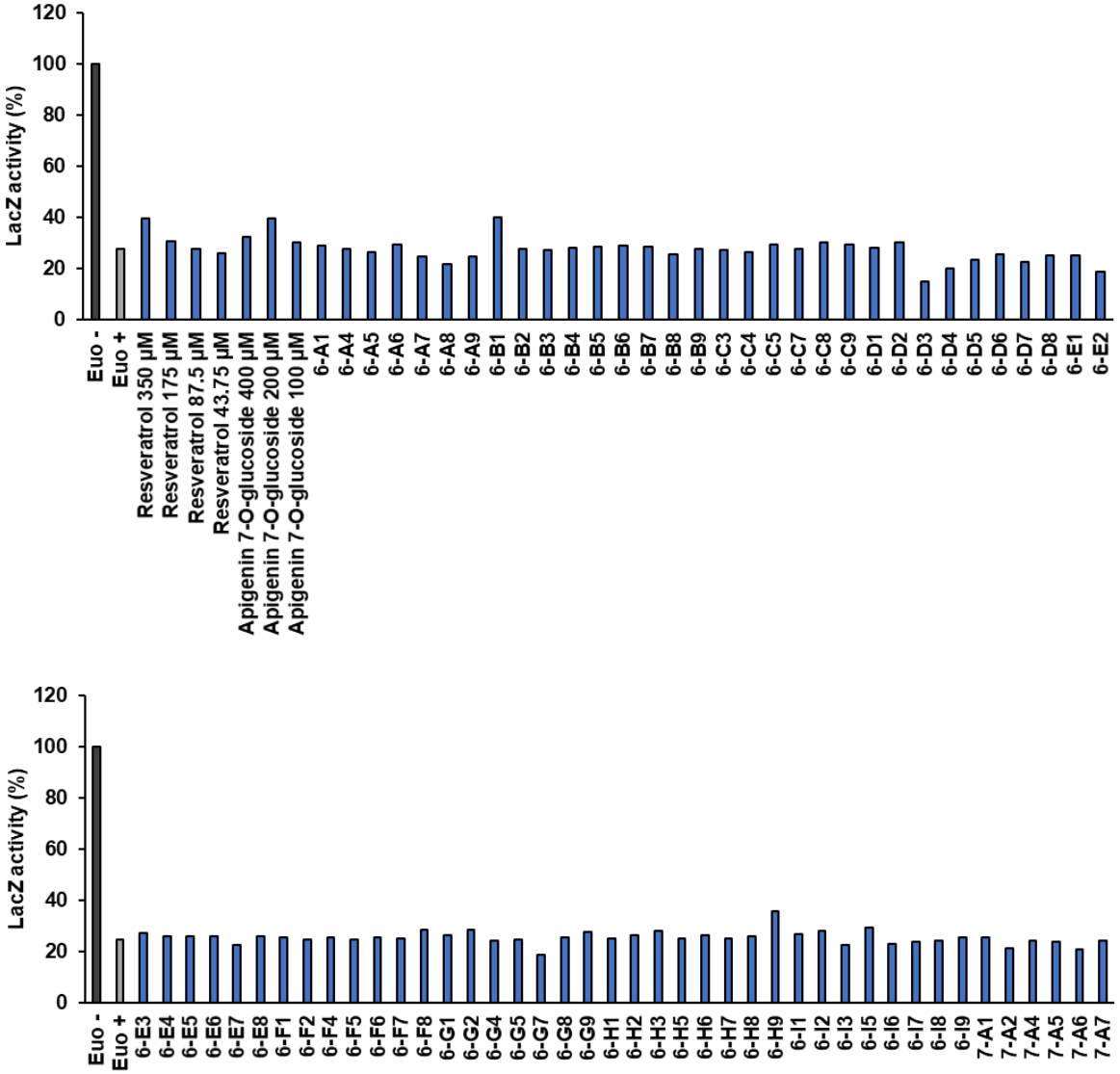

Figure 2.17. Screening results of 74 natural products at 40 µg/mL for Euo repression activity.
Experiments were done in technical duplicates and mean values are represented.

Figure 2.18 shows secondary testing of the natural products resveratrol, apigenin 7-O-glucoside and harmine at different concentrations. Anti-chlamydial activity of resveratrol has been previously described in the literature. This polyphenol was shown to reduce in a dose-dependent manner the number of infected cells, as visualised by monoclonal antibodies against chlamydial lipopolysaccharide [191]. The detailed mechanism of action of the anti-chlamydial activity of resveratrol is not known.

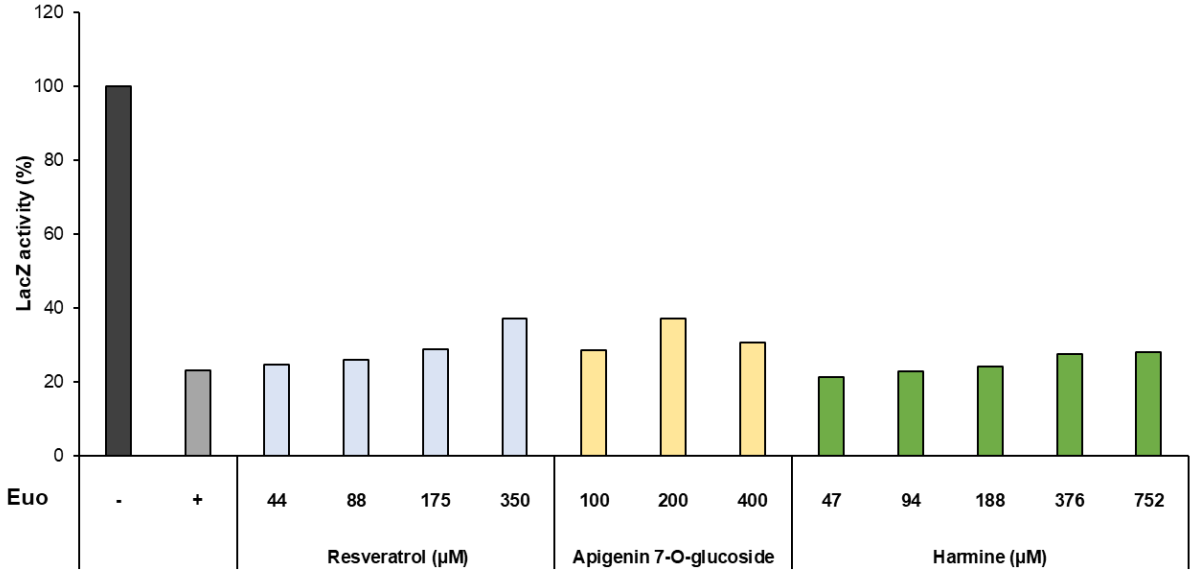

Figure 2.18. LacZ activity of selected natural products.
Resveratrol, apigenin 7-O-glucoside and harmine were tested for Euo repression in Euo+ at different concentrations using method 1. Experiments were performed in technical duplicates and mean value are represented.

All 74 natural products including harmine and quercetin 7-O-glucoside were also tested for repression activity of PhoB (Figure 2.19). Resveratrol, and apigenin 7-O-glucoside were also included at different concentrations. As in the Euo-based assay, a slight repression activity can be seen for harmine (6-H9) and quercetin 7-O-glucoside (6-B1) and a similar dose response is seen in the case of resveratrol, although not for apigenin 7-O-glucoside. However, the effects are marginal, and none of these natural products showed a robust activity when tested in either the Euo or the PhoB functional screen. As for Euo, some natural products showed enhanced repression of PhoB.

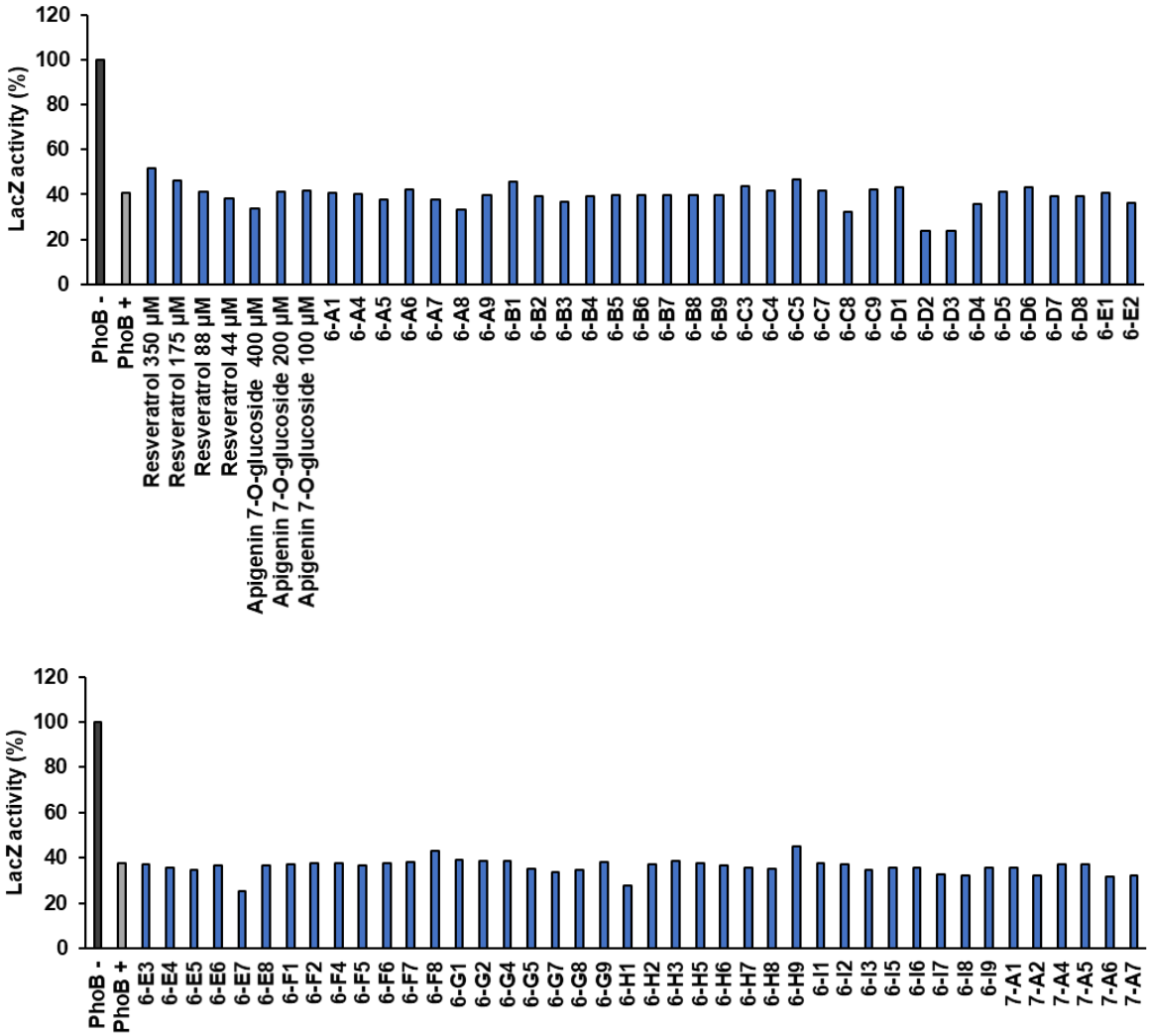

Figure 2.19. Screening results of 74 natural products at 40 µg/mL for PhoB repression activity.
Experiments were done in technical duplicates and mean values are represented.

Furthermore, resveratrol, apigenin 7-O-glucoside and harmine, which showed a weak inhibition of Euo with method 1, did not show inhibitory activity when tested using the optimised method 2 (Figure 2.20). The initial results with apigenin 7-O-glucoside in method 1 is thus likely to be due to the yellow pigmentation of this compound.

In this experiment, three additional flavonoids, naringenin, luteolin and kaempferol were also tested, the two former compounds having been described previously in the literature as having a beneficial effect on *Chlamydiae* pathogenesis [195, 245]. However, none of these compounds showed any repression activity in the Euo-based assay (Figure 2.20).

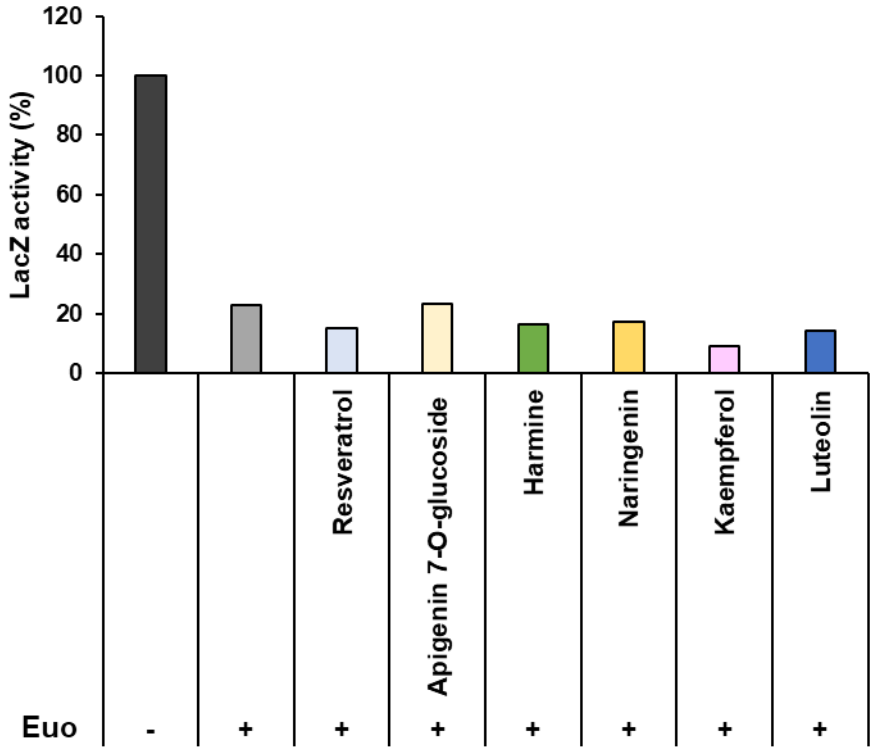

Figure 2.20. LacZ activity measurement of selected natural products.
Natural products were tested at 40 µg/mL using method 2. Experiments were done in biological duplicates and mean values are represented.

Using the revised screening method 2, the natural products library of 2640 compounds was tested for repression of Euo activity. Twelve compounds with a repression inhibition between 10 and 15% were retained.

Randomly chosen 720 natural products (representing 9 plates) were screened in duplicates. Figure 2.21 shows the chemical structures and their corresponding means of repression inhibition of the five compounds measured in duplicates, which showed the highest inhibitory effect. None of the compounds had any influence on growth of *E. coli* during the 3 h incubation step.

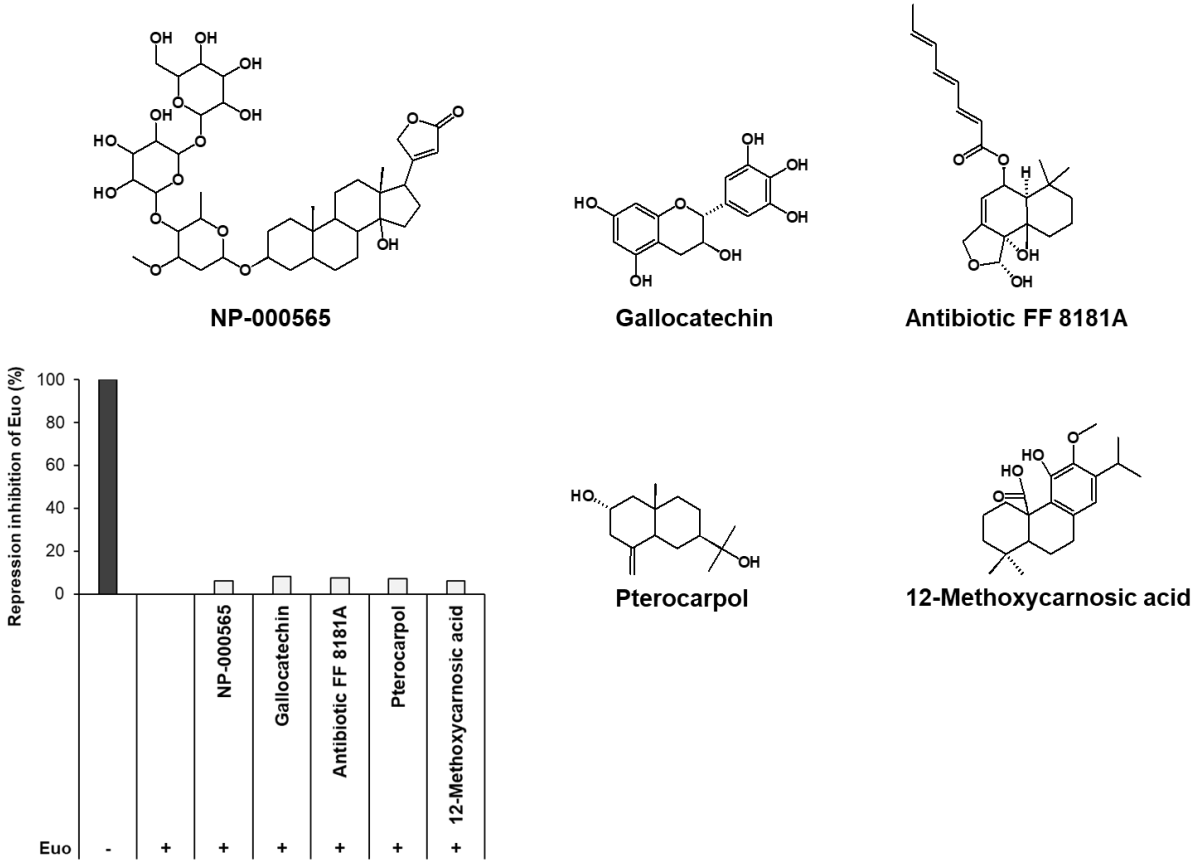

Figure 2.21. The five compounds highest Euo repression inhibition measured in duplicates.

The compound, which showed the strongest effect was (+)-gallocatechin. Gallocatechins have been previously shown to have anti-chlamydial activity when tested for inhibition of proliferation of *C. trachomatis and C. pneumoniae* in cell culture [190, 246]. The inhibitory mechanism to explain the observed decrease in the inclusion count is still unknown, although a damaging effect on the bacterial lipid bilayer has been proposed [247]. Since this compound showed a possible Euo repression effect (8%), the repression activity of both stereoisomers of gallocatechin was evaluated at various concentrations (Figure 2.22).

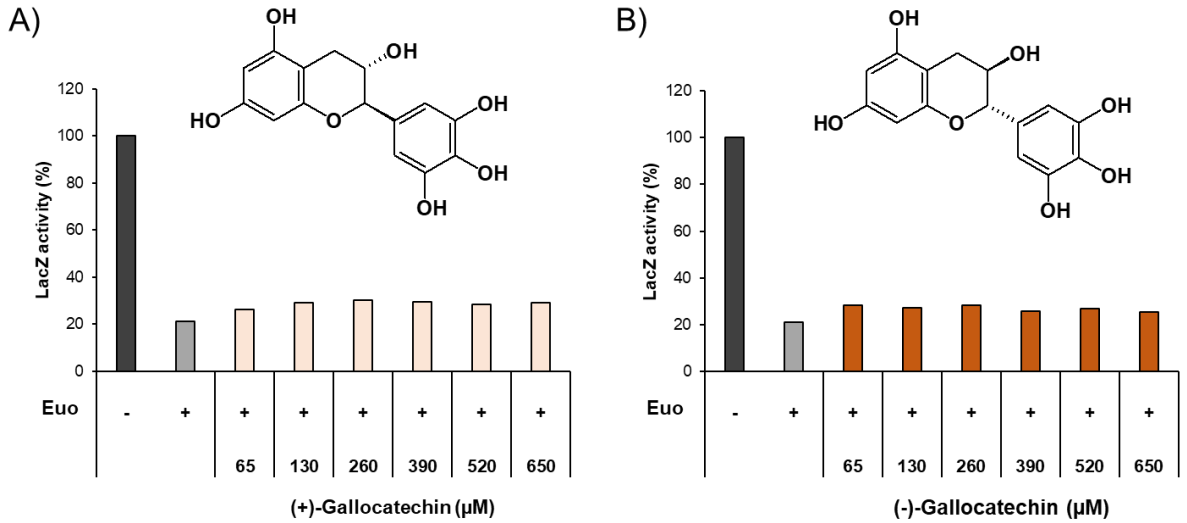

Figure 2.22. LacZ activity of various concentrations of the gallocatechin stereoisomers.
(+)-gallocatechin (A) and (-)-gallocatechin (B). Compounds were tested for Euo repression activity, following method 2 at the concentrations indicated. Experiments were done in technical triplicates and mean values are represented.

No difference in Euo inhibitory effect was seen between the two gallocatechin isomers tested. A compound is considered as a positive result, when its repression activity is at least three times higher (i.e. in this case 23.7%) than that of the control Euo + [229]. None of the screened compounds showed such a high level of repression of Euo activity and therefore none of the compounds tested was considered to be active in this assay.

The cell envelope of Gram-negative bacteria such as *E. coli* consists of an additional outer membrane not present in Gram-positive bacteria, and this confers greater resistance to penetration by antibiotics [248]. Thus, the lack of positive results obtained may be due to specific physicochemical properties of the *E. coli* cell wall. Ebejer *et al.* postulated that the majority of active antibacterial compounds have calculated logP values lying in the range 0–5 [249]. For example, the macrolide and tetracycline classes of antibacterial compounds showed calculated logP values of 3.5 and -0.7, respectively [250]. To investigate the overall distribution of logP values of the 2640 natural products, the Chemicalize database [251] was used (Figure 2.23), and revealed that the majority of molecules had a logP between 0 and 5. Therefore, most of the natural products tested should be capable of passing the *E. coli* cell membrane.

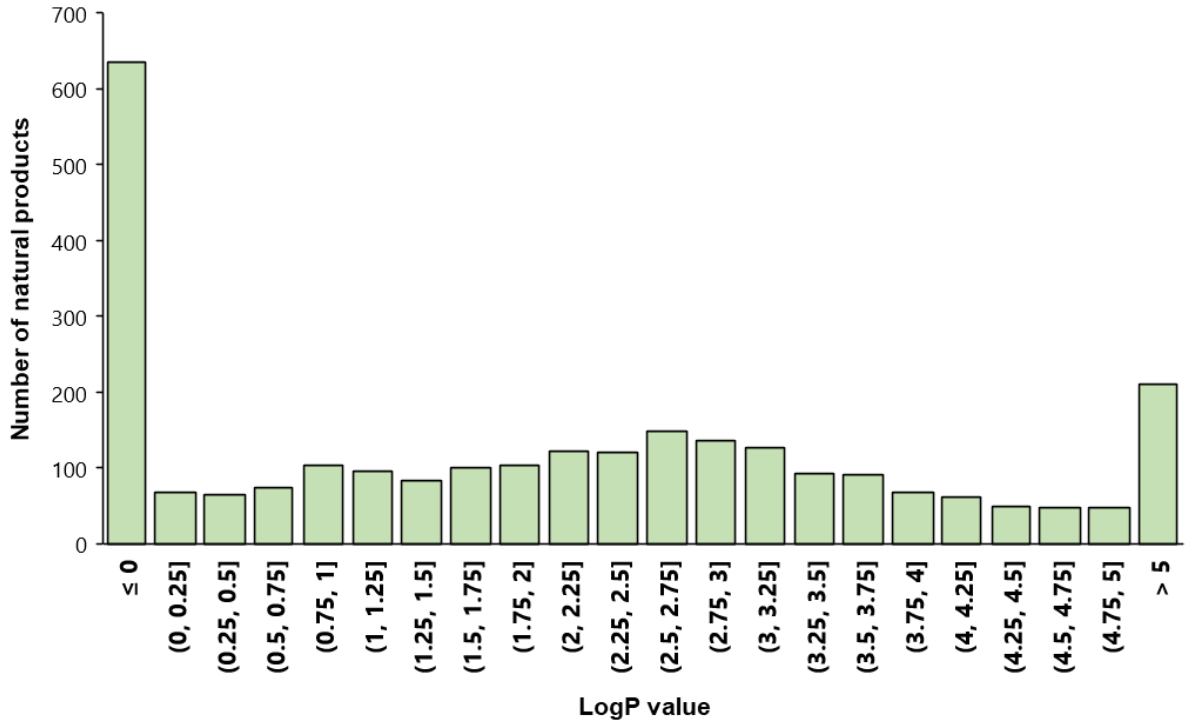

Figure 2.23. Calculated distribution of logP values for the 2640 screened natural products.

2.4 Conclusion

There is clear unmet medical need worldwide for new antibacterial drugs able to combat chlamydial infection. In this section of the project, a high throughput functional assay was developed to screen a collection of plant extracts and natural products for compounds with inhibitory activity against four highly conserved TFs from *W. chondrophila*, NrdR, HrcA, PhoB and Euo. The assay was set up in *E. coli*, and the *lacZ* gene, in which expression was under control of the DNA-binding regions of each of the TFs, provided the readout. All TFs selected are transcriptional repressors and thus the screening was set up to identify antagonistic compounds, which would interfere with TF binding and lead to increased expression of LacZ. Different screening parameters were tested in order to optimise the assay for screening in high throughput mode in 96-well plates. This is the first time such an assay has been developed for *Chlamydia*e.

The main difficulty from the outset of the project was that there are currently no known antagonists for any of the TFs tested, and thus in the absence of a positive control, the assay could not be properly validated. Furthermore, the screening of 175 plant extracts and 2'714 natural products for repression of TF Euo activity failed to identify any positive hits.

Nevertheless, the assay appears to function correctly since robust transcriptional activation of LacZ is observed in the absence of the cognate repressor, and expression is tightly repressed when the TF is co-expressed with the LacZ reporter. Several reasons may be envisaged to explain the lack of hits. The target of the screening as developed, is a single TF and this may be too specific. A chlamydia-specific pathway or even the whole organism could provide a wider screening target, possibly increasing the hit rate. Furthermore, even though some of the compounds used in the screening have known anti-chlamydial activity, this activity does not necessarily work through Euo.

Another issue may be that the *E. coli* Top 10 cell wall is impervious to some or all of the compounds tested, even though the natural product library employed in this screening showed a large number of molecules with low logP values, which theoretically, should have a good chance of crossing the cell membrane. To overcome the problem of low cell permeability, the screening could be established in an *E. coli* mutant strain in which membrane permeability is reduced. For example, mutations such as AS19 or imp4213 showed increased permeability to actinomycin and vancomycin, respectively [252, 253]. Alternatively, molecules such as MAC13243 that render the outer membrane of Gram-negative bacteria more permeable to large-scaffold natural products could be added to the assay buffer [254].

Another explanation could be that the binding affinity of the TFs for their cognate DNA motif may be too high to be displaced by any of the compounds at the concentrations tested. It would be useful to determine the affinity and binding kinetics of the TFs for their different cognate DNA binding motifs. This could be assessed by surface plasmon resonance [255]. Based on such information, the DNA binding affinities could be modified in order to increase the chance that a compound may inhibit the TF interaction with its DNA binding motif. Screening a larger library of compounds could also be useful, and the use of alternative libraries such as small peptides or short DNA or RNA sequences could also be envisaged [256, 257]. Nucleic acid aptamer libraries could be particularly appropriate in the search for inhibitors of TFs.

A further improvement could be to perform an initial pre-screening of the library to select those compounds which are able to bind TFs. Procedures such as electrophoretic mobility shift assay (EMSA) or enzyme-linked immunosorbent assay could be used, and high-throughput procedures for both techniques have been described [258, 259]. Indeed, EMSA has been performed previously using a His_6-tagged Euo protein and a DNA probe that contained the DNA-binding motif of Euo (rhs9) [122]. Any interacting molecules, which emerged from the pre-screening could then be investigated more deeply in a secondary, functional assay.

It is also worth noting that in the screening developed here, some natural products showed an increased Euo repression, and this effect could be investigated further since enhanced repression activity of Euo could also destabilize the bacterial development cycle.

Clearly further optimisation is required and could be performed. This project represents an initial attempt to search for drugs, which could interfere with vital functions required during the infectious cycle of *W. chondrophila,* and while the final outcome was not successful, the methods developed could provide a valuable starting point for further research into chlamydial TFs.

Chapter 3: Functional study of the chlamydial TF DksA

3.1 Introduction

DksA was first described in *E. coli* as a gene that supresses the temperature-sensitive growth and filamentation of a *dnaK* deletion mutant strain [260]. It is highly conserved among Gram-positive and Gram-negative bacteria. In *E. coli*, DksA is a protein (151-amino acids) containing a four-cysteine zinc finger motif. Further analysis revealed that DksA binds directly to the RNA polymerase secondary channel, an opening on the enzyme surface leading to its active centre, thus preventing transcription initiation of several genes involved in bacterial growth [261]. About 7% of all genes in *E. coli* are directly or indirectly regulated by DksA [262].

The main role of DksA is activation of the stringent adaptive response of bacteria to nutritional starvation and other stress conditions. In this role, DksA acts synergistically with the well-described alarmone guanosine pentaphosphate (ppGpp) [263]. Synthesis of ppGpp in *E. coli* is regulated by two enzymes, RelA and SpoT [264, 265]. In response to amino acid limitation, the presence of uncharged tRNAs leads to activation of RelA and synthesis of ppGpp, whereas SpoT has a bifunctional activity, with a weak ppGpp synthase activity and strong ppGpp degrading activity. In conditions of iron limitation, SpoT leads to the accumulation of ppGpp suggesting a role for iron in the SpoT-mediated balance between synthesis and hydrolysis of ppGpp [266]. Overall, the stringent response leads to reduced transcription of stable RNAs (ribosomal and transfer RNA) resulting in a large-scale downregulation of translation [267], which is important for survival in the stationary phase of the bacterial growth cycle. At the same time, synergy between ppGpp and DksA stimulates transcription from promoters upstream of several amino acid biosynthesis genes. DksA is thus a complex DNA-independent TF, which binds to RNA polymerase and, which can be regulated by ppGpp [268, 269].

In other bacteria, DksA has been shown to regulate pathogenicity and also plays a role in biofilm formation [270]. In *P. aeruginosa*, DksA regulates the production of extracellular virulence factors such as elastases, rhamnolipids, phospholipase C, pyoverdine and pyocyanin [271-274], while in *Salmonella typhimurium,* it is important for bacterial virulence, and is involved in the bacterial colonization [275].

Several DksA paralogues exist. For example, some bacteria such as the human pathogen *P. aeruginosa* express 2 DksA proteins [276, 277]. The *P. aeruginosa* DksA2 is positioned downstream of a putative Zur-binding site and the presence of zinc (Zn) leads to the repression of *dksA2* transcription [276]. In Zn-poor environments, this protein serves as a back-up copy of the Zn-dependent DksA1. For example, Zn-limitation has been found to occur in a cystic fibrosis patient infected with *P. aeruginosa,* where Zn was chelated by neutrophil proteins

[278]. It has been proposed that DksA2 plays a role in the Zn homeostasis first by supplying functional copies of DksA and thus increasing cell survival, and second, by liberating Zn from the existing DksA1 molecules. The same mechanism has also been described for Cys-4 Zn-ribbon motifs in some ribosomal protein paralogues [276, 279, 280].

The RNA polymerase (RNAP) binding TFs such as DksA can be divided into sub-groups that act on different domains of RNAP domains. Those, which bind the secondary channel such as DksA are referred to as secondary channel-binding factors (SCBFs). They share a globular C-terminal domain responsible for the RNAP binding and coiled-coil domain, which appears to insert through the secondary channel to modulate transcription [270]. The SCBFs can be subdivided into three functional groups: GreA/B, DksA and factors with unknown function. In *E. coli*, five SCBFs have been identified: GreA, GreB, DksA, TraR and Rnk [262, 281-284].

In the phylum *Chlamydiae,* DksA is part of the coreset of 8 TFs [41] although the mechanism of action of DksA and the presence of ppGpp in these bacteria has not yet been reported, and the two ppGpp synthesizing proteins (RelA and SpoT) are not encoded in the bacterial genome [285, 286]. A proteomics approach designed to identify *C. pneumoniae* proteins expressed during the transition from RBs to EBs revealed a more than 2-fold increase in DksA expression in infected human cells [287]. Applied stress, in form of IFN-γ treatment or heat shock also resulted in a small increase in the expression of DksA, probably involved in induction of the chlamydial persistence response [288]. During the IFN-γ induced persistence, a significant upregulation of proteins involved in amino acid and nucleotide biosynthesis was observed [288, 289]. In addition, the transcriptional response of *C. trachomatis* to iron starvation resulted in a change from bacterial growth to the persistent form for bacterial survival, similar to the stringent response in other bacteria [290]. Surprisingly however, the DksA protein level showed no increase in the iron starvation model.

Chlamydiae are not easily amenable to genetic manipulation and mutants of chlamydial *dksA* have not been described in the literature. Therefore, the function of DksA was tested in a heterologous system. To do this, *W. chondrophila dksA* was cloned into an arabinose-inducible plasmid and transformed into WT or *dksA* mutated strains of *E. coli* and *P. aeruginosa*. The complementation of defects in bacterial growth, ribosomal RNA promoter regulation, DNA repair and the synthesis of virulence factor by the recombinant versions of *W. chondrophila dksA* was then assessed. In general, complementation occurs when a mutated copy of a gene is functionally replaced by a wild-type copy. This approach should allow us to extrapolate our findings in *E. coli* to provide a better understanding of the role of DksA in *Chlamydiae.* This major TF could be an excellent target for new antibacterial agents.

3.2 Materials and Methods

3.2.1 Chemicals

Standard chemicals were obtained from Fluka Chemie AG or Merck KGaA.

3.2.2 Bacterial strains, plasmids and growth conditions

Bacterial strains and plasmids are listed in Table 3.1. Unless otherwise indicated, *E. coli* and *P. aeruginosa* strains were grown at 37°C in LB medium (AppliChem). M9 minimal medium was prepared as described previously [221, 276], and supplemented with 0.2% (w/v) glycerol and 3 mg/mL $FeSO_4 \cdot 7H_2O$. Solid medium in plates (LBA and M9) was prepared by addition of 1.5% (w/v) agar (US Biological). For stable plasmid maintenance in the bacterial host, media were supplemented with antibiotics (all purchased from AppliChem) as follows: tetracycline 10 µg/mL (Tet10) and ampicillin 100 µg/mL (Amp100) were used for *E. coli*, and carbenicillin 200 (Cb200) was used for *P. aeruginosa*. Plasmids were introduced into competent *E. coli* strains by heat-shock at 42°C for 2 min, regenerated for 1h at 37°C in LB without antibiotic then transferred to LBA plates with the appropriate antibiotics and cultured at 37°C overnight [221]. Transformation of *P. aeruginosa* strains was performed by electroporation [291].

Table 3.1. Bacterial strains and plasmids.

Strains and plasmids	Genotype or description	Source
P. aeruginosa		
PT5	PAO1 wild type	Laboratory collection
PAO-RC1	PT5Δ*dksA*, Hg^r	[274]
E. coli		
Top10	F-*mcrA* Δ(*mrr-hsd*RMS-*mcr*BC) Φ80*lac*Z ΔM15 Δ*lac*X74 *rec*A1 *ara*D139 Δ(*araleu*)7697 *gal*U *gal*K *rps*L (Str^R) *end*A1 *nup*G	*
Keio-K12 BW25113	F^- Δ(araD-araB)567 ΔlacZ4787 (::rrnB-3)λ^- rph-1 Δ(rhaD-rhaB) 568 hsdR514	[292]
KeioΔ*dksA*	KeioΔdksA, Tet^r	[293]
RLG5950	VH1000 λrrnB P1 (−61/+1)-lacZ	[294]
RLG7238	RLG5950 Δ*dksA*::tet	[295]
Plasmids		
pBAD24	Cloning vector, Amp^r	[296]
pBAD24-*dksAWC*	*W. chondrophila dksA:His6* on pBAD24; Amp^r	This study
pBAD24-*dksAEC*	*E. coli dksA:His6* on pBAD24; Amp^r	This study
pBAD24-*dksAPA*	*P.* aeruginosa *dksA*:His6 on pBAD24; Amp^r	This study
pBAD24-*dksA_cinAWC*	*W. chondrophila dksA* to *cinA* genes on pBAD24; Amp^r	This study
pHERD20T	Cloning vector, Amp^r	[297]
pHERD20T-*dksAWC*	*W. chondrophila dksA:His6* on pHERD20T; Amp^r	This study
pHERD20T-*dksAEC*	*E. coli dksA:His6* on pHERD20T; Amp^r	This study
pHERD20T-*dksAPA*	*P. aeruginosa dksA:His6* on pHERD20T; Amp^r	This study
pHERD20T-*dksA_cinAWC*	*W. chondrophila dksA* to *cinA* genes on pHERD20T; Amp^r	This study

* Thermo Fisher Scientific.
Abbreviations of selection reagents: Amp: ampicillin; Hg: mercury; Tet: tetracycline.

3.2.3 DNA and protein sequences

Sequences of the *dksA* genes and encoded proteins of *W. chondrophila* (ATCC VR-1470), *E. coli* and *P. aeruginosa* were taken from the Kyoto encyclopedia of genes and genomes database [298]. *W. chondrophila* genomic DNA was a kind gift from Prof. Greub from the Institute of Microbiology of the University Hospital Center and University of Lausanne (CHUV). *In silico* analysis was performed using the Protein Homology/analogY Recognition Engine V 2.0 (Phyre2) (at >90% accuracy) [299] and protein sequences were aligned using protein BLAST [136].

3.2.4 DNA manipulation and cloning procedures

Restriction enzymes, T4 DNA ligase, calf intestinal alkaline phosphatase and *Pfu* DNA polymerase (Promega Corporation). Standard protocols for DNA modification and cloning were followed [221]. For plasmid purification, the GenElute™ plasmid miniprep kit (Sigma-Aldrich) was used according to the supplier's instructions. All plasmid inserts were verified by Sanger DNA sequencing (Fasteris SA) using the primers described in Table 3.2.

Table 3.2. Primers for cloning and Sanger DNA sequencing.

Primers	Gene	Sequence (5'-3')	Purpose
DksA WC His-Tag fwd	*dksA-WC*	GCCCCATGGCGCTCAAGAAAAGTGAAGTTG	*
DksA WC His-Tag rev		GCCAAGCTTTTAATGATGATGATGATGATGC AGCAATCCTTTTTCCATCTGC	
DksA EC His-Tag fwd	*dksA-EC*	GCCCCATGGAAGAAGGGCAAAACCGTAAAAC	*
DksA EC His-Tag rev		GCCAAGCTTTTAATGATGATGATGATGATGGC CAGCCATCTGTTTTTCGC	
DksA PA His-Tag fwd	*dksA-PA*	GCCCCATGGCCACCAAAGCAAAACAACAG	*
DksA PA His-Tag rev		GCCAAGCTTTCAATGATGATGATGATGATGGG AGCCGAGTTGCTTCTCGC	
DksA_cinAWC fwd	*dksA_cinA-WC*	ATACCCGGGATGGCGCTCAAGAAAAGT	*
DksA_cinAWC rev		ATACTGCAGTTACACATTGTACTGCTTACTATATAAGATAAG	
DksA_cinAWC no 1		GATCATGGGGCTCTGCC	°
DksA_cinAWC no 2		GCCTGTTGTGCAGTTGC	°
DksA_cinAWC no 3		GATGTGACGCGGCATG	°
DksA_cinAWC no 4		GTCCGATAGCGGACAGA	°
DksA_cinAWC no 5		GCCAAGCTTGGGAAATGCTTCTTTCCTGC	°

* Cloning/Sequencing
° Sequencing
The restriction sites are underlined.
Abbreviations: WC: *W. chondrophila*; EC: *E. coli*; PA: *P. aeruginosa*.

Plasmid constructs

For complementation assays, the pBAD24 vector was used for *E. coli* strains and the pHERD20T vector for *P. aeruginosa* strains (Table 3.1).

His$_6$ tagged *dksA*: *W. chondrophila dksA* (384 bp), *E. coli dksA* (474 bp) and *P. aeruginosa dksA* (465 bp) were amplified by PCR from genomic DNA using gene-specific primers, which also encoded the C-terminal His$_6$ tag (Table 3.2). PCR amplification products were cloned into the strain-specific vectors after digestion with *NcoI* and *HindIII* and gel purification [221]. Final plasmid constructs (Table 3.1) were confirmed by DNA sequencing using the primers shown in Table 3.2. Plasmids were then transformed as appropriate into the *E. coli dksA* mutants (KeioΔ*dksA* and RLG7238), the *E. coli* parent strain (Keio K-12), the *P. aeruginosa dksA* mutant (PAO-RC1) or *P. aeruginosa* parent strain (PT5).

pBAD24-*dksA_cinAWC* in *E. coli*: A 2850 bp fragment containing the *W. chondrophila* genomic region extending from the *dksA* gene down to and including the *cinA* gene, was amplified by PCR from genomic DNA using primers shown in Table 3.2. The PCR amplification product was digested with *PstI* and *SmaI* and cloned into the corresponding sites of pBAD24. This construct (Table 3.1) was sequenced with primers DksA_cinAWC, nos. 1-4 from Table 3.2 and transformed into the *E. coli* strains KeioΔ*dksA* and Keio-K12.

pHERD20T-*dksA_cinAWC* in *P. aeruginosa*: the pBAD24-*dksA_cinAWC* plasmid and the pHERD20T vector were digested with *PstI* and *SmaI* and the corresponding DNA fragments were purified and ligated to obtain pHERD20T-*dksA_cinAWC* (Table 3.1). This construct was sequenced with primer DksA_cinAWC no 5 from Table 3.2 and transformed into *the P. aeruginosa* strains PAO-RC1 and PT5.

Simplified nomenclature: the parent strains *E. coli* Keio K-12, *E. coli* RLG5950 and *P. aeruginosa* PT5 containing empty plasmid were referred as wild type (wt). Keio∆*dksa* containing pBAD24-*dksAWC*, pBAD24-*dksAEC*, pBAD24-*dksAPA,* pBAD24-*dksA_cinA* or pBAD24-*Ø*, and PAO1-RC1 containing pHERD20T-*dksAWC*, pHERD20T-*dksAEC*, pHERD20T-*dksAPA,* pHERD20T-*dksA_cinAWC* or pHERD20T-*Ø* are referred to as p*dksA-WC*, p*dksA-EC*, p*dksA-PA,* p*dksA_cinA* and ∆*dksA*, respectively. *E. coli* RLG7238 containing pBAD24-*dksAWC*, pBAD24-*dksAEC*, pBAD24-*dksAPA* are referred to as p*dksA-WC*, p*dksA-EC*, p*dksA-PA* and ∆*dksA*, respectively.

3.2.5 Western blot

Buffers, solutions and reagents for Western blotting were prepared as previously described [221]. Overnight cultures of Keio∆*dksa* or PAO1-RC1 containing p*dksA-WC*, p*dksA-EC* or p*dksA-PA* were diluted to an OD_{600} of 0.05 in LB. Induction of *dksA* with 0.02% arabinose (Fluka Chemie) was started after 2 h at 37 °C and 260 rpm. After 3 h of induction (5 h for *P. aeruginosa* strains), the OD_{600} was measured and 1 mL of each culture was centrifuged at maximal speed to pellet the cells. Supernatants were discarded and the cell pellets were resuspended in 2x sample buffer to obtain a final protein concentration of 2 mg/mL, assuming that 1 OD_{600} unit corresponds to 5 x 10^8 cells and 0.175 mg/mL of total protein. Samples were sonicated to fragment the DNA and proteins were denaturated at 90°C for 5 min. 30 µg of each sample was loaded on a 4-20% Mini-PROTEAN® TGX™ precast protein gels (Pierce™, Bio-Rad, Hercules, CA, USA) and run at 30 mA in Native Page™ running buffer (AppliChem) containing 0.1% (v/v) SDS (AppliChem). The PageRuler™ pre-stained protein ladder (Thermo Fisher Scientific) provided molecular weight standards. Proteins were transferred to a 0.2 µM nitrocellulose membrane using the iBlot™ 2 system (Thermo Fisher Scientific). Homogeneous transfer of proteins to the membrane was checked by staining with 2% Ponceau S solution. Non-specific binding to membranes was blocked using 4% (w/v) milk powder in TBST for 1 h with constant agitation. Primary antibody against penta-His tag (Thermo Fisher Scientific) was diluted 1:5000 in 4% (w/v) milk-TBST. Membranes were incubated with antibody for 2 h at RT with gentle agitation. After 3 washes with TBST and once with 4% (w/v) milk-TBST for 10 min, membranes were incubated with peroxidase-coupled anti-mouse IgG (whole molecule) (Sigma-Aldrich) diluted 1:5000 in 4% (w/v) milk-TBST for 45 min with gentle agitation. Proteins were detected by chemiluminescence as previously described [300]. Membranes were exposed immediately to autoradiographic film and images were developed using the SRX-101A film processor (Konica Corporation, Tokyo, Japan).

3.2.6 Complementation tests

3.2.6.1 Growth test in liquid M9 medium

Cultures of Keio∆*dksa,* Keio-K12, PAO1-RC1, each transformed with p*dksA-WC*, p*dksA-EC*, p*dksA-PA* or vector alone (∆*dksA)* were grown overnight in LB. Cells were washed with M9 medium, and normalized to an OD_{600} of 0.05 with M9 medium. Induction of *dksA* was started by addition of 0.02 or 0.2% arabinose. Bacterial growth was measured at OD_{600} for 24 h at 37°C with continuous shaking using the Synergy HT microplate reader. Expression tests using

Keio∆*dksa*, Keio-K12, PAO1-RC1 and PT5 containing the p*dksA_cinAWC* construct or the empty plasmid were performed as described above.

Metal salts and supplements for growth experiment: 0.2% (w/v) casamino acids (Becton, Dickinson and Co., Franklin Lakes, NJ, USA), 25 µM $ZnCl_2$, 25 µM $NiSO_4$, 25 µM mM $CoCl_2$; 25 µM $CuSO_4$, and 100 µM Ethylenediaminetetraacetic acid (EDTA) (AppliChem) were added as indicated.

3.2.6.2 Growth test on solid medium

For M9 medium plates: Overnight cultures of Keio∆*dksa,* Keio-K12, PAO1-RC1 or PT5 containing p*dksA-WC*, p*dksA-EC*, p*dksA-PA* or vector alone in LB were washed three times with M9 medium and normalized to an OD_{600} of 1. To test bacterial growth, 10 µL of each culture was spread on agar plates containing M9 medium, without or with 0.02 or 0.2% arabinose, and incubated for 24 h at 37°C.

For LBA plates: Overnight cultures of Keio∆*dksa,* Keio-K12, PAO1-RC1 or PT5 containing p*dksA-WC*, p*dksA-EC*, p*dksA-PA* or ∆*dksA*, were diluted to an OD_{600} of 0.05. To test bacterial growth, 10 µL of each culture was spread on LBA plates containing 0.02 or 0.2% arabinose and incubated for 24 h at 37°C.

3.2.6.3 Mitomycin C assay

Cultures of Keio-K12 and Keio∆*dksa* containing p*dksA-WC*, p*dksA-EC*, p*dksA-PA* or ∆*dksA*, were grown overnight in LB and normalized with LB medium to an OD_{600} of 1. To test bacterial growth, 10 µL of each culture was spread on LBA plates containing 0.5 µg/mL mitomycin C (Sigma-Aldrich), without or with 0.02 or 0.2% arabinose [301]. Plates were incubated at 37°C for 24 h.

3.2.6.4 LacZ activity assay

For these experiments the strain RLG7238, an *E. coli dksA* mutant strain was used, which contains an integrated copy of the *rrn* P1 promoter-*lacZ* fusion.

Overnight cultures of RLG7238 transformed with p*dksA-WC*, p*dksA-EC*, p*dksA-PA* or vector alone (∆*dksA*) in LB were diluted to an OD_{600} of 0.5 in fresh LB. After incubation for 2 h, 200 rpm at 30°C, cultures were induced by addition of 0.02 or 0.2% arabinose and incubated for a further 3 h, 200 rpm at 30°C. Non-transformed wt cells were processed in parallel. To measure

OD_{600}, 100 µL of each bacterial culture was transferred to black 96-well clear bottom plates (Corning Incorporated) and cells were lysed by addition of FastBreak™ reagent to a final concentration of 10% (v/v) followed by incubation for 15 min at RT on an orbital shaker at 250 rpm. To measure LacZ activity, the galactosidase substrate, DDAOG (Thermo Fisher Scientific), was added to a final concentration of 5.5 µM and the fluorescence signal at $F_{590/680}$ was recorded for 10 min at 28°C using a Synergy HT microplate reader (gain: 60, optics position: top, read height: 1.00 mm) and calculated using the Gen5 version 2.04.11 software (BioTek® Instruments). LacZ activity in DDAOG units was calculated after 9 min as follows:

$$\text{LacZ activity (DDAOG Units)} = \frac{F_{590/680}}{(OD_{600} * t)}$$

Time (t) calculated in min
$F_{590/680}$: excitation/emission at 590/680 nm

3.2.6.5 Pyocyanin assay

To purify pyocyanin, overnight cultures of PAO1-RC1 containing pHERD20T-*dksAWC*, pHERD20T-*dksAEC*, pHERD20T-*dksAPA* or pHERD20T-Ø, and PT5 containing pHERD20T-Ø were grown in LB Lennox, which contains half the amount of NaCl compared to standard LB and which was prepared as previously described [221]. LB Lennox was used to enhance the production of pyocyanin in these strains. Cultures were diluted to an OD_{600} of 0.01 with fresh LB Lennox, and incubated for 24 h at 37°C, 260 rpm in the presence or absence of 0.02% arabinose. Pyocyanin was isolated from 10 mL of culture supernatant using TPP® (Greiner Bio-One, St. Gallen, Switzerland), chloroform resistant centrifuge tubes as previously described [302]. Detection was performed at OD_{520} in acidic solution using the WPA Biowave DNA Life Science spectrophotometer. The concentrations, expressed as micrograms of pyocyanin produced per milliliter of culture supernatant, were determined by multiplying the OD_{520} by 17.072 [303].

3.2.7 Experimental design

Experimental replicates were performed using starting cultures derived from independent bacterial colonies as described in the legends to Figures. Standard deviations were calculated when at least three biological replicates were performed.

3.3 Results and Discussion

3.3.1 Primary sequence and structural similarities between DksA proteins of *W. chondrophila*, *E. coli* and *P. aeruginosa*

Predicted secondary structures of *W. chondrophila*, *E. coli* and *P. aeruginosa* DksA proteins are shown in Figure 3.1. All structures are highly similar with a central coiled-coil domain consisting of two long alpha helices connected by a linker, as well as an additional alpha helical domain at the C-terminus.

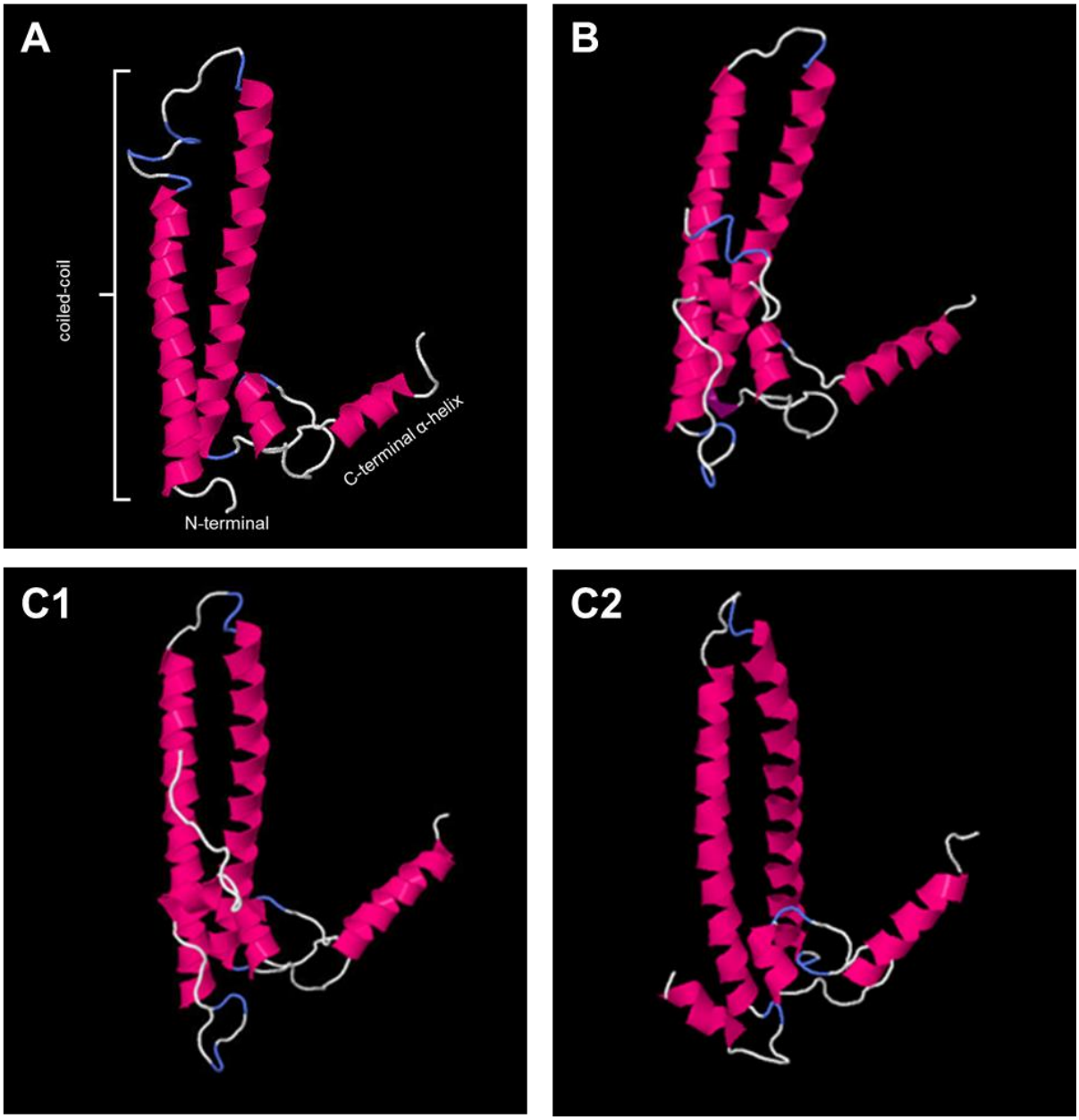

Figure 3.1. Protein structure predictions of *W. chondrophila* DksA (A), *E. coli* DksA (B) and *P. aeruginosa* DksA1 (C1) and DksA2 (C2).
α-helix secondary structures are shown in pink and *β*-turns in blue.

The central coiled-coil domain together with the DXXDXA motif within the linker were found to be important for the binding of DksA to the RNA polymerase secondary channel [304], although in *W. chondrophila,* the DXXDXA motif is absent (Figure 3.2A) and the linker is longer (Figure 3.1A). Amino acid sequence alignment of the *W. chondrophila*, *E. coli* and *P. aeruginosa* proteins shows that the canonical Cys4 zinc finger motif present in *E. coli* DksA and *P. aeruginosa* DksA1 is missing in *W. chondrophila* DksA, which also contains a shorter N-terminus (Figure 3.2A). Like *W. chondrophila,* the *P. aeruginosa* DksA2 also lacks the Cys4 zinc finger motif [276], although interestingly, *P. aeruginosa* DksA2 was able to complement the *E. coli dksA* deletion.

A phylogram based on these sequences showed that *W. chondrophila* DksA is most closely related to *P. aeruginosa* DksA2 (Figure 3.2B). Protein sequence alignments of *W. chondrophila* DksA with *E. coli* DksA and *P. aeruginosa* DksA1 and DksA2, showed 26, 29 and 28% identity, respectively. (*E. coli* Dksa aligned with *P. aeruginosa* DksA1 and DksA2 showed 75 and 37% identity, respectively). Overall, *W. chondrophila* DksA had the shortest protein sequence and was most similar to *P. aeruginosa* DksA2.

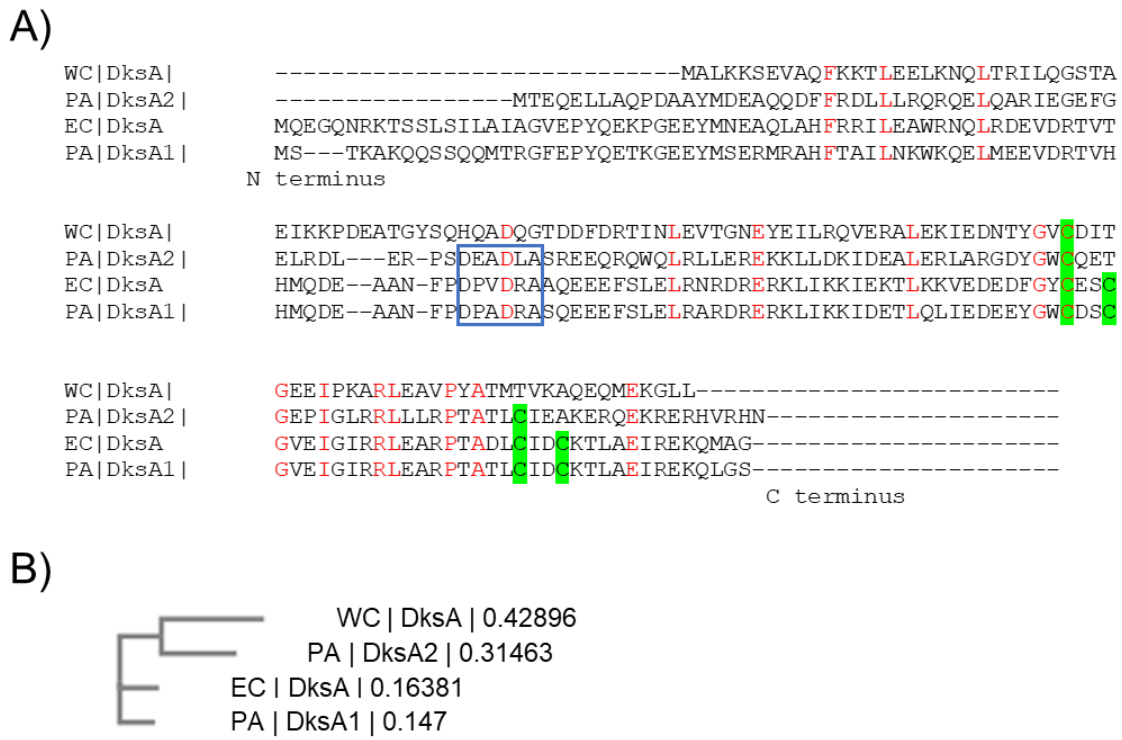

Figure 3.2. Alignment (A) and phylogram (B) of DksA sequences of *W. chondrophila, E. coli* and *P. aeruginosa* (DksA1 and DksA2).
Protein sequences comparison and phylogram of *W. chondrophila* (WC), *P. aeruginosa* (PA) (DksA1 and DksA2) and *E. coli* (EC) DksA made by Clustal Omega [305]. Identical amino acids are shown in red, the zinc finger domain is shown in green and DXXDXA motif is framed in blue.

3.3.2 Expression of *dksA* from *E. coli*, *W. chondrophila* and *P. aeruginosa* in *dksA* mutants of *E. coli* and *P. aeruginosa*

For the complementation experiments, *W. chondrophila dksA* was fused to a 3' His_6-Tag and cloned into the appropriate arabinose inducible vector. The corresponding His_6-tagged versions of *dksA* from *E. coli* and *P. aeruginosa* were also prepared as control plasmids. All three plasmids were transformed into the *dksA*-deleted strains of *E. coli* and *P. aeruginosa* and expression of the His_6-tagged proteins following arabinose induction was monitored by western blotting using the anti-His_6 antibody (Figure 3.3).

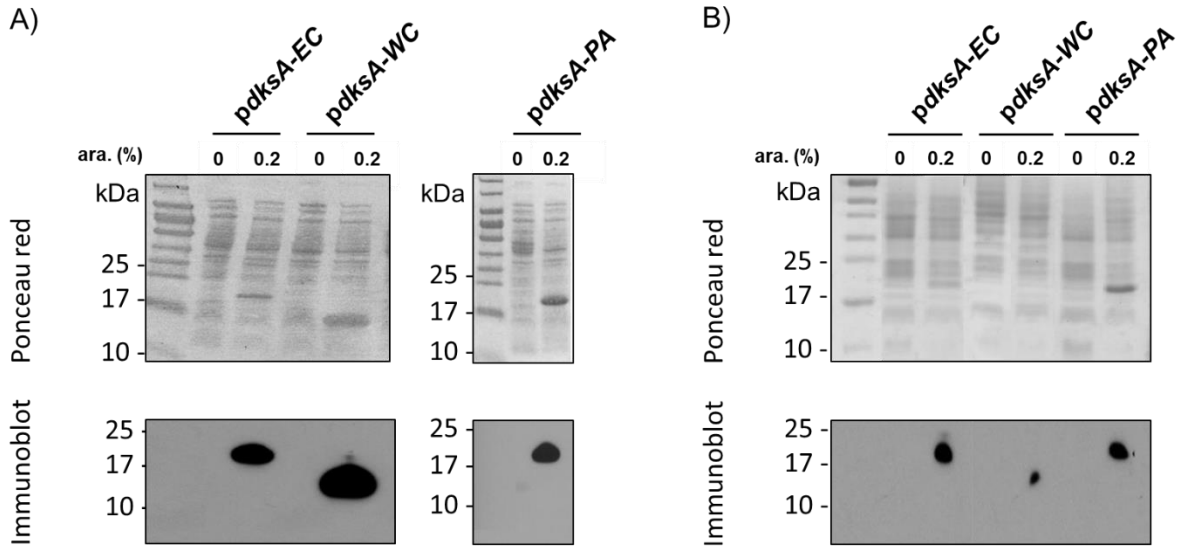

Figure 3.3. Immunoblot of DksA from *E. coli, W. chondrophila* and *P. aeruginosa*.
Loading controls (upper panels) and western blots (lower panels) performed on total protein extracts from *E. coli dksA* mutant (A) and *P. aeruginosa dksA* mutant (B). The expression plasmids and arabinose (ara.) concentration are indicated.

Protein bands of around 18 kDa, 14 kDa and 18 kDa, corresponding to the predicted molecular weights of the *E. coli, W. chondrophila* and *P. aeruginosa* DksAs, respectively, were seen in the arabinose-induced samples in both hosts. The level of *W. chondrophila* DksA in *P. aeruginosa* appears to be somewhat lower than in *E. coli* although this may be due in part to a problem of protein transfer during western blotting. Nevertheless, these results confirm that both heterologous hosts are able to express the full length *W. chondrophila* DksA.

3.3.3 Toxicity test of overexpressed *W. chondrophila dksA* in *E. coli* and *P. aeruginosa*

To test whether overexpression of *W. chondrophila* DksA may be toxic for the heterologous host, the *W. chondrophila dksA* gene was overexpressed in the *E. coli* parent strain grown in minimal M9 medium. This medium contains only salts and nitrogen without amino acids, and will only support growth of *E. coli* when *dksA* is functional, while no growth is seen in the Δ*dksA* strain (Figure 3.4).

Overexpression of *E. coli dksA* in these cells showed a slight reduction in growth rate, whereas overexpression of both *W. chondrophila dksA* and *P. aeruginosa dksA* in 0.2% arabinose showed a severe growth inhibition of the *E. coli* parent strain. This effect could be somewhat mitigated using 0.02% arabinose to induce transcription, and this was especially the case for *W. chondrophila dksA*. Furthermore, the higher toxicity of *W. chondrophila* DksA compared to the *E. coli* protein could be at least in part due to its higher protein expression as evidenced by western blotting (Figure 3.3A). Toxicity of DksA overexpression has been reported previously, and shown to be the result of negative regulation of rrnB P1, which is important for bacterial growth [306].

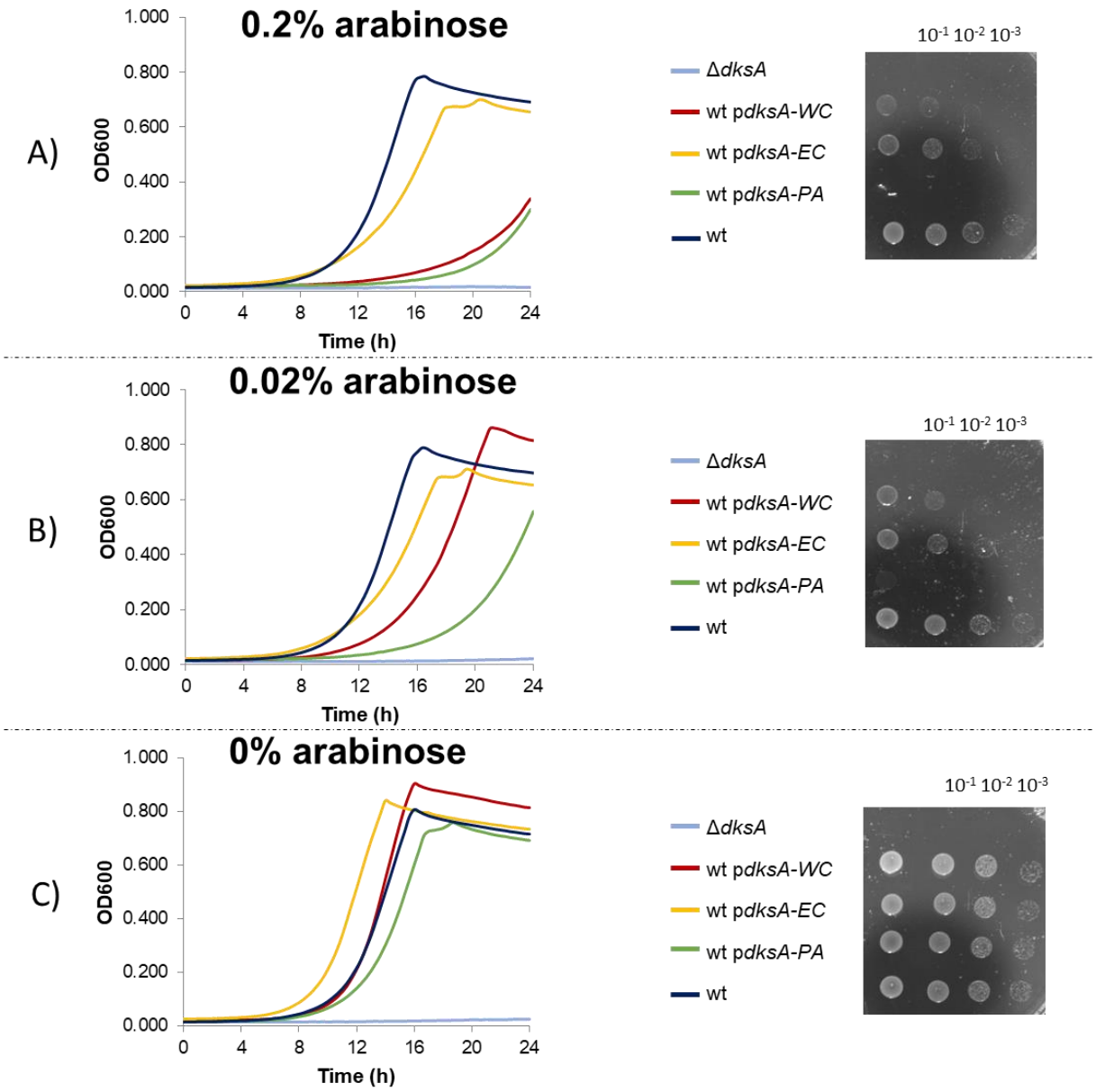

Figure 3.4. Overexpression of *dksA* in *E. coli* wildtype.
(Left) Growth curves of Δ*dksA*, wt containing p*dksA-WC*, p*dksA-EC* or p*dksA-PA*, and wt in M9 minimal medium with 0.2% arabinose (A), with 0.02% arabinose (B) and without arabinose (C) are shown. Experiments were done in technical triplicates and mean values are represented. (Right) The same strains were plated on solid minimal M9 medium with the indicated arabinose concentrations: None, 10^{-1}, 10^{-2} and 10^{-3} dilutions of normalized cultures in minimal M9 medium are shown.

To test if the toxic effect is only related to the stringent response, *W. chondrophila dksA* was expressed in the *E. coli* and *P. aeruginosa dksA* mutant strains and grown on LBA plates containing 0, 0.02 and 0.2% arabinose (Figure 3.5). Induction of *W. chondrophila dksA* did not affect growth of either host in rich medium, and the same result was seen in parallel experiments using the *E. coli dksA* and *P. aeruginosa dksA* control plasmids. These results demonstrated that the toxic effect of DksA overexpression is only associated with the stringent response. In the next step, several complementation assays with *W. chondrophila dksA* in *E. coli* and *P. aeruginosa dksa* mutants were performed.

Figure 3.5. Overexpression of DksA in the *dksA* deletion strains of *E. coli* and *P. aeruginosa*.
The strains indicated were plated on LBA medium containing arabinose as shown and incubated at 37°C for 24 h.

3.3.4 Complementation tests in *E. coli* and *P. aeruginosa*

3.3.4.1 Suppression tests of the amino acid auxotrophy

3.3.4.1.1 Auxotrophy suppression in *E. coli* and *P. aeruginosa dksA* mutants

Deletion of the *E. coli dksA* gene leads to amino acid auxotrophy and this strain requires exogenous amino acids in the medium in order to grow. To determine whether expression of *W. chondrophila* DksA can functionally replace DksA of *E. coli* and/or *P. aeruginosa*, plasmids containing the arabinose inducible *dksA* genes from *W. chondrophila, E. coli* and *P. aeruginosa* were transformed into the *dksA* mutant strains of *E. coli* and *P. aeruginosa* and grown in minimal M9 medium lacking amino acids (Figure 3.6). The results show that *W. chondrophila dksA* is not able to complement the growth defect of the *E. coli* and *P. aeruginosa dksA* mutants.

The overexpression of *dksA* from all three bacteria using 0.2% arabinose was toxic for growth of the *E. coli dksA* mutant (Figure 3.6A), which was already seen for *P. aeruginosa dksA1* [276, 306] even though surprisingly, toxicity was not observed in the wt strain (Figure 3.6A). Toxicity might be reduced using a lower concentration of arabinose to induce transcription, as

seen previously by Potrykus *et al.* [306]. However, even in the absence of the inducer, the phenotype of *E. coli dksA* mutant was rescued by *P. aeruginosa dksA and E. coli dksA,* probably due to basal expression of their promoters.

For unknown reason, the strong toxicity effect is higher in *E. coli dksA* mutant (Figure 3.6A) than in wt (Figure 3.6A). This could indicate that the His_6 tag may in part be responsible for the increased toxicity.

In the *P. aeruginosa dksA* mutant, the toxic effect due to overexpression of *P. aeruginosa dksA* and *E. coli dksA* was less apparent (Figure 3.6B) and for *P. aeruginosa dksA and E. coli dksA,* the level of complementation followed the concentrations of arabinose. However, this was not seen for *W. chondrophila dksA*. Overall, these results showed that *W. chondrophila dksA* was not able to rescue the amino acid auxotrophy of *E. coli dksA* (Figure 3.6A) or *P. aeruginosa dksA* (Figure 3.6B).

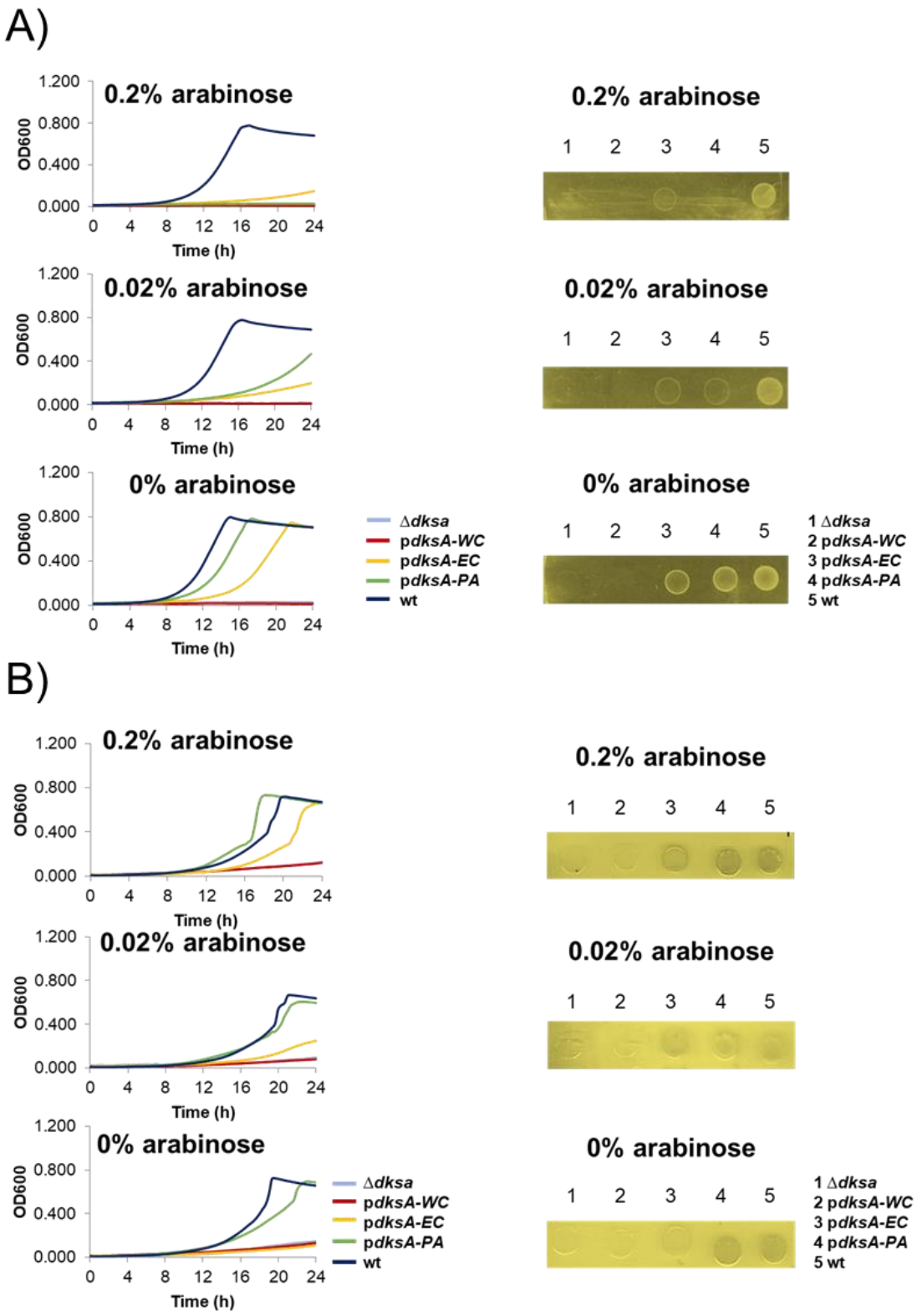

Figure 3.6. Complementation of *E. coli* and *P. aeruginosa* growth.
Growth experiments in liquid M9 medium (left) and on solid M9 medium plate (right) using different arabinose concentrations were done with indicated *E. coli dksA mutants* (A), and *P aeruginosa dksA mutants* (B). Δ*dksA* and wt were used as controls. Experiments were done in technical triplicates and performed at least twice. Mean values are represented.

3.3.4.1.2 Auxotrophy suppression in *E. coli* and *P. aeruginosa dksA* mutants using the complete putative *dksA* operon.

From the genomic sequence of *W. chondrophila* it is likely that *dksA* may be part of an operon containing other co-expressed genes (Figure 3.7), and thus it is possible that the genes located downstream of *dksA* and transcribed in the same orientation are required for full *W. chondrophila* DksA function. The protein encoded upstream of *dksA,* NrdR, is another TF, which has a different mode of action from DksA and is not involved in the stringent response, thus it is unlikely to be part of the same operon. The *lspA* gene is located 9 bp downstream of the *dksA* gene and encodes a lipoprotein signal peptidase that removes the signal peptide from prolipoproteins thus releasing the mature protein into the periplasm [307]. A further 13 bp downstream of *lspA*, the *wcw_1748* gene encodes a hypothetical protein of unknown function. The *cinA* gene is located 268 bp downstream of *wcw_1748* and it is not clear whether it is part of the same operon. Nevertheless, it was included in the expression construct. It should be noted that in *E. coli* and *P. aeruginosa,* the *dksA* genes are not located within the same gene cluster.

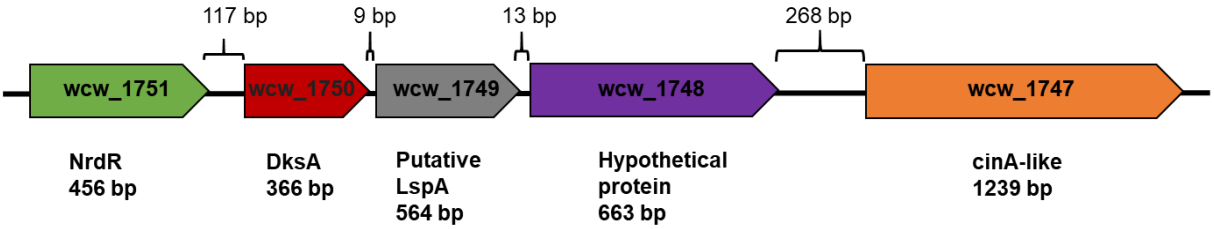

Figure 3.7. Gene(s) located up- and downstream of *W. chondrophila dksA*.
Genes located up- and downstream of the *dksA* (wcw_1750) in the *W. chondrophila* genome are shown. The corresponding protein names and their size in base pairs (bp) are presented below each gene, and between the genes, the intergene distances are shown in bp.

The experiments described in Figure 3.6 using *W. chondrophila dksA* alone were repeated using new constructs, which express the entire genomic region from the *dksA* gene to the *cinA*-like gene. These plasmids are referred to as pBAD24-dksA_cinAWC, and pHERD20T-dksA_cinAWC for expression in *E. coli and P. aeruginosa*, respectively. The plasmids were transformed into both the *dksA* mutant and the corresponding wt strains.

The previously observed toxicity of the *W. chondrophila dksA* gene for growth of the *E. coli* parent strain was also seen using the extended construct expressing the entire region (Figure 3.8A), although compared to Figure 3.6, the expression of *W. chondrophila dksA_cinA* genes in wt cells showed lower toxicity in both 0.02 and 0.2% arabinose. As discussed above, this may be due to an effect of the His_6 tag, which is missing in the extended construct. Another

possibility could be that the *dksA_cinA* genes are less well expressed. This toxic effect was not seen in *P. aeruginosa* parent strain (Figure 3.8B), however, the complementation results showed that *W. chondrophila dksA_cinA* could not rescue the growth defect seen in the *E. coli* and *P. aeruginosa dksA* mutants.

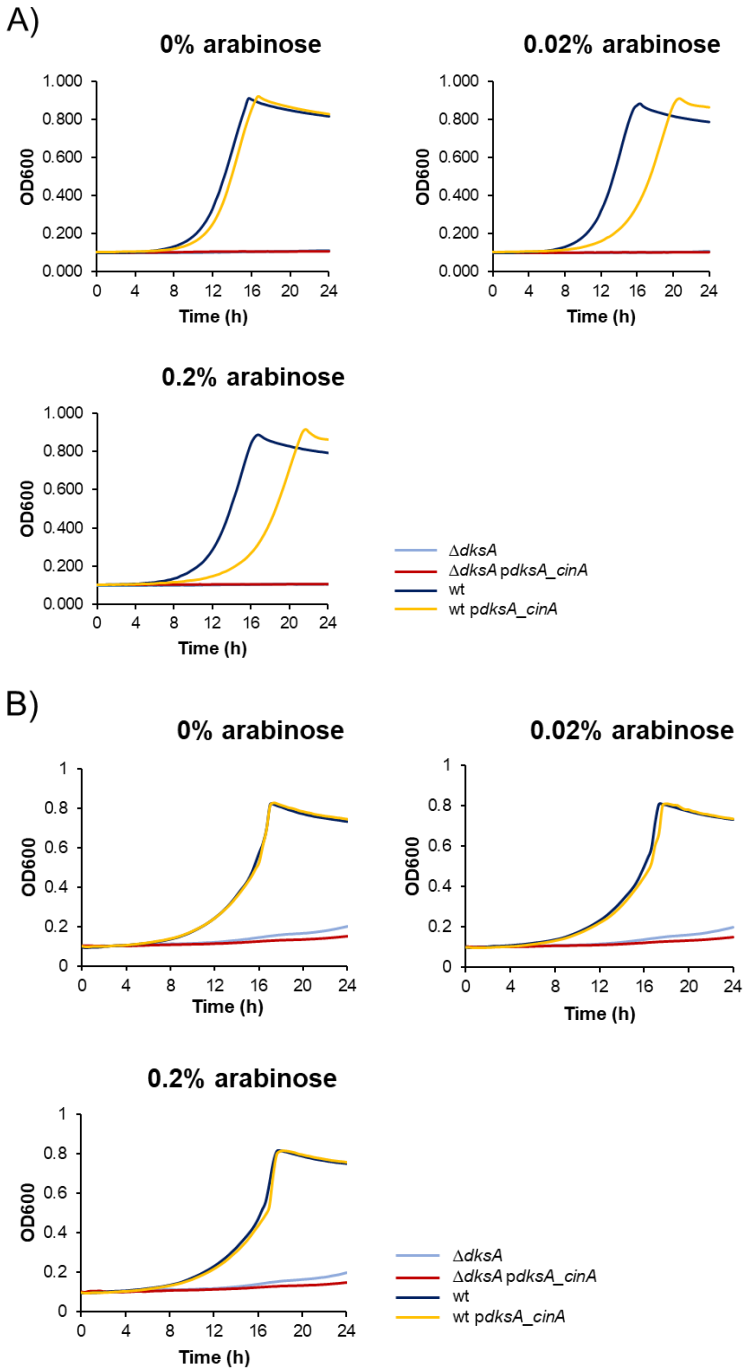

Figure 3.8. Growth test of genes located downstream of *W. chondrophila dksA*.
Growth curves of *E. coli dksA* mutant and wt (A), and *P. aeruginosa dksA* mutant and wt (B) containing either empty plasmid or pDksA_cinA. Experiments were performed in liquid M9 medium containing the supplements indicated. Experiments were done in technical triplicates and mean values are represented.

3.3.4.1.3 Effect of metal depletion on the auxotrophic phenotype of the *E. coli dksA* mutant

In the literature, it has been reported that when EDTA is added to M9 medium *P. aeruginosa dksA2* was able to functionally replace *P. aeruginosa dksA* [276]. EDTA is a metal chelator that can lead to metal depletion. In *P. aeruginosa,* EDTA together with Co or Ni were able to suppress the growth defect of a *P. aeruginosa dksA* mutant [276]. In our experiments, growth of *E. coli* transformed with p*dksA-WC* was followed using liquid M9 medium containing EDTA and supplemented with different metals (Figure 3.9). These experiments showed that none of the metals added in combination with EDTA could restore the functionality of *E. coli dksA*. As a positive control, addition of casamino acids (consisting of a mixture of amino acids) to M9 medium was able to substantially restore normal bacterial growth.

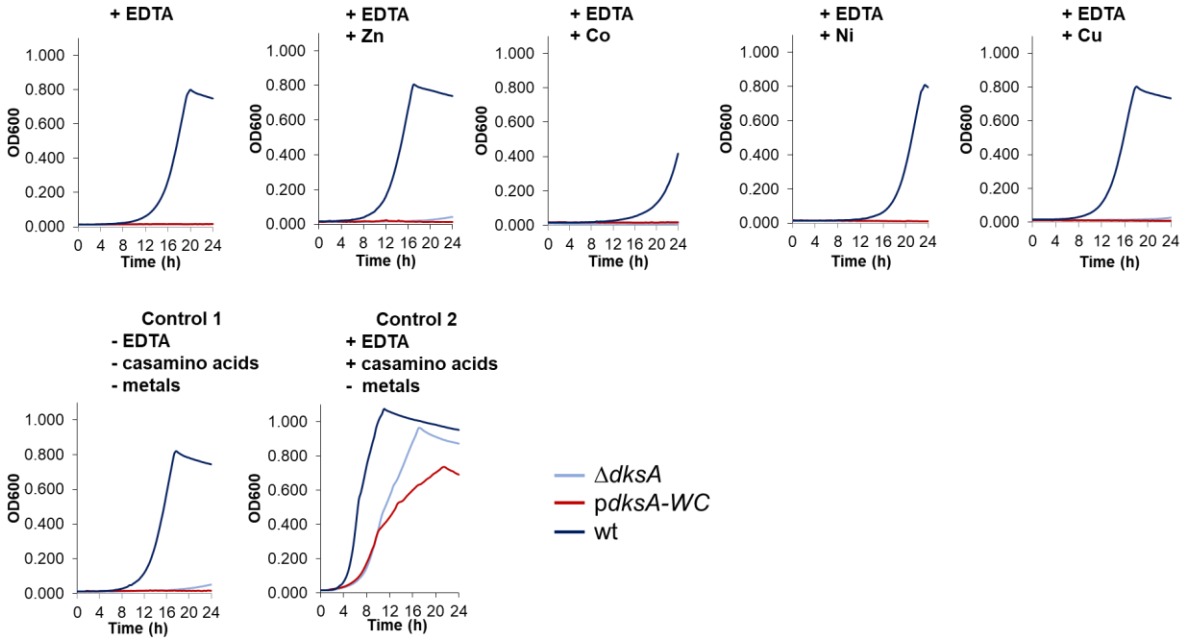

Figure 3.9. Rescue test of *E. coli dksA* phenotypes using different metals.
Growth curves of *E coli* strains KeioΔ*dksA,* KeioΔ*dksA* transformed with p*dksA-WC* and Keio (wt) in liquid M9 medium ± 100 µM EDTA and ± 25 mM of each metal indicated. Control 1: M9 medium lacking EDTA, casamino acids and metals. Control 2: M9 medium containing 100 µM EDTA, 0.2% casamino acids and no metal supplements. All M9 media were supplemented with 0.02% arabinose. Experiment performed in technical duplicates and mean values are represented.

3.3.4.1.4 Effect of pH on the auxotrophic phenotype of the *E. coli dksA* mutant

A previously published study found that the SCBF TF GfhI from *Thermus thermophilus*, is only active at acidic pH, and an increase to a pH above 7.0 prevents GfhI binding to the RNA-polymerase [308]. *C. trachomatis* inclusion and cell cytoplasm measurement showed a pH of around 7.25 in both cases, although change in pH during the development cycle has not been evaluated [309].

In the light of these observations, experiments were conducted to test the effect of pH on the rescue of the *E. coli dksA* phenotype by *W. chondrophila dksA*. For this, cells were grown in minimal M9 medium and the pH range of the medium was varied between 6.4 and 8.4. Results showed that changes in the pH did not restore growth of the *E. coli dksA* mutant (Figure 3.10). It should be noted that arabinose-induced expression of *W. chondrophila dksA* did not affect the growth of wt cells. This indicates that the presence of the *W. chondrophila* TF *per se* is not toxic to *E. coli*, but rather that it is unable functionally to replace the *E. coli* protein. This is in accordance with the observations described in Figure 3.9 showing that addition of casamino acids to the M9 medium was also able to restore growth of the *E. coli dksA* mutant expressing *W. chondrophila dksA*.

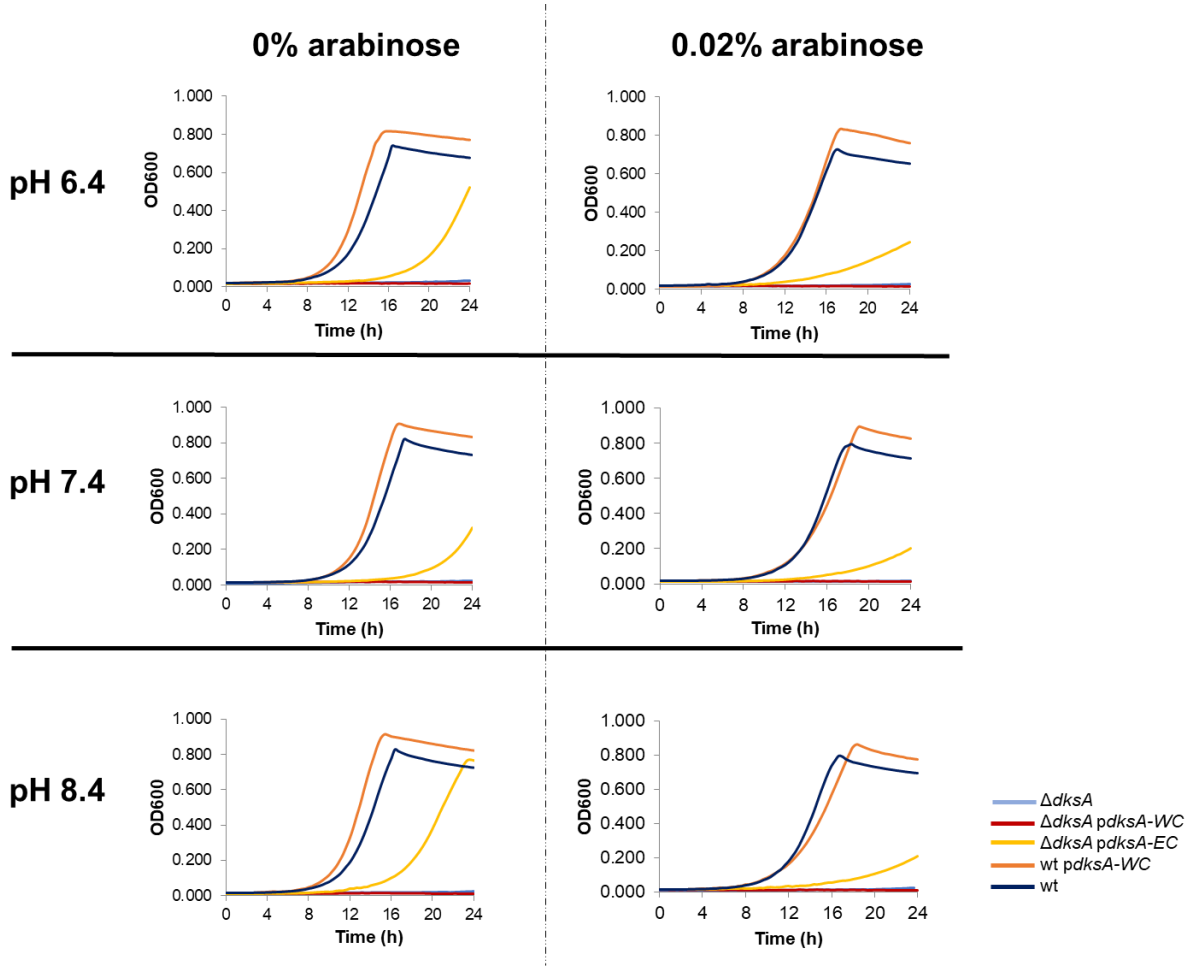

Figure 3.10. Effect of medium pH on bacterial growth.
The strains as indicated were grown for 24 h at 37°C in M9 medium adjusted to different starting pH values. Arabinose was present as indicated. Experiments were done in technical duplicates and mean values are represented.

3.3.4.2 DNA repair mechanism in *E. coli*

To test the effect of DksA on DNA repair, the *E. coli* strain KeioΔdksA was grown on plates containing mitomycin C, a known inhibitor of DNA replication, which acts by preventing the separation of the complementary DNA strands [310, 311]. Deletion of *dksA* in *E. coli* has previously been found to confer sensitivity to mitomycin C [301]. The results in Figure 3.11 showed that *W. chondrophila dksA* could not complement loss of the *E. coli* protein in the mitomycin C assay neither at 0.02% nor at 0.2% arabinose. In contrast, the control plasmid pBAD24-dksAEC, which expresses *E. coli dksA* was able to rescue the growth arrest phenotype at both concentrations of arabinose. Interestingly, the *P. aeruginosa dksA* was also able to complement *E. coli dksA* mutant.

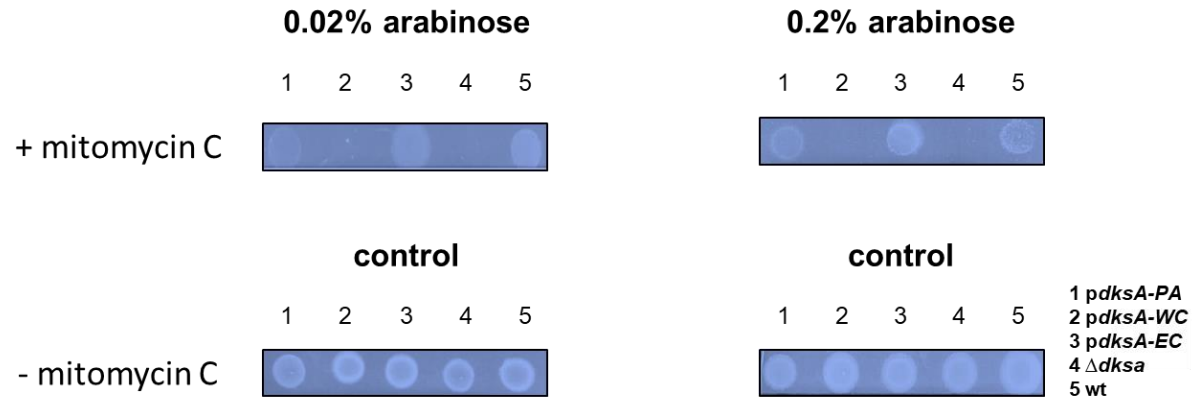

Figure 3.11. Sensitivity to mitomycin C.
The strains indicated were plated on LBA medium containing mitomycin C and arabinose as shown and incubated at 37°C for 24 h.

3.3.4.3 rrnB P1 promoter regulation in *E. coli*

DksA has been shown to exert both positive and negative regulatory effects on the expression of different genes involved in the stringent response [263]. One of these effects is the negative regulation of ribosomal RNA (rRNA) gene transcription [306]. In *E. coli*, there are 7 rRNA operons, *rrnA, rrnB, rrnC, rrnD, rrnE, rrnG* and *rrnH*, each under the control of a tandem P1-P2 promoter. Each operon contributes differentially to the rRNA expression in a cell [294]. In rapidly growing cells, the *rrnB* operon accounts for around 70% of the total rRNA synthesis. DksA suppresses transcription of rRNA by binding RNAP, thus detaching it from the *rrnB* promoters [312]. To test the repressive activity of *W. chondrophila dksA* in *E. coli*, the strain RLG7238 was used in which the *rrnB P1* promoter fused to *lacZ* had been inserted into the *E. coli* chromosomal DNA. This strain was transformed with *dksA-WC,* the control plasmids *dksA-EC* or *dksA-PA* and the empty vector (Δ*dksA)*. Expression of dksA was induced using 0.02% or 0.2% arabinose and lacZ activity was determined as described (see section 3.2.7.4).

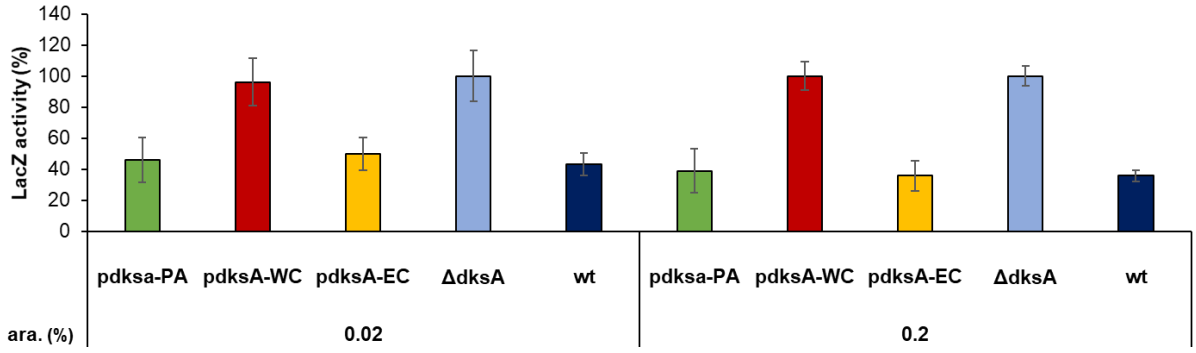

Figure 3.12. Function of *W. chondrophila dksA* in *E. coli*.
The strains, as indicated were induced using 0.02 or 0.2% arabinose (ara.) and LacZ activity was measured using DDAOG substrate. Experiments were done in technical triplicates and performed three times. Error bars represent the standard deviations and values were compared to Δ*dksA* (set to 100%).

As previously described in the literature [295], and shown in Figure 3.12, the control, *E. coli dksA* was able to repress *rrnB* P1 activity to virtually the same extent as in the wt cells, and similar results were obtained using *P. aeruginosa dksA*. However, *W. chondrophila dksA* was inactive in this assay and unable to repress the promoter *rrnB* P1. The readout for this assay, which involves expression of LacZ, requires that cells be actively growing. Thus, in this case, the failure of *W. chondrophila dksA* to repress synthesis of lacZ is not due to toxicity of the *W. chondrophila* protein. This assay therefore demonstrates definitively that even though well expressed, the *W. chondrophila dksA* is non-functional in *E. coli.*

3.3.4.4 Pyocyanin production in *P. aeruginosa*

To test functionality of *W. chondrophila* dksA in a different heterologous host, the production of pyocyanin in *P. aeruginosa* was investigated. Pyocyanin is considered as a quorum sensing (QS) dependent virulence factor and is responsible for the blue-green colour characteristic of *P. aeruginosa*. Expression of pyocyanin is regulated by the las and rhl quorum sensing (QS) systems [313], and DksA is required for translation of two QS-regulated genes, *lasB* and *rhlAB*, required for pyocyanin biosynthesis [274, 314, 315]. Thus, pyocyanin is not produced in the *P. aeruginosa* strain lacking *dksA* (Figure 3.13, inset).

The strain deleted for *dksA* (PAO1-RC1) and the wt strain (PT5) were transformed with the plasmids pHERD20T-dksAWC, pHERD20T-dksAEC, pHERD20T-dksAPA or pHERD20T-Ø, and pyocyanin production was assayed colorimetrically in absence and presence of 0.02% arabinose (Figure 3.13). *E. coli dksA* was able to complement the *P. aeruginosa dksA* in 0.02% arabinose, resulting in pyocyanin production similar to that seen in the wild-type strain. In contrast, *W. chondrophila dksA* was not able to rescue pyocyanin production in *P. aeruginosa*. Expression of the recombinant *P. aeruginosa* DksA was able to fully restore the production of pyocyanin, and strangely, this effect was independent of the presence or absence of arabinose. This is presumably due to basal level of expression of this protein in the homologous cells [276]. A similar effect was already seen in Figure 3.6B.

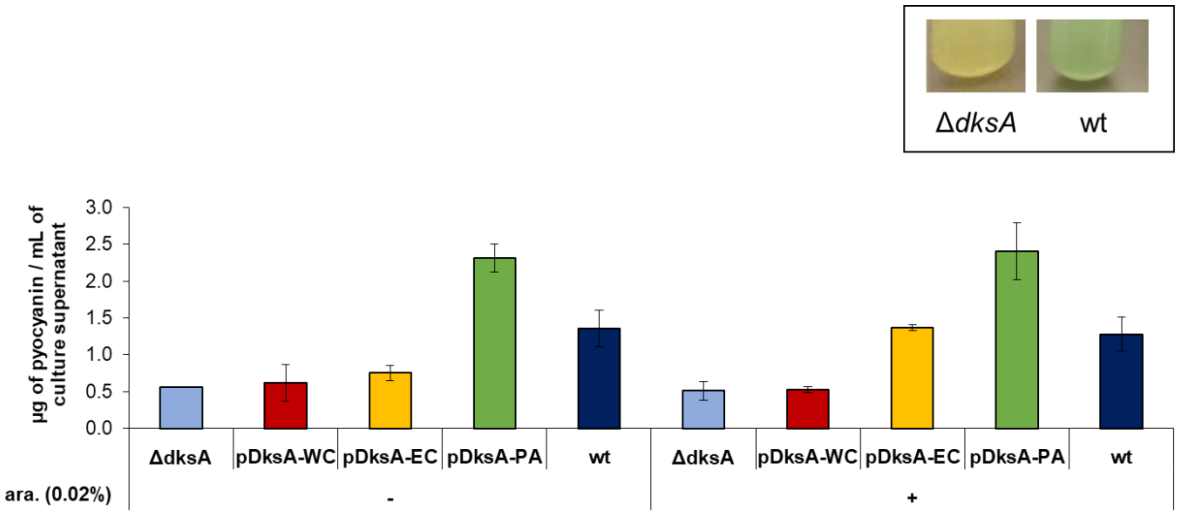

Figure 3.13. Rescue test of *P. aeruginosa dksA* phenotype by *W. chondrophila*, *E. coli* and *P. aeruginosa dksA* gene.
Pyocyanin production of various strains was measured in absence or presence of 0.02% arabinose (ara.) in LB. Overnight cultures of *P. aeruginosa* lacking *dksA* was transformed with the plasmids indicated, and compared to the wt strain. Cultures were grown in the absence or presence of 0.02% arabinose as shown. The inset shows colour development in overnight cultures of Δ*dksA* and wt. Experiments were performed in triplicate and error bars represent the standard deviations.

3.4 Conclusion

The goal of this part of the project was to establish an assay for functional expression of the *W. chondrophila* TF *dksA* in a heterologous bacterial host, since this could provide a cell-based platform for investing the biology of this protein. DksA is widespread in bacteria. It is a DNA-independent TF, which acts through binding to RNA polymerase to either suppress or activate transcription of genes involved in the stringent response to environmental stress. It is likely to be a good target for therapeutic intervention. With this in mind, functional complementation assays were set up using both *E. coli* and *P. aeruginosa* host strains in which the endogenous *dksA* gene had been deleted.

W. chondrophila DksA is well expressed in both hosts as evidenced by Western blotting, although overexpression from the arabinose-inducible promoter results in dose dependent toxicity in wt *E. coli.* On the other hand, overexpression of recombinant *E. coli dksA* was not toxic, suggesting that overexpression of *dksA per se* is not deleterious to the cell, and suggesting rather that the *W. chondrophila* DksA is not fully functional in *E. coli*, thus leading to a dominant negative phenotype due to non-productive interactions with the host cell targets.

This conclusion is consistent with our different complementation studies. When grown in Minimal M9 medium lacking amino acids, the *E coli dksA* deletion fails to grow and cannot be complemented by expression of the *W. chondrophila dksA* even though addition of casamino acids does allow these cells to grow. This suggests that *W. chondrophila* DksA is unable to activate transcription of the amino acid biosynthetic genes. Secondly the transcriptional repressive activity of *W. chondrophila* DksA is also non-functional as evidenced by its failure to suppress expression from the rrnB P1 promoter, responsible for most of the rRNA expression in actively growing cells; and thirdly, in the *E. coli dksA* deletion strain, *W. chondrophila dksA* was unable to restore resistance to mitomycin C, even though the recombinant *E. coli* protein was able to do so.

In the light of the failure of *W. chondrophila* DksA to complement the *E. coli* deletions, several attempts were made to improve its *in vivo* activity. These included expression of the neighboring genes in the *W. chondrophila* genome, which could provide other elements in a co-expressed operon; testing different pH environments, which was shown to be important for the activity of GfhI, a related SCBF and addition of different metal ions, whose importance had been indicated in studies of *P. aeruginosa* DksA2. However, none of these modifications to our assay enabled us to increase the activity of *W. chondrophila* DksA in *E. coli.*

The question remains therefore, why is *W. chondrophila* DksA non-functional in a heterologous bacterial host? One explanation could be that the protein is either not correctly

folded or not correctly modified post-translationally in *E. coli* as has been shown for other TFs in prokaryotes [316]; or alternatively that it is correctly folded but is not recognized by essential interacting proteins in the heterologous host. In this respect, it is noteworthy that even though the structural predictions of the DksA proteins are highly similar between the different bacteria studied here, there are several, possibly significant, differences seen in the primary sequences of these proteins. The *W. chondrophila* DksA has a shortened N-terminus; it contains only a single conserved cysteine residue of the canonical Zn-finger domain and it lacks the DXXDXA motif in the so-called tip region. It is therefore possible that the conformation of this protein once folded is not compatible with full activity in *E. coli*, and thus overexpression of a partially active protein may lead to a dominant negative phenotype and the observed toxicity.

Another possibility is that the mechanism of action of *W. chondrophila* DksA may be quite different. There is no indication at present that the alarmone ppGpp is required for activity of the *W. chondrophila* DksA, and indeed the enzymes, which control synthesis of ppGpp, *SpoT* and *RelA* are not present in the *Chlamydiae* genome. It is possible therefore that unlike in *E. coli*, the *Chlamydia* DksA functions in the absence of ppGpp.

In this context, it is interesting that a functional homologue of DksA, TraR, has been identified in *E. coli*, which is not dependent on ppGpp either for transcriptional repression of the rrnB P1 promoter, or activation of amino acid biosynthesis/transport genes [284]. TraR also has a truncated N-terminus, similar to *W. chondrophila* DksA, which does not affect its interaction with RNAP. However, unlike the *W. chondrophila* DksA, TraR retains the Zn-finger motif and other conserved amino acids, which may therefore be key for its function.

Observations in *Bacillus subtilis* may also be pertinent. The DNA-independent TF YlyA, a probable functional homologue of DksA, also lacks the DXXDXA motif and contains only the first conserved cysteine residue of the zinc finger motif. This protein is required during spore formation, however it binds RNA polymerase at a different site from that bound by DksA [317]. It is possible therefore that the *W. chondrophila* DksA, which shows similar features to *B. subtilis* YlyA, also binds a different site on RNA polymerase, which may not exist or be different on the *E. coli* and *P. aeruginosa* enzymes. It would be interesting to investigate this possibility in more detail.

Chapter 4: Metabolomic analysis of the *W. chondrophila* intracellular development cycle

4.1 Introduction

Metabolomics is a rapidly growing field of research for studying the small molecule composition of biological systems under different conditions. Typically, molecules less than 1500 Da are investigated. By systematically identifying the vast numbers of primary and secondary metabolites, which characterize the metabolic state of the cell, this approach provides a perspective, which can complement the genomics and proteomics approaches.

The metabolome is largely determined by the signaling pathways and transcription factors active in the cell [318]. Members of the phylum *Chlamydiae* are known to share a core set of TFs, involved in their intracellular development cycle, and regulation of gene expression by these factors would be expected to result in the presence of specific metabolites characteristic for each phase of bacterial infection. Therefore, an untargeted metabolomic approach was performed to identify and measure the metabolites produced during infectious cycle of *W. chondrophila* in a natural host cell. For these experiments, Vero cells were infected with *W. chondrophila* and the metabolites were analyzed by MS-based techniques at 24 and 72 h post infection (p.i.). These two time points correspond to the maximal presence of the RB and EB forms of *W. chondrophila* respectively (Figure 1.2), thus the analysis aims to highlight changes in the signaling molecules present during these two development stages. This is the first metabolomic analysis describing the infectious cycle of *W. chondrophila*.

The principal steps involved in the metabolomic analysis can be briefly summarized as sample collection, sample processing, instrumental analysis, data processing, data analysis and interpretation, as illustrated in Figure 4.1. While multiple techniques and softwares are available at each step of the process, only the most widely used will be mentioned here.

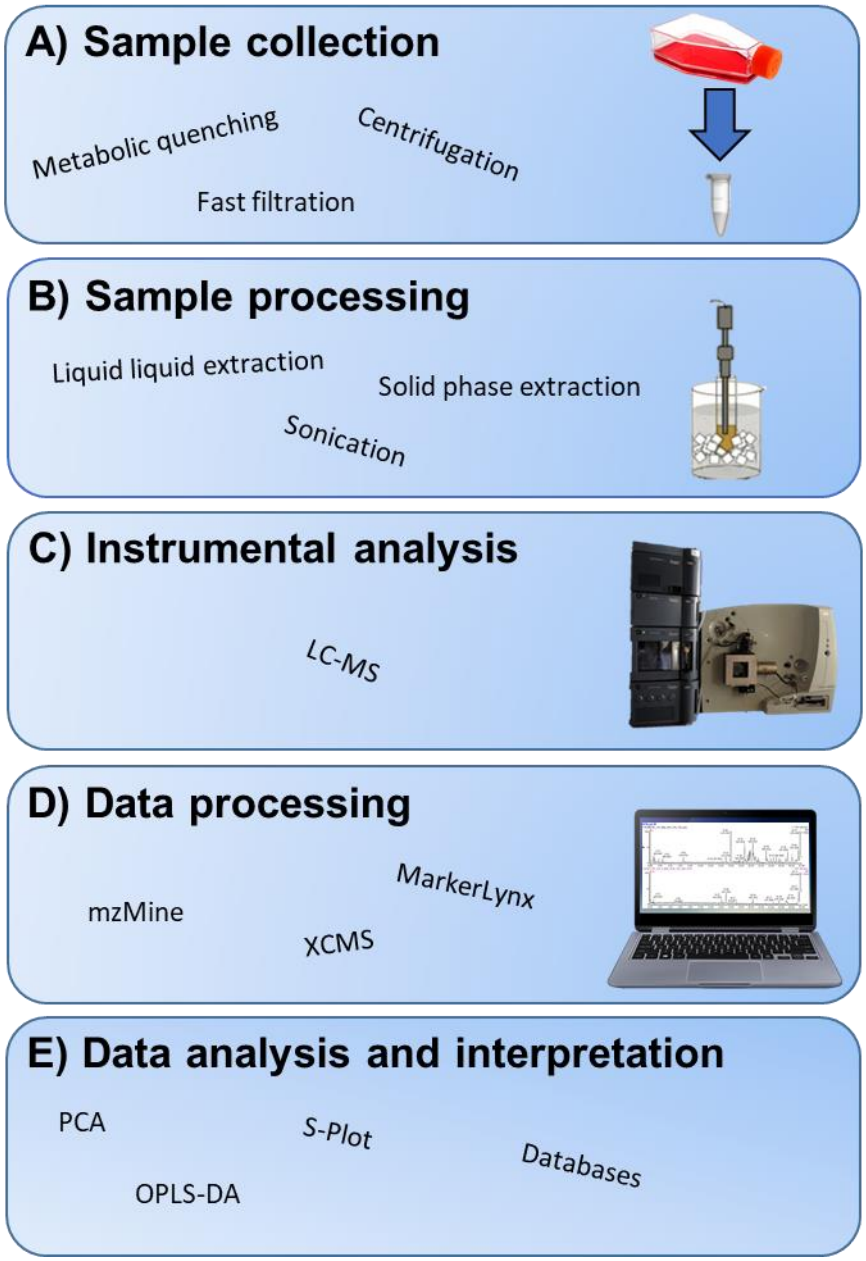

Figure 4.1. Summary of the workflow for untargeted metabolomic analysis using LC-MS.

Sample collection for a metabolic analysis, which focuses on identification of intracellular metabolites (the endo-metabolome) involves an initial rapid metabolic quenching in order to stop all the metabolic (enzymatic) activities (Figure 4.1A) [163]. For this, the extracellular medium is removed and the cells are rapidly rinsed in phosphate buffer saline (PBS). The quenching step is then performed in situ by treating cells with low-temperature organic solvents such as methanol at -80°C or liquid nitrogen. The exo-metabolome, which is the extracellular culture medium following filtration or rapid centrifugation can be processed in parallel as required by the experiment. Sample processing (Figure 4.1B) involves either liquid-liquid extraction using (different) immiscible solvents, or solid phase extraction (SPE) in combination with sonication or similar techniques for destruction of the bacterial cell wall. The extracts thus obtained can then be separated using LC methods, such as reversed-phase liquid chromatography (RP-LC), hydrophilic interaction liquid chromatography (HILIC) or ultra-high performance liquid chromatography (UHPLC), depending on the biological sample complexity and the purpose of the study [319].

An interface connects the separation device with the MS detector, which transfers separated metabolites from the liquid phase into the gas phase. One ionization system, which is widely used in metabolomics is the electrospray ionization (ESI). The ESI source in combination with a LC system (LC-ESI-MS) can be applied to complex biological samples, and was the technique of choice in the present study. This “soft ionization” method, in which the extent of fragmentation is limited, leaves mainly intact molecular ions for detection [320]. In a full MS spectrum, molecular weight determination can be achieved based on the presence of protonated ($[M+H]^+$) or deprotonated ($[M-H]^-$) molecules, or through the formation of adducts generated in the presence of reagents such as formic acid (FA) [321]. A wide choice of mass analyzers is now available, including the TOF and the Orbitrap high resolution mass detectors (HRMS), both of which are capable of generating highly accurate MS spectra. Both instrument types were employed during the course of this metabolomic study. In general, a mass detector with a higher resolution significantly reduces the number of possible elemental compositions for an ion of interest compared to instruments having lower resolution [321, 322], thus giving greater confidence in spectra interpretation and metabolite identification. The data of the samples analyzed by LC-MS in Figure 4.1C consist in the retention time (RT), the mass-to-charge ratio (*m/z)* and the signal intensity. The most challenging step in performing metabolomic experiments is translating the information acquired into metabolite chemical identities [323]. For the LC-MS data processing (Figure 4.1D), several widely used software packages exist such as the open access, mzMine and XCMS, as well as proprietary software MarkerLynx [324, 325].

The last step in the workflow includes data analysis and interpretation (Figure 4.1E). Multivariate data analysis can be performed to highlight differences such as an increase or decrease in a given metabolite between two chosen samples. In a procedure known as dereplication, the metabolites can then be compared with metabolite databases, such as Chemical entities of biological interest (ChEBI), Dictionary of natural products (DNP), *E. coli* metabolome database (ECMDB), Human metabolome database (HMDB), LIPID MAPS and METLIN as a way to facilitate the identification of a specific metabolite [326-330].

Unfortunately, current databases used for the identification of masses are often incomplete with result that some of the masses detected cannot be assigned to specific molecules. Indeed, Jansson *et al.* estimated that known metabolites represent only around 10% of the data, which can be obtained in a typical LC-MS metabolomic experiment. Thus, it can be very challenging to annotate with certainty many of the "hits" identified in a complex sample [331]. In the best case, a tentative assignment of a spectrum to a specific metabolite can be achieved by including a known isotopically-labeled reference compound in the sample for tandem MS (MS^2) analysis. The method of choice for structural elucidation is NMR, even though NMR has the disadvantage of lower sensitivity compared to MS, and thus is not suitable for determining the structures of low abundant metabolites.

Overall, using this approach, novel metabolites and possible biomarkers of the *W. chondrophila* development cycle may be identified. Such metabolites can then provide a starting point for further investigation, and potentially can offer novel antimicrobial drug targets and pathways.

4.2 Materials and Methods

4.2.1 Chemicals

Extractions were performed with ULC/MS-grade methanol (MeOH) or ULC/MS-grade water. Analyses were performed using UHPLC-grade acetonitrile or water containing 0.1% (v/v) FA). All chemicals were purchased from Biosolve (Valkenswaard, The Netherlands).

4.2.2 Biological materials

Vero cells isolated from green monkey (*Cercopithecus aethiops)* kidney (ATCC® CCL-81™)*, Acanthamoeba castellanii* infected with *W. chondrophila* strain WSU86-1044 (ATCC number VR-1470), *Staphylococcus aureus* (ATCC number 29213) and *E. coli* (ATCC number 25922) were purchased from ATCC (Manassas, VA, USA).

4.2.3 Sample preparation

Vero cells were grown in 25 cm^2-cell culture flasks (Corning, NY, USA) and infected with *W. chondrophila* as previously described by Kebbi-Beghdadi *et al*. [129]. Cells were quenched by addition of -80°C MeOH (2 mL MeOH used for 4 cell culture flasks), collected and stored at -80°C. Purified EBs were obtained from *Acanthamoeba castellanii* infected with same *W. chondrophila* strain as described by Goy and Greub [126]. These experiments were performed in the laboratory of Prof. Greub (Institute of Microbiology, University Hospital Center and University of Lausanne, Lausanne, Switzerland).

The workflow of the experimental procedure for the sample extraction used in this metabolomic study, including the controls of non-infected cells and culture medium is outlined in Figure 4.2. Adherent Vero cells infected with *W. chondrophila*, non-infected cells and culture medium alone were collected at 24 and at 72 h. For this, the culture medium was removed (Figure 4.2a) and flasks were rinsed with phosphate-buffered saline (PBS). Adherent cells were then quenched with MeOH prechilled to -80°C (Figure 4.2b), detached using a cell scraper and centrifuged at 13,500 rpm, 4°C for 15 min (Figure 4.2c). Supernatants were removed (Figure 4.2d) and analyzed by UHPLC–TOF-MS. In parallel, cell pellets were resuspended by addition of 400 µL precooled MeOH and extracted in an acetone-dry ice cooling bath below -60°C using the Sonifier 450 from Branson Ultrasonics Corporation, Danbury, CT, USA operated at 45 W for 10 cycles of 30 s pulse “on” and 30 s pulse “off”

(Figure 4.2e). To avoid particles in the solution, the extracts were centrifuged and supernatants were analyzed, as previously described.

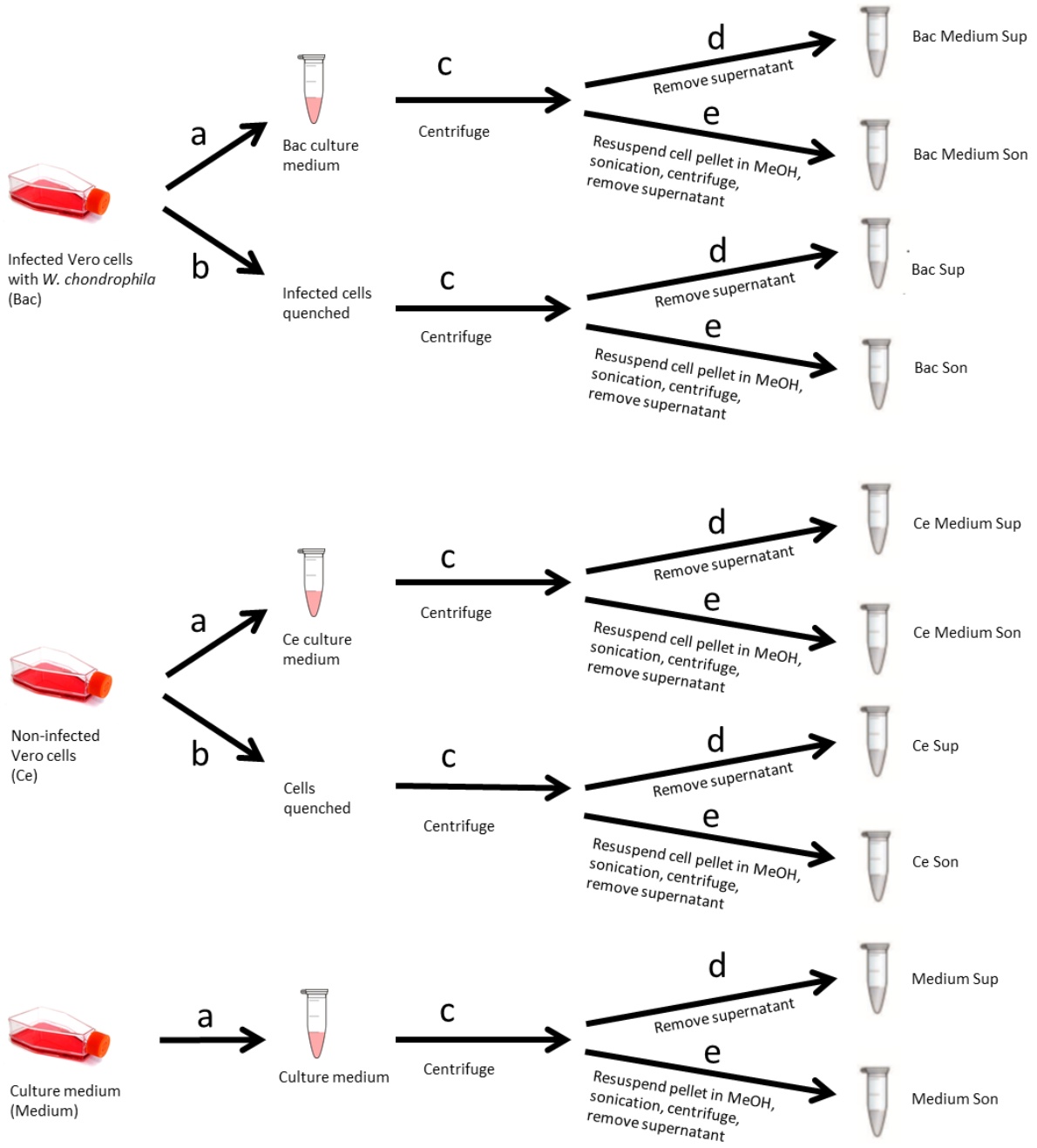

Figure 4.2. Experimental procedure of sample extractions.
Vero cells infected with *W. chondrophila* (Bac) were incubated for 24 and at 72 h p.i., and control flasks containing either non-infected cells (Ce) or culture medium alone were incubated in parallel. Culture medium was removed (a) and flasks were rinsed with PBS. Quenching was performed by addition of cold MeOH to each flask (b), and the cells were detached using a cell scraper, transferred to Eppendorf tubes and centrifuged at 13'500 rpm, 4°C for 15 min (c). The supernatants were collected (d) for analysis by UHPLC–TOF-MS. The cell pellets were resuspended in cold MeOH and disrupted by sonication (e). Particulate material was removed from the cell extracts by centrifugation at 13'500 rpm, 4°C for 15 min and supernatants were analyzed by UHPLC–TOF-MS.

4.2.4 *S. aureus* and *E. coli* growth conditions

E. coli and *S. aureus* were grown overnight at 37°C in Luria-Bertani broth. The next morning, 1 mL of culture was centrifuged at 10'000 rpm for 1 min. Supernatants were collected and cell pellets were washed with PBS. Cells were then extracted as described for *W. chondrophila*-infected Vero cells. Ongoing metabolism was quenched by addition of 400 µL precooled MeOH and cells were disrupted using a Sonifier 450 (Branson Ultrasonics Corporation, Danbury, CT, USA) operated at 45 W for 10 cycles of 30 s pulse "on" and 30 s pulse "off".

4.2.5 SPE

For solid-phase extraction (SPE), the C_{18} cartridge 100 mg/mL (Teknokroma, Barcelona, Spain) was used. Vero cells infected with *W. chondrophila* 24 h p.i. were extracted using MeOH as described in 4.2.3. Supernatants of extracted samples were collected by centrifugation at 10,000 rpm, 15 min, 4°C, diluted 1:1 in water and loaded on the SPE C_{18} cartridge. Elution was made with MeOH 85%.

4.2.6 Sample randomization list

Samples were randomized as previously described by Want *et al.* [332], with the following modifications: the standard mixture containing 20 µg/mL rutin (Fluka AG), 10 µg/mL glycyrrhizic acid, 40 µg/mL piperine and 40 µg/mL echinocystic acid in MeOH (all from Carl Roth, Karlsruhe, Germany), the individual samples and a quality control (QC) sample, consisting of an equal mixture of all biological samples after extraction were injected as described in Table 4.1. In addition, a blank (MeOH) was injected after every six biological samples and three times at the start and the end of the experiment.

Table 4.1. Randomized sample list.

	INJECTION NO° (NUMBER OF SAMPLES)	SAMPLE NAME
START	1 - 5 (5)	Standard mixture
	6 - 8 (3)	Blank
	9 - 13 (5)	QC
	14 -…	Biological sample
	After every 6 biological samples	Blank and QC
	After every 14 injections	Standard mixture
END	200 - 204 (5)	QC
	205 - 207 (3)	Blank
	208 - 212 (5)	Standard mixture

4.2.7 UHPLC–TOF-MS analysis (long run)

Chromatographic separation was performed on an Acquity UPLC system (Waters, Milford, MA, USA) interfaced to a Micromass-LCT Premier TOF MS from Waters, using an ESI source. The separation was performed on an Acquity BEH C_4 UPLC column (150 x 2.1 mm i.d.;1.7 µm, Waters) and on an Acquity BEH C_{18} UPLC column (150 x 2.1 mm i.d.; 1.7 µm, Waters). Gradient mode was set at a flow rate of 0.46 mL/min with the following solvent system: (A) 0.1% (v/v) FA in water; (B) 0.1% (v/v) FA in acetonitrile. The gradient was increased linearly from 5 to 95% B in 30.0 min. The column was then washed for 10.0 min with 95% B, reconditioned with 5% B for 0.5 min and finally equilibrated with 5% B for 0.5 min. Column temperature was maintained at 40°C and the injection volume was set to 2 µL. Detection was performed in negative and positive ion modes. The *m/z* range was set to 100–1300 Da in centroid mode with a scan time of 0.3 s and an inter-scan delay of 0.01 s. The ESI conditions were as follows: capillary voltage of 2800 V (negative and positive ion modes), cone voltage of 40 V, source temperature of 120°C, desolvation temperature of 300°C, cone-gas flow of 20 L/h and desolvation-gas flow 800 L/h. Waters Acquity Autosampler temperature was set at 4.0°C. For internal calibration, a 0.25 µg/mL solution of leucine-enkephalin (Sigma-Aldrich) was infused through the lock-mass probe at a flow rate of 5 µL/min using an additional Shimadzu LC-10ADvp LC pump (Duisburg, Germany).

4.2.8 UHPLC–TOF-MS analysis (short run)

Chromatographic separation was performed on an Acquity UPLC system (Waters) interfaced to TOF MS from Waters, using an ESI source. The separation was performed on an Acquity BEH C_{18} UPLC column (50 x 1 mm i.d.; 1.7 µm, Waters) in gradient mode at a flow rate of 0.3 mL/min with the solvent system described above. The gradient was increased from 5 to 95% B in 4.0 min. The column was then washed for 0.8 min with 95% B, reconditioned with 5% B for 0.1 min and finally equilibrated with 5% B for 1.1 min. Column temperature was maintained at 40°C and injection volume was set to 1 µL. Detection was performed in negative and positive ion modes. The *m/z* range was set to 100–1300 Da in centroid mode with a scan time of 0.25 s and an inter-scan delay of 0.01 s. The ESI conditions were as follows: capillary voltage of 2400 V (negative ion mode) or 2800 V (positive ion mode), cone voltage of 40 V, source temperature of 120°C, desolvation temperature of 300°C, cone-gas flow of 20 L/h, and desolvation-gas flow 600 L/h. Waters Acquity Autosampler was at 4.0°C. For internal calibration, a 0.25 µg/mL solution of leucine-enkephalin (Sigma-Aldrich) was infused through

the lock-mass probe at a flow rate of 5 µL/min using an additional Shimadzu LC-10ADvp LC pump.

4.2.9 UHPLC-HRMS and MS^2 analysis

Chromatography was performed on an UltiMate 3000 UHPLC system (Thermo Fisher Scientific) coupled to a Q Exactive Plus Orbitrap MS from Thermo Fisher Scientific, using a heated ESI (HESI-II) source. The LC conditions were as follows: Acquity BEH C_{18} UPLC column (100 x 2.1 mm i.d., 1.7 µm, Waters) in gradient mode at a flow rate of 0.6 mL/min with the solvent system described above. The gradient was increased from 5 to 100% B in 8.0 min. The column was then washed for 3.0 min with 95% B, reconditioned with 5% B for 0.2 min and finally equilibrated with 5% B for 3.8 min. The temperature was maintained at 40°C. Detection was achieved in positive and negative ion modes: Spray voltage 3500 V (positive ion mode) or 2500 V (negative ion mode), sheath gas flow rate (N_2) 47.50 units, auxiliary gas flow rate 11.25 units, capillary temperature 256.25°C (positive and negative ion modes), probe heater temperature 412.5°C, S-Lens RF level 50, maximum injection time was 60 ms for full scan MS and 50 ms for MS^2 scans, and resolution 35,000 for full scan MS and 17,500 for MS^2. The *m/z* range was set to *m/z* 150–1300 Da in centroid mode. Waters Acquity Autosampler temperature was set at 4.0°C and the injection volume was set to 1 µL. The mass analyzer was calibrated according to the manufacturer's instructions by direct injection of a mixture of caffeine, methionine−arginine− phenylalanine−alanine−acetate (MRFA), sodium dodecyl sulfate, sodium taurocholate, and Ultramark 1621 in an acetonitrile-MeOH-H_2O solution containing 1% formic acid. Chromatograms were treated using Xcalibur v.3.0.63 software (Thermo Fisher Scientific).

4.2.10 Data analysis

The raw UHPLC–TOF-MS data were converted to the open MS format (.mzXML) using the MSconvert, part of the ProteoWizard package [333] and to NetCDF using DataBridge (Waters). A peak list containing RT, *m/z* and signal intensity was generated by the enhanced statistical program for multivariate data analysis, MarkerLynx™, a part of MassLynx XS™ software version 4.1 (Waters), using the parameters as shown in Table 4.2.

Table 4.2. Properties and values used during automatic peak picking procedure by MarkerLynx.

PROPERTY	VALUE	
	Negative mode	Positive mode
FUNCTION	1*	1*
INITIAL RT (MIN)	0.00	0.00
FINAL RT (MIN)	4.00	4.00
LOW MASS (*M/Z*)	100.00	100.00
HIGH MASS (*M/Z*)	1300.00	1300.00
MASS TOLERANCE (DA)	0.05	0.05
USE RT TIME	No	No
APEX TRACK PEAK PARAMETERS		
PEAK WIDTH AT 5% HEIGHT (SECONDS)	1.00[2]	1.00[2]
PEAK-TO-PEAK BASELINE NOISE2	0.00[2]	0.00[2]
COLLECTION PARAMETERS		
MASS PER RT	20	60
MINIMUM INTENSITY (AS A PERCENTAGE OF BPI)	20.00	20.00
MASS WINDOW (DA)	0.05	0.05
RT WINDOW (MIN)	0.20	0.20
NOISE ELIMINATION LEVEL	4.00	4.00
DEISOTOPE DATA?	Yes	Yes

*Usually MS data is acquired as function 1; [2]Peak width automatically determined by MarkerLynx.

For dereplication, the following databases were used: ChEBI (https://www.ebi.ac.uk/chebi), DNP (http://dnp.chemnetbase.com/), ECMDB (www.ecmdb.ca), HMDB (http://www.hmdb.ca/), METLIN (http://metlin.scripps.edu/index.php), and LIPIDMAPS (http://www.lipidmaps.org/).

Unsupervised principal component analysis (PCA) and supervised orthogonal partial least squares discriminant analysis (OPLS-DA plot) and S-plot multivariate analyses with samples (pareto scaled) were done using SIMCA-P software version 13.0 (Umetrics, Umea, Sweden). Exact p-values were calculated by nonparametric Wilcoxon-Mann Whitney test using GraphPad prism software version 7.02 (Graph-Pad software, La Jolla, CA, USA).

4.2.11 Molecular network analysis

The molecular network was generated following the online workflow at GNPS [334] using default parameters, with parent mass peak tolerance of 2.0 Da and MS^2 peak tolerance of 0.5 Da. Edges were filtered to have a cosine score above 0.7 and more than 6 matched peaks. Further edges between two nodes were kept in the network only if each of the nodes appeared in each other's respective top 10 most similar nodes. The spectra in the network were then searched against GNPS' spectral libraries. All matches kept between network spectra and library spectra were required to have a score above 0.7 and at least 6 matched peaks.

4.3 Results and Discussion

4.3.1 Sample preparation to study *W. chondrophila* infected Vero cells

In the first step, several extraction methods and separation techniques were tested for their suitability prior to analysis of metabolites from Vero cells infected with *W. chondrophila*. The detection of low abundance metabolites required enrichment to enable better detection. Therefore, a small volume of MeOH (400 µL) was used for metabolite extraction from cells infected with *W. chondrophila* 24 h p.i with additional sonication. This extraction solvent is widely used and was shown to have excellent reproducibility and recovery for polar and mid-polar metabolites in biological system analysis [335-338]. Cold MeOH was also used as quenching agent to reduce the handling steps. Furthermore, the chromatographic separation of the extracts was achieved by performing UHPLC–TOF-MS in the long run mode to obtain a better peak separation and therefore an extended view of the number of metabolites in the extract.

In Figure 4.3, the UHPLC–TOF-MS chromatogram of the 1/10 diluted extract after analysis in positive ion mode (Figure 4.3B) was compared to the non-diluted sample (Figure 4.3A). No peak saturation and good intensities were observed following direct injection of extracts, indicating no need for extract dilution prior to LC-MS analysis. The same findings were observed in negative ion mode (data not shown). These analyses also showed that the extraction method using MeOH, combined with sonication of the cell pellet, resulted in the detection of peaks, which can further be interpreted. In parallel, SPE prior to the LC-MS analysis was tested to remove highly nonpolar compounds and other interfering substances such as salts. In Figure 4.3C the base peak chromatogram of the extract after SPE is shown. Significantly fewer peaks were observed in negative and positive mode (latter data not shown) compared to the non-diluted sample, and this approach was not pursued further. In a further test, the extracts were separated on a C_4 column (Acquity BEH C_4) and the chromatogram obtained was compared to the separation using a C_{18} column. The C_4 column resulted in an accumulation of middle polar metabolites at around 22 min in both positive (Figure 4.3D) and negative ion mode (data not shown). These results showed that a better separation of peaks was obtained using the C_{18} column.

Since this study aims to highlight the maximum number of metabolite changes in the *W. chondrophila* development cycle, optimizing the chromatographic separation was important to reduce possible matrix interference in the ionization process. The subsequent metabolomic analyses were therefore performed using a C_{18} column for metabolite separation, without

dilution and SPE steps during extract preparation. To perform metabolite extraction, MeOH was used as solvent, even though very apolar metabolites are unlikely to be extracted.

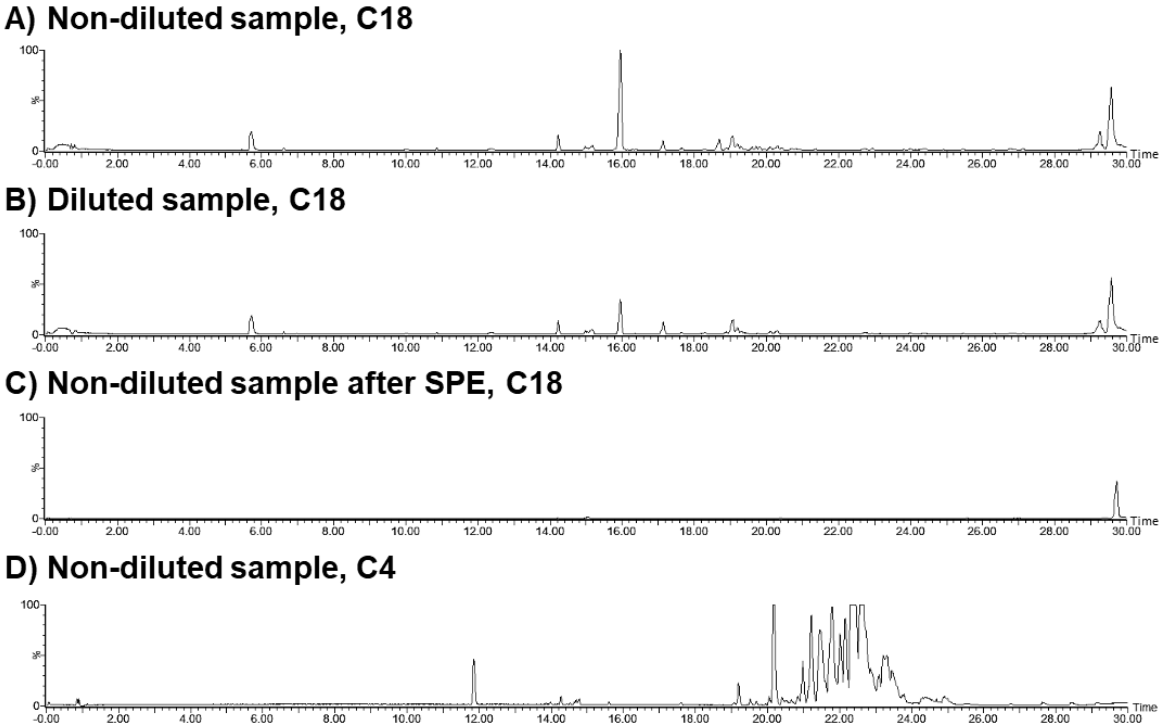

Figure 4.3. UHPLC–TOF-MS chromatograms in positive ion mode of non-diluted (A), diluted (B), SPE (C) samples (All long run, C_{18} column) and non-diluted (Long run, C_4 column) (D) sample.

To compare the metabolites present in *W. chondrophila*-infected Vero cells at 24 and 72 h p.i., a preliminary study was performed to check that the method developed above could be applied. Thus, cells at 24 and 72 h p.i. together with the corresponding non-infected Vero cells, were quenched and extracted with MeOH as described above and analyzed by UHPLC–TOF-MS in long run mode. The detection was performed in both positive and negative ion modes in order to monitor the largest possible number of metabolites. However, since both modes produced the same result, only the chromatograms in positive ion mode are shown (Figure 4.4). The results using this protocol, showed differences between the extracts from infected cells at 24 and 72 h p.i., and also between the infected and non-infected cell samples (data not shown). To conclude, the method described is suitable for the metabolomic analyses described here.

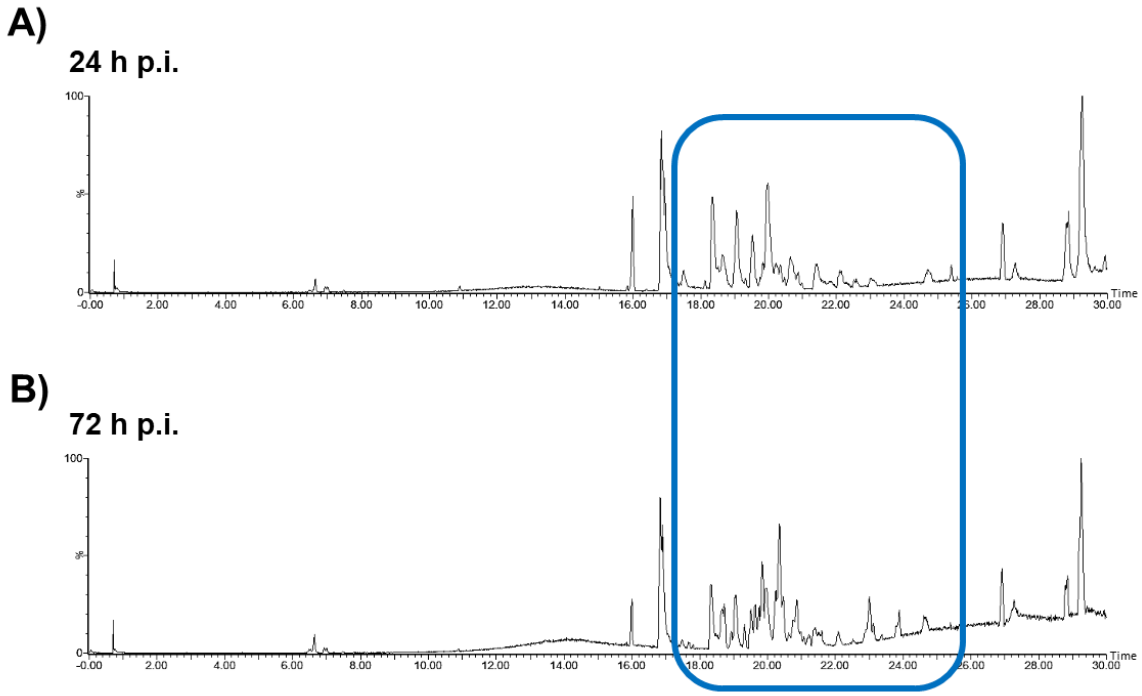

Figure 4.4. UHPLC–TOF-MS chromatograms in positive ion mode of Vero cells infected with *W. chondrophila* at 24 (A) and 72 h p.i. (B).
Areas of some visible metabolite changes are framed in blue. (All long run, C_{18} column).

In order to enable statistical analysis and to minimize the biological variance within samples, experiments were performed in triplicate on two different days giving a total of six replicates. The reported standard for metabolomic analyses recommends a minimum of three biological replicates, with five replicates preferred. Multiple replicates are essential to provide a valid statistical basis for data evaluation and interpretation [339].

Samples were analyzed using the UHPLC–TOF-MS short run mode to avoid extended analysis times. Madala *et al*. compared the resolution of short chromatograms of 5 and 10 min, with the higher resolution chromatograms of 20 and 40 min. Equivalent biological information was obtained using lower resolution, short chromatograms when the results were analyzed by multivariate data analysis e.g. PCA in combination with OPLS-DA [340]. Three replicates were analyzed together (batch 1) and the other three replicates (batch 2) on the next day. Since certain types of molecules are better ionized in positive ion mode and others in negative ion mode (based on their chemical functionality), biological samples were analyzed in both modes to maximize the metabolome coverage. For data analysis, LC-MS data processing results of the six replicates were combined. Following the steps of peak picking, normalization, deisotoping, RT alignment, and noise filtering, a peak table was generated

using the MarkerLynx software. The method parameters applied to the data are described in Material and Methods part 4.2.10 and Table 4.2, although the algorithms used are not publicly available from the software developer. The resulting two-dimensional data matrix in form of a peak-table generally comprises the *m/z* values, the RT and the corresponding signal intensity of every detectable peak.

4.3.2 Testing system suitability and method variability

A standard mixture of known compounds was used to verify the performance of the system (system suitability test, SST) and to ensure the quality of the MS measurements [341-343]. To check instrument stability, extracted ion chromatograms of selected ions were compared in negative and positive ion modes ($[M-H]^-$/$[M+H]^+$) to assess RT, signal intensity (area) and *m/z* value (Table 4.3). The RT and m/z data for rutin, (RT 0.98/0.97 min, *m/z* 609.14/611.16), glycyrrhetic acid (RT 2.96/2.96 min, *m/z* 469.33/471.35), and echinocystic acid with $[M+H-H_2O]^+$ in positive ion mode, (RT 2.82/2.81 min, *m/z* 471.35/455.35) were obtained. Overall, a coefficient of variation (CV) of less than 2% in RT shift was estimated in both ion modes, with the highest variation (1.3%) at an early RT of 0.97 min. Furthermore, the *m/z* values showed no variation in negative and positive ion modes. The largest CV was found in the signal intensity, with around 30% in positive ion mode and 15% in negative ion mode. This higher CV in positive ion mode could be attributed to the functional groups of the test metabolites. Overall, the SST showed a good system stability as judged by measurements of RT, signal intensity (area) and *m/z* value obtained in two independent experiments.

Table 4.3. RT, *m/z*, signal intensity (area) and the corresponding CV (%) of standard mixture samples (n=30) in negative and positive ion modes.

		RT [min]	*m/z*	Signal intensity (area)
Negative ion mode	**Rutin**	0.98 ± 0.6	609.14 ± 0.0	844.12 ± 14.0
	Glycyrrhetic acid	2.96 ± 0.2	469.33 ± 0.0	948.16 ± 8.7
	Echinocystic acid	2.82 ± 0.2	471.35 ± 0.0	1690.21 ± 7.3
Positive ion mode	**Rutin**	0.97 ± 1.3	611.16 ± 0.0	20.74 ± 31.5
	Glycyrrhetic acid	2.96 ± 0.3	471.35 ± 0.0	1486.44 ± 14.8
	Echinocystic acid	2.81 ± 0.2	455.35 ± 0.0	237.48 ± 20.8

For the additional multivariate analysis, the QC samples provide an estimate of the variability in the analytical technique during the analysis. Therefore, the quality of measurement was verified retrospectively in the next step by the QC samples.

4.3.3 Biomarker identification using multivariate statistical tools

Metabolomic studies generate very complex datasets, where the three dimensions are represented by RT, *m/z* value and signal intensity. To summarize and visualize the MS data generated, multivariate statistical tools such as unsupervised PCA, and supervised method such as OPLS-DA and S-plot were employed on the pareto scaled data. Such a scaling is commonly used for MS data in order to increase the contributory effects of low concentration metabolites with no amplification of involved noise and artefacts in the data [344, 345].

In general, the PCA score plot is used to highlight the systematic trends and relationships among all the samples, e.g. clustering and time trends, and reduces the complex data set to a 2D plot [346, 347]. In this PCA, all six biological replicates (n=104) and the QC sample injections (n=36) were included. The PCA score plots were generated with two components, resulting in R2X(cum) 0.215 and Q2(cum) 0.161 in negative ion mode and R2X(cum) 0.324 and Q2(cum) 0.264 in positive ion mode (Figure 4.5). Therefore, the PCA captured a greater percentage variance in the data in positive ion mode (32.4%) than in negative ion mode (21.5%). The ellipse represented the Hotelling's T^2 with a 95% confidence, the ions located outside of it being called outliers. In the negative ion mode PCA, four observations could be identified as outliers and one in the positive ion mode. A total of 140 observations were present, resulting in statistically seven (140*0.05) observations, which were expected to be outside Hotelling's T^2 tolerance 95% confidence ellipse. Therefore, the small numbers of outliers obtained were neglected for further data analysis.

In the PCA score plots obtained, five clusters could be identified: a cluster of samples with non-infected and infected cells after sonication (Bac/Ce Son), a cluster with non-infected and infected cells before sonication (Bac/Ce Sup), a cluster of all media after sonication (Media Son), a cluster of all media before sonication (Media Sup) and a cluster of QC samples, representing the analytical variation in the system [348]. These clusters represent the relationships of metabolites within them. Since the repeated QC injections were widely spread, with a larger variation than the biological samples in the PCA score plot, a difference between 24 and 72 h p.i. samples must be interpreted with caution.

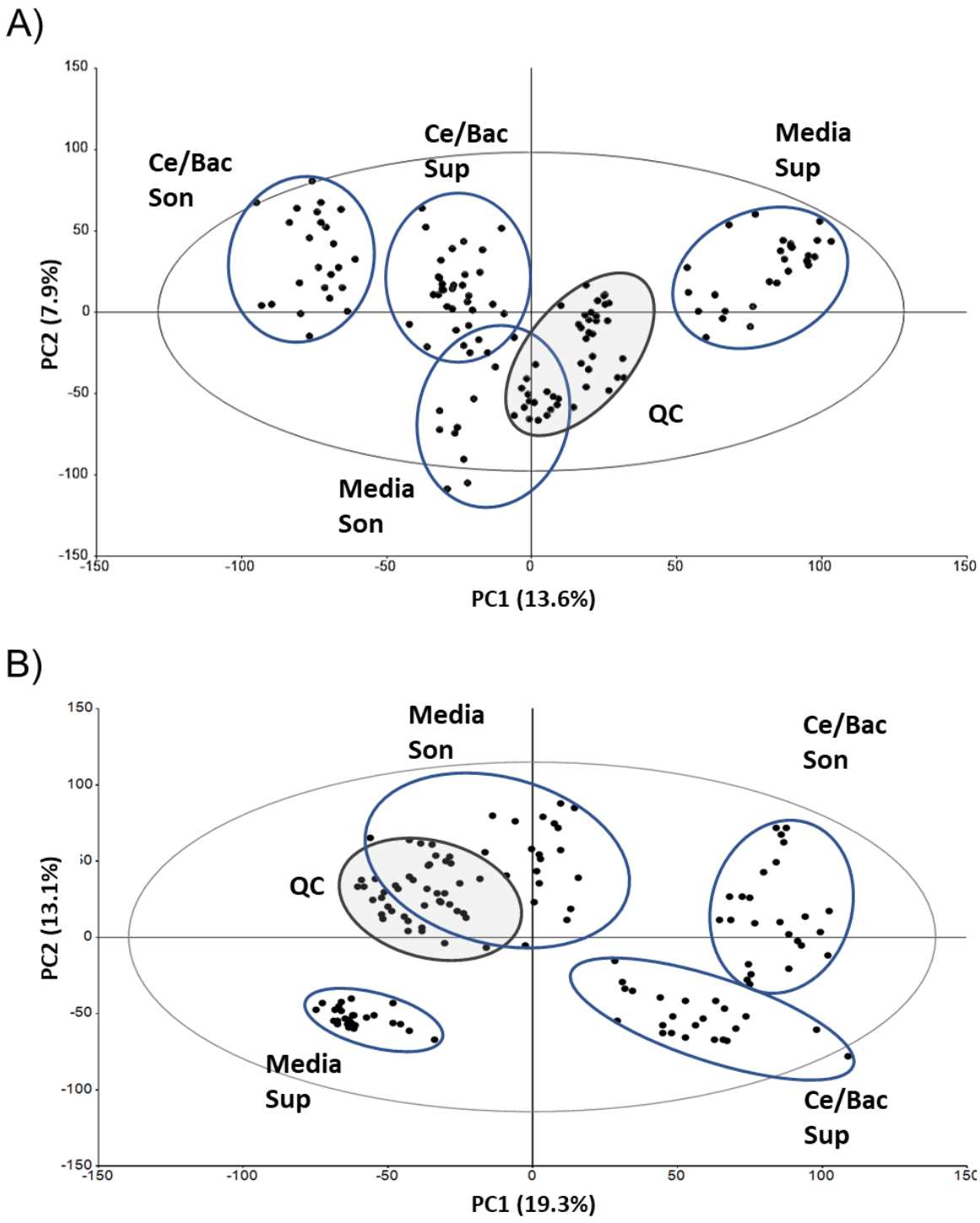

Figure 4.5. PCA score plots of the 6 biological replicates and the QC samples (grey) in negative (A) and positive (B) ion modes.
Abbreviations: Ce/Bac: Non-infected/*W. chondrophila* infected Vero cells; Sup: Before sonication; Son: After sonication; QC: Quality control; Media: no cells.
The ellipse in grey represents the Hotelling's T^2 with a 95% confidence.

As this work is focusing on changes of intracellular metabolites produced by the bacteria, samples of Vero cells infected with *W. chondrophila* after sonication (Bac son) at 24 and 72 h p.i. were chosen for further data analyses. The other samples, infected cells after sonication and media were considered as controls. PCA score plots of theses six replicates and QC samples were generated in negative and positive ion modes (Figure 4.6), resulting in R2X(cum) 0.629 and Q2(cum) 0.477 in positive ion mode, and R2X(cum) 0.493 and Q2(cum) 0.396 in negative ion mode with 2 components. A significant separation between the two clusters 24 and 72 h p.i. was observed in negative ion mode. In this mode, the biological samples were also clustered closer together at 72 h p.i. than at 24 h p.i. when compared to QC samples. In contrast, the PCA score plots generated in positive ion mode showed a larger biological variation than between the QC samples, including five outliers.

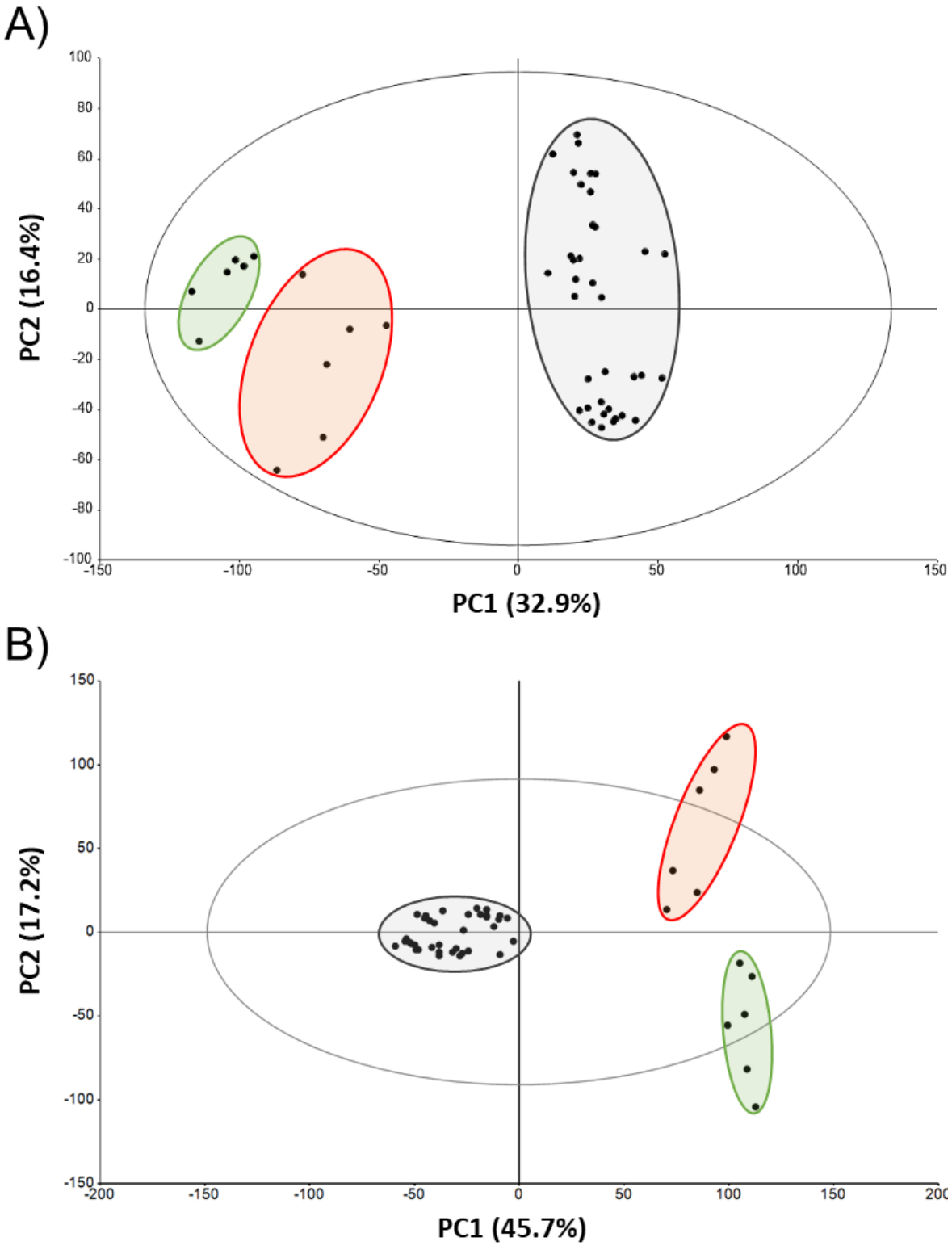

Figure 4.6. PCA score plots of the 6 biological replicates of infected cells at 24 (red) and 72 h p.i. (green), and the QC samples (grey) in negative (A) and positive (B) ion modes.
The ellipse in grey represents the Hotelling's T^2 with a 95% confidence.

To discriminate better between cells infected with *W. chondrophila* at 24 and 72 h p.i. and therefore to identify potential marker metabolites, OPLS-DA plots were generated from the data in positive and negative ion modes (Figure 4.7A). The OPLS-DA identifies the variables, where there are differences between extracts at 24 and 72 h p.i. The previously performed PCA model (Figure 4.6) provided evidence that the forced group differences provided by OPLS-DA model are statistically reliable. Then, as shown in the study by Worley and Powers [349], PCA only reveals differences between measurements in its scores if those differences are major contributors to the total variability. Both ion modes showed a high value in model interpretation rate (R2(cum) 1 and 1) and in OPLS-DA model prediction ability (Q2(cum) 0.948 and 0.921), implying that this is a good model for further data analysis. This model explained 77.3% of the systematic data variability (R2X(cum)) in negative, and 89.6% in positive ion mode, with a noise rest of 22.7 and 10.4%, respectively. In the next step, for the visualization and interpretation of the OPLS-DA model results (Figure 4.7A), the detected features explaining the differences between these two groups are shown in the S-plot (Figure 4.7B). This plot allows visualization of both correlation and covariance between the metabolites and the modelled class designation. Each point represents an individual *m/z*-RT pair. The y-axis (P(corr)) denotes correlation/reliability of a variable as a marker. The further a data point is from the value 0, the greater its contribution within the sample group. The x-axis (loading p-value) in the S-plot allows visualization of the contribution/covariance of a particular marker to the group differences. The further away from 0, the greater its contribution to the variance from the sample [345]. Both of these two parameters have a theoretical minimum of −1 and maximum of 1. *m/z* values on both ends of the S-shaped curve represent the leading contributing ions from each sample group with the highest confidence. The most interesting ions in this metabolomic analysis are the ions which are located in the upper right and lower left quadrants of the plot. Thus, the S-plot helps to identify statistically significant and potentially biochemically significant metabolites, based on contributions to the model and their reliability. The resulting list of variable importance in projection (VIP)-value, ranked according to their importance, is shown in Figure 4.7C. Those greater than 1 are indicated in red. The VIP-value combined with the corresponding loading p-value was used as a screening criterion to identify metabolites which were significantly different. Metabolites were selected if the two conditions, VIP-value >1 and p-value >0.05 were met. The OPLS-DA, the S-plot and the list of VIP-values were also generated in the positive ion mode (data not shown).

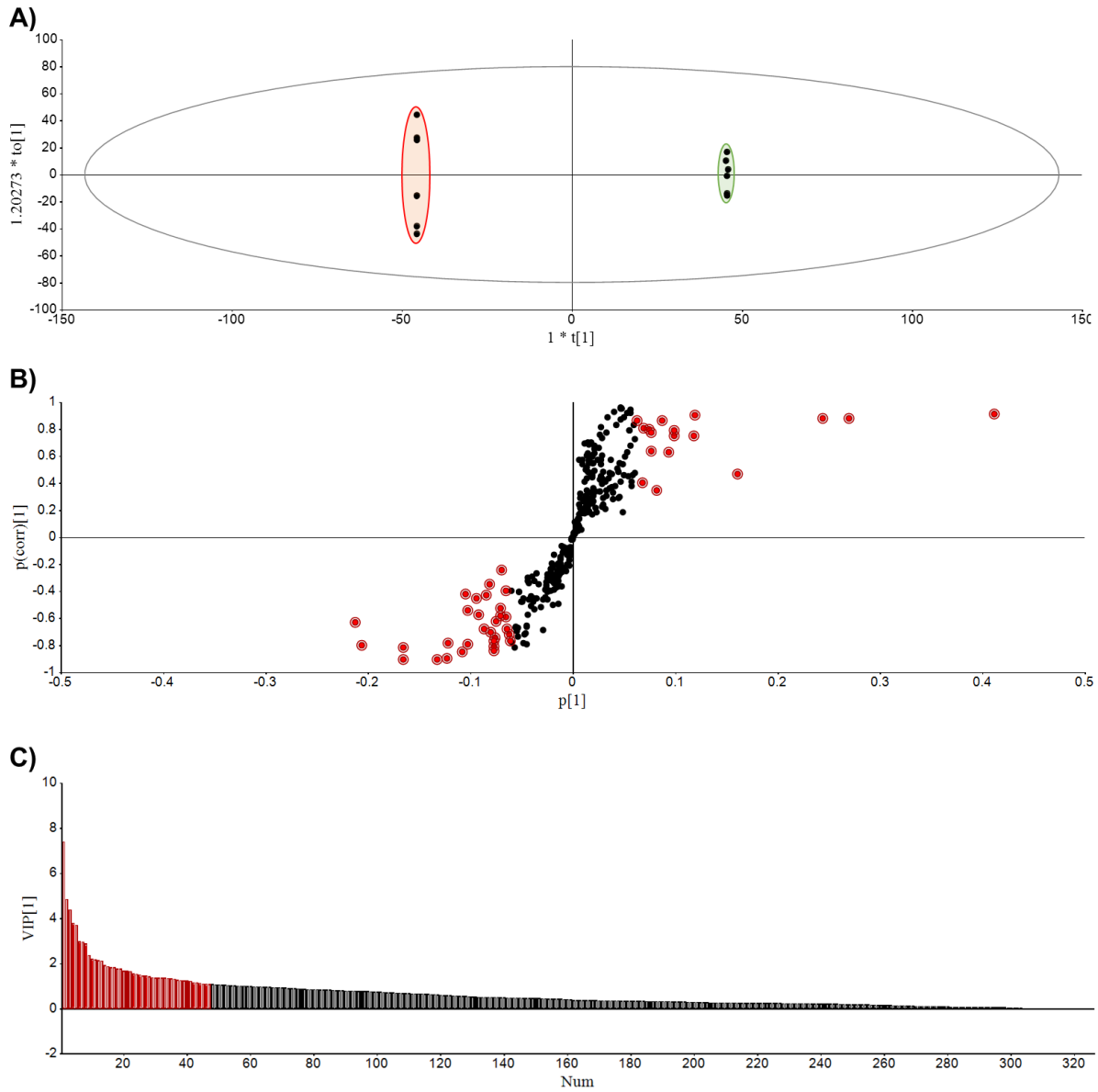

Figure 4.7. Analysis of OPLS-DA in Vero cells infected with *W. chondrophila*.
(A) OPLS-DA score plot of Vero cells infected at 72 (green) and 24 h p.i (red) in negative ion mode. The grey ellipse represents the Hotelling's T^2 with a 95% confidence. (B) S-plot generated using the OPLS-DA model. The most discriminating features are highlighted in red (upper right and lower left), having the highest correlation coefficients. (C) Numbers of VIP-values. VIP-values >1 are highlighted in red.

Metabolites with a p-value of covariance >0.05 and VIP >1 were selected in both negative and positive ion modes and ranked in order of their importance. This untargeted metabolomic approach led to 60 potential hits in negative ion mode and 19 potential metabolites in positive ion mode, (Tables 4.4). The ion with *m/z* 587.407 at RT 3.65 min was identified as the most significant metabolite at the confidence level of 0.911 in negative ion mode. The corresponding ion also showed a high correlation in the positive ion mode (*m/z* 589.422 at RT 3.65 min).

A heuristic rule was then applied, which took only VIP into consideration, detectable in at least 3 of 6 replicates. In addition, exact p-values were calculated using the non-parametric Wilcoxon-Mann Whitney test for the ions which change in abundance between 24 and 72 h p.i., suggesting significant differences in the metabolites present [175]. With this rule and the calculated p-value <0.05, 6 ions were found in both negative (Figure 4.8A) and positive ion modes (Figure 4.8B), which were not present in the non-infected cells or culture medium. All were shown to be significantly increased at 72 h p.i.

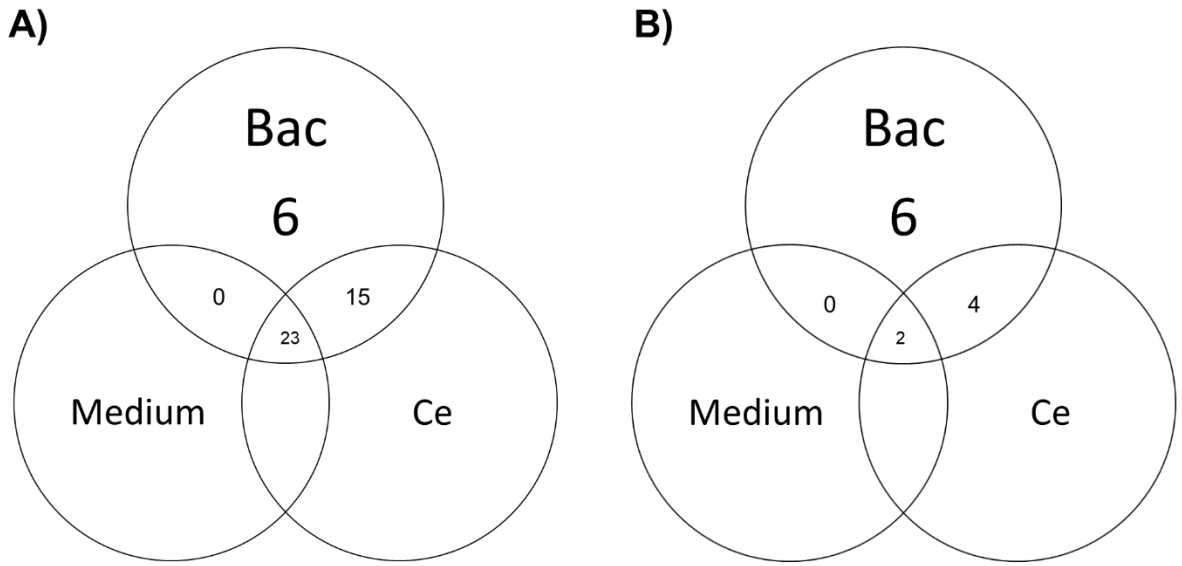

Figure 4.8. Venn diagrams displaying the distribution of metabolites following *W. chondrophila* infection of Vero cells.
The diagram displays the numbers of metabolites uniquely present in Vero cells infected with *W. chondrophila* (Bac), and those shared with non-infected Vero cells (Ce) and culture medium without cells (Medium). Metabolites were detected in negative (A) and positive ion modes (B) and the same six metabolites specific to *W. chondrophila* infected Vero cells were identified in both modes. Only those ions which showed a significant change in abundance between 24 and 72 h p.i. are represented.

The multivariate data analysis also revealed 34 VIP in negative ion mode and 8 in positive ion mode, which were decreased when compared to non-infected cells. Of these, 25 in negative and 4 in positive ion modes were shown to be significantly decreased when tested using Wilcoxon-Mann-Whitney test.

Table 4.4. VIP-values higher than 1 are shown in negative and positive ion modes, ranked according to their importance.

Negative ion mode										
No°	**RT [min]**	***m/z***	**VIP**	**Covariance**	**Correlation**	**Wilcoxon–Mann–Whitney test (n=6) (p-value)**	**In infected cells**	**In non-infected cells**	**In culture medium**	**I / D**
1 (M1)	3.65	587.407	7.4	0.411	0.911	0.0022				I
2 (M2)	3.74	571.409	4.9	0.270	0.880	0.0022				I
3	3.32	480.308	4.4	0.244	0.876	0.0022				I
4	3.72	681.295	3.8	-0.212	-0.635	0.0043				D
5	0.20	268.802	3.7	-0.206	-0.804	0.0022				D
6	2.75	500.276	3.0	-0.166	-0.907	0.0022				D
7	0.20	266.805	3.0	-0.165	-0.817	0.0022				D
8	3.60	747.557	2.9	0.161	0.467	0.0411				I
9	2.75	524.276	2.4	-0.132	-0.904	0.0022				D
10	2.76	303.232	2.2	-0.123	-0.900	0.0022				D
11	0.20	326.761	2.2	-0.122	-0.782	0.0022				D
12	2.94	452.278	2.2	0.120	0.904	0.0022				I
13	3.34	508.339	2.1	0.119	0.748	0.0022				I
14	2.83	526.293	1.9	-0.107	-0.849	0.0022				D
15*	2.64	265.144	1.9	-0.104	-0.425	0.4805				D
16	0.20	560.589	1.8	-0.102	-0.794	0.0022				D
17	3.86	492.344	1.8	-0.102	-0.540	0.0411				D
18	3.67	201.051	1.8	0.099	0.751	0.0281				I
19 (M3)	3.95	514.387	1.8	0.099	0.793	0.0152				I
20*	0.17	248.96	1.7	-0.094	-0.457	0.2403				D
21	3.44	464.312	1.7	0.094	0.628	0.0260				I
22*	0.20	215.035	1.7	-0.092	-0.572	0.0606				D
23	3.04	436.281	1.6	0.087	0.863	0.0022				I
24	0.23	160.842	1.6	-0.086	-0.680	0.0260				D
25*	0.17	316.948	1.5	-0.084	-0.433	0.2403				D
26*	3.81	885.552	1.5	0.081	0.345	0.3939				I
27*	3.92	832.608	1.5	-0.082	-0.346	0.3030				D
28	2.38	558.117	1.4	-0.080	-0.705	0.0260				D
29	0.18	374.907	1.4	-0.077	-0.768	0.0043				D
30	2.75	327.233	1.4	-0.077	-0.807	0.0022				D
31	3.03	528.308	1.4	-0.077	-0.844	0.0022				D
32	3.42	585.39	1.4	0.077	0.778	0.0022				I
33	3.66	655.417	1.4	0.077	0.638	0.0152				I
34	0.19	278.832	1.4	-0.076	-0.746	0.0043				D
35	3.90	255.232	1.4	-0.075	-0.627	0.0260				D
36	3.78	534.354	1.3	0.074	0.795	0.0022				I
37	0.20	502.632	1.3	-0.071	-0.524	0.0411				D
38*	0.17	306.919	1.3	-0.070	-0.586	0.0931				D
39*	2.12	449.149	1.3	-0.069	-0.244	0.9394				D
40	2.93	255.232	1.3	0.069	0.805	0.0022				I
41*	3.51	885.552	1.2	0.068	0.405	0.5455				I
42*	2.90	528.271	1.2	-0.066	-0.397	0.6970				D
43	0.17	238.932	1.2	-0.065	-0.595	0.0411				D
44	0.18	296.89	1.2	-0.064	-0.679	0.0152				D
45	3.86	560.36	1.1	0.062	0.865	0.0022				I
46	0.23	164.837	1.1	-0.062	-0.720	0.0152				D
47	3.59	564.343	1.1	-0.061	-0.767	0.0043				D
48	2.73	279.233	1.1	0.061	0.726	0.0152				I

49*	3.32	283.265	1.1	0.061	0.472	0.2403				I
50*	0.17	384.935	1.1	-0.060	-0.399	0.3095				D
51	2.83	329.249	1.1	-0.059	-0.779	0.0022				D
52	3.13	466.296	1.1	0.059	0.830	0.0152				I
53*	3.82	788.548	1.1	0.058	0.462	0.1818				I
54*	2.60	885.551	1.0	0.058	0.378	0.4459				I
55*	3.80	802.561	1.0	0.057	0.408	0.1818				I
56	3.02	331.264	1.0	-0.057	-0.815	0.0022				D
57*	2.91	683.391	1.0	0.057	0.916	0.1818				I
58	2.95	540.329	1.0	0.056	0.677	0.0411				I
59	2.67	769.427	1.0	0.056	0.940	0.0022				I
60	0.18	286.862	1.0	-0.056	-0.664	0.0152				D

Positive ion mode

No°	RT [min]	*m/z*	VIP	Covariance	Correlation	Wilcoxon–Mann–Whitney test (n=6) (p-value)	In infected cells	In non-infected cells	In culture medium	I / D
1	3.65	369.355	4.2	0.430	0.913	0.0022				I
2*	3.72	637.305	3.8	-0.387	-0.606	0.0649				D
3 (M1)	3.65	589.422	3.3	0.334	0.778	0.0152				I
4	3.93	369.352	2.8	0.282	0.947	0.0022				I
5	3.65	221.080	2.2	0.229	0.933	0.0022				I
6*	3.72	682.362	2.0	-0.202	-0.519	0.0649				D
7 (M2)	3.73	573.427	1.8	0.184	0.742	0.0216				I
8 (M3)	3.94	516.404	1.6	0.162	0.935	0.0022				I
9*	2.14	657.243	1.6	0.160	0.545	0.1818				I
10*	2.38	437.194	1.5	-0.158	-0.573	0.0649				D
11	2.74	361.275	1.4	-0.139	-0.727	0.0022				D
12*	3.34	524.373	1.3	0.136	0.664	0.0281				I
13	3.33	341.305	1.2	0.127	0.944	0.0022				I
14	2.11	366.156	1.2	0.121	0.560	0.1818				I
15	2.83	387.290	1.1	-0.117	-0.778	0.0152				D
16	2.74	385.274	1.1	-0.116	-0.724	0.0087				D
17*	3.17	440.409	1.1	-0.109	-0.635	0.1277				D
18	0.20	262.079	1.1	-0.108	-0.607	0.0087				D
19*	0.20	246.096	1.1	0.108	0.703	0.0606				I

Ions present are highlighted in green and those absent in red. Ions present only in infected cells and significantly increased at 72 h p.i. are highlighted in yellow. *p-value from Wilcoxon–Mann–Whitney test (n=6) >0.05. Metabolites M1, M2 and M3 are present only in infected cells and were detected in both negative and positive modes.

Abbreviations: I: Increased; D: Decreased.

Chemical formula prediction (<5 ppm deviation), based on the HRMS data was performed for the 6 metabolites increased in both negative and positive ion modes. The Mzmine based software was used. This prediction took also into account the heuristic rules [350] and resulted in the putative chemical formulas as shown in Figures 4.9 and 4.10.

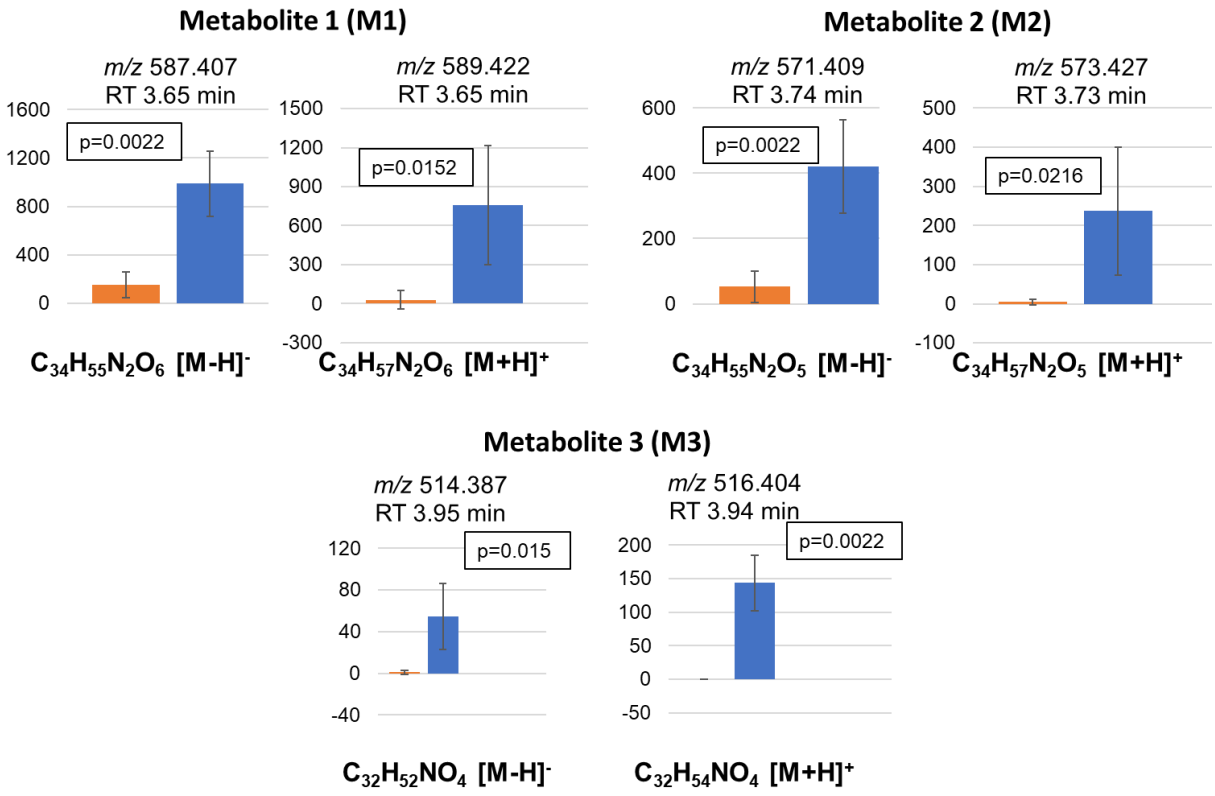

Figure 4.9. Increased ions (only present in infected cells) detected in negative and positive ion modes.
Vero cells infected with *W. chondrophila* at 24 h p.i. are shown in orange and at 72 h p.i. in blue.
Signal intensities (UPLC–TOF-MS) (average, +standard deviation, n=6) with elemental composition. p-value from Wilcoxon–Mann–Whitney test (n=6).

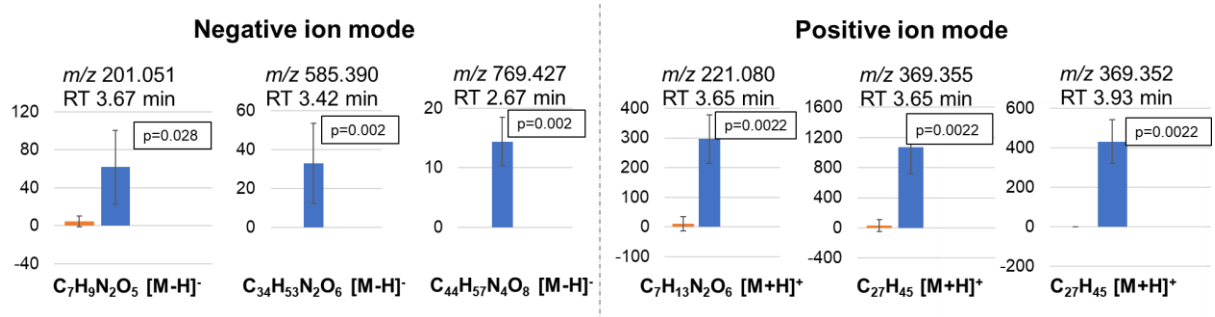

Figure 4.10. Increased ions (only present in infected cells) detected in negative or positive ion modes.
Vero cells infected with *W. chondrophila* at 24 h p.i. are shown in orange and at 72 h p.i. in blue.
Signal intensities (UPLC–TOF-MS) (average, +standard deviation, n=6) with elemental composition. p-value from Wilcoxon–Mann–Whitney test (n=6).

The workflow for selection of metabolites for elemental composition calculation is represented in Figure 4.11. It takes into account the fact that the host and the pathogen metabolisms are interconnected. With this method for data analysis, two groups of metabolites were of interest: one group which is present exclusively in cells infected with bacteria; and a second group which is present in non-infected cells and/or medium and which is significantly changed as a result of bacterial infection.

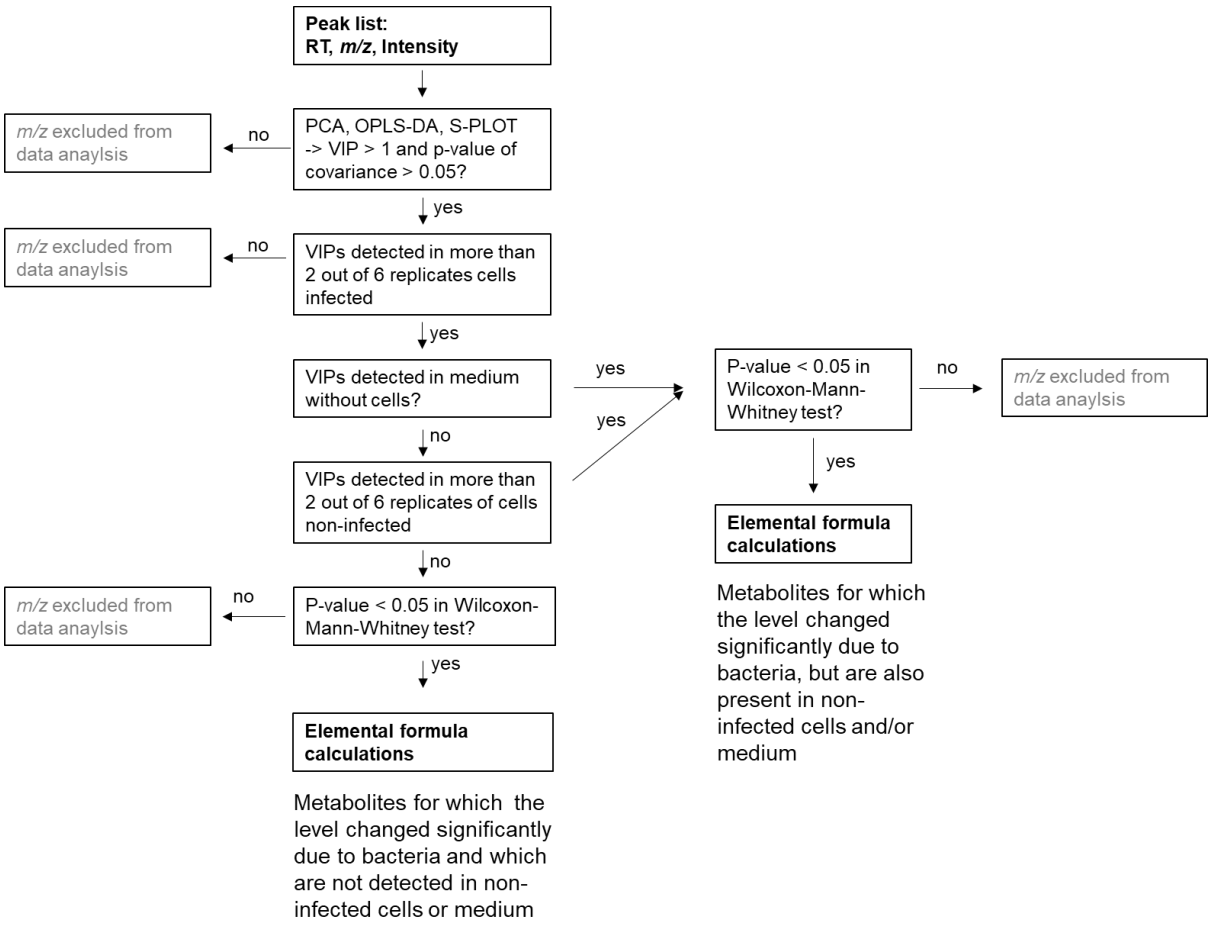

Figure 4.11. Criteria for candidate selection.
Flowchart summarizing the decision tree for cleaning and analysis of LC-MS-based metabolomic data.

Of significant importance were the ions **M1** (*m/z* 587.407 $[M-H]^-$; *m/z* 589.422 $[M-H]^+$), **M2** (*m/z* 571.409 $[M-H]^-$; *m/z* 573.427 $[M-H]^+$) and **M3** (*m/z* 514.387 $[M-H]^-$; *m/z* 516.404 $[M-H]^+$), detected in both negative and positive ion modes. These three metabolites were also identified in the preliminary study using UPLC–TOF-MS in long run mode (data not shown), confirming that their presence is associated with bacterial infection.

Other metabolites (*m/z* 221.080, *m/z* 369.355 and *m/z* 369.352) were found to be increased at 72 h p.i. in positive ion mode. The two ions with the same *m/z* 369.35, but different RT (3.65 min and 3.93 min) might be isomers. Two ions, the *m/z* 221.080 and *m/z* 369.355 have the same RT (3.65 min) as **M1** and therefore may be two fragment ions derived from the parent ion **M1** rather than separate metabolites. The mass difference of 16 between *m/z* **M1** and **M2** suggests a loss of oxygen, which is in accordance with their UPLC-HRMS predicted molecular formulas. Furthermore, both potential metabolites showed a late RT on the C_{18} column in short run mode, suggesting a more lipophilic nature of the compounds.

The mass spectra in Figure 4.12 show the metabolite **M1** at RT 3.65 min in negative and positive ion modes. The ion at *m/z* 633.4211 was recognized as the corresponding formate adduct $[M+FA-H]^-$ and the ion at *m/z* 1175.8198 as the corresponding cluster of two molecules $[2M-H]^-$. Furthermore, the ion at *m/z* 1177.8512 in positive ion mode was identified as the same cluster $[2M+H]^+$. A similar analysis was performed on the mass spectra of **M2** at RT 3.74 min and **M3** at RT 3.95 min (Figure 4.13 and 4.14).

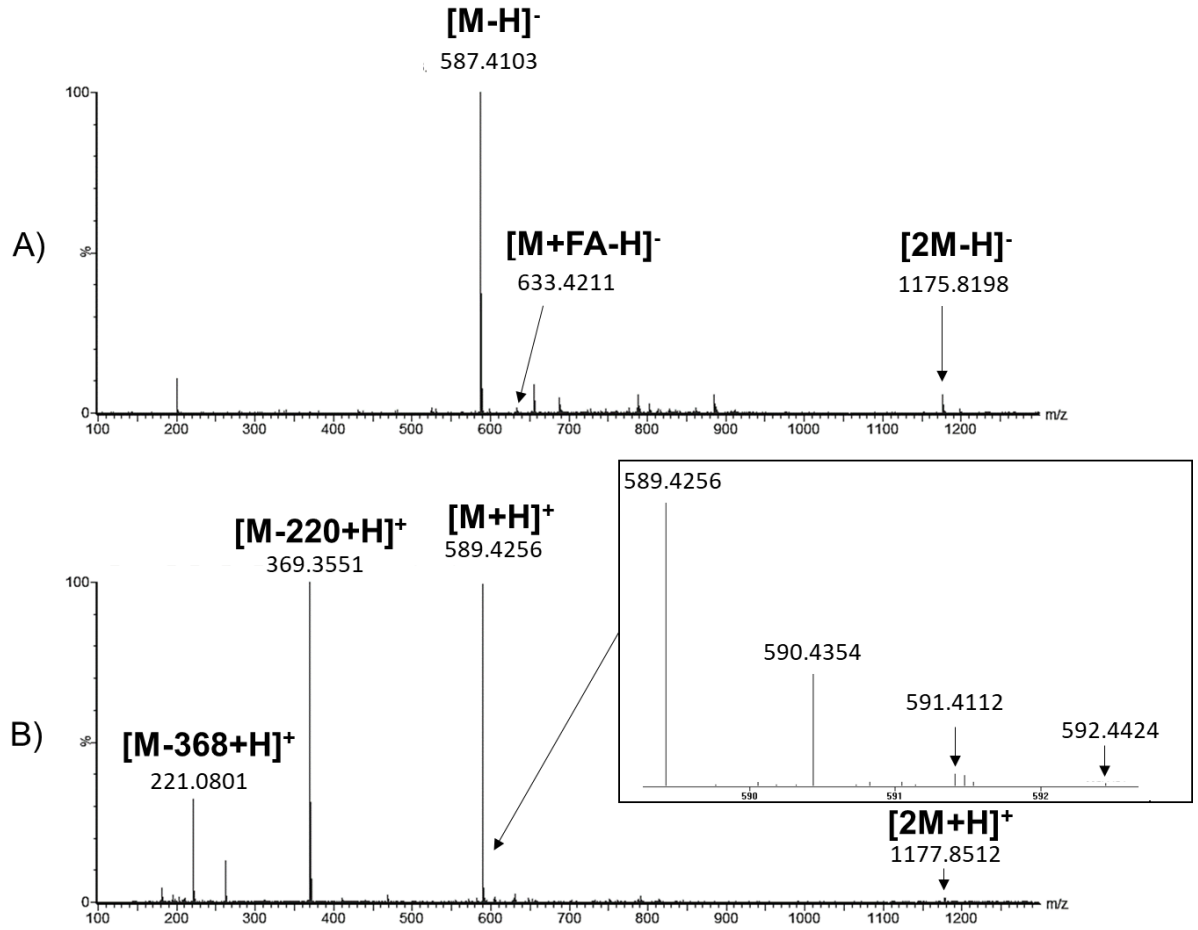

Figure 4.12. Mass spectra of M1 at RT 3.65 min in negative (A) and positive (B) ion modes.

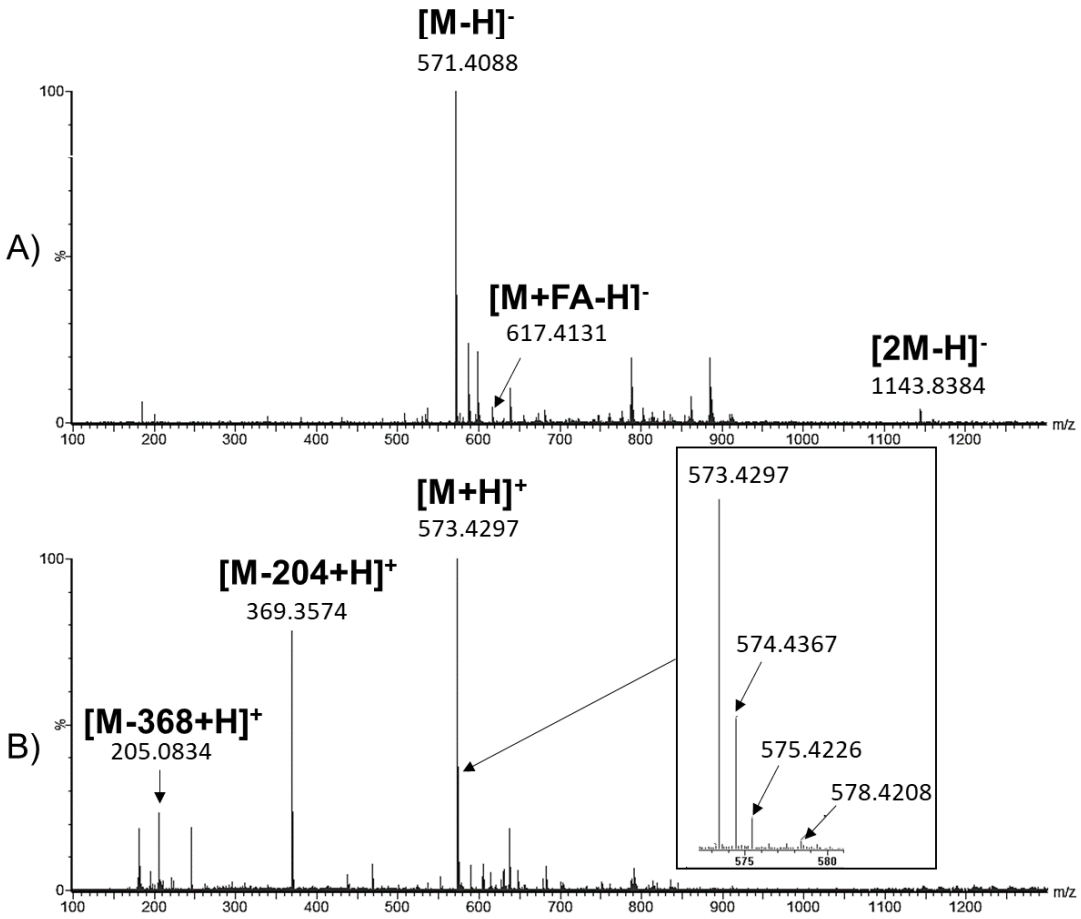

Figure 4.13. Mass spectra of M2 at RT 3.74 min in negative (A) and positive (B) ion modes.

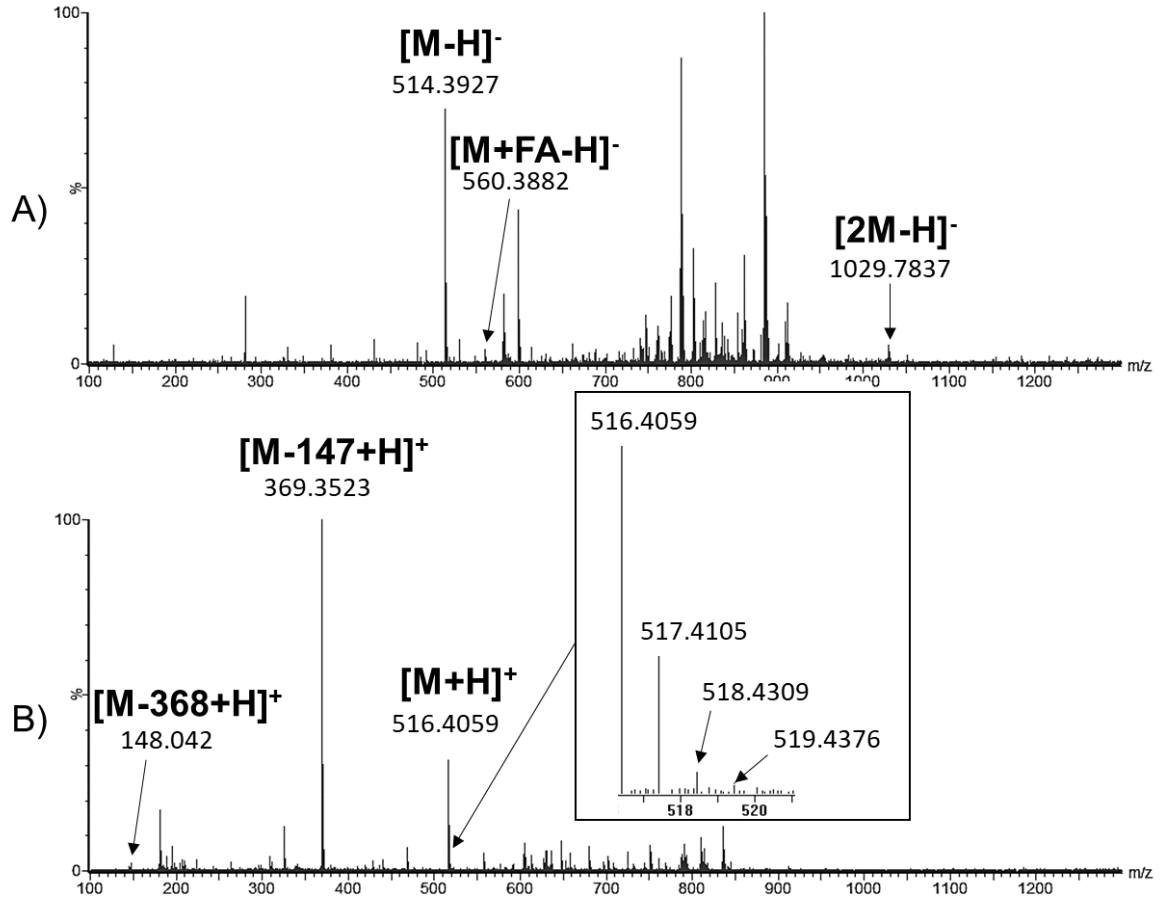

Figure 4.14. Mass spectra of M3 at RT 3.95 min in negative (A) and positive (B) ion modes.

An in-source fragmentation of the parent ion **M1** using the ESI system was observed in positive ion mode (Figure 4.12B). The isotopic pattern of **M1** (Figure 4.12B, inset) showed equal intervals of one mass unit indicating that the parent ion is singly charged. Furthermore, the isotope distribution of **M1** (Intensity: 100.00%) and 590.4354 (^{13}C) (Intensity: 35.89%) resulted in a calculated number of 32 ^{12}C atoms, which is near the HRMS elemental composition prediction of C34, (view Figure 4.9). In general, ions with an even *m/z* value have an odd number of nitrogen atoms, while ions with an odd *m/z* value have an even number or zero nitrogen atoms [351]. The previously calculated elemental compositions of the increased metabolites were in agreement with the nitrogen rule. Another parameter to assist the metabolite identification is the polarity of the molecule, expressed as RT in the chromatogram. These results suggested that **M2** (3.73 min) is slightly more hydrophobic than **M1** (3.65 min) and that **M3** (3.94 min) is even more strongly apolar. Detailed information on the molecular

formula elucidation, including the ring and double bond equivalent (RDBE) evaluation is summarized in Table 4.5.

Table 4.5. List of increased ions in negative and positive ion modes of statistical significance.

		RT [min]	TOF-HRMS [*m/z*]	$[M-H]^-$ / $[M+H]^+$	Mass error [ppm]	RDBE	Nitrogen rule	Number of calculated C^{12} atoms in M
Negative ion mode	**Increased**	3.65	587.4068 (**M1**)	$C_{34}H_{55}N_2O_6$	0.4	8.5	Even	32
		3.74	571.4127 (**M2**)	$C_{34}H_{55}N_2O_5$	1.8	8.5	Even	35
		2.67	769.427	$C_{44}H_{57}N_4O_8$	3.4	18.5	Even	35
		3.67	201.051	$C_7H_9N_2O_5$	-1.5	4.5	Even	7
		3.95	514.387 (**M3**)	$C_{32}H_{52}NO_4$	-1.4	7.5	Odd	37
		3.90	585.390	$C_{34}H_{53}N_2O_6$	3.4	9.5	Even	31
Positive ion mode	**Increased**	3.65	589.4217 (**M1**)	$C_{34}H_{57}N_2O_6$	-0.9	7.5	Even	32
		3.73	573.4232 (**M2**)	$C_{34}H_{57}N_2O_5$	3.1	7.5	Even	34
		3.94	516.4051 (**M3**)	$C_{32}H_{54}NO_4$	-1.4	6.5	Odd	39
		3.65	221.0853	$C_7H_{13}N_2O_6$	6.3	2.5	Even	9
		3.65	369.3518	$C_{27}H_{45}$	-2.4	4.5	-	28
		3.93	369.3518	$C_{27}H_{45}$	-2.4	4.5	-	28

Abbreviations: M: Molecular formula; RDBE: Ring and double bond equivalent (RDBE = X-(1/2)Y + (1/2)Z + 1, where X: Carbon, Y: Hydrogen, Z: Nitrogen).

4.3.4 Molecular networking

A higher-energy C-trap dissociation (HCD) experiment was performed using Orbitrap MS to provide further information about the detected increased metabolites (**M1**, **M2** and **M3**) and the composition of the extract at 72 h p.i. in positive ion mode. Therefore, a molecular network was generated from the high-resolution MS fragmentation data (UHPLC-$HRMS^2$) in positive ion mode of the sample 72 h p.i. using the internet platform GNPS (http://gnps.ucsd.edu) (Figure 4.15). This MS^2-based data network analysis provided an overview for comparison of mass fragmentation pattern spectra allowing identification of chemical relationships and clustering based on similarity. In this analysis, each node in the network represents a single chemical species and the relatedness between the spectra is represented as an edge [352]. Therefore, a global view of the metabolomic data could be created. The network visualization of the metabolomic data in positive ion mode showed five clusters with more than three nodes.

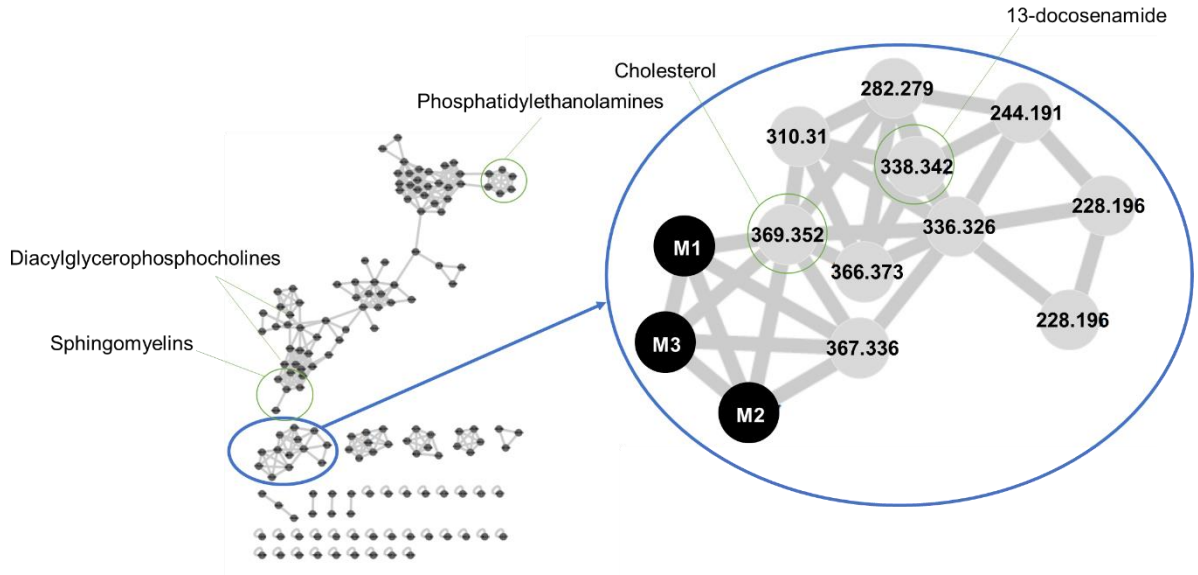

Figure 4.15. Molecular network of UHPLC-HRMS^2 data obtained from Vero cells infected with *W. chondrophila* at 72 h p.i. in positive ion mode.
Nodes indicate MS^2 spectra of ions; edges indicate significant similarity between the MS^2 fragmentation patterns of different spectra, mostly between intermediates/variants of the same compounds. The selected network cluster of increased metabolites is highlighted in blue.

Among these five clusters, the separated cluster containing the ions *m/z* 228.196, *m/z* 244.191, *m/z* 282.279, *m/z* 310.31, *m/z* 336.326, *m/z* 338.342, *m/z* 367.336, *m/z* 369.352, *m/z* 366.373, also contained the previously described increased ions **M1**, **M2** and **M3** (Figure 4.15, highlighted in blue). **M1**, **M2** and **M3** are in direct connection with each other and with the *m/z* 367.336 and *m/z* 369.352, suggesting a group of molecules with similar chemical structure and properties. The ion with *m/z* 338.342, which was also part of this cluster, could be dereplicated as putative 13-docosenamide, a fatty acid amide, which was in agreement with the predicted elemental composition of $C_{22}H_{44}NO$ (Δ= 0.232 ppm) at a RT 4.99 min based on the UHPLC-HRMS data. Furthermore, four ions, which are part of the biggest cluster in the molecular network could be dereplicated as lipids from MS^2 data: *m/z* 703.574, *m/z* 689.559, *m/z* 701.550 containing the characteristic head group peak *m/z* 184 as sphingomyelin or phosphatidylcholine [353], and *m/z* 774.544 as phosphatidylethanolamine. However, these ions were not significantly changed between 24 and 72 h p.i.

4.3.5 MS^2 spectra anaylsis

To obtain more structural information about relationships between **M1**, **M2**, and **M3**, the previously generated MS^2 spectra were compared (Figure 4.16-4.18). In negative mode, fragments with a mass difference of *m/z* 386.35 from the parent ions **M1** and **M2**, and a mass difference of *m/z* 397.35 from **M3** could be observed. In positive ion mode, the fragmentation patterns revealed an ion with *m/z* 369.351 common to all three increased metabolites. Furthermore, the second most intense signal for all three ions showed a mass difference of *m/z* 368.34 from the parent ion. Several fragments, including *m/z* 81.070, *m/z* 109.101, *m/z* 147.116 and *m/z* 175.148 were also present in all 3 spectra as well as in the spectrum for *m/z* 369.351, suggesting a common precursor metabolite.

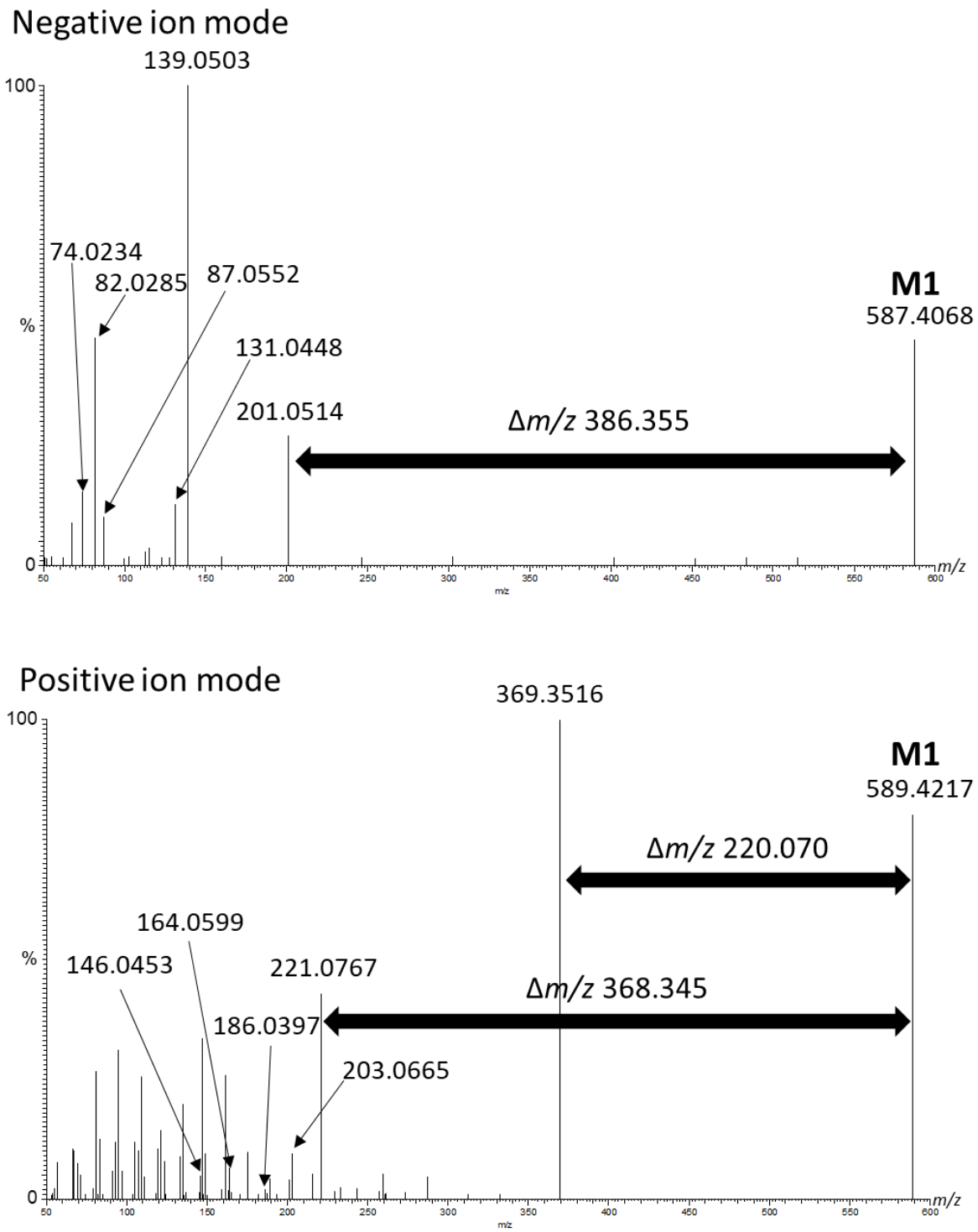

Figure 4.16. Fragmentation patterns of M1 in negative and positive ion modes.

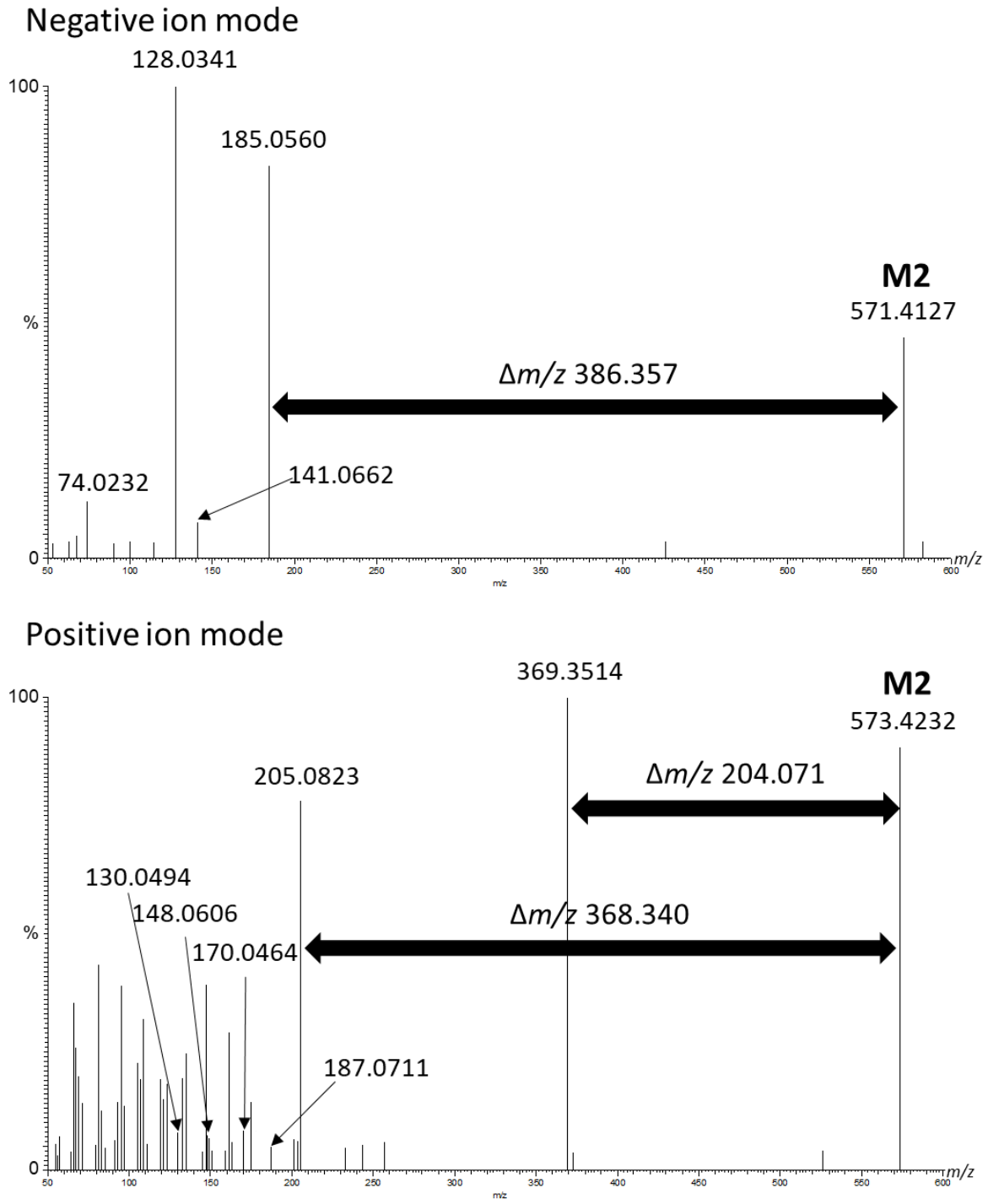

Figure 4.17. Fragmentation patterns of M2 in negative and positive ion modes.

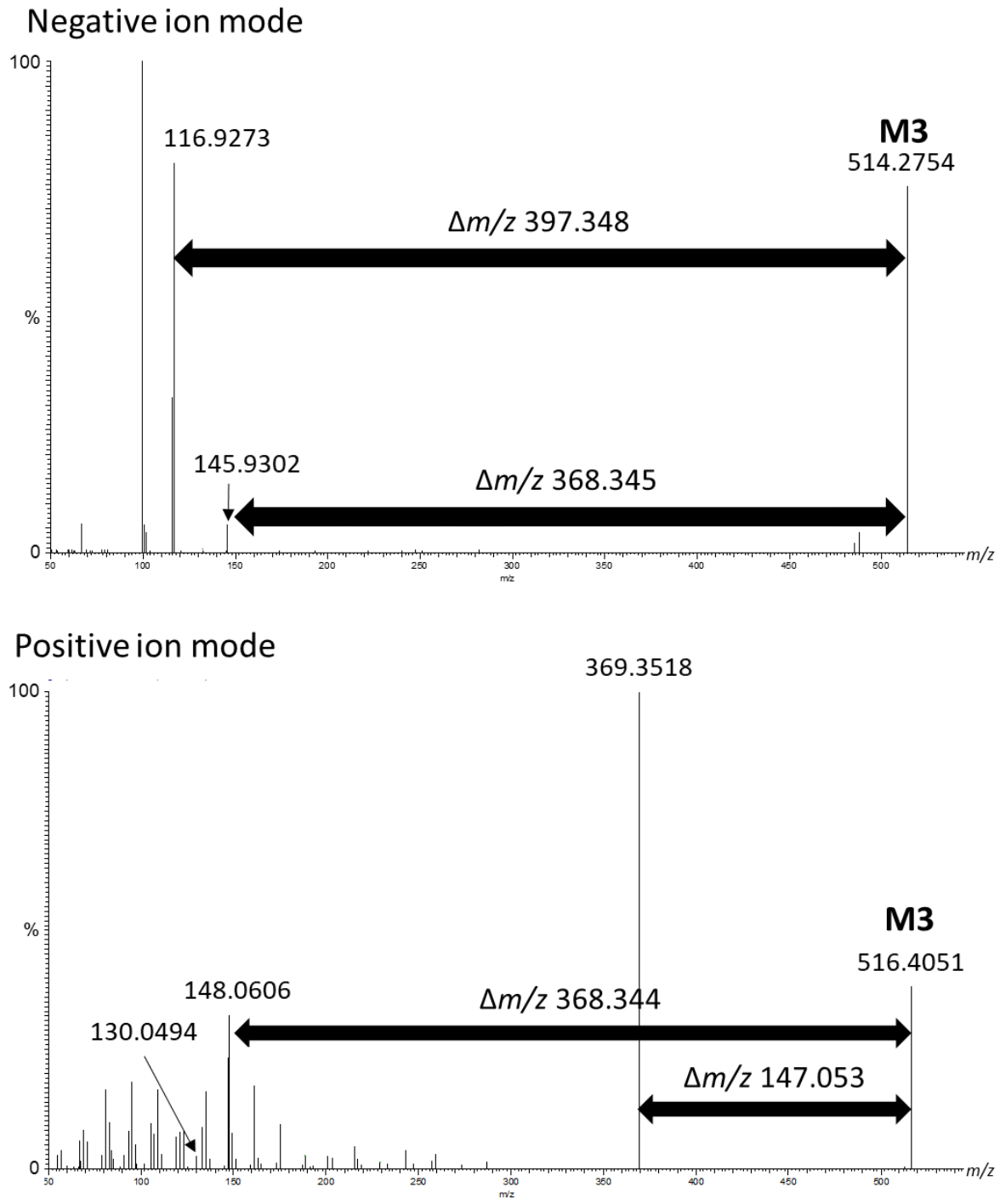

Figure 4.18. Fragmentation pattern of M3 in negative and positive ion modes.

This fragmentation pattern in positive ion mode is typical for a cholesteryl ester with the cholesterol head group at *m/z* 369.3516, which could most probably be annotated as $[M-H_2O+H]^+$ with M being putatively assigned to cholesterol. In Figure 4.19, the fragmentation pattern of **M1** is shown, with the corresponding signal annotation of the cholesterol MS^2 fragmentation pattern, taken from literature [354].

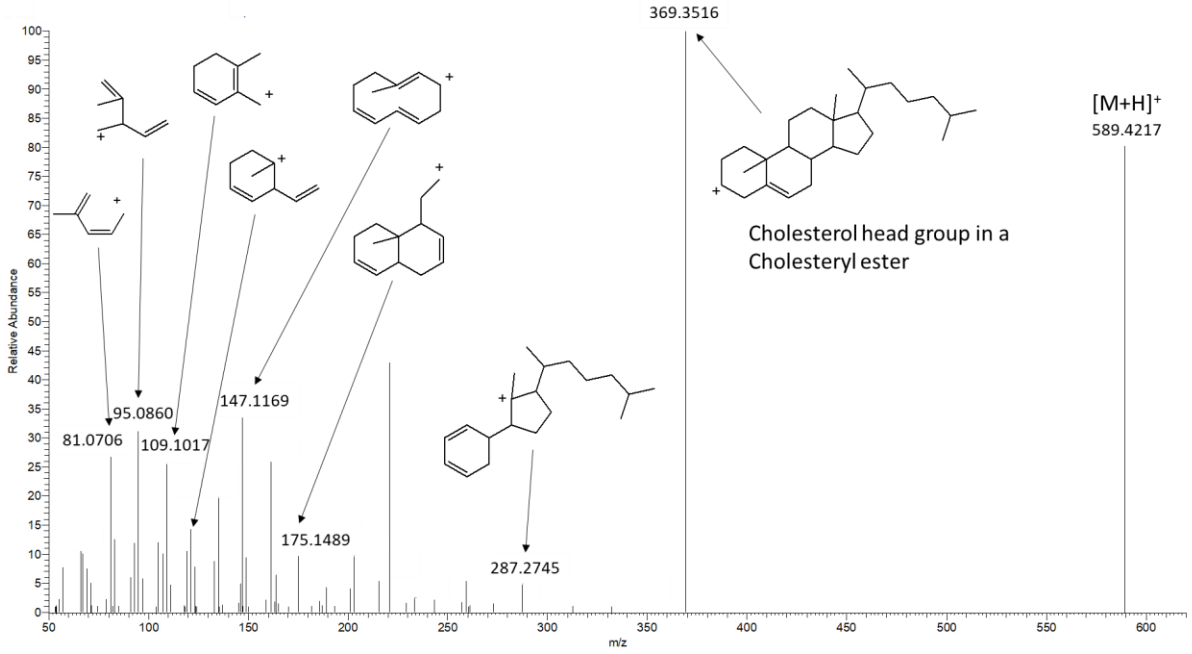

Figure 4.19. MS^2 spectrum of M1 in positive ion mode.
Annotated masses are based on data from Thermo Fisher scientific analysis [354].

The clustering of **M1**, **M2** and **M3** in the previously generated molecular network and their common fragmentation pattern in positive ion mode led to the conclusion that these molecules are most probably lipids with a common skeletal structure based on cholesterol. Dereplication with these masses in databases gave no hits related to *Chlamydiae, W. chondrophila* or Vero cells. Overall, a strong correlation of the increased ions **M1**, **M2** and **M3** and cholesterol is postulated.

A spectrum search for cholesterol (*m/z* 387.3627) in the six replicates resulted in a putative cholesterol peak at RT 4.29 min in positive ion mode. Comparison of the annotated cholesterol RT (4.29 min) with the increased ions **M3** (RT 3.94 min), **M2** (RT 3.73 min) and **M1** (RT 3.65 min) in positive ion mode led to the conclusion that all three putative novel metabolites must be more hydrophilic than cholesterol. Furthermore, extraction of mammalian cells using MeOH extracted polar and nonpolar lipids such as phospholipids, glycoproteins and cholesterol [355,

356]. Therefore, it can be concluded that the proposed cholesterol derivatives may be detected in our MeOH extract.

Since the deduced molecular formula of the three increased ions in Vero cells infected with *W. chondrophila* at 72 h p.i. most probably contained nitrogen atom(s), it was hypothesized that their cholesteryl ester side-chain had an amino acid-based character. Furthermore, these increased ions were detectable in both negative and positive ion modes, which suggested the possibility that amine ($-NH_2$) and carboxyl (-COOH) functional groups may be components of the side chains. This would be in agreement with the previous indication that the molecular formula contains nitrogen atom(s). Data in the literature indicate that the main changes in the metabolites present during chlamydial infection are lipids, carbohydrates and amino acids [175], thus the presence of a cholesterol ester with an amino side chain would be consistent with these observations. For further interpretation of the structures, their corresponding fragmentation patterns in positive and negative ion modes were analyzed in more detail as described below.

Fragmentation pattern in positive ion mode

The fragmentation pattern of these three metabolites in positive ion mode (Figure 4.16-4.18) showed mainly fragments in the low weight range (*m/z* 50-250). Some fragments, such as *m/z* 221.0767, *m/z* 203.0665, *m/z* 186.0397, *m/z* 164.0599 and *m/z* 146.0453 were present in the fragmentation pattern of **M1** and with a mass difference of 16 (*m/z* 205.0823, *m/z* 187.0711, *m/z* 170.0446, *m/z* 148.0606 and *m/z* 130.0494) in the fragmentation pattern of the parent ion **M2**. Another fragment *m/z* 164.0599 was only detected in the fragmentation pattern of **M1**. In addition, two fragments (*m/z* 130.0494 and *m/z* 148.0606), which were absent in **M1** were present in the fragmentation pattern of **M2** and **M3**. Further interpretation of these fragments is difficult, since such fragments can be obtained either from another fragment or from the parent ion. To distinguish between these possibilities, and to predict the fragmentation pathways of these metabolites, ESI-MS^n spectra should be performed, which unfortunately was not available during the course of this study.

Fragmentation pattern in negative ion mode

The negative ion mode of the three increased ions (Figure 4.16-4.18) showed a neutral loss of *m/z* 386.35 (putative cholesterol), which suggested that the fragments observed in these MS^2 spectra were most probably derived from the side chains. Furthermore, cholesterol is only very weakly ionized in negative ion mode. Therefore, this ion mode was more suitable for elucidating the molecular formula of the side chains. The metabolites **M1** and **M2** differed by *m/z* 16, which could be an oxidation event performed by the bacteria. This suggests that they may be more closely related to each other than to **M3**. The neutral loss of cholesterol (*m/z* 386.35) from the **M1** and **M2** parent ions was observed, but this was not the case for **M3**. Furthermore, the fragment *m/z* 74.023 was only detected in the parent ions **M1** and **M2**, but not in **M3**.

Based on this information, a list of fragments of **M1** and **M2** was generated in negative ion mode (Table 4.6). Elemental compositions were calculated at high mass accuracy (<6 ppm), RDBEs evaluated and nitrogen rules determined. Since the masses of the parent ions were odd numbers, and their biggest fragments (*m/z* 201.0514 and *m/z* 185.0560) also showed an odd number of nitrogens, it could be concluded that all nitrogen atoms in the structure were located in the side chain. Furthermore, the difference of *m/z* 16, between these two fragments suggested that the oxidation occurs on the *m/z* 185.0560 side chain.

Table 4.6. List of fragments of M1 and M2 in negative ion mode.

Parent ion	Orbitrap-HRMS [*m/z*]	$[M-H]^-$	Mass error [ppm]	RDBE	Nitrogen rule
M1	201.0514	$C_7H_9N_2O_5$	3.890	4.5	Odd
	139.0503	$C_6H_7N_2O_2$	0.475	4.5	Odd
	131.0448	$C_4H_7N_2O_3$	-2.431	0.5	Odd
	87.0552	$C_3H_7N_2O$	-1.487	1.0	Odd
	82.0285	C_4H_4NO	-2.808	1.5	Even
	74.0234	$C_2H_4NO_2$	-3.984	1.5	Even
M2	185.0560	$C_7H_9N_2O_4$	1.549	4.5	Odd
	141.0662	$C_6H_9N_2O_2$	2.169	3.5	Odd
	128.0341	$C_5H_6NO_3$	-1.012	3.5	Even
	74.0232	$C_2H_4NO_2$	-5.740	1.5	Even

Abbreviations: M: Molecular formula; RDBE: Ring and double bond equivalent (RDBE = X-(1/2)Y + (1/2)Z + 1, where X: Carbon, Y: Hydrogen, Z: Nitrogen)

Since the side chain was hypothesized to be attached to the cholesterol head by an esterification, the possible chemical reactions with *m/z* 204.0746 and *m/z* 220.0695 are shown in Figure 4.20. This conjugation is probably enzymatic. In mammalian cells, cholesteryl esters are formed in the liver through the action of acyl-coenzyme A (CoA):cholesterol acyltransferase (ACAT). This enzyme has not been described in the *Chlamydia* [130]. However, *Chlamydia* express the esterase CT149 [357], which catalyzes ester hydrolysis. In *W. chondrophila* the proteins wcw_0511 and wcw_1298 were reported to have a hydrolase function.

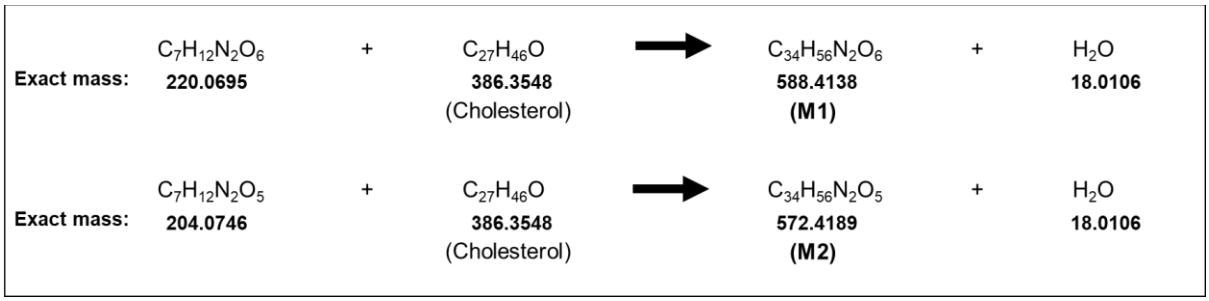

Figure 4.20. Proposed chemical reactions for the cholesteryl derivatives M1 and M2 with annotated calculated exact masses.

Dereplication of the exact mass 220.0695 resulted in possible dipeptide metabolites e.g. aspartyl-serine ($C_7H_{12}N_2O_6$). Further analysis should be performed to confirm their elemental composition. This will be discussed further in the Perspectives section.

4.3.6 Analysis of metabolites in *E. coli* and *S. aureus* extracts

To test if the increased metabolites are produced in free living bacteria, *E. coli* and the Gram-positive bacteria *S. aureus* were extracted using a procedure similar to that described for Vero cells infected with *W. chondrophila,* and analyzed using the same UPLC–TOF-MS method in negative ion mode. Corresponding chromatograms are shown in Figure 4.21A and the ion extraction spectra for *m/z* 587.4 in Figure 4.21B. The results showed that the m/z 587.4 ion was only detectable in Vero cells infected with *W. chondrophila* even at a low mass accuracy of 50 ppm.

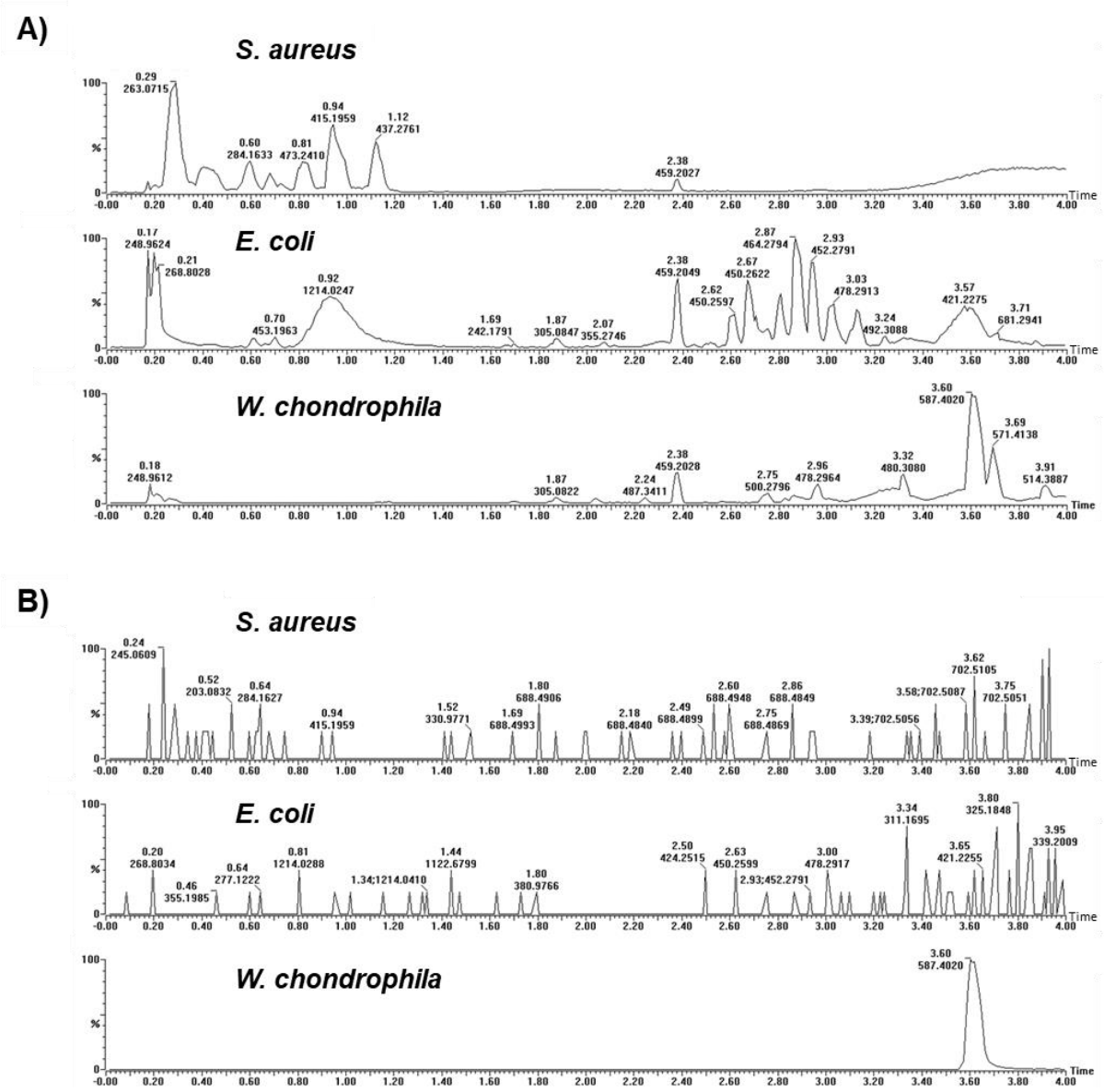

Figure 4.21. Base peak intensity chromatograms (A) and mass extraction spectra (*m/z* 587.4) at 50 ppm (B) of *S. aureus*, *E. coli* and *W. chondrophila*-infected Vero cells at 72 h p.i. in negative ion mode.
UPLC–TOF-MS analyses were done in short run mode using a C_{18} column.

Likewise, the increased metabolite (**M2**) was also not detected in *E. coli* and *S. aureus* in negative ion mode (data not shown). These findings are in agreement with the hypothesis that these metabolites are derived from cholesterol produced by mammalian cells, and consistent with the finding that *E. coli, S. aureus* and *W. chondrophila* do not encode all the enzymes required for cholesterol biosynthesis [358]. Interestingly however, the *W. chondrophila* genome, unlike the *Chlamydia* genome [130], encodes sterol delta-7 reductase (wcw_1842), which is known to catalyze the last step in cholesterol synthesis. The presence of the gene might therefore indicate an important role for cholesterol in *W. chondrophila* even though the

function of this predicted delta-7 reductase in *W. chondrophila* has not been described in the literature. Sterol delta-7 reductase is also expressed in another intracellular Gram-negative bacterium, *Coxiella burnetii* [359]. In this organism, the parasitophorous vacuole membrane is enriched in cholesterol, and thus cholesterol biosynthesis is essential for bacterial proliferation [360].

In the system described here, since the increased metabolites were not detected in non-infected Vero cells, it can be concluded that the production of these metabolites is dependent on the presence of *W. chondrophila*.

4.3.7 Analysis of metabolites in *Acanthamoeba castellanii* host and in purified EBs

To investigate if these metabolites were specifically produced in Vero cells, another host, *Acanthamoeba castellanii,* infected with *W. chondrophila*, as well as the purified EBs were extracted and analyzed in the same way as previously described for Vero cells. Since amoebae produce ergosterol instead of cholesterol, the presence of a mass at *m/z* 397.3833 with a RT of 3.90 in the non-infected amoebae could be annotated as ergosterol. Metabolites with a mass defect of 0.4 and with a RT higher than 2.8 min, which were not present in uninfected amoebae, but detectable in both positive and negative ion modes at 72 h p.i. with *W. chondrophila*, were investigated further. Based on these criteria, four metabolites *m/z* 527.3975, *m/z* 584.4189, *m/z* 598.4246, and *m/z* 600.4138 (Table 4.7) were found. The same four metabolites were also detected in preparations of purified EBs.

Table 4.7. List of ions present in negative and positive ion modes in amoebae infected with *W. chondrophila* at 72 h p.i., but absent in non-infected amoebae.

	RT LC [min]	TOF-HRMS [*m/z*]	$[M-H]^-$ / $[M+H]^+$	Mass error [ppm]	RDBE	Nitrogen rule
Negative ion mode	3.59	599.4011	$C_{35}H_{55}N_2O_6$	-7.3	9.5	Even
	3.66	583.4095	$C_{35}H_{55}N_2O_5$	-11.8	9.5	Even
	3.77	597.4281	$C_{36}H_{57}N_2O_5$	12.9	9.5	Even
	3.87	526.3917	$C_{33}H_{52}NO_4$	0.0	8.5	Odd
Positive ion mode	3.60	601.4236	$C_{35}H_{57}N_2O_6$	9.0	8.5	Even
	3.67	585.4224	$C_{35}H_{57}N_2O_5$	-0.6	8.5	Even
	3.78	599.4400	$C_{36}H_{59}N_2O_5$	0.3	8.5	Even
	3.88	528.4091	$C_{33}H_{54}NO_4$	4.2	7.5	Odd

Abbreviations: M: Molecular formula; RDBE: Ring and double bond equivalent (RDBE = X-(1/2)Y + (1/2)Z + 1, where X: Carbon, Y: Hydrogen, Z: Nitrogen)

Since this analysis was only performed once, the results should be interpreted with caution. Nevertheless, the same decreasing order in RT of these metabolites (*m/z* 528.409; RT 3.88 min, *m/z* 585.422; RT 3.67 min, *m/z* 601.424; RT 3.60 min) could be seen in positive ion mode as was found previously for the increased metabolites in infected Vero cells (**M3**; RT 3.94 min, **M2**; RT 3.73 min, **M1**; RT 3.65 min).

In general, cholesterol and ergosterol play a similar role in maintaining membrane fluidity in mammalian cells and protozoa, respectively, and in modulating cellular functions as second messenger. The significant increase in all three metabolites during the bacterial infection from 24 to 72 h p.i led to the hypothesis that these metabolites are required during the transition phase when RBs differentiate back into EBs and exit the cells. It can be hypothesized that the bacteria use these metabolites in assembling the EB cell wall.

As described in Chapter 1, *W. chondrophila* obtains many precursors such as amino acids, nucleosides and lipids from its host. In general, lipids are synthesized in the ER and are transported via the Golgi apparatus to the chlamydial inclusion, where they form part of the inclusion membrane, which protects RBs from the host immune response during the replication phase [361]. Müller *et al.* showed that in HEp-2 cells infected with *C. pneumoniae* at 24 h p.i., significantly less cholesterol could be measured compared to that present in non-infected cells [175]. These findings are consistent with the results presented here showing increased cholesterol metabolism and the formation of derivatives such as cholesteryl esters.

Unlike the *Chlamydia*, the inclusion of *W. chondrophila* is found in close contact with the host cell mitochondria and ER, possibly as a means to ensure the availability of large amounts of ATP and lipids [45, 129, 362]. In contrast, the fragmentation of the Golgi apparatus and the transport of sphingomyelin into the inclusion, and the degradation of host cell proteins by proteolytic activity, which occurs during the infection with *C. trachomatis* were not observed following infection with *W. chondrophila* [362]. Thus, it can be hypothesized that *W. chondrophila* metabolizes the cholesterol from its host to generate the cell envelope rather than using host-derived sphingomyelin.

The three metabolites M1, M2 and M3 were not described in other members of the phylum *Chlamydiae* and thus appear to be uniquely produced by *W. chondrophila*.

4.4 Conclusion

A non-targeted metabolomic approach based on UHPLC–TOF-MS was performed with Vero cells infected with *W. chondrophila*. The workflow illustrated graphically in Figure 4.1 and 4.11 was used to compare two different time points during the bacterial infectious cycle to detect metabolites that were significantly altered during bacterial development. The two time points chosen were 24 and 72 h p.i. reflecting the two stages of infection. At 24 h p.i. mainly RBs are present and at 72 h p.i. the EBs predominate.

The use of UHPLC-HRMS enabled the assignment of accurate masses to UPLC–TOF-MS signals, which in addition allowed determination of the elemental composition necessary for further structure determination. In addition, the unsupervised multivariate statistical analysis done by PCA showed that the extraction method used was adequate to detect metabolites, by clustering the samples according to their different origins (see Figure 4.5).

By using the supervised multivariate tool OPLS-DA, metabolic differences between the two time points could be determined. The performed innovative data analysis strategy highlighted changes in the whole system (intracellular bacteria and host cell), although only a limited number of metabolic differences were detected. The use of very low temperature methanol (-80°C) during the extraction process might also have a negative effect on solubility, resulting in fewer detectable metabolites. On the other hand, the use of low temperature was considered necessary in order to preserve the chemical integrity of labile metabolites and to stop possible biochemical reactions leading to metabolite degradation. The limited number of differences between the two time points could be also due to technical difficulties, since many metabolites, especially signaling molecules, are known to be present only in trace amounts [363]. The overall metabolome coverage could be enhanced by using a combination of solvents e.g. water/MeOH/chloroform to extract polar and apolar metabolites at the same time. Additionally, the combination of HILIC and RP UHPLC–TOF-MS analysis could be performed on the same samples. The separated medium and supernatant samples, which were collected during this MS approach, could be studied further. Changes in the culture conditions could also stimulate the production of additional metabolites.

The MS^2-based molecular networking analysis highlighted the presence of several distinct clusters of molecules. Furthermore, the molecular network showed that the MeOH extract of the biological sample contained lipids. One of these clusters included three putative novel cholesterol derivatives, which were found to be present only in cells infected with *W. chondrophila* and which were significantly increased at 72 h p.i. While these metabolites could not be dereplicated using currently available databases, similar metabolites were identified in

Acanthamoeba castellanii infected with *W. chondrophila* and in their purified EBs. These appear to be cholesterol derivatives with an amino acid-based side chain, although further analyses to determine the individual structures need to be performed. Nevertheless, these ions could be used as potential biomarkers to distinguish Vero cells infected with *W. chondrophila* at 72 h compared to at 24 h p.i.

Overall, this untargeted metabolomic approach was able to identify changes in the biological system of an intracellular bacteria and led to the hypothesis that the metabolites detected are synthesized by *W. chondrophila* and may be required during the late stage of the bacterial development cycle, possibly for the generation of the EB cell wall. This hypothesis could be tested further as described in the Perspectives section.

Chapter 5: General conclusion and future work

5.1 General conclusion

Despite considerable ongoing research into chlamydial biology, and the search for novel therapeutic agents, chlamydial infections are still increasing worldwide. Detailed knowledge on the biology of bacterial development and infectivity remains largely obscure, and furthermore, attempts to study *Chlamydiae* are complicated due to its obligate intracellular development cycle. The three experimental approaches described in this thesis were aimed at studying different aspects of the chlamydial development cycle. The work presented includes an investigation of several highly conserved TFs, which are probable regulators of the bacterial development cycle, and an investigation into the changes in specific metabolites produced during the transition between the early and late stages of infection.

The screening assay developed in the first experimental section (chapter 2) to identify inhibitors of several key chlamydial TFs was designed to exploit the advantages of using *E. coli* as a heterologous system. In this organism, the throughput is rapid compared to screening based on a mammalian host cell; the protocol is generic and can easily be adapted to different TFs; and it is possible to use the lacZ enzymatic readout for which there are numerous substrates available, and which can be easily scaled up to a multiwell plate format. Following evaluation of different TF targets, the Early Upstream Open reading frame (Euo) was considered to be the most promising candidate. Euo is specific to *Chlamydia* and is known to be a master regulator active during the late phase of the *Chlamydia* development cycle [364]. Conditions for the growth and cell lysis were optimised and different screening parameters were evaluated in order to screen a relatively small, but chemically diverse collection of plant extracts and natural products. These are sources that in the past have proved to be particularly rich in antimicrobial compounds. Unfortunately, the 175 plant extracts and 2'714 natural products tested failed to identify compounds with inhibitory activity against Euo. Possible reasons for this are discussed in the Conclusion to chapter 2, and are likely to be a consequence of the intracellular life cycle of *Chlamydia* and the specific role of the Euo TF in this process.

Given that this screening approach did not lead to potential drug candidates, an alternative experimental strategy was adopted (chapter 3). For these experiments, another chlamydial TF, DksA, was selected for study. DksA is highly conserved between all members of the phylum *Chlamydiae* and its expression increases during progression from the EB to RB stages suggesting an involvement in the developmental cycle. DksA is a DNA-independent TF, which modulates transcription by binding to RNA polymerase. In *E. coli* it is a central player in the stringent response to stress conditions, such as amino acid limitation and changes in pH of

the environment. Under these conditions, its principal activities include down-regulation of the rRNA transcription and upregulation of the biosynthetic genes for certain amino acids. DksA is also present in other experimentally tractable bacteria including *P. aeruginosa,* suggesting the possibility of using a genetic complementation approach to explore the activity of the *Chlamydia* DksA. For these experiments, *E. coli* and *P. aeruginosa* strains deleted for the *dksA* gene were transformed with *W. chondrophila* DksA expressed from an arabinose-inducible promoter, and the functionality of *W. chondrophila* DksA was tested under different stress conditions including amino acid limitation, metal ion depletion and changes in pH of the medium. However, results showed that the *W. chondrophila* DksA was not able to complement the *dksA* mutation in the two bacteria tested. At present, the role of DksA in *Chlamydiae* remains largely unknown and these results suggest that its function is related more specifically to chlamydial biology such as progression through the developmental cycle, and consequently, studying its activity may be possible only in mammalian or amoeboid host cell environments.

Since the research on chlamydial TFs in heterologous bacteria failed to deliver useful ways of developing anti-chlamydial reagents, a different approach using metabolomics was adopted in an attempt to understand the biology of *Chlamydia* development cycle in a natural host cell environment (chapter 4). In these experiments, the focus was on the identification of metabolites which fluctuate during the chlamydial development cycle. Vero cells were infected with *W. chondrophila* and two time points were investigated, 24 and 72 h p.i., when mainly RBs and EBs, respectively are present. A group of three putative novel metabolites was found to be significantly increased at the later stage of the developmental cycle, and further analysis provided evidence that these molecules are novel cholesterol derivatives. Furthermore, this study revealed many metabolites which are not currently annotated, and which correspond to potentially novel molecules of unknown biological importance. These molecules remain to be explored. This metabolic study again demonstrated the difficulties in working with obligate intracellular bacteria. Nevertheless, the results led to a new hypothesis, which could be tested as discussed in the Perspectives section below.

Overall, the work presented in this thesis describes a multidisciplinary approach combining microbiology, molecular biology and metabolomics to explore different aspects of chlamydial biology, and ultimately to identify new anti-chlamydial targets and drugs. This research has opened new avenues for further investigation of this important group of intracellular bacteria.

5.2 Perspectives

The possible explanations for the failure to find active compounds against the TF Euo were discussed in chapter 2. Since this screening approach was not seen as a promising perspective in the future, other approaches can be envisaged. A completely different approach would be to perform *in silico* drug design. Although, the though obtained putative candidates have to be experimentally proven. For example, Euo has been shown to dimerize *in vitro* in the presence of DNA [2], and it is likely that this is important for its DNA-binding activity, even though the importance of dimerization has yet to be demonstrated experimentally. On the other hand, structure-based drug design relies on a knowledge of the 3D structure of the biological target and currently, neither X-ray crystallography nor NMR spectroscopy data are available for the *Chlamydia* TFs. Furthermore, post-translational modifications such as methylation, glycosylation, lipidation, carboxylation, phosphorylation, are known to occur in the case of TFs from other prokaryotic organisms [316, 365]. Such modifications could be investigated for *Chlamydia* TFs and may lead to enzymatic targets, which may be easier to inhibit with small molecules than targets, which rely on protein-DNA interactions and/or protein conformational changes.

The attempts to complement *E. coli* and *P. aeruginosa dksa* mutants using *W. chondrophila* DksA failed to show functional equivalence between these proteins (chapter 3). Difference in the biology of *W. chondrophila* may again provide an explanation. The alarmone ppGpp, which is reported to act synergistically with DksA in the stringent response [263], has not been described in *W. chondrophila*, and in the light of the results obtained in chapter 3, the function of *W. chondrophila* DksA might be more related to that of *E. coli* TF TraR, which has been reported to regulate gene expression in absence of ppGpp [284]. TraR lacks the residues that interact with ppGpp in DksA, and TraR binding to RNAP occupies residues in the RNAP β' rim helices that contribute to the ppGpp binding site in the DksA-ppGpp-RNAP complex. Thus, a model can be proposed in which TraR mimics the effects of DksA and ppGpp together by binding directly to the region of the RNAP secondary channel that otherwise binds ppGpp. In this configuration, the N-terminal region of TraR, like the coiled-coil tip of DksA, engages the active-site region of the enzyme and affects transcription allosterically. Thus, TraR binds the secondary channel of RNAP using interactions which are similar, but not identical to those of *E. coli* DksA [366], and attempts to complement *E. coli* TraR may be more productive.

However, TraR is a member of the LuxR family of quorum-sensing (QS) transcription factors, which requires the signaling molecule acyl-homoserine lactone as a co-inducer for functional activity [367, 368], and *E. coli* TraR was shown to bind DNA in the presence of N-(3-oxo-

octanoyl)-L-homoserine lactone [369]. In Gram-negative bacteria, other acyl-homoserine lactones are described [370], which could be tested as co-inducers for *W. chondrophila* DksA activity. In *Chlamydiae*, such QS signalling molecules have not been documented, making it likely that the bacteria acquire them from the mammalian host cell [371]. Furthermore, *W. chondrophila* is an obligate intracellular bacterium, and thus relies heavily on the natural host encoded proteins. *E. coli* and *P. aeruginosa*, while convenient to work with, are taxonomically distinct from *Chlamydia* and thus the chlamydial proteins such as DksA may not interact functionally with the heterologous bacterial proteins. A screening using mammalian cells could be performed even though this would be technically more difficult to set up.

The metabolomics approach led to the identification of three putative novel biomarkers (chapter 4), which were highly increased in Vero cells infected with *W. chondrophila* at 72 h p.i. These were all identified as cholesterol ester derivatives. Preliminary results of UHPLC–TOF-MS analysis also showed their presence in another natural host, *Acanthamoeba castellanii*, and in purified EBs. Since these three potential biomarkers have not been detected in other bacteria, elucidating their structure could provide useful tools for monitoring chlamydial infections. Identifying the structure of these molecules would first involve determination of their elemental composition by Fourier-transform ion cyclotron resonance MS, which combines excellent mass accuracy and ultra-high resolution. Fragmentation pathways could be studied by MS^n spectra and the structures elucidated by NMR. However, a large number of infected cells would be needed to do this. Tests to isolate these compounds showed that a one liter cell culture was not sufficient. Alternatively, MS and MS^2 analysis of reference compounds could be performed in parallel, and compared to the 3 biomarkers. Furthermore, since the side chains of these biomarkers are likely to contain nitrogen, and nitrogen can be found e.g. in amino acids, the change of amino acid composition during the bacterial development cycle could be studied and might lead to further information about the side chains of these cholesteryl esters. Having elucidated the structure of these molecules, their biological function would be a subsequent task. Similar compounds, conjugates of cholesterol with amino acids such as tyrosine, have been shown to have anticancer activities [372]. It may also be interesting to link the increase of these metabolites at 72 h p.i. with the expression of host genes involved in cholesterol metabolism such as 7-dehydrocholesterol reductase (wcw_1842), phospholipase/carboxylesterase (wcw_0054), and putative BAAT (wcw_0412). Transcriptomic data would therefore be useful in this respect.

Another interesting track would be to evaluate the occurrence of these metabolites during other phases of the life cycle such as in the resistance form (AB) and in purified metabolically active RBs. Other members of the phylum *Chlamydiae*, including the human pathogen *C.*

trachomatis could also be investigated. The host interactions of *W. chondrophila* are known to differ slightly from those of *C. trachomatis* and *C. pneumoniae.* For example, *W. chondrophila* remains in the inclusion, surrounded by an inner layer of tightly associated mitochondria, which interact with a dense ER network. In contrast, in the other two members of the genus, such intimate contact with mitochondria has not been reported [128]. Since the increased putative novel molecules identified thus far are all lipids, a metabolomic approach, which specifically targets lipids could be performed to investigate the global change in the lipid components. A database containing authentic lipid reference standards could be generated to compare the observed mass changes with different phases of the development cycle. To investigate the production of the three biomarkers, isotopically labelled cholesterol could be added to the culture medium of cholesterol-dependent Vero cells previously infected with *W. chondrophila.* The metabolomic modifications of cholesterol in the *W. chondrophila* infected cells could then be tracked.

A further approach to study the possible importance of lipids during the development cycle of *W. chondrophila* could make use of high resolution imaging technologies such as Nanoscale secondary ion mass spectrometry (NanoSIMS). This analytical procedure was used by Doughty *et al*. [373] to study the subcellular localization of the hopanoid lipids in bacteria. Hopanoids are sterol-like pentacyclic compounds, which can functionally replace sterols in bacterial membranes [374], although they have not yet been described in *Chlamydia* [375]. Finally, a study could be performed using NMR, an alternative and well-established technique, which has been used for metabolomic approaches in bacteria for identification and quantification of possible biomarkers [376]. This approach might provide a completely different perspective on the metabolite composition of the infected cells and thus increase the global view of the bacterial development cycle.

Overall, this work has provided new options for future studies of the chlamydial development cycle, and the metabolomic approach could be especially promising. Since chlamydial infections worldwide are still not under control, this work may offer new approaches for further research into this into this clinically important organism.

References

1. Davies, J. and Davies, D., *Origins and evolution of antibiotic resistance.* Microbiol Mol Biol Rev, 2010, **74**: 417-433.
2. Silver, L.L., *Challenges of antibacterial discovery.* Clin Microbiol Rev, 2011, **24**: 71-79.
3. Miesel, L., Greene, J., and Black, T.A., *Genetic strategies for antibacterial drug discovery.* Nat Rev Genet, 2003, **4**: 442-456.
4. World Health Organization, *Antibacterial agents in clinical development: an analysis of the antibacterial clinical development pipeline, including tuberculosis*, 2017.
5. O'Neill, J., *Antimicrobial resistance: tackling a crisis for the health and wealth of nations.* Review on Antimicrobial Resistance, 2014, **20**: 1-16.
6. Taylor, H.R., Burton, M.J., Haddad, D.*, et al.*, *Trachoma.* The Lancet, 2014, **384**: 2142-2152.
7. Centers for Disease Control Prevention, *Chlamydia trachomatis genital infections--United States, 1995*, 1997.
8. World Health Organization, *Progress report of the implementation of the global strategy for prevention and control of sexually transmitted infections: 2006-2015: document for the World Health Assembly*, 2015.
9. World Health Organization, *WHO guidelines for the treatment of Chlamydia trachomatis*, 2016.
10. Atlanta: U.S. Department of Health and Human Services, *Sexually Transmitted Disease Surveillance 2015*, 2016.
11. Brunham, R.C., Gottlieb, S.L., and Paavonen, J., *Pelvic inflammatory disease.* N Engl J Med, 2015, **372**: 2039-2048.
12. Brunham, R.C. and Rey-Ladino, J., *Immunology of Chlamydia infection: implications for a Chlamydia trachomatis vaccine.* Nat Rev Immunol, 2005, **5**: 149-161.
13. Bavoil, P.M., Hsia, R.C., and Ojcius, D.M., *Closing in on Chlamydia and its intracellular bag of tricks.* Microbiology, 2000, **146**: 2723-2731.
14. Miyairi, I., Ramsey, K.H., and Patton, D.L., *Duration of untreated chlamydial genital infection and factors associated with clearance: review of animal studies.* J Infect Dis, 2010, **201**: S96-S103.
15. Owusu-Edusei Jr, K., Chesson, H.W., Gift, T.L.*, et al.*, *The estimated direct medical cost of selected sexually transmitted infections in the United States, 2008.* Sex Transm Dis, 2013, **40**: 197-201.
16. Laga, M., Manoka, A., Kivuvu, M.*, et al.*, *Non-ulcerative sexually transmitted diseases as risk factors for HIV-1 transmission in women: Results from a cohort study.* Aids, 1993, **7**: 95-102.

17. Karim, S., Souho, T., Benlemlih, M.*, et al.*, *Cervical cancer induction enhancement potential of Chlamydia trachomatis: A systematic review.* Curr Microbiol, 2018: 1-8.
18. Bell, T.A., Stamm, W.E., Wang, S.*, et al.*, *Chronic Chlamydia trachomatis infections in infants.* JAMA, 1992, **267**: 400-402.
19. Dean, D., Suchland, R.J., and Stamm, W.E., *Evidence for long-term cervical persistence of Chlamydia trachomatis by omp1 genotyping.* J Infect Dis, 2000, **182**: 909-916.
20. Hahn, D.L. and McDonald, R., *Can acute Chlamydia pneumoniae respiratory tract infection initiate chronic asthma?* Ann Allergy Asthma Immunol, **81**: 339-344.
21. Gaydos, C.A. and Quinn, T.C., *The role of Chlamydia pneumoniae in cardiovascular disease.* Adv Intern Med, 2000, **45**: 139-173.
22. Villareal, C., Whittum-Hudson, J.A., and Hudson, A.P., *Persistent Chlamydiae and chronic arthritis.* Arthritis Res, 2001, **4**: 5-9.
23. Kuo, C.-C., Jackson, L.A., Campbell, L.A.*, et al.*, *Chlamydia pneumoniae (TWAR).* Clin Microbiol Rev, 1995, **8**: 451-461.
24. Vanrompay, D., Harkinezhad, T., van de Walle, M.*, et al.*, *Chlamydophila psittaci transmission from pet birds to humans.* Emerg Infect Dis, 2007, **13**: 1108-1110.
25. Wagner, M. and Horn, M., *The Planctomycetes, Verrucomicrobia, Chlamydiae and sister phyla comprise a superphylum with biotechnological and medical relevance.* Curr Opin Biotechnol, 2006, **17**: 241-249.
26. Gupta, R.S., Naushad, S., Chokshi, C.*, et al.*, *A phylogenomic and molecular markers based analysis of the phylum Chlamydiae: proposal to divide the class Chlamydiia into two orders, Chlamydiales and Parachlamydiales ord. nov., and emended description of the class Chlamydiia.* Antonie Van Leeuwenhoek, 2015, **108**: 765-781.
27. Chua, P.K., Corkill, J.E., Hooi, P.S.*, et al.*, *Isolation of Waddlia malaysiensis, a novel intracellular bacterium, from fruit bat (Eonycteris spelaea).* Emerg Infect Dis, 2005, **11**: 271-277.
28. Everett, K.D., Bush, R.M., and Andersen, A.A., *Emended description of the order Chlamydiales, proposal of Parachlamydiaceae fam. nov. and Simkaniaceae fam. nov., each containing one monotypic genus, revised taxonomy of the family Chlamydiaceae, including a new genus and five new species, and standards for the identification of organisms.* Int J Syst Bacteriol, 1999, **49**: 415-440.
29. Rurangirwa, F.R., Dilbeck, P.M., Crawford, T.B.*, et al.*, *Analysis of the 16S rRNA gene of micro-organism WSU 86-1044 from an aborted bovine foetus reveals that it is a member of the order Chlamydiales: proposal of Waddliaceae fam. nov., Waddlia chondrophila gen. nov., sp. nov.* Int J Syst Bacteriol, 1999, **49 Pt 2**: 577-581.

30. Thomas, V., Casson, N., and Greub, G., *Criblamydia sequanensis, a new intracellular Chlamydiales isolated from Seine river water using amoebal co-culture.* Environ Microbiol, 2006, **8**: 2125-2135.
31. Kuo, C., Horn, M., and Stephens, R., *The order Chlamydiales.* Bergey's manual of systematic bacteriology-the Planctomycetes, Spriochaetes, Fibrobacteres, Bacteriodetes and Fusobacteria, 2011: 37-40.
32. Stride, M.C., Polkinghorne, A., Miller, T.L., *et al.*, *Molecular characterization of "Candidatus Parilichlamydia carangidicola," a novel Chlamydia-like epitheliocystis agent in yellowtail kingfish, Seriola lalandi (Valenciennes), and the proposal of a new family, "Candidatus Parilichlamydiaceae" fam. nov. (order Chlamydiales).* Appl Environ Microbiol, 2013, **79**: 1590-1597.
33. Taylor-Brown, A., Vaughan, L., Greub, G., *et al.*, *Twenty years of research into Chlamydia-like organisms: a revolution in our understanding of the biology and pathogenicity of members of the phylum Chlamydiae.* Pathog Dis, 2015, **73**: 1-15.
34. Stephens, R.S., Tam, M.R., Kuo, C.C., *et al.*, *Monoclonal antibodies to Chlamydia trachomatis: antibody specificities and antigen characterization.* J Immunol, 1982, **128**: 1083-1089.
35. Caldwell, H.D. and Schachter, J., *Antigenic analysis of the major outer membrane protein of Chlamydia spp.* Infect Immun, 1982, **35**: 1024-1031.
36. Harris, S.R., Clarke, I.N., Seth-Smith, H.M., *et al.*, *Whole-genome analysis of diverse Chlamydia trachomatis strains identifies phylogenetic relationships masked by current clinical typing.* Nat Genet, 2012, **44**: 413-419.
37. Stephens, R.S., Kalman, S., Lammel, C., *et al.*, *Genome sequence of an obligate intracellular pathogen of humans: Chlamydia trachomatis.* Science, 1998, **282**: 754-759.
38. Blattner, F.R., Plunkett, G., Bloch, C.A., *et al.*, *The complete genome sequence of Escherichia coli K-12.* Science, 1997, **277**: 1453-1462.
39. Voigt, A., Schofl, G., and Saluz, H.P., *The Chlamydia psittaci genome: a comparative analysis of intracellular pathogens.* PLoS One, 2012, **7**: e35097.
40. Collingro, A., Tischler, P., Weinmaier, T., *et al.*, *Unity in variety—the pan-genome of the Chlamydiae.* Mol Biol Evol, 2011, **28**: 3253-3270.
41. Domman, D. and Horn, M., *Following the footsteps of chlamydial gene regulation.* Mol Biol Evol, 2015, **32**: 3035-3046.
42. Pérez-Rueda, E. and Collado-Vides, J., *The repertoire of DNA-binding transcriptional regulators in Escherichia coli K-12.* Nucleic Acids Res, 2000, **28**: 1838-1847.

43. Moulder, J.W., *Interaction of Chlamydiae and host cells in vitro.* Microbiol Rev, 1991, **55**: 143-190.
44. Hackstadt, T., Fischer, E.R., Scidmore, M.A*., et al.*, *Origins and functions of the chlamydial inclusion.* Trends Microbiol, 1997, **5**: 288-293.
45. Croxatto, A. and Greub, G., *Early intracellular trafficking of Waddlia chondrophila in human macrophages.* Microbiology, 2010, **156**: 340-355.
46. Hybiske, K. and Stephens, R.S., *Mechanisms of host cell exit by the intracellular bacterium Chlamydia.* Proc Natl Acad Sci U S A, 2007, **104**: 11430-11435.
47. Wyrick, P.B., *Intracellular survival by Chlamydia.* Cell Microbiol, 2000, **2**: 275-282.
48. Shaw, E., Dooley, C., Fischer, E*., et al.*, *Three temporal classes of gene expression during the Chlamydia trachomatis developmental cycle.* Mol Microbiol, 2000, **37**: 913-925.
49. Nicholson, T.L., Olinger, L., Chong, K*., et al.*, *Global stage-specific gene regulation during the developmental cycle of Chlamydia trachomatis.* J Bacteriol, 2003, **185**: 3179-3189.
50. Abdelrahman, Y.M. and Belland, R.J., *The chlamydial developmental cycle.* FEMS Microbiol Rev, 2005, **29**: 949-959.
51. Hogan, R.J., Mathews, S.A., Mukhopadhyay, S*., et al.*, *Chlamydial persistence: beyond the biphasic paradigm.* Infect Immun, 2004, **72**: 1843-1855.
52. Kintner, J., Lajoie, D., Hall, J*., et al.*, *Commonly prescribed beta-lactam antibiotics induce C. trachomatis persistence/stress in culture at physiologically relevant concentrations.* Front Cell Infect Microbiol, 2014, **4**: 1-10.
53. Campbell, R.P., Kintner, J., Whittimore, J*., et al.*, *Chlamydia muridarum enters a viable but non-infectious state in amoxicillin-treated BALB/c mice.* Microbes Infect, 2012, **14**: 1177-1185.
54. Wyrick, P.B., *Chlamydia trachomatis persistence in vitro: an overview.* J Infect Dis, 2010, **201**: S88-S95.
55. Raulston, J.E., *Response of Chlamydia trachomatis serovar E to iron restriction in vitro and evidence for iron-regulated chlamydial proteins.* Infect Immun, 1997, **65**: 4539-4547.
56. Harper, A., Pogson, C.I., Jones, M.L*., et al.*, *Chlamydial development is adversely affected by minor changes in amino acid supply, blood plasma amino acid levels, and glucose deprivation.* Infect Immun, 2000, **68**: 1457-1464.
57. Bertelli, C., Collyn, F., Croxatto, A*., et al.*, *The Waddlia genome: a window into chlamydial biology.* PLoS One, 2010, **5**: e10890.

58. Nans, A., Saibil, H.R., and Hayward, R.D., *Pathogen–host reorganization during Chlamydia invasion revealed by cryo-electron tomography.* Cell Microbiol, 2014, **16**: 1457-1472.

59. Betts, H., Twiggs, L., Sal, M.*, et al.*, *Bioinformatic and biochemical evidence for the identification of the type III secretion system needle protein of Chlamydia trachomatis.* J Bacteriol, 2008, **190**: 1680-1690.

60. Nans, A., Ford, C., and Hayward, R.D., *Host-pathogen reorganisation during host cell entry by Chlamydia trachomatis.* Microbes Infect, 2015, **17**: 727-731.

61. Wolf, K., Betts, H., Chellas-Géry, B.*, et al.*, *Treatment of Chlamydia trachomatis with a small molecule inhibitor of the Yersinia type III secretion system disrupts progression of the chlamydial developmental cycle.* Mol Microbiol, 2006, **61**: 1543-1555.

62. Dautry-Varsat, A., Subtil, A., and Hackstadt, T., *Recent insights into the mechanisms of Chlamydia entry.* Cell Microbiol, 2005, **7**: 1714-1722.

63. Elwell, C., Mirrashidi, K., and Engel, J., *Chlamydia cell biology and pathogenesis.* Nat Rev Microbiol, 2016, **14**: 385-390.

64. Wesolowski, J. and Paumet, F., *Taking control: reorganization of the host cytoskeleton by Chlamydia.* F1000Res, 2017, **6**: 1-18.

65. Kern, J., Maass, V., and Maass, M., *Molecular pathogenesis of chronic Chlamydia pneumoniae infection: a brief overview.* Clin Microbiol Infect, 2009, **15**: 36-41.

66. Bastidas, R.J., Elwell, C.A., Engel, J.N.*, et al.*, *Chlamydial intracellular survival strategies.* Cold Spring Harb Perspect Med, 2013, **3**: a010256.

67. Zaas, D.W., Duncan, M., Wright, J.R.*, et al.*, *The role of lipid rafts in the pathogenesis of bacterial infections.* Biochim Biophys Acta, 2005, **1746**: 305-313.

68. Hackstadt, T., Rockey, D., Heinzen, R.*, et al.*, *Chlamydia trachomatis interrupts an exocytic pathway to acquire endogenously synthesized sphingomyelin in transit from the Golgi apparatus to the plasma membrane.* EMBO J, 1996, **15**: 964-977.

69. Heuer, D., Rejman Lipinski, A., Machuy, N.*, et al.*, *Chlamydia causes fragmentation of the Golgi compartment to ensure reproduction.* Nature, 2009, **457**: 731-735.

70. Beatty, W.L., *Trafficking from CD63-positive late endocytic multivesicular bodies is essential for intracellular development of Chlamydia trachomatis.* J Cell Sci, 2006, **119**: 350-359.

71. Derré, I., Swiss, R., and Agaisse, H., *The lipid transfer protein CERT interacts with the Chlamydia inclusion protein IncD and participates to ER-Chlamydia inclusion membrane contact sites.* PLoS Pathog, 2011, **7**: e1002092.

72. Ouellette, S.P., Dorsey, F.C., Moshiach, S.*, et al.*, *Chlamydia species-dependent differences in the growth requirement for lysosomes.* PLoS One, 2011, **6**: e16783.
73. Tipples, G. and McClarty, G., *The obligate intracellular bacterium Chlamydia trachomatis is auxotrophic for three of the four ribonucleoside triphosphates.* Mol Microbiol, 1993, **8**: 1105-1114.
74. Case, E.D., Akers, J.C., and Tan, M., *CT406 encodes a chlamydial ortholog of NrdR, a repressor of ribonucleotide reductase.* J Bacteriol, 2011, **193**: 4396-4404.
75. Liang, S.Y. and Reno, H.E.L., *Sexually transmitted diseases treatment guidelines, 2015.* Annals of Emergency Medicine, 2015, **66**: 526-528.
76. Moulder, J.W., *Why is Chlamydia sensitive to penicillin in the absence of peptidoglycan?* Infect Agents Dis, 1993, **2**: 87-99.
77. Barbour, A.G., Amano, K.-i., Hackstadt, T.*, et al.*, *Chlamydia trachomatis has penicillin-binding proteins but not detectable muramic acid.* J Bacteriol, 1982, **151**: 420-428.
78. McCoy, A.J. and Maurelli, A.T., *Building the invisible wall: updating the chlamydial peptidoglycan anomaly.* Trends Microbiol, 2006, **14**: 70-77.
79. Hatch, T.P., Allan, I.t., and Pearce, J., *Structural and polypeptide differences between envelopes of infective and reproductive life cycle forms of Chlamydia spp.* J Bacteriol, 1984, **157**: 13-20.
80. Lambden, P.R., Pickett, M.A., and Clarke, I.N., *The effect of penicillin on Chlamydia trachomatis DNA replication.* Microbiology, 2006, **152**: 2573-2578.
81. Misyurina, O., Chipitsyna, E., Finashutina, Y.*, et al.*, *Mutations in a 23S rRNA gene of Chlamydia trachomatis associated with resistance to macrolides.* Antimicrob Agents Chemother, 2004, **48**: 1347-1349.
82. Wyrick, P.B. and Knight, S.T., *Pre-exposure of infected human endometrial epithelial cells to penicillin in vitro renders Chlamydia trachomatis refractory to azithromycin.* J Antimicrob Chemother, 2004, **54**: 79-85.
83. Reveneau, N., Crane, D.D., Fischer, E.*, et al.*, *Bactericidal activity of first-choice antibiotics against gamma interferon-induced persistent infection of human epithelial cells by Chlamydia trachomatis.* Antimicrob Agents Chemother, 2005, **49**: 1787-1793.
84. Hocking, J.S., Kong, F.Y., Timms, P.*, et al.*, *Treatment of rectal Chlamydia infection may be more complicated than we originally thought.* J Antimicrob Chemother, 2014, **70**: 961-964.
85. Gieffers, J., Fullgraf, H., Jahn, J.*, et al.*, *Chlamydia pneumoniae infection in circulating human monocytes is refractory to antibiotic treatment.* Circulation, 2001, **103**: 351-356.

86. Horner, P.J., *Azithromycin antimicrobial resistance and genital Chlamydia trachomatis infection: duration of therapy may be the key to improving efficacy.* Sex Transm Infect, 2012, **88**: 154-156.
87. Bailey, R. and Lietman, T., *The SAFE strategy for the elimination of trachoma by 2020: will it work?* Bull World Health Organ, 2001, **79**: 233-236.
88. Satpathy, G., Behera, H., and Ahmed, N., *Chlamydial eye infections: Current perspectives.* Indian J Ophthalmol, 2017, **65**: 97-102.
89. Centers for Disease Control Prevention, *Sexually transmitted diseases treatment guidelines, 2010, https://www.cdc.gov*, Accessed: November 13, 2018.
90. Low, N., Redmond, S., Uusküla, A.*, et al.*, *Screening for genital Chlamydia infection.* Cochrane Database Syst Rev, 2013: 1-15.
91. Rank, R.G. and Whittum-Hudson, J.A., *Protective immunity to chlamydial genital infection: evidence from animal studies.* J Infect Dis, 2010, **201**: S168-S177.
92. Poston, T.B., Gottlieb, S.L., and Darville, T., *Status of vaccine research and development of vaccines for Chlamydia trachomatis infection.* Vaccine, 2017: 1-16.
93. Liu, X., Afrane, M., Clemmer, D.E.*, et al.*, *Identification of Chlamydia trachomatis outer membrane complex proteins by differential proteomics.* J Bacteriol, 2010, **192**: 2852-2860.
94. Tanzer, R.J. and Hatch, T.P., *Characterization of outer membrane proteins in Chlamydia trachomatis LGV serovar L2.* J Bacteriol, 2001, **183**: 2686-2690.
95. Caldwell, H.D., Kromhout, J., and Schachter, J., *Purification and partial characterization of the major outer membrane protein of Chlamydia trachomatis.* Infect Immun, 1981, **31**: 1161-1176.
96. Bøje, S., Olsen, A.W., Erneholm, K.*, et al.*, *A multi-subunit Chlamydia vaccine inducing neutralizing antibodies and strong IFN-γ+ CMI responses protects against a genital infection in minipigs.* Immunol Cell Biol, 2016, **94**: 185-195.
97. Pal, S., Theodor, I., Peterson, E.M.*, et al.*, *Immunization with the Chlamydia trachomatis mouse pneumonitis major outer membrane protein can elicit a protective immune response against a genital challenge.* Infect Immun, 2001, **69**: 6240-6247.
98. Sun, Y., Tippmann, E.M., and Platz, M.S., *A search for carbene-solvent interactions using time-resolved infrared spectroscopy.* Org Lett, 2003, **5**: 1305-1307.
99. Longbottom, D., *Chlamydial vaccine development.* J Med Microbiol, 2003, **52**: 537-540.
100. Olsen, A.W., Follmann, F., Erneholm, K.*, et al.*, *Protection against Chlamydia trachomatis infection and upper genital tract pathological changes by vaccine-*

promoted neutralizing antibodies directed to the VD4 of the major outer membrane protein. J Infect Dis, 2015, **212**: 978-989.

101. Agger, E.M., Rosenkrands, I., Hansen, J.*, et al.*, *Cationic liposomes formulated with synthetic mycobacterial cordfactor (CAF01): a versatile adjuvant for vaccines with different immunological requirements.* PLoS One, 2008, **3**: e3116.
102. Karunakaran, K.P., Yu, H., Jiang, X.*, et al.*, *Outer membrane proteins preferentially load MHC class II peptides: Implications for a Chlamydia trachomatis T cell vaccine.* Vaccine, 2015, **33**: 2159-2166.
103. He, Q., Martinez-Sobrido, L., Eko, F.O.*, et al.*, *Live-attenuated influenza viruses as delivery vectors for Chlamydia vaccines.* Immunology, 2007, **122**: 28-37.
104. Harvey, A., *Strategies for discovering drugs from previously unexplored natural products.* Drug Discov Today, 2000, **5**: 294-300.
105. Brown, M.A., Potroz, M.G., Teh, S.W.*, et al.*, *Natural products for the treatment of Chlamydiaceae infections.* Microorganisms, 2016, **4**: 1-30.
106. Li, J.L., Yang, N., Huang, L.*, et al.*, *Pyocyanin inhibits Chlamydia infection by disabling infectivity of the elementary body and disrupting intracellular growth.* Antimicrob Agents Chemother, 2018, **26**: 1-41.
107. Hall, S., McDermott, C., Anoopkumar-Dukie, S.*, et al.*, *Cellular effects of pyocyanin, a secreted virulence factor of Pseudomonas aeruginosa.* Toxins, 2016, **8**: 1-14.
108. Lazarev, V.N., Shkarupeta, M.M., Polina, N.F.*, et al.*, *Antimicrobial peptide from spider venom inhibits Chlamydia trachomatis infection at an early stage.* Arch Microbiol, 2013, **195**: 173-179.
109. Abdelmohsen, U.R., Cheng, C., Reimer, A.*, et al.*, *Antichlamydial sterol from the Red Sea sponge Callyspongia aff. implexa.* Planta Med, 2015, **81**: 382-387.
110. Li, J.L., Chen, D., Huang, L.*, et al.*, *Antichlamydial dimeric indole derivatives from marine actinomycete Rubrobacter radiotolerans.* Planta Med, 2017, **83**: 805-811.
111. Gootz, T.D., *Discovery and development of new antimicrobial agents.* Clin Microbiol Rev, 1990, **3**: 13-31.
112. Testa, C.A. and Johnson, L.J., *A whole-cell phenotypic screening platform for identifying methylerythritol phosphate pathway-selective inhibitors as novel antibacterial agents.* Antimicrob Agents Chemother, 2012, **56**: 4906-4913.
113. Tam, J.E., Davis, C.H., and Wyrick, P.B., *Expression of recombinant DNA introduced into Chlamydia trachomatis by electroporation.* Can J Microbiol, 1994, **40**: 583-591.
114. Bastidas, R.J. and Valdivia, R.H., *Emancipating Chlamydia: advances in the genetic manipulation of a recalcitrant intracellular pathogen.* Microbiol Mol Biol Rev, 2016, **80**: 411-427.

115. Workowski, K.A. and Berman, S., *Sexually transmitted diseases treatment guidelines.* MMWR Recomm Rep 2010, **59**: 1-110.
116. Monaghan, R.L. and Barrett, J.F., *Antibacterial drug discovery--then, now and the genomics future.* Biochem Pharmacol, 2006, **71**: 901-909.
117. Silver, L.L., *Multi-targeting by monotherapeutic antibacterials.* Nat Rev Drug Discov, 2007, **6**: 41-55.
118. Silver, L.L., *Appropriate targets for antibacterial drugs.* Cold Spring Harb Perspect Med, 2016, **6**: 1-7.
119. Baud, D., Goy, G., Osterheld, M.-C.*, et al.*, *Waddlia chondrophila: from bovine abortion to human miscarriage.* Clin Infect Dis, 2011, **52**: 1469-1471.
120. Haider, S., Collingro, A., Walochnik, J.*, et al.*, *Chlamydia-like bacteria in respiratory samples of community-acquired pneumonia patients.* FEMS Microbiol Lett, 2008, **281**: 198-202.
121. Dilbeck, P.M., Evermann, J.F., Crawford, T.B.*, et al.*, *Isolation of a previously undescribed rickettsia from an aborted bovine fetus.* J Clin Microbiol, 1990, **28**: 814-816.
122. de Barsy, M., Frandi, A., Panis, G.*, et al.*, *Regulatory (pan-)genome of an obligate intracellular pathogen in the PVC superphylum.* ISME J, 2016, **10**: 2129-2144.
123. Goy, G., Croxatto, A., and Greub, G., *Waddlia chondrophila enters and multiplies within human macrophages.* Microbes Infect, 2008, **10**: 556-562.
124. Tosetti, N., Croxatto, A., and Greub, G., *Amoebae as a tool to isolate new bacterial species, to discover new virulence factors and to study the host–pathogen interactions.* Microb Pathog, 2014, **77**: 125-130.
125. Froquet, R., Lelong, E., Marchetti, A.*, et al.*, *Dictyostelium discoideum: a model host to measure bacterial virulence.* Nat Protoc, 2008, **4**: 25-30.
126. Goy, G. and Greub, G., *Antibiotic susceptibility of Waddlia chondrophila in Acanthamoeba castellanii amoebae.* Antimicrob Agents Chemother, 2009, **53**: 2663-2666.
127. Lamoth, F., Pillonel, T., and Greub, G., *Waddlia: An emerging pathogen and a model organism to study the biology of Chlamydiae.* Microbes Infect, 2015: 732-737.
128. Derre, I., *Chlamydiae interaction with the endoplasmic reticulum: contact, function and consequences.* Cell Microbiol, 2015, **17**: 959-966.
129. Kebbi-Beghdadi, C., Cisse, O., and Greub, G., *Permissivity of Vero cells, human pneumocytes and human endometrial cells to Waddlia chondrophila.* Microbes Infect, 2011, **13**: 566-574.

130. UniProt, C.T., *UniProt: the universal protein knowledgebase.* Nucleic Acids Res, 2016, **45**: D158-D169.
131. Lange, R.P., Locher, H.H., Wyss, P.C.*, et al.*, *The targets of currently used antibacterial agents: lessons for drug discovery.* Curr Pharm Des, 2007, **13**: 3140-3154.
132. Dougherty, T.J., Barrett, J.F., and Pucci, M.J., *Microbial genomics and novel antibiotic discovery: new technology to search for new drugs.* Curr Pharm Des, 2002, **8**: 1119-1135.
133. Fleischmann, R.D., Adams, M.D., White, O.*, et al.*, *Whole-genome random sequencing and assembly of Haemophilus influenzae Rd.* Science, 1995, **269**: 496-512.
134. NCBI, *Database resources of the National Center for Biotechnology Information.* Nucleic Acids Res, 2018, **46**: D8-D13.
135. Kanz, C., Aldebert, P., Althorpe, N.*, et al.*, *The EMBL nucleotide sequence database.* Nucleic Acids Res, 2005, **33**: D29-D33.
136. Altschul, S.F., Madden, T.L., Schäffer, A.A.*, et al.*, *Gapped BLAST and PSI-BLAST: a new generation of protein database search programs.* Nucleic Acids Res, 1997, **25**: 3389-3402.
137. Pearson, W.R. and Lipman, D.J., *Improved tools for biological sequence comparison.* Proc Natl Acad Sci U S A, 1988, **85**: 2444-2448.
138. McDevitt, D. and Rosenberg, M., *Exploiting genomics to discover new antibiotics.* Trends Microbiol, 2001, **9**: 611-617.
139. Turab Naqvi, A.A., Rahman, S., Rubi*, et al.*, *Genome analysis of Chlamydia trachomatis for functional characterization of hypothetical proteins to discover novel drug targets.* Int J Biol Macromol, 2017, **96**: 234-240.
140. Lubec, G., Afjehi-Sadat, L., Yang, J.W.*, et al.*, *Searching for hypothetical proteins: theory and practice based upon original data and literature.* Prog Neurobiol, 2005, **77**: 90-127.
141. Gentry, D.R., Ingraham, K.A., Stanhope, M.J.*, et al.*, *Variable sensitivity to bacterial methionyl-tRNA synthetase inhibitors reveals subpopulations of Streptococcus pneumoniae with two distinct methionyl-tRNA synthetase genes.* Antimicrob Agents Chemother, 2003, **47**: 1784-1789.
142. Gwynn, M.N., Portnoy, A., Rittenhouse, S.F.*, et al.*, *Challenges of antibacterial discovery revisited.* Ann N Y Acad Sci, 2010, **1213**: 5-19.
143. Wasinger, V.C., Cordwell, S.J., Cerpa-Poljak, A.*, et al.*, *Progress with gene-product mapping of the Mollicutes: Mycoplasma genitalium.* Electrophoresis, 1995, **16**: 1090-1094.

144. O'Farrell, P.H., *High resolution two-dimensional electrophoresis of proteins.* J Biol Chem, 1975, **250**: 4007-4021.

145. Linn, T. and Losick, R., *The program of protein synthesis during sporulation in Bacillus subtilis.* Cell, 1976, **8**: 103-114.

146. Agabian, N. and Unger, B., *Caulobacter crescentus cell envelope: effect of growth conditions on murein and outer membrane protein composition.* J Bacteriol, 1978, **133**: 987-994.

147. Thorén, K., Gustafsson, E., Clevnert, A.*, et al.*, *Proteomic study of non-typable Haemophilus influenzae.* J Chromatogr B Analyt Technol Biomed Life Sci, 2002, **782**: 219-226.

148. Bini, L., Sanchez-Campillo, M., Santucci, A.*, et al.*, *Mapping of Chlamydia trachomatis proteins by Immobiline-polyacrylamide two-dimensional electrophoresis: Spot identification by N-terminal sequencing and immunoblotting.* Electrophoresis, 1996, **17**: 185-190.

149. Vandahl, B.B., Birkelund, S., Demol, H.*, et al.*, *Proteome analysis of the Chlamydia pneumoniae elementary body.* Electrophoresis, 2001, **22**: 1204-1223.

150. Shevchenko, A., Wilm, M., Vorm, O.*, et al.*, *Mass spectrometric sequencing of proteins silver-stained polyacrylamide gels.* Anal Chem, 1996, **68**: 850-858.

151. Brotz-Oesterhelt, H., Bandow, J.E., and Labischinski, H., *Bacterial proteomics and its role in antibacterial drug discovery.* Mass Spectrom Rev, 2005, **24**: 549-565.

152. VanBogelen, R.A., Schiller, E.E., Thomas, J.D.*, et al.*, *Diagnosis of cellular states of microbial organisms using proteomics.* Electrophoresis, 1999, **20**: 2149-2159.

153. Molestina, R.E., Klein, J.B., Miller, R.D.*, et al.*, *Proteomic analysis of differentially expressed Chlamydia pneumoniae genes during persistent infection of HEp-2 cells.* Infect Immun, 2002, **70**: 2976-2981.

154. Wehrl, W., Meyer, T.F., Jungblut, P.R.*, et al.*, *Action and reaction: Chlamydophila pneumoniae proteome alteration in a persistent infection induced by iron deficiency.* Proteomics, 2004, **4**: 2969-2981.

155. Shaw, A.C., Vandahl, B.B., Larsen, M.R.*, et al.*, *Characterization of a secreted Chlamydia protease.* Cell Microbiol, 2002, **4**: 411-424.

156. Zhong, G., Fan, P., Ji, H.*, et al.*, *Identification of a chlamydial protease–like activity factor responsible for the degradation of host transcription factors.* J Exp Med, 2001, **193**: 935-942.

157. Zhong, G., *Killing me softly: chlamydial use of proteolysis for evading host defenses.* Trends Microbiol, 2009, **17**: 467-474.

158. Huang, Z., Feng, Y., Chen, D.*, et al.*, *Structural basis for activation and inhibition of the secreted Chlamydia protease CPAF.* Cell Host Microbe, 2008, **4**: 529-542.

159. Heuer, D., Brinkmann, V., Meyer, T.F.*, et al.*, *Expression and translocation of chlamydial protease during acute and persistent infection of the epithelial HEp-2 cells with Chlamydophila (Chlamydia) pneumoniae.* Cell Microbiol, 2003, **5**: 315-322.

160. Chen, A.L., Johnson, K.A., Lee, J.K.*, et al.*, *CPAF: a chlamydial protease in search of an authentic substrate.* PLoS Pathog, 2012, **8**: e1002842.

161. Fiehn, O., *Metabolomics—the link between genotypes and phenotypes.* Plant Mol Biol, 2002, **48**: 155-171.

162. Nicholson, J.K., Lindon, J.C., and Holmes, E., *'Metabonomics': understanding the metabolic responses of living systems to pathophysiological stimuli via multivariate statistical analysis of biological NMR spectroscopic data.* Xenobiotica, 1999, **29**: 1181-1189.

163. Villas-Boas, S.G., Mas, S., Akesson, M.*, et al.*, *Mass spectrometry in metabolome analysis.* Mass Spectrom Rev, 2005, **24**: 613-646.

164. Durot, M., Bourguignon, P.-Y., and Schachter, V., *Genome-scale models of bacterial metabolism: reconstruction and applications.* FEMS Microbiol Rev, 2008, **33**: 164-190.

165. Frediani, J.K., Jones, D.P., Tukvadze, N.*, et al.*, *Plasma metabolomics in human pulmonary tuberculosis disease: a pilot study.* PLoS One, 2014, **9**: e108854.

166. Mohamed, R., Varesio, E., Ivosev, G.*, et al.*, *Comprehensive analytical strategy for biomarker identification based on liquid chromatography coupled to mass spectrometry and new candidate confirmation tools.* Anal Chem, 2009, **81**: 7677-7694.

167. Zhou, B., Xiao, J.F., Tuli, L.*, et al.*, *LC-MS-based metabolomics.* Mol Biosyst, 2012, **8**: 470-481.

168. van der Werf, M.J., Overkamp, K.M., Muilwijk, B.*, et al.*, *Microbial metabolomics: toward a platform with full metabolome coverage.* Anal Biochem, 2007, **370**: 17-25.

169. Weckwerth, W., *Metabolomics in systems biology.* Annu Rev Plant Biol, 2003, **54**: 669-689.

170. Ramautar, R., Somsen, G.W., and de Jong, G.J., *CE-MS in metabolomics.* Electrophoresis, 2009, **30**: 276-291.

171. Zhou, P., Zhou, N., Shao, L.*, et al.*, *Diagnosis of Clostridium difficile infection using an UPLC–MS based metabolomics method.* Metabolomics, 2018, **14**: 1-11.

172. dos Santos, B.S., da Silva, L.C.N., da Silva, T.D.*, et al.*, *Application of omics technologies for evaluation of antibacterial mechanisms of action of plant-derived products.* Front Microbiol, 2016, **7**: 1-13.

173. Gao, P. and Xu, G., *Mass-spectrometry-based microbial metabolomics: recent developments and applications.* Anal Bioanal Chem, 2015, **407**: 669-680.
174. Tang, J., *Microbial Metabolomics.* Current Genomics, 2011, **12**: 391-403.
175. Müller, C., Dietz, I., Tziotis, D.*, et al.*, *Molecular cartography in acute Chlamydia pneumoniae infections—a non-targeted metabolomics approach.* Anal Bioanal Chem, 2013, **405**: 5119-5131.
176. Byrne, G.I., *Chlamydia uncloaked.* Proc Natl Acad Sci U S A, 2003, **100**: 8040-8042.
177. Wang, Y., *Etiology of trachoma: a great success in isolating and cultivating Chlamydia trachomatis.* Chin Med J (Engl), 1999, **112**: 938-941.
178. Kohlhoff, S.A. and Hammerschlag, M.R., *Treatment of chlamydial infections: 2014 update.* Expert Opin Pharmacother, 2015, **16**: 205-212.
179. Engel, J.N., *Azithromycin-induced block of elementary body formation in Chlamydia trachomatis.* Antimicrob Agents Chemother, 1992, **36**: 2304-2309.
180. Beatty, W.L., Morrison, R.P., and Byrne, G.I., *Reactivation of persistent Chlamydia trachomatis infection in cell culture.* Infect Immun, 1995, **63**: 199-205.
181. Kutlin, A., Roblin, P.M., and Hammerschlag, M.R., *Effect of prolonged treatment with azithromycin, clarithromycin, or levofloxacin on Chlamydia pneumoniae in a continuous-infection model.* Antimicrob Agents Chemother, 2002, **46**: 409-412.
182. Stamm, W.E., *Potential for antimicrobial resistance in Chlamydia pneumoniae.* J Infect Dis, 2000, **181**: 456-459.
183. Somani, J., Bhullar, V.B., Workowski, K.A.*, et al.*, *Multiple drug-resistant Chlamydia trachomatis associated with clinical treatment failure.* J Infect Dis, 2000, **181**: 1421-1427.
184. Sukuru, S.C.K., Jenkins, J.L., Beckwith, R.E.*, et al.*, *Plate-based diversity selection based on empirical HTS data to enhance the number of hits and their chemical diversity.* J Biomol Screen, 2009, **14**: 690-699.
185. Pelaez, F., *The historical delivery of antibiotics from microbial natural products—can history repeat?* Biochem Pharmacol, 2006, **71**: 981-990.
186. Butler, M.S. and Buss, A.D., *Natural products—the future scaffolds for novel antibiotics?* Biochem Pharmacol, 2006, **71**: 919-929.
187. Li, J.W.-H. and Vederas, J.C., *Drug discovery and natural products: end of an era or an endless frontier?* Science, 2009, **325**: 161-165.
188. Newman, D.J. and Cragg, G.M., *Natural products as sources of new drugs from 1981 to 2014.* J Nat Prod, 2016, **79**: 629-661.

189. Chandra, H., Bishnoi, P., Yadav, A.*, et al.*, *Antimicrobial resistance and the alternative resources with special emphasis on plant-based antimicrobials—A review.* Plants (Basel), 2017, **6**: 1-16.

190. Yamazaki, T., Inoue, M., Sasaki, N.*, et al.*, *In vitro inhibitory effects of tea polyphenols on the proliferation of Chlamydia trachomatis and Chlamydia pneumoniae.* Jpn J Infect Dis, 2003, **56**: 143-145.

191. Petyaev, I.M., Zigangirova, N.A., Morgunova, E.Y.*, et al.*, *Resveratrol inhibits propagation of Chlamydia trachomatis in mccoy cells.* Biomed Res Int, 2017, **1**: 1-7.

192. Soleas, G.J., Diamandis, E.P., and Goldberg, D.M., *Resveratrol: a molecule whose time has come? And gone?* Clin Biochem, 1997, **30**: 91-113.

193. Takaoka, M., *Of the phenolic substrate of hellebore (Veratrum grandiflorum Loes. fil.).* J Fac Sci Hokkaido Imper Univ, 1940, **3**: 1-16.

194. Ma, D.S.L., Tan, L.T.-H., Chan, K.-G.*, et al.*, *Resveratrol—Potential antibacterial agent against foodborne pathogens.* Front Pharmacol, 2018, **9**: 1-16.

195. Tormakangas, L., Vuorela, P., Saario, E.*, et al.*, *In vivo treatment of acute Chlamydia pneumoniae infection with the flavonoids quercetin and luteolin and an alkyl gallate, octyl gallate, in a mouse model.* Biochem Pharmacol, 2005, **70**: 1222-1230.

196. Vuorela, P., Leinonen, M., Saikku, P.*, et al.*, *Natural products in the process of finding new drug candidates.* Curr Med Chem, 2004, **11**: 1375-1389.

197. Shaw, E.I., Dooley, C.A., Fischer, E.R.*, et al.*, *Three temporal classes of gene expression during the Chlamydia trachomatis developmental cycle.* Mol Microbiol, 2000, **37**: 913-925.

198. Belland, R.J., Zhong, G., Crane, D.D.*, et al.*, *Genomic transcriptional profiling of the developmental cycle of Chlamydia trachomatis.* PNAS, 2003, **100**: 8478-8483.

199. Wilson, A.C. and Tan, M., *Functional analysis of the heat shock regulator HrcA of Chlamydia trachomatis.* J Bacteriol, 2002, **184**: 6566-6571.

200. Hanson, B.R. and Tan, M., *Transcriptional regulation of the Chlamydia heat shock stress response in an intracellular infection.* Mol Microbiol, 2015, **97**: 1158-1167.

201. Hsieh, Y.J. and Wanner, B.L., *Global regulation by the seven-component pi signaling system.* Curr Opin Microbiol, 2010, **13**: 198-203.

202. Rosario, C.J., Hanson, B.R., and Tan, M., *The transcriptional repressor euo regulates both subsets of Chlamydia late genes.* Mol Microbiol, 2014, **94**: 888-897.

203. Zhang, L., Douglas, A.L., and Hatch, T.P., *Characterization of a Chlamydia psittaci DNA binding protein (Euo) synthesized during the early and middle phases of the developmental cycle.* Infect Immun, 1998, **66**: 1167-1173.

204. Xue, Y., Zheng, H., Mai, Z.*, et al.*, *An in vitro model of azithromycin-induced persistent Chlamydia trachomatis infection.* FEMS Microbiol Lett, 2017, **364**: 1-8.

205. Kaul, R., Hoang, A., Yau, P.*, et al.*, *The chlamydial euo gene encodes a histone H1-specific protease.* J Bacteriol, 1997, **179**: 5928-5934.

206. Ma, C., Yang, X., and Lewis, P.J., *Bacterial transcription as a target for antibacterial drug development.* Microbiol Mol Biol Rev, 2016, **80**: 139-160.

207. Rizzo, A., Carratelli, C.R., Losacco, A.*, et al.*, *Antimicrobial effect of natural polyphenols with or without antibiotics on Chlamydia pneumoniae infection in vitro.* Microb Drug Resist, 2014, **20**: 1-10.

208. Roblin, P.M., Dumornay, W., and Hammerschlag, M.R., *Use of HEp-2 cells for improved isolation and passage of Chlamydia pneumoniae.* J Clin Microbiol, 1992, **30**: 1968-1971.

209. Silhavy, T.J., *Gene fusions.* J Bacteriol, 2000, **182**: 5935-5938.

210. Miller, J.H., *Experiments in molecular genetics. CSHL Press, Cold spring Harbor, NY.* 1972.

211. Gee, K.R., Sun, W.C., Bhalgat, M.K.*, et al.*, *Fluorogenic substrates based on fluorinated umbelliferones for continuous assays of phosphatases and beta-galactosidases.* Anal Biochem, 1999, **273**: 41-48.

212. Gong, H., Zhang, B., Little, G.*, et al.*, *Beta-Galactosidase activity assay using far-red-shifted fluorescent substrate DDAOG.* Anal Biochem, 2009, **386**: 59-64.

213. Vidal-Aroca, F., Giannattasio, M., Brunelli, E.*, et al.*, *One-step high-throughput assay for quantitative detection of beta-galactosidase activity in intact Gram-negative bacteria, yeast, and mammalian cells.* BioTechniques, 2006, **40**: 433-438.

214. Bronstein, I., Fortin, J., Stanley, P.E.*, et al.*, *Chemiluminescent and bioluminescent reporter gene assays.* Anal Biochem, 1994, **219**: 169-181.

215. Pearson, B., Wolf, P.L., and Vazquez, J., *A comparative study of a series of new indolyl compounds to localize beta-galactosidase in tissues.* Lab Invest, 1963, **12**: 1249-1259.

216. Beck, E., Ludwig, G., Auerswald, E.A.*, et al.*, *Nucleotide sequence and exact localization of the neomycin phosphotransferase gene from transposon tn5.* Gene, 1982, **19**: 327-336.

217. Thomson, V.J., Bhattacharjee, M.K., Fine, D.H.*, et al.*, *Direct selection of IS903 transposon insertions by use of a broad-host-range vector: isolation of catalase-deficient mutants of Actinobacillus actinomycetemcomitans.* J Bacteriol, 1999, **181**: 7298-7307.

218. Sticher, P., Jaspers, M.C., Stemmler, K.*, et al.*, *Development and characterization of a whole-cell bioluminescent sensor for bioavailable middle-chain alkanes in contaminated groundwater samples.* Appl Environ Microbiol, 1997, **63**: 4053-4060.

219. Yun, C. and DasGupta, R., *Luciferase reporter assay in Drosophila and mammalian tissue culture cells.* Curr Protoc Chem Biol, 2014, **6**: 7-23.

220. Schenborn, E. and Groskreutz, D., *Reporter gene vectors and assays.* Mol Biotechnol, 1999, **13**: 29-44.

221. Sambrook, J., and Russell, D., *Molecular cloning: a laboratory manual*. 3rd ed. 2001, NY: CSHL Press. Cold Spring Harbor.

222. Gober, J.W. and Shapiro, L., *A developmentally regulated Caulobacter flagellar promoter is activated by 3'enhancer and IHF binding elements.* Mol Biol Cell, 1992, **3**: 913-926.

223. Karimova, G., Ullmann, A., and Ladant, D., *Protein-protein interaction between Bacillus stearothermophilus tyrosyl-tRNA synthetase subdomains revealed by a bacterial two-hybrid system.* J Mol Microbiol Biotechnol, 2001, **3**: 73-82.

224. Jaspers, M.C., Suske, W.A., Schmid, A.*, et al.*, *HbpR, a new member of the XylR/DmpR subclass within the NtrC family of bacterial transcriptional activators, regulates expression of 2-hydroxybiphenyl metabolism in Pseudomonas azelaica HBP1.* J Bacteriol, 2000, **182**: 405-417.

225. Khan, S.R., Gaines, J., Roop, R.M.*, et al.*, *Broad-host-range expression vectors with tightly regulated promoters and their use to examine the influence of traR and traM expression on ti plasmid quorum sensing.* Appl Environ Microbiol, 2008, **74**: 5053-5062.

226. Wiegand, I., Hilpert, K., and Hancock, R.E., *Agar and broth dilution methods to determine the minimal inhibitory concentration (MIC) of antimicrobial substances.* Nat Protoc, 2008, **3**: 163-175.

227. Eloff, J., *A sensitive and quick microplate method to determine the minimal inhibitory concentration of plant extracts for bacteria.* Planta Med, 1998, **64**: 711-713.

228. Bauer, A.W., Kirby, W.M., Sherris, J.C.*, et al.*, *Antibiotic susceptibility testing by a standardized single disk method.* Am J Clin Pathol, 1966, **45**: 493-496.

229. Zhang, J.H., Chung, T.D., and Oldenburg, K.R., *A simple statistical parameter for use in evaluation and validation of high throughput screening assays.* J Biomol Screen, 1999, **4**: 67-73.

230. Griffith, K.L. and Wolf, R.E., Jr., *Measuring beta-galactosidase activity in bacteria: cell growth, permeabilization, and enzyme assays in 96-well arrays.* Biochem Biophys Res Commun, 2002, **290**: 397-402.

231. Jacob, F. and Monod, J., *Genetic regulatory mechanisms in the synthesis of proteins.* J Mol Biol, 1961, **3**: 318-356.

232. Kercher, M.A., Lu, P., and Lewis, M., *Lac repressor-operator complex.* Curr Opin Struct Biol, 1997, **7**: 76-85.

233. Archetti, M., Döring, T.F., Hagen, S.B.*, et al.*, *Unravelling the evolution of autumn colours: an interdisciplinary approach.* Trends Ecol Evol, 2009, **24**: 166-173.

234. Sui, Y. and Wu, Z., *Alternative statistical parameter for high-throughput screening assay quality assessment.* J Biomol Screen, 2007, **12**: 229-234.

235. Hidalgo, G., Chan, M., and Tufenkji, N., *Inhibition of Escherichia coli CFT073 flic expression and motility by cranberry materials.* Appl Environ Microbiol, 2011, **77**: 6852-6857.

236. Chen, A.L., Wilson, A.C., and Tan, M., *A Chlamydia-specific c-terminal region of the stress response regulator HrcA modulates its repressor activity.* J Bacteriol, 2011, **193**: 6733-6741.

237. Wilson, A.C. and Tan, M., *Stress response gene regulation in Chlamydia is dependent on HrcA-CIRCE interactions.* J Bacteriol, 2004, **186**: 3384-3391.

238. Tan, M., Wong, B., and Engel, J.N., *Transcriptional organization and regulation of the dnaK and groE operons of Chlamydia trachomatis.* J Bacteriol, 1996, **178**: 6983-6990.

239. Hickey, J.M., Weldon, L., and Hefty, P.S., *The atypical OmpR/PhoB response regulator ChxR from Chlamydia trachomatis forms homodimers in vivo and binds a direct repeat of nucleotide sequences.* J Bacteriol, 2011, **193**: 389-398.

240. Jackson, A.P., Thomas, G.H., Parkhill, J.*, et al.*, *Evolutionary diversification of an ancient gene family (rhs) through c-terminal displacement.* BMC genomics, 2009, **10**: 1-16.

241. Kung, V.L., Khare, S., Stehlik, C.*, et al.*, *An rhs gene of Pseudomonas aeruginosa encodes a virulence protein that activates the inflammasome.* Proc Natl Acad Sci U S A, 2012, **109**: 1275-1280.

242. Kosinski, M.J., Rinas, U., and Bailey, J.E., *Isopropyl-β-D-thiogalactopyranoside influences the metabolism of Escherichia coli.* Appl Microbiol Biotechnol 1992, **36**: 782–784.

243. Thibodeau, S.A., Fang, R., and Joung, J.K., *High-throughput beta-galactosidase assay for bacterial cell-based reporter systems.* BioTechniques, 2004, **36**: 410-415.

244. Smith, J.G., Sconiers, W., Spasojevic, M.J.*, et al.*, *Phenological changes in alpine plants in response to increased snowpack, temperature, and nitrogen.* Arct Antarct Alp Res, 2012, **44**: 135-142.

245. Yilma, A.N., Singh, S.R., Morici, L., *et al.*, *Flavonoid naringenin: a potential immunomodulator for Chlamydia trachomatis inflammation.* Mediators Inflamm, 2013, **2013**: 1-13.

246. Yamazaki, T., Kishimoto, T., Shiga, S., *et al.*, *Biosynthesized tea polyphenols inactivate Chlamydia trachomatis in vitro.* Antimicrob Agents Chemother, 2005, **49**: 2501-2503.

247. Ikigai, H., Nakae, T., Hara, Y., *et al.*, *Bactericidal catechins damage the lipid bilayer.* Biochim Biophys Acta, 1993, **1147**: 132-136.

248. Delcour, A.H., *Outer membrane permeability and antibiotic resistance.* Biochim Biophys Acta Proteins Proteom, 2009, **1794**: 808-816.

249. Ebejer, J.-P., Charlton, M.H., and Finn, P.W., *Are the physicochemical properties of antibacterial compounds really different from other drugs?* J Cheminform, 2016, **8**: 1-9.

250. O'Shea, R. and Moser, H.E., *Physicochemical properties of antibacterial compounds: implications for drug discovery.* J Med Chem, 2008, **51**: 2871-2878.

251. ChemAxon Ltd. , *ChemAxon Ltd: Chemicalize, https://chemicalize.com*, Accessed: November 13, 2018.

252. Sekiguchi, M. and Iida, S., *Mutants of Escherichia coli permeable to actinomycin.* Proc Natl Acad Sci U S A, 1967, **58**: 2315-2320.

253. Ruiz, N., Falcone, B., Kahne, D., *et al.*, *Chemical conditionality: a genetic strategy to probe organelle assembly.* Cell, 2005, **121**: 307-317.

254. Muheim, C., Gotzke, H., Eriksson, A.U., *et al.*, *Increasing the permeability of Escherichia coli using MAC13243.* Sci Rep, 2017, **7**: 1-11.

255. Smith, E.A., Erickson, M.G., Ulijasz, A.T., *et al.*, *Surface plasmon resonance imaging of transcription factor proteins: interactions of bacterial response regulators with DNA arrays on gold films.* Langmuir, 2003, **19**: 1486-1492.

256. Mondragón, E. and Maher, L.J., *Anti-transcription factor RNA aptamers as potential therapeutics.* Nucleic Acid Ther, 2016, **26**: 29-43.

257. Fontaine, F., Overman, J., and François, M., *Pharmacological manipulation of transcription factor protein-protein interactions: opportunities and obstacles.* Cell Regen (Lond), 2015, **4**: 1-12.

258. Pan, Y., Duncombe, T.A., Kellenberger, C.A., *et al.*, *High-throughput electrophoretic mobility shift assays for quantitative analysis of molecular binding reactions.* Anal Chem, 2014, **86**: 10357-10364.

259. Alonso, N., Guillen, R., Chambers, J.W.*, et al.*, *A rapid and sensitive high-throughput screening method to identify compounds targeting protein-nucleic acids interactions.* Nucleic Acids Res, 2015, **43**: 1-8.

260. Kang, P. and Craig, E.A., *Identification and characterization of a new Escherichia coli gene that is a dosage-dependent suppressor of a dnaK deletion mutation.* J Bacteriol, 1990, **172**: 2055-2064.

261. Perederina, A., Svetlov, V., Vassylyeva, M.N.*, et al.*, *Regulation through the secondary channel-structural framework for ppGpp-DksA synergism during transcription.* Cell, 2004, **118**: 297-309.

262. Aberg, A., Fernandez-Vazquez, J., Cabrer-Panes, J.D.*, et al.*, *Similar and divergent effects of ppGpp and DksA deficiencies on transcription in Escherichia coli.* J Bacteriol, 2009, **191**: 3226-3236.

263. Paul, B.J., Barker, M.M., Ross, W.*, et al.*, *DksA: a critical component of the transcription initiation machinery that potentiates the regulation of rRNA promoters by ppGpp and the initiating NTP.* Cell, 2004, **118**: 311-322.

264. Cashel M, G.D., Hernandez VJ, Vinella D, *The stringent response in Escherichia coli and Salmonella typhimurium*. 2nd ed. 1987, Washington DC: ASM Press.

265. Xiao, H., Kalman, M., Ikehara, K.*, et al.*, *Residual guanosine 3', 5'-bispyrophosphate synthetic activity of relA null mutants can be eliminated by spoT null mutations.* J Biol Chem, 1991, **266**: 5980-5990.

266. Vinella, D., Albrecht, C., Cashel, M.*, et al.*, *Iron limitation induces SpoT-dependent accumulation of ppGpp in Escherichia coli.* Mol Microbiol, 2005, **56**: 958-970.

267. Paul, B.J., Ross, W., Gaal, T.*, et al.*, *rRNA transcription in Escherichia coli.* Annu Rev Genet, 2004, **38**: 749-770.

268. Paul, B.J., Berkmen, M.B., and Gourse, R.L., *DksA potentiates direct activation of amino acid promoters by ppGpp.* Proc Natl Acad Sci U S A, 2005, **102**: 7823-7828.

269. Magnusson, L.U., Gummesson, B., Joksimovic, P.*, et al.*, *Identical, independent, and opposing roles of ppGpp and DksA in Escherichia coli.* J Bacteriol, 2007, **189**: 5193-5202.

270. Zenkin, N. and Yuzenkova, Y., *New insights into the functions of transcription factors that bind the RNA polymerase secondary channel.* Biomolecules, 2015, **5**: 1195-1209.

271. Ulmer, A.J., Pryjma, J., Tarnok, Z.*, et al.*, *Inhibitory and stimulatory effects of Pseudomonas aeruginosa pyocyanine on human T and B lymphocytes and human monocytes.* Infect Immun, 1990, **58**: 808-815.

272. Meyer, J.-M., Neely, A., Stintzi, A.*, et al.*, *Pyoverdin is essential for virulence of Pseudomonas aeruginosa.* Infect Immun, 1996, **64**: 518-523.

273. Berka, R., Gray, G., and Vasil, M., *Studies of phospholipase c (heat-labile hemolysin) in Pseudomonas aeruginosa.* Infect Immun, 1981, **34**: 1071-1074.
274. Jude, F., Kohler, T., Branny, P.*, et al.*, *Posttranscriptional control of quorum-sensing-dependent virulence genes by DksA in Pseudomonas aeruginosa.* J Bacteriol, 2003, **185**: 3558-3566.
275. Turner, A.K., Lovell, M.A., Hulme, S.D.*, et al.*, *Identification of Salmonella typhimurium genes required for colonization of the chicken alimentary tract and for virulence in newly hatched chicks.* Infect Immun, 1998, **66**: 2099-2106.
276. Blaby-Haas, C.E., Furman, R., Rodionov, D.A.*, et al.*, *Role of a Zn-independent Dksa in Zn homeostasis and stringent response.* Mol Microbiol, 2011, **79**: 700-715.
277. Wippel, K. and Long, S.R., *Contributions of Sinorhizobium meliloti transcriptional regulator DksA to bacterial growth and efficient symbiosis with Medicago sativa.* J Bacteriol, 2016, **198**: 1374-1383.
278. Clohessy, P. and Golden, B., *Calprotectin-mediated zinc chelation as a biostatic mechanism in host defence.* Scand J Immunol, 1995, **42**: 551-556.
279. Natori, Y., Nanamiya, H., Akanuma, G.*, et al.*, *A fail-safe system for the ribosome under zinc-limiting conditions in Bacillus subtilis.* Mol Microbiol, 2007, **63**: 294-307.
280. Gabriel, S.E., Miyagi, F., Gaballa, A.*, et al.*, *Regulation of the Bacillus subtilis yciC gene and insights into the DNA-binding specificity of the zinc-sensing metalloregulator Zur.* J Bacteriol, 2008, **190**: 3482-3488.
281. Opalka, N., Chlenov, M., Chacon, P.*, et al.*, *Structure and function of the transcription elongation factor GreB bound to bacterial RNA polymerase.* Cell, 2003, **114**: 335-345.
282. Sekine, S., Murayama, Y., Svetlov, V.*, et al.*, *The ratcheted and ratchetable structural states of RNA polymerase underlie multiple transcriptional functions.* Mol Cell, 2015, **57**: 408-421.
283. Tagami, S., Sekine, S., Kumarevel, T.*, et al.*, *Crystal structure of bacterial RNA polymerase bound with a transcription inhibitor protein.* Nature, 2010, **468**: 978-982.
284. Blankschien, M.D., Potrykus, K., Grace, E.*, et al.*, *TraR a homolog of a RNAP secondary channel interactor, modulates transcription.* PLoS Genet, 2009, **5**: 1-13.
285. Mittenhuber, G., *Comparative genomics and evolution of genes encoding bacterial (p)ppGpp synthetases/hydrolases (the Rel, RelA and SpotT proteins).* J Mol Microbiol Biotechnol, 2001, **3**: 585-600.
286. Hauryliuk, V., Atkinson, G.C., Murakami, K.S.*, et al.*, *Recent functional insights into the role of (p)ppGpp in bacterial physiology.* Nat Rev Microbiol, 2015, **13**: 298-309.

287. Mukhopadhyay, S., Good, D., Miller, R.D., *et al.*, *Identification of Chlamydia pneumoniae proteins in the transition from reticulate to elementary body formation.* Mol Cell Proteomics, 2006, **5**: 2311-2318.

288. Mukhopadhyay, S., Miller, R.D., Sullivan, E.D., *et al.*, *Protein expression profiles of Chlamydia pneumoniae in models of persistence versus those of heat shock stress response.* Infect Immun, 2006, **74**: 3853-3863.

289. Ouellette, S.P., Hatch, T.P., AbdelRahman, Y.M., *et al.*, *Global transcriptional upregulation in the absence of increased translation in Chlamydia during IFNgamma-mediated host cell tryptophan starvation.* Mol Microbiol, 2006, **62**: 1387-1401.

290. Brinkworth, A.J., Wildung, M.R., and Carabeo, R.A., *Genomewide transcriptional responses of iron-starved Chlamydia trachomatis reveal prioritization of metabolic precursor synthesis over protein translation.* mSystems, 2018, **3**: 1-22.

291. Smith, A.W. and Iglewski, B.H., *Transformation of Pseudomonas aeruginosa by electroporation.* Nucleic Acids Res, 1989, **17**: 10509.

292. Datsenko, K.A. and Wanner, B.L., *One-step inactivation of chromosomal genes in Escherichia coli K-12 using PCR products.* Proc Natl Acad Sci U S A, 2000, **97**: 6640-6645.

293. Baba, T., Ara, T., Hasegawa, M., *et al.*, *Construction of Escherichia coli K-12 in-frame, single-gene knockout mutants: the Keio collection.* Mol Syst Biol, 2006, **2**: 1-11.

294. Hirvonen, C.A., Ross, W., Wozniak, C.E., *et al.*, *Contributions of up elements and the transcription factor fis to expression from the seven rrn P1 promoters in Escherichia coli.* J Bacteriol, 2001, **183**: 6305-6314.

295. Rutherford, S.T., Lemke, J.J., Vrentas, C.E., *et al.*, *Effects of DksA, GreA, and GreB on transcription initiation: insights into the mechanisms of factors that bind in the secondary channel of RNA polymerase.* J Mol Biol, 2007, **366**: 1243-1257.

296. Guzman, L.M., Belin, D., Carson, M.J., *et al.*, *Tight regulation, modulation, and high-level expression by vectors containing the arabinose pBAD promoter.* J Bacteriol, 1995, **177**: 4121-4130.

297. Qiu, D., Damron, F.H., Mima, T., *et al.*, *PBAD-based shuttle vectors for functional analysis of toxic and highly regulated genes in Pseudomonas and Burkholderia spp. and other bacteria.* Appl Environ Microbiol, 2008, **74**: 7422-7426.

298. Kanehisa, M., Furumichi, M., Tanabe, M., *et al.*, *KEGG: new perspectives on genomes, pathways, diseases and drugs.* Nucleic Acids Res, 2017, **45**: D353-D361.

299. Kelley, L.A., Mezulis, S., Yates, C.M., *et al.*, *The Phyre2 web portal for protein modeling, prediction and analysis.* Nat Protoc, 2015, **10**: 845-858.

300. Durrant, I., *Light-based detection of biomolecules.* Nature, 1990, **346**: 297-298.

301. Trautinger, B.W., Jaktaji, R.P., Rusakova, E.*, et al.*, *RNA polymerase modulators and DNA repair activities resolve conflicts between DNA replication and transcription.* Mol Cell, 2005, **19**: 247-258.

302. Farrell, H., Garvey, M., Cormican, M.*, et al.*, *Investigation of critical inter-related factors affecting the efficacy of pulsed light for inactivating clinically relevant bacterial pathogens.* J Appl Microbiol, 2010, **108**: 1494-1508.

303. Kurachi, M., *Studies on the biosynthesis of pyocyanine.(III): on the effect of iron and other heavy metals.* Bull Inst Chem Res Kyoto Univ, 1958, **36**: 188-196.

304. Parshin, A., Shiver, A.L., Lee, J.*, et al.*, *DksA regulates RNA polymerase in Escherichia coli through a network of interactions in the secondary channel that includes sequence insertion 1.* Proc Natl Acad Sci U S A, 2015, **112**: E6862-E6871.

305. Sievers, F., Wilm, A., Dineen, D.*, et al.*, *Fast, scalable generation of high-quality protein multiple sequence alignments using clustal omega.* Mol Syst Biol, 2011, **7**: 1-6.

306. Potrykus, K., Vinella, D., Murphy, H.*, et al.*, *Antagonistic regulation of Escherichia coli ribosomal RNA rrnB P1 promoter activity by GreA and DksA.* J Biol Chem, 2006, **281**: 15238-15248.

307. Paetzel, M., Karla, A., Strynadka, N.C.*, et al.*, *Signal peptidases.* Chem Rev, 2002, **102**: 4549-4580.

308. Laptenko, O., Kim, S.S., Lee, J.*, et al.*, *PH-dependent conformational switch activates the inhibitor of transcription elongation.* EMBO J, 2006, **25**: 2131-2141.

309. Grieshaber, S., Swanson, J.A., and Hackstadt, T., *Determination of the physical environment within the Chlamydia trachomatis inclusion using ion-selective ratiometric probes.* Cell Microbiol, 2002, **4**: 273-283.

310. Wakaki, S., Marumo, H., Tomioka, K.*, et al.*, *Isolation of new fractions of antitumor mitomycins.* Antibiot Chemother (Northfield), 1958, **8**: 228-240.

311. Schwartz, H.S., Sodergren, J., and Philips, F., *Mitomycin C: chemical and biological studies on alkylation.* Science, 1963, **142**: 1181-1183.

312. Zhou, Y.N. and Jin, D.J., *The rpoB mutants destabilizing initiation complexes at stringently controlled promoters behave like "stringent" RNA polymerases in Escherichia coli.* Proc Natl Acad Sci U S A, 1998, **95**: 2908-2913.

313. Jayaseelan, S., Ramaswamy, D., and Dharmaraj, S., *Pyocyanin: production, applications, challenges and new insights.* World J Microbiol Biotechnol, 2014, **30**: 1159-1168.

314. Branny, P., Pearson, J.P., Pesci, E.C.*, et al.*, *Inhibition of quorum sensing by a Pseudomonas aeruginosa dksA homologue.* J Bacteriol, 2001, **183**: 1531-1539.

315. Lau, G.W., Hassett, D.J., Ran, H.*, et al.*, *The role of pyocyanin in Pseudomonas aeruginosa infection.* Trends Mol Med, 2004, **10**: 599-606.
316. Cain, J.A., Solis, N., and Cordwell, S.J., *Beyond gene expression: The impact of protein post-translational modifications in bacteria.* J Proteomics, 2014, **97**: 265-286.
317. Traag, B.A., Ramirez-Peralta, A., Wang Erickson, A.F.*, et al.*, *A novel RNA polymerase-binding protein controlling genes involved in spore germination in Bacillus subtilis.* Mol Microbiol, 2013, **89**: 113-122.
318. McKnight, S.L., *On getting there from here.* Science, 2010, **330**: 1338-1339.
319. Patti, G.J., Yanes, O., and Siuzdak, G., *Innovation: Metabolomics: the apogee of the omics trilogy.* Nat Rev Mol Cell Biol, 2012, **13**: 263-269.
320. Yamashita, M. and Fenn, J.B., *Electrospray ion source. Another variation on the free-jet theme.* J Phys Chem A, 1984, **88**: 4451-4459.
321. Holcapek, M., Jirasko, R., and Lisa, M., *Basic rules for the interpretation of atmospheric pressure ionization mass spectra of small molecules.* J Chromatogr A, 2010, **1217**: 3908-3921.
322. Bowen, B.P. and Northen, T.R., *Dealing with the unknown: metabolomics and metabolite atlases.* J Am Soc Mass Spectrom, 2010, **21**: 1471-1476.
323. Dunn, W.B., Erban, A., Weber, R.J.*, et al.*, *Mass appeal: metabolite identification in mass spectrometry-focused untargeted metabolomics.* Metabolomics, 2013, **9**: 44-66.
324. Katajamaa, M. and Orešič, M., *Processing methods for differential analysis of LC/MS profile data.* BMC bioinformatics, 2005, **6**: 1-12.
325. Smith, C.A., Want, E.J., O'Maille, G.*, et al.*, *XCMS: processing mass spectrometry data for metabolite profiling using nonlinear peak alignment, matching, and identification.* Anal Chem, 2006, **78**: 779-787.
326. Smith, C.A., O'Maille, G., Want, E.J.*, et al.*, *METLIN: a metabolite mass spectral database.* Ther Drug Monit, 2005, **27**: 747-751.
327. Wishart, D.S., Tzur, D., Knox, C.*, et al.*, *HMDB: the human metabolome database.* Nucleic Acids Res, 2007, **35**: D521-D526.
328. Fahy, E., Subramaniam, S., Brown, H.A.*, et al.*, *A comprehensive classification system for lipids.* J Lipid Res, 2005, **46**: 839-862.
329. Degtyarenko, K., de Matos, P., Ennis, M.*, et al.*, *ChEBI: a database and ontology for chemical entities of biological interest.* Nucleic Acids Res, 2008, **36**: D344-D350.
330. Sajed, T., Marcu, A., Ramirez, M.*, et al.*, *ECMDB 2.0: A richer resource for understanding the biochemistry of E. coli.* Nucleic Acids Res, 2016, **44**: D495-D501.
331. Jansson, J., Willing, B., Lucio, M.*, et al.*, *Metabolomics reveals metabolic biomarkers of Crohn's disease.* PLoS One, 2009, **4**: e6386.

332. Want, E.J., Wilson, I.D., Gika, H.*, et al.*, *Global metabolic profiling procedures for urine using UPLC-MS.* Nat Protoc, 2010, **5**: 1005-1018.

333. Chambers, M.C., Maclean, B., Burke, R.*, et al.*, *A cross-platform toolkit for mass spectrometry and proteomics.* Nat Biotechnol, 2012, **30**: 918-920.

334. GNPS, *Global natural products social molecular networking, http://gnps.ucsd.edu*, Accessed: November 13, 2018.

335. Marcinowska, R., Trygg, J., Wolf-Watz, H.*, et al.*, *Optimization of a sample preparation method for the metabolomic analysis of clinically relevant bacteria.* J Microbiol Methods, 2011, **87**: 24-31.

336. Theodoridis, G., Gika, H.G., and Wilson, I.D., *Mass spectrometry-based holistic analytical approaches for metabolite profiling in systems biology studies.* Mass Spectrom Rev, 2011, **30**: 884-906.

337. Theodoridis, G., Gika, H.G., and Wilson, I.D., *LC-MS-based methodology for global metabolite profiling in metabonomics/metabolomics.* Trends Analyt Chem, 2008, **27**: 251-260.

338. Pinu, F.R., Villas-Boas, S.G., and Aggio, R., *Analysis of intracellular metabolites from microorganisms: quenching and extraction protocols.* Metabolites, 2017, **7**: 1-20.

339. Sumner, L.W., Amberg, A., Barrett, D.*, et al.*, *Proposed minimum reporting standards for chemical analysis Chemical Analysis Working Group (CAWG) Metabolomics Standards Initiative (MSI).* Metabolomics, 2007, **3**: 211-221.

340. Madala, N.E., Tugizimana, F., Steenkamp, P.A.*, et al.*, *The short and long of it: shorter chromatographic analysis suffice for sample classification during UHPLC-MS-mased metabolic fingerprinting.* Chromatographia, 2013, **76**: 279-285.

341. Dunn, W.B., Wilson, I.D., Nicholls, A.W.*, et al.*, *The importance of experimental design and QC samples in large-scale and MS-driven untargeted metabolomic studies of humans.* Bioanalysis, 2012, **4**: 2249-2264.

342. Gika, H.G., Theodoridis, G.A., Wingate, J.E.*, et al.*, *Within-day reproducibility of an HPLC− MS-based method for metabonomic analysis: application to human urine.* J Proteome Res, 2007, **6**: 3291-3303.

343. Gika, H.G., Macpherson, E., Theodoridis, G.A.*, et al.*, *Evaluation of the repeatability of ultra-performance liquid chromatography–TOF-MS for global metabolic profiling of human urine samples.* J Chromatogr B Analyt Technol Biomed Life Sci, 2008, **871**: 299-305.

344. Cloarec, O., Dumas, M.E., Trygg, J.*, et al.*, *Evaluation of the orthogonal projection on latent structure model limitations caused by chemical shift variability and improved*

visualization of biomarker changes in 1H NMR spectroscopic metabonomic studies. Anal Chem, 2005, **77**: 517-526.

345. Wiklund, S., Johansson, E., Sjostrom, L.*, et al.*, *Visualization of GC/TOF-MS-based metabolomics data for identification of biochemically interesting compounds using OPLS class models.* Anal Chem, 2008, **80**: 115-122.
346. Wilson, I.D., Nicholson, J.K., Castro-Perez, J.*, et al.*, *High resolution "ultra performance" liquid chromatography coupled to oa-TOF mass spectrometry as a tool for differential metabolic pathway profiling in functional genomic studies.* J Proteome Res, 2005, **4**: 591-598.
347. Goodacre, R., Vaidyanathan, S., Dunn, W.B.*, et al.*, *Metabolomics by numbers: acquiring and understanding global metabolite data.* Trends Biotechnol, 2004, **22**: 245-252.
348. Sangster, T.P., Wingate, J.E., Burton, L.*, et al.*, *Investigation of analytical variation in metabonomic analysis using liquid chromatography/mass spectrometry.* Rapid Commun Mass Spectrom, 2007, **21**: 2965-2970.
349. Worley, B. and Powers, R., *PCA as a practical indicator of OPLS-DA model reliability.* Current Metabolomics, 2016, **4**: 97-103.
350. Kind, T. and Fiehn, O., *Seven golden rules for heuristic filtering of molecular formulas obtained by accurate mass spectrometry.* BMC Bioinformatics, 2007, **8**: 105-125.
351. Karni, M. and Mandelbaum, A., *The 'even-electron rule'.* Organic Mass Spectrometry, 1980, **15**: 53-64.
352. Wang, M., Carver, J.J., Phelan, V.V.*, et al.*, *Sharing and community curation of mass spectrometry data with Global Natural Products Social Molecular Networking.* Nat Biotechnol, 2016, **34**: 828-837.
353. Milne, S., Ivanova, P., Forrester, J.*, et al.*, *Lipidomics: An analysis of cellular lipids by ESI-MS.* Methods, 2006, **39**: 92-103.
354. ThermoFisher Scienctific, *Planet Orbitrap, http://planetorbitrap.com/cholesterol-metabolites#tab:mass-spectrometry*, Accessed: November 13, 2018.
355. Ferraz, T., Fiuza, M., Dos Santos, M.*, et al.*, *Comparison of six methods for the extraction of lipids from serum in terms of effectiveness and protein preservation.* J Biochem Biophys Methods, 2004, **58**: 187-193.
356. Fei, F., Bowdish, D.M., and McCarry, B.E., *Comprehensive and simultaneous coverage of lipid and polar metabolites for endogenous cellular metabolomics using HILIC-TOF-MS.* Anal Bioanal Chem, 2014, **406**: 3723-3733.

357. Peters, J., Onguri, V., Nishimoto, S.K., *et al.*, *The Chlamydia trachomatis CT149 protein exhibits esterase activity in vitro and catalyzes cholesteryl ester hydrolysis when expressed in HeLa cells.* Microbes Infect, 2012, **14**: 1196-1204.

358. Carabeo, R.A., Mead, D.J., and Hackstadt, T., *Golgi-dependent transport of cholesterol to the Chlamydia trachomatis inclusion.* Proc Natl Acad Sci U S A, 2003, **100**: 6771-6776.

359. Moliner, C., Raoult, D., and Fournier, P.-E., *Evidence that the intra-amoebal Legionella drancourtii acquired a sterol reductase gene from eukaryotes.* BMC research notes, 2009, **2**: 51.

360. Howe, D. and Heinzen, R.A., *Coxiella burnetii inhabits a cholesterol-rich vacuole and influences cellular cholesterol metabolism.* Cell Microbiol, 2006, **8**: 496-507.

361. Samanta, D., Mulye, M., Clemente, T.M., *et al.*, *Manipulation of host cholesterol by obligate intracellular bacteria.* Front Cell Infect Microbiol, 2017, **7**: 1-14.

362. de Barsy, M. and Greub, G., *Waddlia chondrophila: from biology to pathogenicity.* Microbes Infect, 2013, **15**: 1033-1041.

363. Van der Werf, M.J., Overkamp, K.M., Muilwijk, B., *et al.*, *Comprehensive analysis of the metabolome of Pseudomonas putida S12 grown on different carbon sources.* Mol Biosyst, 2008, **4**: 315-327.

364. Rosario, C.J. and Tan, M., *The early gene product EUO is a transcriptional repressor that selectively regulates promoters of Chlamydia late genes.* Mol Microbiol, 2012, **84**: 1097-1107.

365. Mijakovic, I., Grangeasse, C., and Turgay, K., *Exploring the diversity of protein modifications: special bacterial phosphorylation systems.* FEMS Microbiol Rev, 2016, **40**: 398-417.

366. Gopalkrishnan, S., Ross, W., Chen, A.Y., *et al.*, *TraR directly regulates transcription initiation by mimicking the combined effects of the global regulators DksA and ppGpp.* Proc Natl Acad Sci U S A, 2017, **114**: E5539-E5548.

367. Luo, Z.Q. and Farrand, S.K., *Signal-dependent DNA binding and functional domains of the quorum-sensing activator TraR as identified by repressor activity.* Proc Natl Acad Sci U S A, 1999, **96**: 9009-9014.

368. Zhu, J. and Winans, S.C., *The quorum-sensing transcriptional regulator TraR requires its cognate signaling ligand for protein folding, protease resistance, and dimerization.* Proc Natl Acad Sci U S A, 2001, **98**: 1507-1512.

369. Vannini, A., Volpari, C., Gargioli, C., *et al.*, *The crystal structure of the quorum sensing protein TraR bound to its autoinducer and target DNA.* EMBO J, 2002, **21**: 4393-4401.

370. Papenfort, K. and Bassler, B.L., *Quorum sensing signal–response systems in Gram-negative bacteria.* Nat Rev Microbiol, 2016, **14**: 576-588.
371. Ismail, A.S., Valastyan, J.S., and Bassler, B.L., *A host-produced autoinducer-2 mimic activates bacterial quorum sensing.* Cell Host Microbe, 2016, **19**: 470-480.
372. Wang, H., Feng, Z., Wu, D.*, et al.*, *Enzyme-regulated supramolecular assemblies of cholesterol conjugates against drug-resistant ovarian cancer cells.* J Am Chem Soc, 2016, **138**: 10758-10761.
373. Doughty, D.M., Dieterle, M., Sessions, A.L.*, et al.*, *Probing the subcellular localization of hopanoid lipids in bacteria using NanoSIMS.* PLoS One, 2014, **9**: e84455.
374. Dufourc, E.J., *Sterols and membrane dynamics.* J Chem Biol, 2008, **1**: 63-77.
375. Sohlenkamp, C. and Geiger, O., *Bacterial membrane lipids: diversity in structures and pathways.* FEMS Microbiol Rev, 2016, **40**: 133-159.
376. Halouska, S., Zhang, B., Gaupp, R.*, et al.*, *Revisiting protocols for the NMR analysis of bacterial metabolomes.* J Integr OMICS, 2013, **3**: 120-137.